CONCEPTUAL DESIGN OF MOLTEN SALT TEST LOOP FOR FUSION REACTOR HEAT TRANSFER, TRITUM BREEDING, BYPRODUCT FILTERING AND STORAGE

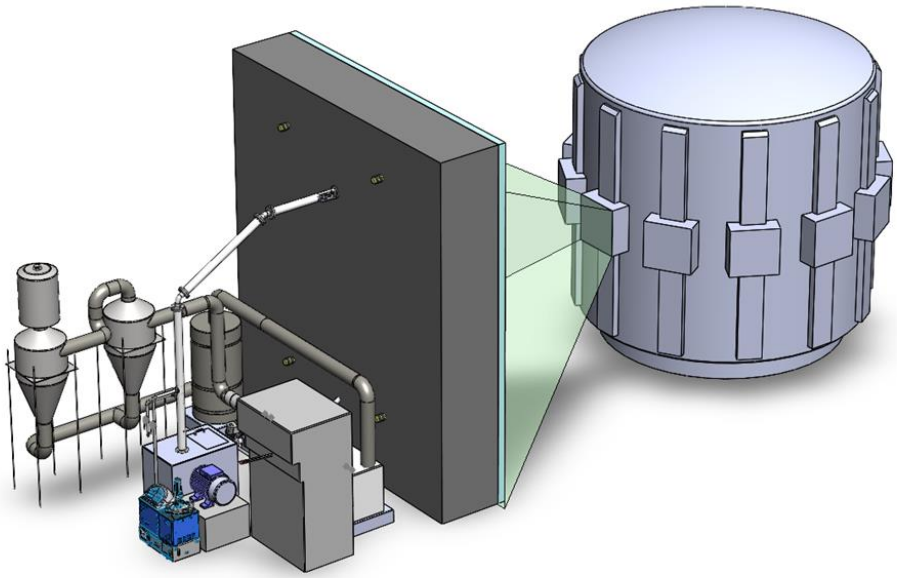

By

Samuel Haga

Benjamin Kraus

Austin Michael

Logan Powers

Jackson Stanley

THIS PAGE PURPOSELY BLANK

A SENIOR CAPSTONE REPORT

Presented to the faculty of

The College of Engineering and Applied Science at the University of Cincinnati

In Partial Fulfillment of the Requirements

For the Bachelor of Science in Mechanical Engineering

MECH5051/5052 Senior Design

Under the supervision of:

Thomas Huston PhD

Jude Iroh PhD

Henry Spitz PhD

Cincinnati, OH

April 2024

Project Overview

University of Cincinnati Molten Salt Test Loop
UC-MSTL

University of Cincinnati
BSME Class of 2024

THIS PAGE PURPOSELY BLANK

TABLE OF CONTENTS

PROJECT OVERVIEW

1. FOREWORD 10
2. OVERVIEW OF REPORT 12
3. PROJECT DESCRIPTION 13
   3.1. Project Scope 13
4. ENGINEERING STANDARDS AND CODES 13
   4.1. 10 CFR 30 13
   4.2. 49 CFR 173 14
   4.3. 10 CFR 71 14
5. CONSTRAINTS 15
   5.1. Economic 15
   5.2. Environmental 16
   5.3. Sustainability 16
   5.4. Manufacturability 16
   5.5. Ethical 16
   5.6. Health & Safety 16
   5.7. Specifications 16
6. METHODOLOGY 17
   6.1. Team Members and Roles: 17
   6.2. Deliverables 17
   6.3. Deliverable Breakdown 18

LITERATURE REVIEW

1. INTRODUCTION 22
   1.1. Purpose of Document 22
   1.2. Document Scope 22
   1.3. Background 22
   1.4. Scope 22
2. EXECUTIVE SUMMARY 23
   2.1. Summary Introduction 23
   2.2. General Fusion Materials 23
   2.3. Sensing 24
   2.4. Previous Loop Examples 24
   2.5. FLiBe Salt 25
   2.6. Filtering 26
3. LITERATURE REVIEW 28
   3.1. General Fusion Materials 28
   3.2. Sensing 36
   3.3. Previous Molten Salt Loops 40
   3.4. FLiBe Salt 45
   3.5. Filtering 52

FUNCTIONAL REQUIREMENTS DOCUMENT

1. INTRODUCTION 67
   1.1. Purpose of Document 67
   1.2. Document Scope 67
   1.3. Background 67
   1.4. System Description 67
   1.5. Scope 68
2. FUNCTIONAL REQUIREMENTS 70
   2.1. FLiBe Test Loop (System) 70
   2.2. FLiBe (LiF-BeF_2, Subsystem) 71
   2.3. Pump System (Subsystem) 72
   2.4. Filtering (Subsystem) 72
   2.5. Support Equipment (Balance of Plant, Subsystem) 73
   2.6. Controls (Subsystem) 74
   2.7. Samples (Subsystem) 75

SYSTEM DESIGN DESCRIPTION

1. INTRODUCTION 80
   1.1. Purpose of Document 80
   1.2. Document Scope 80
   1.3. Background 80
   1.4. System Description 80
   1.5. Project Scope 81
2. OVERVIEW OF MSTL DESIGN 82
   2.1. Heat Transfer 85
   2.2. Irradiation Zone and Non-Irradiation Zone 86
   2.3. Zone Material Selection and Layout 87
3. BREAKDOWN OF SUBSYSTEM DESIGN 89
   3.1. FLiBe (LiF-BeF_2) 89
   3.2. Pump 91
   3.3. Filter 93
   3.4. Supporting Equipment 97
   3.5. Controls 98
   3.6. Sampling 99

DETERMINISTIC AND STOCHASTIC CALCULATIONS

1. INTRODUCTION 110
   1.1. Purpose of Document 110
   1.2. Document Scope 110
   1.3. Background 110
   1.4. System Description 110
   1.5. Project Scope 111
2. INTRODUCTION TO NEUTRONICS AND NUCLEAR FUSION ENGINEERING 112
   2.1. Simplified Definition of Neutronics 112
   2.2. Fusion Energy and the Neutron 112
   2.3. Equations for Neutronics Modeling 114
3. OVERVIEW OF LOOP CONCEPTUAL DESIGN 115
4. DETERMINISTIC CALCULATIONS 115
   4.1. Shielding Calculations 115
   4.2. Neutron Activation Analysis (NAA) 117
5. STOCHASTIC CALCULATIONS 129
   5.1. Constructing the Model 129
   5.2. Assumptions 132
   5.3. Requested Data 134
   5.4. Convergence Study 134
   5.5. Shielding Sensitivity Study 140
   5.6. Tritium Production Experimental Study 147
6. FUTURE WORK 152

FILTERING MECHANISM THEORY, EXPERIMENTAL PLAN, AND ANALYSIS

1. INTRODUCTION 220
   1.1. Purpose of Document 220
   1.2. Document Scope 220
   1.3. Background 220
   1.4. Scope 221
2. INTRODUCTION TO METAL-ORGANIC FRAMEWORKS 222
   2.1. Reticular Chemistry 222
   2.2. Metal-Organic Frameworks 222
   2.3. MOF Decision Matrix 223
   2.4. Methods of Analysis 225
   2.5. Stoichiometric Calculations 229
3. BACKGROUND 233
4. EXPERIMENTAL INSTRUCTIONS 233
   4.1. Safety 238
   4.2. Materials: 238
5. MOF RESULTS AND ANALYSIS 240
   5.1. Porosity 240
   5.2. Imaging 245
   5.3. Energy Signatures 248
6. CONCLUSION 250
7. FUTURE WORK 250

MASTER DOCUMENT

1. PEOPLE 260
2. DELIVERABLES 260
3. MEETING NOTES 261
4. ASSIGNED PROJECT-BASED WORK 274
5. PROJECT SCHEDULE 290

THIS PAGE PURPOSELY BLANK

1. Foreword

The five engineers who worked towards this project provide in this report, to the best of their technical training as degreed mechanical engineers, a comprehensive and conceptual design for a molten salt test loop to be implemented within the proximity of a fusion demonstration device. This test loop, namely the University of Cincinnati Molten Salt Test Loop (UC-MSTL), validates heat transfer characteristics, tritium breeding, and byproduct storage.

The UC-MSTL group could not have completed this project without the dedication and support from Commonwealth Fusion Systems, who provided their time diligently over countless hours in order to make this project successful. The staff at the Massachusetts Institute of Technology Plasma Science and Fusion Center (MIT-PSFC) provided essential guidance towards the development of the Monte Carlo results documented in this report. Without their guidance, these results would have never materialized. Finally, the UC-MSTL group would like to thank Dr. Henry Spitz, Dr. Will Hawkins, and Dr. Jude Iroh of the University of Cincinnati, who gave their time at all hours and with no bounds to verify the results of the project.

The group would like to thank all those who supported us in this mission not mentioned.

Jackson Stanley

Jackson N. Stanley

2. Overview of Report

This report serves as the final and total deliverable for the senior capstone project, as required for the completion of a Bachelor of Science in Mechanical Engineering at the University of Cincinnati.

This document is partitioned into sections pertaining to specific deliverables as defined at the beginning of the project. Some of these deliverables are specific to grading for the senior capstone, while others have a more general appreciation. As such, each deliverable contains its own set of references and document content. This is for ease of distribution to supporting parties and for partitioning prior to submission. Grading for the capstone requirements should take into account the breakdown of the deliverables based on individual and group contribution.

The following Deliverables were completed by all team members:

Literature Review

Functional Requirements Document

System Design Description

The following deliverable(s) were completed by Sam Haga:

Complete Conceptual Model Utilizing SolidWorks

The following deliverable(s) were completed by Jackson Stanley and Austin Michael:

Neutronics and Nuclear Engineering Calculation Report

The following deliverable(s) were completed by Ben Kraus and Logan Powers:

Filtering Mechanism Theory, Experimental Plan, and Analysis

Some of the deliverables provide code or procedures. These will be truncated for the purpose of demonstrating the goal of deliverables. Full code sets and results may be requested by contacting Jackson Stanley at jstanley1998@outlook.com or (781)-364-0570 or Benjamin Kraus at blk4805@gmail.com or (513) 504-6413.

3. Project Description

The University of Cincinnati senior design group researched open-space and readily available fusion reactor devices, such as those developed by Commonwealth Fusion Systems (CFS) and other fusion energy startups (General Atomics, et al.). In line with this, the group aimed to undertake a conceptual design project focused on a molten salt test loop. This test loop is designed to simulate the nuclear, thermo-fluid, and heat transfer properties of liquid salt, specifically for applications in heat transfer within a fusion device. The project, known as the UC Molten Salt Test Loop (UC-MSTL), documented anticipated engineering challenges, current and required empirical data, and preliminary results derived from heating, fluid flow, and neutronics calculations. Additionally, the team explored steady-state solutions for tritium capture and storage.

The goal of the MSTL is to utilize the high neutron flux environment to simulate critical aspects of fusion device operations including tritium breeding, heat transfer, thermo-hydraulic flow, and thermodynamic aspects of FLiBe. The test loop incorporates real and delayed nuclear data gathering techniques, FLiBe material sample mechanisms, and innovative byproduct removal subsystems in order to provide a basis for fusion device construction.

3.1. Project Scope

The project scope has been determined by the University of Cincinnati (UC) to be limited to a comprehensive conceptual design of a MSTL. The conceptual design limitation allows for equipment identification, layout, and small-scale experiments, but does not approach final material selection or mid-design status. The deliverables highlighted in this project plan are to be completed solely by the students specified on the project and subproject teams. It is important to highlight that the MSTL is not a product of CFS-UC affiliation. CFS personnel have agreed to support the senior student design project while remaining unaffiliated; there is no existing memorandum of understanding. In light of transparency, work scope may also be supported by advisors assigned to the project via the University of Cincinnati College of Engineering and Applied Science (UC-CEAS) per capstone requirements and guidelines. All external support from UC-CEAS staff will be documented in the project plan and each deliverable.

4. Engineering Standards and Codes

4.1. 10 CFR 30

4.1.1. Regulation

10 CFR 30: RULES OF GENERAL APPLICABILITY TO DOMESTIC LICENSING OF BYPRODUCT MATERIAL

4.1.2. Utility

“Prescribes rules applicable to all persons in the United States governing domestic licensing of byproduct material under the Atomic Energy Act of 1954, as amended (68 Stat. 919), and under title II of the Energy Reorganization Act of 1974 (88 Stat. 1242), and exemptions from the domestic licensing requirements permitted by Section 81 of the Act.”

4.1.3. Description

Applied to fusion industry, commercial fusion enterprises, particle accelerator facilities, etc. as enacted by the NRC in April 2022.

4.2. 49 CFR 173

4.2.1. Regulation

49 CFR 173: SHIPPERS—GENERAL REQUIREMENTS FOR SHIPMENTS AND PACKAGINGS

4.2.2. Utility

“This part includes definitions of hazardous materials for transportation purposes, requirements to be observed in preparing hazardous materials for shipment by air, highway, rail, or water, or any combination thereof; and inspection, testing, and retesting responsibilities for persons who retest, recondition, maintain, repair and rebuild containers used or intended for use in the transportation of hazardous materials.”

4.2.3. Description

Applied to the transportation of hazardous materials including activated waste products and byproducts.

4.3. 10 CFR 71

4.3.1. Regulation

10 CFR 71: PACKAGING AND TRANSPORTATION OF RADIOACTIVE MATERIAL

4.3.2. Utility

“This part establishes requirements for packaging, preparation for shipment, and transportation of licensed material, and procedures and standards for NRC approval of packaging and shipping procedures for fissile material and for a quantity of other licensed material in excess of a Type A quantity.”

4.3.3. Description

Applied to the proper packaging and storage of radioactive material including but not limited to transuranic waste, fissile material, and activated waste.

5. Constraints

5.1. Economic

No private funding has been identified for this project, and no memorandum of understanding exists between the MSTL project and any private organizations. A total of $400 was requested and approved by the UC College of Engineering and Applied Science department of Mechanical Engineering for this project to aide in the procurement of chemicals for the chemical engineering experiments to be performed to support filter development. In all, $376 of departmental funding was utilized for the project. The following table shows the breakdown of all costs on this project.

Table 1 – UC MSTL Cost Breakdown

	Description	Intended Use	Vendor	Quantity Purchased	Cost
DMF	N-Dymethylformamide ACS reagent, 500 mL, >99.8% CAS Number: 68-12-2 SKU: 319937-500ML	Used as a solvent for synthesizing NU-2100	Sigma Aldrich	500 mL	$132.00
$CuCl_2$	Copper (II) Chloride, 5 grams, anhydrous, powder, >99.995% trace metals basis, CAS #: 7447-39-4, SKU #: 451665-5G	Used as a reactant for synthesizing NU-2100	Sigma Aldrich	5 grams	$94.60
H_2BBTA	[CAS No. 7221-63-8] 1,5-Dihydrobenzo[1,2-d:4,5-d']bis([1,2,3]triazole) Cat. No.: A1154723, 100 mg	Used as a reactant for synthesizing NU-2100	Ambeed	100 mg	$99.00
$ZnCl_2$	Zinc Chloride anhydrous, 5 grams, powder, >99.995% trace metals basis, CAS Number: 7646-85-7, SKU: 429430-5G	Used as a reactant for synthesizing NU-2100	UC Department of Chemistry: Dr. Guan's Laboratory	1 gram	$0.00
SEM/EDS	Electron-based microscope capable of observing materials at a scale of micrometers. Only works for conductive materials	Used as a type of characterizing analysis; It is for observing NU-2100	Advanced Materials Characterization Center	1 hour	$50.00
				Total:	$375.60

5.2. Environmental

The MSTL prioritizes environmental integrity on a conceptual level. It Is important to note that this is a conceptual design, and no actual environmental impact will be created during this project. This project will, however, identify the potential hazards associated with the design, and limit them to comply with regulatory standards.

5.3. Sustainability

The MSTL embodies sustainability principles through its efficient energy utilization and minimal environmental footprint. By employing molten salt as a heat transfer medium, the system maximizes energy efficiency and contributes to the advancement of clean energy technologies. Its closed-loop design minimizes resource consumption and waste generation, promoting long-term sustainability. The conceptual model will intensely focus on disposability as it pertains to activated waste byproduct and treatment of the molten salt, as described through the System Design Description (SDD).

5.4. Manufacturability

The MSTL is a concept model and involves no physical construction other than that of the filtering and metal organic framework experiments. All concept designs will however focus on realistic construction techniques and will not rely upon advanced or otherwise hypothetical construction concepts.

5.5. Ethical

The MSTL is a concept model to aid in the engineering behind feasible fusion energy generation. Its ethical scope expands into the well-being of the next frontier of clean energy.

5.6. Health & Safety

The MSTL is a concept model to aid in the engineering behind feasible fusion energy generation and poses no physical health and safety concerns. All concept designs will however document conceptual health and safety hazards from MSTL construction and operation through the System Design Description (SDD).

5.7. Specifications

The MSTL is a concept model to aid in the engineering behind feasible fusion energy generation. No specifications for MSTL construction have been written. All drawings of the MSTL will be labeled “CONCEPT MODEL - NOT FOR CONSTRUCTION”.

6. Methodology

6.1. Team Members and Roles:

- Jackson Stanley (stanljn@mail.uc.edu): Project Leader, Nuclear Engineering Lead
  - Subsystems – FLiBe, Samples
- Austin Michael (michaeau@mail.uc.edu): Heat Transfer and Fluid Flow Lead
  - Subsystems – Pump System
- Benjamin Kraus (krausbl@mail.uc.edu): Impurity Removal and Material Lead
  - Subsystems - Filtering
- Logan Powers (powerslg@mail.uc.edu): Impurity Removal and Material Engineer
  - Subsystems – Filtering, Controls
- Sam Haga (hagass@mail.uc.edu): Drafter and Design Engineer
  - Subsystems – Support Equipment – Balance of Plant

6.2. Deliverables

Project meeting notes, breakdown of task status, and gantt chart can be found the end of this final report in the Master Doc (see final document table of contents).

Table 2 – UC-MSTL Project Deliverables

Deliverable	Status	Completion and Date	Work Delegation
Literature Review	Completed.	Completed November 13th 2023.	Whole team, separated by subsystems.
Functional Requirements Document (FRD)	Completed.	Completed December 11th 2023.	Whole team, separated by subsystems.
Rough Design (SolidWorks) of loop and System Design Description (SDD)	Completed.	Completed March 25th 2024.	Whole team, separated by subsystems.
Laboratory processes for gaseous byproduct removal and FLiBe chemical composition	Completed.	Completed April 11th, 2024	Ben Kraus, Logan Powers
Shielding calculations and OpenMC models using unstructured mesh for irradiation of FLiBe.	Completed.	Completed March 3rd 2024.	Jackson Stanley, Austin Michael

Complete conceptual design report of MSTL (report, standards and codes applicable for loop, and sub-system design)	Completed	Completed April 15th 2024.	Whole team, separated by subsystems

6.3. Deliverable Breakdown

6.3.1. Literature Review

The literature review will provide a logical starting point for the progression of the project. It will lay out what is known and what is required for task fulfillment. Sources will be collected to develop an understanding of subsystem background and usable project information. This start and end point will provide a general idea of what might be required to fill the gaps in information, enabling further document reviews to determine how to fill these informational gaps.

6.3.2. Functional Requirements Document (FRD)

The Functional Requirements Document (FRD) defines the scope of each subsystem and outlines the specifications and expectations for the conceptual heat transfer LiF-BeF_2 (FLiBe) salt test loop being developed by UC. The primary objective of this document is to provide a comprehensive understanding of the functional requirements that govern the design, development, and performance of the test loop. This is done by defining the high-level requirements and their justifications for each subsystem of the test loop.

6.3.3. Rough Design (SolidWorks) of loop and System Design Description (SDD)

The rough loop design will be used as the basis for the shielding calculations and OpenMC models to be completed later in the project. The loop design will also contribute to the final report, as it will define what codes, standards, power requirements, maintenance, etc. Although there are many examples of test FLiBe loops in research applications, many aspects of the loop design will be based on assumptions about the project or decisions that will need to be made upfront. Both will influence the system (shielding/production) downstream. The totality of these results will be documented in a conceptual System Design Description (SDD).

6.3.4. Laboratory processes for gaseous byproduct removal and FLiBe chemical composition

FLiBe salt is chosen as the test loop working fluid due to its history in fast reactor design and high tritium breeding ratio, but existing studies on removing radioactive decay products from its Li-6 interactions indicate no clear results. Thus, experiments will be performed on Metal-organic frameworks (MOFs) to enhance understanding of gaseous byproduct removal from FLiBe salt. Some MOFs are highly porous and capable of absorbing different target molecules. Various kinds of MOFs and substrates that can both capture and contain different amounts of Tritium and Helium will be explored through

experimentation. Filter material composition will be greatly scrutinized to determine its maximum activity and its byproduct activation for disposal.

6.3.5. Shielding calculations, Neutron Activation Analysis, and OpenMC Workflow Using CSG Geometry for Irradiation of FLiBe

A major component of the conceptual design being developed for the UC-MSTL is neutronics modeling and subsequent data processing. Neutronics analysis will provide much needed preliminary information on the irradiation of molten salts, tritium breeding ratios, distances for effective irradiation, and preliminary images of local heating. The neutronics portion of the conceptual design will be conducted with OpenMC 0.12.1, and will involve raw data outputs, imaging of select tally results, and verification of neutronic hand calculations.

6.3.6. Complete conceptual Design Report of UC-MSTL (report, standards and codes applicable for loop, and sub-system design)

A final report will be generated for completion of the senior capstone graduation requirements and the documentation of results to be provided to the University of Cincinnati and industry supporters. The report will likely be hundreds of pages long and incorporate all aspects of the project. A high-level overview section will break down the report into project management segments or results segments, such that the work reflects the utility of results separately to industry versus academic readers.

Literature Review

University of Cincinnati Molten Salt Test Loop
UC-MSTL

University of Cincinnati
BSME Class of 2024

THIS PAGE PURPOSELY BLANK

1. Introduction

1.1. Purpose of Document

The purpose of this literature review is to critically examine existing research and developments in the field of molten salt test loops to aid in the development of the conceptual heat transfer LiF-BeF_2 (FLiBe) salt test loop being developed by private fusion energy companies such as Commonwealth Fusion Systems, General Atomics, et al. The review will focus on identifying gaps in current research, evaluating the methodologies employed in previous studies, and extracting valuable insights that can inform future developments in the field.

The document is composed of one high level section and five research sections. The high-level section is the executive summary. The executive summary is a brief overview of the findings documented in the subsequent sections and their significance in the development of the conceptual system. Each paper referenced in the executive summary utilizes the paper's title, for ease of access. The five research sections are general fusion materials, sensing, previous molten salt loops, FLiBe salt, and filtering. Each section uses the same standardized table to document the findings of the paper of interest.

1.2. Document Scope

The scope of this literature review encompasses a thorough examination of research and developments related to molten salt test loops, including but not limited to, thermophysical properties, heat transfer mechanisms, material compatibility, experimental methodologies, chemical composition, and radiation damage.

1.3. Background

The University of Cincinnati senior design group is conducting research into the open space and readily available fusion reactor devices such as those being produced by Commonwealth Fusion Systems (CFS) and other Fusion energy start-ups (General Atomics, et. al). As such, the group would like to complete a conceptual design on a molten salt test loop, which simulates the nuclear, thermo-fluid, and heat transfer properties of liquid salt for the purposes of heat transfer in a fusion device. The concept under development is the Molten Salt Test Loop (MSTL). The ultimate goal of the conceptual design is to document expected engineering challenges, current and needed empirical data, and preliminary results from heating, fluid flow, and neutronics calculations. This is to be completed by senior mechanical engineering students of the class of 2024 to satisfy graduation requirements per a capstone project.

1.4. Scope

1.4.1. Users

Users of this Functional Requirement Document include but are not limited to future system designers and engineers, project managers, stakeholders, and regulatory bodies, such as the Department of Energy (DOE) and Nuclear Regulatory Commission (NRC).

1.4.2. Need

The literature review will provide essential research in order to validate the operational assumptions for fusion powerplants. Previously published results and data provide a basis for the conceptual loop functional requirements, subsequent fusion device manufacturing, and plasma physics research.

2. Executive Summary

2.1. Summary Introduction

In an era where fusion energy solutions are paramount, the exploration and optimization of molten salt test loops stand at the forefront of technological innovation. Their significance is tied to the complex matter in which heat is transferred from a fusion device to a usable power production cycle. This executive summary provides a concise overview of the comprehensive literature review focused on molten salt test loops- a pivotal component in the development of advanced nuclear reactors. By synthesizing a wealth of research and developments, this review delves into the thermophysical properties, heat transfer mechanisms, materials compatibility, experimental methodologies, challenges, and opportunities within the domain. With a diverse audience in mind, ranging from researchers and engineers to policymakers and investors, this summary highlights the significance of the literature review in advancing our understanding of current molten salt research and previous loop designs. The insights presented herein aim to guide future research, shape technological advancements, and contribute to the development of functional requirements for a conceptual salt test loop design.

2.2. General Fusion Materials

A major concern of salt-fusion material interactions is corrosion. Corrosion control could involve passivation techniques, coatings, or the addition of specific materials to manage the corrosion of structural components in the presence of fluoride salts- with less emphasis on the base material of the loop (Was).

However, the loop base material is still a significant contributor to total activation and disposal protocols. Elements which provide activation concerns include Fe, Cr, Mo, W, V, Nb, and Ta. Another concern is that of helium embrittlement. The instance of He embrittlement of steels could become an issue on timescales similar to the required lifetimes (5-10 years) of components in fusion reactors. More complex models to characterize this should utilize migration barriers and grain size, (Gilbert, “Neutron Induced”).

Further analysis of helium embrittlement, gas production, and transmutation provides guidance on material selection in fusion devices. Even at low concentrations, gas particles can have severe life altering consequences for materials, with He being a particular problem because of: low solubility in the crystal lattice, cluster accumulation, dislocations at the grain boundary, and swelling/embrittlement. Pure tungsten (in plasma facing componentry or as a component to stainless steel alloys) should be avoided in the divertor region, as self-shielding can have impact on the population of low energy neutrons in the blanket which contribute significantly to tritium breeding, (Gilbert, “An Integrated”).

Although neutron irradiation is of major concern, ionizing irradiation, in particular protons generated via (n,p) reactions, were also investigated. Research has showed that proton irradiation decelerated intergranular corrosion in Ni-20Cr alloys in molten salt. The research proposed that the presence of radiation-generated interstitials enhanced the transport of alloy constituents to the grain boundaries, thus slowing down corrosion (Zhou).

2.3. Sensing

Sensing of transmutation byproducts and localized neutron irradiation requires compact measurement techniques. An example of this was the analysis of silicon sensors in neutron environments. Mature silicon sensors could prove appropriate as transmission detectors or in applications where high spatial resolution and high time resolution are necessary. However, a low detection efficiency (typically < 5%) remains a shortcoming.

Significant advancements in real time-neutron detection have been made in the past few years. These advancements include electron-tracking based gamma-ray reconstruction and 3D volumetric or scene-fusion gamma-ray imaging in large-scale detection systems (Vetter). These sensing techniques will be imperative to validate loop characteristics.

Existing neutronic measurement technologies include carbon-based scintillators, which have the ability to measure real-time flux. These scintillators are, in particular, accurate given their ability to relate the chemistry of scintillator to sensitivity between neutron and gamma ray measurements- allowing to shift focus between measurements of non-ionizing and ionizing particles (Vetter). Carbon based scintillators will most certainly be involved in the loop design.

2.4. Previous Loop Examples

Previous examples of loops have documented the conceptual design stage. A molten salt test loop was designed, built, and commissioned to advance the technical readiness level of molten salt components and instruments in the NEXT Lab on the Abeline Christian University (ACU) campus in Abeline, TX. The Molten Salt Test Loop (MSTL), developed high level requirements for this system which include the ability to store, melt, and circulate salt, use materials readily available and capable of ensuring safe operations, minimize hazards of all types, provide test opportunities for instruments, components, and controls, and utilize a previously procured pump and heating system. The advances in molten salt components and instruments made possible by the MSTL have informed plans for future gas-tight, high-temperature salt systems and paved the way for commercial applications of molten salts, including advanced reactors. Findings through this experiment will dictate future research, especially around salt effects on loop qualities. A more corrosive or hazardous salt will need to be loaded into the system as a liquid transferred without contact with the air to minimize risk to people and reduce opportunities for ingress of water and oxygen into the system (Head).

Another example of a test loop was conducted by the Texas A&M University Thermal-Hydraulic Research Laboratory in College Station, TX. The experimental test facility has been utilized to characterize the thermal–hydraulic behavior of typical molten salts under steady-state and transient, forced flow conditions, by employing innovative measurement methods to improve measurements which are needed for a permanent molten salt application in reactors. Applications

of OFDTS (Optical Fiber Distributed Temperature Sensors) in forced convection molten salt environments present more challenges, and are subsequently not yet fully explored, as documented by Texas A&M (Arora).

2.5. FLiBe Salt

FLiBe salt has been studied for applications in the nuclear industry since the early 1950's. One of the most comprehensive studies on the effectiveness of using FLiBe in fusion energy applications was conducted by Dr. Charles Forsberg at the MIT-PSFC. In this 2019 study, several parameters in the application of FLiBe salts were explored, including the characteristics of FLiBe salts, the status of the technology, the options for tritium capture and control in the salt, heat exchangers, secondary heat transfer loops, and the coupling to power cycles with heat storage. Expert opinion includes that FLiBe shall be constantly moving, and stagnation limited. Formation of vortexes in the FLiBe could cause relatively stationary fluid flow, which could cause rapid local heating to the boiling point and large variations of FLiBe being tested. To measure these parameters, infrared imaging can detect hotspots associated with the first wall through the FLiBe. Cherenkov radiation imaging diagnostics from neutron interactions with FLiBe salt may enable direct measurement of fusion power, both of which are imperative to loop design. After powering down, a significant gamma radiation field will be produced from the FLiBe salt flowing outside the reactor and a small amount of decay heat for weeks after shutdown due to the activated byproducts of the FLiBe salt (Forsberg). This will have to be accounted for in the post-operational timeline of the loop.

Other studies focused on byproducts produced via the irradiation of FLiBe salt. One study addresses the issue of controlling hydrogen fluoride (HF) in molten FLiBe ($2LiF \cdot BeF_2$) used as a cooling and tritium breeding medium in fusion reactors. The study focused on the effectiveness of beryllium (Be) as a redox control agent to prevent HF and free fluorine ions from reacting with structural materials. As concluded by the study, beryllium acts as a redox control agent in the presence of HF. It undergoes a redox reaction where it reacts with HF, converting it into less corrosive compounds. Controlling HF concentration through beryllium redox reactions enhances the safety of the fusion reactor, reducing the risk of corrosion-related issues and potential leaks of HF, which can be hazardous to both the system and personnel (Smolik).

Corrosion of structural material by FLiBe salt interactions still remains one of the largest engineering challenges. One study aimed to address the challenges associated with structural materials in various nuclear reactors, including molten salt reactors and fusion reactors. It investigates the corrosion, radiation damage, and high-temperature embrittlement issues in these systems, and discusses potential materials and strategies to mitigate these problems. It was concluded that there exists a preferential dissolution of chromium over iron and nickel when exposed to fluoride salts. Thus, the use of additives and coatings will aid in the control of fluorine potential in salt systems. Identification of advanced materials like ODS steels and high-nickel alloys for improved performance in nuclear environments were also discussed (Was). Base material types will be guided by this research.

2.6. Filtering

Filtering byproducts of FLiBe irradiation, particularly tritium and helium, will be essential to quantifying the effectiveness of a conceptual loop. One material of interest is ceramics, which have been utilized in particulate filtering studies conducted in diesel and gasoline applications. Studies have focused on the optimization of cell wall thickness and cell wall density in ceramic honeycomb filters and hydrocarbon particulate filtration in gasoline and diesel emissions (Bardhan).

Other studies have focused on polysulfone membrane filters. Polysulfone filters show promise, given the temperatures at which tritium and helium gas will be produced from FLiBe irradiation. Aerosol and gas penetration rates through PSF membrane filters were studied, with optimal pore sizes in PSF membrane filters to maximize flow rate. Results found that aerosol penetration decreased with a decrease in porosity and aerosol penetration increases when flow rate increases (Huang).

Advanced materials of consideration include metal organic frameworks (MOFs). MOFs operate via the activation of pore sites by binding metal receptors to organic ligands. Previously, MOFs have been used to filter organic contaminants and micro-level particulates from industrial processes in waterways (Akeremale). Given their novelty, MOFs have not been studied as in depth as other filter technologies. However, their applications in helium capture have been shown to be promising in preliminary studies. In one study, the MOFs GYPCUQ01, HUTZAX01, and PEHBIO showed helium selectivity as well as high helium permeability. In addition, MOF membranes were predicted to have a higher helium permeability than polymeric and zeolite membranes, (Kadioglu). Realistically, the conceptual design of the test loop will invoke many of these material types.

Other studies have focused on the application of tritium capture. A tritium-adsorbing MOF called VSB-5 (a nickel phosphate based nanoporous MOF) shoes promise given VSB-5 has one of the highest measured initial heats of adsorption, showing 1.5 kJ/mol more selectivity for Deuterium than Hydrogen. This is believed to be one of the highest measured initial D2/H2 selectivity in any material at a temp above 120 K, (Sharma).

Tritium capture through water has also been studied. In fission applications, safe methods for tritium removal from heavy water moderators is necessary since other methods cause possible hydrogen explosions. Engineered MOFs show promise in creating detritiation systems for heavy water reactors, (Fu).

THIS PAGE PURPOSELY BLANK

3. Literature Review

3.1. General Fusion Materials

Research Article (Provide proper Reference and Title of published article)	Materials for future nuclear energy systems https://www.sciencedirect.com/science/article/pii/S0022311519312334?via%3Dihub Was, B.S., et al. "Materials for Future Nuclear Energy Systems." Journal of Nuclear Materials, Volume 527, 2019, https://doi.org/10.1016/j.jnucmat.2019.151837.
Problems Addressed / Identified	Need for advanced structural materials and fuels for future nuclear energy systems Challenges related to higher temperatures, radiation damage, and severe chemical environments Specific issues: corrosion, tritium control, fission product removal, and radiation effects Significance of materials' performance in advanced reactor concepts with extended lifetimes
Aim & Objectives of article	To review material requirements for advanced nuclear reactors Identify promising options for structural materials and fuels Address specific problems, such as corrosion and radiation effects Contribute to the realization of advanced reactor concepts
Novelty/Rationale and Significance: Why was the research was worth undertaking?	Development of materials to withstand harsh operating conditions Facilitation of advanced reactor concepts with extended lifetimes Potential solutions for problems in advanced reactor systems Enhanced safety and efficiency in future nuclear energy systems
Limitations and Weaknesses What limitations were encountered when performing the experiment for the article, if any mentioned?	Lack of specific experimental data and results in the article The focus on requirements and potential materials rather than testing Specific limitations of materials or concepts not addressed Emphasis on review rather than primary research
Implementation Details/Experimental Setup Dataset [Ref],No of Attributes,, Environment/Tool and	The article was focused on discussion and meta-analysis of other research articles as well as application of known knowledge bases within the field.

Technique, Compared and validated with Techniques [Name and parameters compared]	
Findings and Conclusions	The article provides findings related to tritium extraction methods from the hot flowing fluid within the fusion reactor. Corrosion control could involve passivation techniques, coatings, or the addition of specific materials to manage the corrosion of structural components in the presence of fluoride salts. A list of materials that could work in a molten salt environment are listed and potential risks, such as grain boundary helium embrittlement are discussed.
Areas of improvement/ Future Direction	In-depth studies on material performance under various conditions Potential improvements and innovations in materials Detailed investigations into the longevity of materials in advanced nuclear reactor

Research Article (Provide proper Reference and Title of published article)	Neutron-induced dpa, transmutations, gas production, and helium embrittlement of fusion materials Gilbert, M.R., et al. "Neutron-Induced DPA, Transmutations, Gas Production, and Helium Embrittlement of Fusion Materials." Journal of Nuclear Materials, Volume 442, Issues 1-3, Supplement 1, 2013, https://doi.org/10.1016/j.jnucmat.2013.03.085.
Problems Addressed / Identified	Gaps in research understood by DEMO simulations with neutron transport and helium production. He = f(n,p) He production has a threshold of 3.7 MeV Elements of concern: - Fe - Cr - Mo - W - V - Nb - Ta The issue of He embrittlement of GBs could become an issue on timescales similar to the required lifetimes (5-10 years) of components in fusion reactors. -Concentrations in range of 400 appm are known to cause a change in fracture behavior of neutron irradiated steels.
Aim & Objectives of article	Fill holes existing in DEMO experiment results.
Novelty/Rationale and Significance: Why was the research was worth undertaking?	Materials modeling for fusion reactors is becoming more pertinent in the future.
Limitations and Weaknesses What is not understood?	More complex models should utilize migration barriers and grain size. DPA cannot be trusted as a sole contributor to material defections- further complex models should take into account higher flux values without DPA directly introduced.

What limitations were encountered when performing the experiment for the article, if any mentioned?	
Implementation Details/Experimental Setup Dataset [Ref],No of Attributes,, Environment/Tool and Technique, Compared and validated with Techniques [Name and parameters compared]	N/A
Findings and Conclusions	A more sophisticated DEMO model shows that helium induced dpa will be a concern for fusion reactor materials within a 5–10-year period of usage.
Areas of improvement/ Future Direction	More complex models that do not homogenize/discount macroscopic material details.

Research Article (Provide proper Reference and Title of published article)	An integrated model for materials in a fusion power plant: transmutation, gas production, and helium embrittlement under neutron irradiation. Gilbert, M.R., et al. "An Integrated Model for Materials in a Fusion Power Plant: Transmutation, Gas Production, and Helium Embrittlement under Neutron Irradiation." Nuclear Fusion, 52 083019, 2012, https://iopscience.iop.org/article/10.1088/0029-5515/52/8/083019.
Problems Addressed / Identified	- Even at low concentrations, gas particles can have severe life altering consequences for materials, with He being a particular problem because of: Low solubility in the crystal lattice, cluster accumulation, dislocations at the grain boundary, and swelling/embrittlement. - Pure tungsten (in plasma facing componentry or as a component to s.s. allow) should be avoided in the divertor region, as self-shielding can have impact on the population of low energy neutrons in the blanket which contribute significantly to tritium breeding. - Beryllium is a significant contributor to helium production and is known to swell significantly under neutron irradiation. -
Aim & Objectives of article	Broaden the existing base of knowledge surrounding neutron irradiation of materials in future built fusion power plants.
Novelty/Rationale and Significance: Why was the research was worth undertaking?	More complete and realistic models help validate assumptions in the fusion powerplant building industry.
Limitations and Weaknesses What is not understood?	Experimental testing of materials in a fully realistic fusion neutron-irradiation powerplant environment in not feasible.

What limitations were encountered when performing the experiment for the article, if any mentioned?	
Implementation Details/Experimental Setup Dataset [Ref],No of Attributes,, Environment/Tool and Technique, Compared and validated with Techniques [Name and parameters compared]	N/A
Findings and Conclusions	An expansion of materials analysis provides more realistic depictions of neutron-induced embrittlement.
Areas of improvement/ Future Direction	Full-fledged designs of cycle calculations for neutron embrittlement.

Research Article (Provide proper Reference and Title of published article)	Proton irradiation-decelerated intergranular corrosion of Ni-Cr alloys in molten salt Zhou, W., Yang, Y., Zheng, G. et al. “Proton irradiation-decelerated intergranular corrosion of Ni-Cr alloys in molten salt”. Nat Commun 11, 3430 (2020). https://doi.org/10.1038/s41467-020-17244-y
Problems Addressed / Identified	The paper addresses the impact of ionizing radiation, specifically proton irradiation, on the corrosion of Ni-Cr alloys in molten fluoride salt at high temperatures. It challenges the common understanding that radiation damage usually accelerates corrosion and explores the unique effects of radiation in this specific environment.
Aim & Objectives of article	The primary aim of the article is to investigate and understand the effects of proton irradiation on intergranular corrosion of Ni-Cr alloys in molten fluoride salt at 650°C. The article seeks to determine whether proton irradiation can decelerate the corrosion process, which goes against the usual assumption that radiation accelerates corrosion.
Novelty/Rationale and Significance: Why was the research was worth undertaking?	The research is significant because it challenges the conventional view that radiation damage typically accelerates corrosion. The findings have implications for the development of advanced reactors, where high temperatures, corrosive coolants, and intense particle fluxes are common challenges. If radiation can decelerate corrosion, it can lead to the development of more corrosion-resistant materials for advanced nuclear reactors.
Limitations and Weaknesses What limitations were encountered when performing the experiment for the article, if any mentioned?	While the research provides valuable insights into the interplay between proton irradiation and corrosion in Ni-Cr alloys, it primarily focuses on one specific type of irradiation (proton) and one specific alloy (Ni-Cr). The findings might not be directly transferable to other materials and environments.

	More research would be needed to generalize the results.
Implementation Details/Experimental Setup Dataset [Ref],No of Attributes,, Environment/Tool and Technique, Compared and validated with Techniques [Name and parameters compared]	Thin foil samples of Ni-20Cr were exposed to proton irradiation and molten salt at 650°C. The central region of each sample was exposed to both protons and salt, while the outer region was exposed only to salt. The researchers used a simultaneous irradiation/corrosion facility to conduct the experiments. They quantified the corrosion depth, analyzed the salt-facing side of the foils with scanning electron microscopy (SEM), and prepared TEM specimens for transmission electron microscopy (TEM) analysis.
Findings and Conclusions	The research showed that proton irradiation decelerated intergranular corrosion in Ni-20Cr alloys in molten salt. In the irradiated region, salt penetration and corrosion were significantly reduced compared to the unirradiated region. Cross-sectional analysis revealed that the depth of corrosion-induced voids was much shallower in the irradiated region, indicating the deceleration of corrosion. The research proposed a mechanism for radiation-decelerated corrosion, suggesting that radiation-enhanced bulk diffusion played a crucial role in inhibiting void formation along grain boundaries. The presence of radiation-generated interstitials enhanced the transport of alloy constituents to the grain boundaries, thus slowing down corrosion.
Areas of improvement/ Future Direction	Additional alloys tested to determine generalized attributes that can be used to validate anti-corrosion materials or determine other similar materials. Testing of additional radiation types to understand what material properties best react (or in this case, reduce reactivity).

3.2. Sensing

Research Article (Provide proper Reference and Title of published article)	Characterization of boron-coated silicon sensors for thermal neutron detection Mehendale, Shruti, et al. “Characterization of Boron-Coated Silicon Sensors for Thermal Neutron Detection.” Nuclear Instruments and Methods in Physics Research, Section A, Volume 972, 2020, https://doi.org/10.1016/j.nima.2020.164124.
Problems Addressed / Identified	
Aim & Objectives of article	Study of thermal neutron capture by silicon diodes coated with boron carbide
Novelty/Rationale and Significance: Why was the research was worth undertaking?	
Limitations and Weaknesses What limitations were encountered when performing the experiment for the article, if any mentioned?	Applications are for neutron imaging and nuclear security applications. - No data on fast neutron environments, max eV in results is one order of magnitude less than eV in ARC
Implementation Details/Experimental Setup Dataset [Ref],No of Attributes,, Environment/Tool and Technique, Compared and validated with Techniques [Name and parameters compared]	
Findings and Conclusions	- mature silicon sensors could prove appropriate as transmission detectors or in applications where high spatial resolution and high time resolution are necessary. However, a low detection efficiency (typically < 5%) remains a shortcoming
Areas of improvement/ Future Direction	

Research Article (Provide proper Reference and Title of published article)	Multi-sensor radiation detection, imaging, and fusion Kai Vetter, Department of Nuclear Engineering, University of California, Berkeley; Nuclear Science Division, Lawrence Berkeley National Laboratory Vetter, Kai. "Multi-Sensor Radiation Detection, Imaging, and Fusion." Nuclear Instruments and Methods in Physics Research, Section A, Volume 805, Pages 127-134, 2016, https://doi.org/10.1016/j.nima.2015.08.078.
Problems Addressed / Identified	recent highlights in research and outreach: - electron-tracking based gamma-ray reconstruction - 3D volumetric or scene-fusion gamma-ray imaging - large-scale detection systems - Berkeley Radwatch program which led to the recent establishment of the Institute for Resilient Communities
Aim & Objectives of article	Provide insight on advancements in radiation technology research
Novelty/Rationale and Significance: Why was the research was worth undertaking?	UC Berkeley and Lawrence National Laboratory
Limitations and Weaknesses What limitations were encountered when performing the experiment for the article, if any mentioned?	Focus more on gamma rays and less conclusions on neutrons
Implementation Details/Experimental Setup Dataset [Ref],No of Attributes,, Environment/Tool and Technique, Compared and validated with Techniques	Radiological Multisensor Acquisition Platform (RadMAP) contains arrays of HPGe, NaI(Tl), and liquid scintillator detectors that enable standoff detection of gamma rays and neutrons - Systematic mapping of radiation backgrounds - "development of the Nuclear Street View [17]. A systematic mapping of

[Name and parameters compared]	radiation backgrounds in a range of environments with their temporally and temporary variations is important in order to evaluate and develop improved detection concepts.”
Findings and Conclusions	- HPGe detectors provide excellent spectroscopic detection capabilities -
Areas of improvement/ Future Direction	

Research Article (Provide proper Reference and Title of published article)	Scintillation Counter for Detecting Fast Neutrons Harding, G.N.. “A Scintillation Counter for Detecting Fast Neutrons.” Nature 167, 437, 1951. https://www.nature.com/articles/167437a0#citeas.
Problems Addressed / Identified	Relates chemistry of scintillator to sensitivity between neutron and gamma ray measurements
Aim & Objectives of article	Provide a scintillator chemistry for measuring fast neutrons
Novelty/Rationale and Significance: Why was the research was worth undertaking?	
Limitations and Weaknesses What limitations were encountered when performing the experiment for the article, if any mentioned?	May be lacking newer technology – written in 1951
Implementation Details/Experimental Setup Dataset [Ref],No of Attributes,, Environment/Tool and Technique, Compared and validated with Techniques [Name and parameters compared]	
Findings and Conclusions	- Using anthracene, the ratio of the number of neutron counts to the number of y-counts has a maximum value of 2.2 - The number of 2·5-MeV. neutrons counted would then be 0·8 per cent of those falling on a detector 2 cm. thick
Areas of improvement/ Future Direction	Increasing energy of fast neutrons

3.3. Previous Molten Salt Loops

Research Article (Provide proper Reference and Title of published article)	A molten salt test loop for component and instrumentation testing Head, T.L., et al. "A Molten Salt Test Loop for Component and Instrumentation Testing." Annals of Nuclear Energy, Volume 186, 109772, 2023, https://doi.org/10.1016/j.anucene.2023.109772.
Problems Addressed / Identified	High level requirements to consider: - Store, melt, and circulate salt - Use materials readily available and capable of ensuring safe operations - Minimize hazards of all types - Provide test opportunities for instruments, components, and controls. - Utilize previously procured pump and heating system. Specific requirements to SPARC: - The working salt will be a eutectic mixture of FLiBe - The system will hold at least xx L of liquid salt. - The system will be able to operate up to xx °C. - The system will be constructed from xx. - The system will be capable of flow rates from xx L/min. - The system will have a nitrogen cover gas system. - The system will provide means of salt and cover gas sampling.

	- The system will be remotely operated and monitored. - The system will be equipped with instrumentation beyond the minimum control requirements. - ingress of air into the system will cause corrosion. - The major leak points identified in this system are the pump-shaft seal and the pump mounting flange seal.
Aim & Objectives of article	Development of concept and outline for molten salt test loop for msr smr's.
Novelty/Rationale and Significance: Why was the research was worth undertaking?	Molten salt reactors are making a comeback, and will require significant advancements in salt technologies.
Limitations and Weaknesses What is not understood? What limitations were encountered when performing the experiment for the article, if any mentioned?	Applications using fluoride salts or radioactive materials should utilize gas spaces with slightly negative pressures with respect to atmosphere so that harmful materials do not leave the system- the full effect of which is no yet fully understood. Usage of a different type of shaft seal will be required for systems containing more highly corrosive salts. A more corrosive or hazardous salt will need to be loaded into the system as a liquid transferred without contact with the air to minimize risk to people and reduce opportunities for ingress of water and oxygen into the system.
Implementation Details/Experimental Setup Dataset [Ref],No of Attributes,, Environment/Tool and	

Technique, Compared and validated with Techniques [Name and parameters compared]	
Findings and Conclusions	A molten salt test loop was designed, built, and commissioned to advance the technical readiness level of molten salt components and instruments in the NEXT Lab on the ACU campus.
Areas of improvement/ Future Direction	The advances in molten salt components and instruments made possible by the MSTL have informed plans for future gas-tight, high-temperature salt systems and paved the way for commercial applications of molten salts, including advanced reactors.

Research Article (Provide proper Reference and Title of published article)	Advanced flow and temperature measurements in a forced convection molten salt test loop Arora, Ojasvin, et al. “Advanced Flow and Temperature Measurements in a Forced Convection Molten Salt Test Loop.” Annals of Nuclear Energy, Volume 159, 108269, 2021, https://doi.org/10.1016/j.anucene.2021.108269.
Problems Addressed / Identified	- forced convection, closed loop able to operate under high temperature (up to 700 C). - The test loop consists of five major segments, or legs. Instrumentation is installed at specific locations within the loop and the tank to measure major system-level thermal–hydraulic parameters, including flow rate through the test loop, fluid and pipe wall temperatures, system pressure, and pressure drop across the loop. The two electric heaters surrounding the sump tank are used to achieve and maintain the desired fluid operating temperature during the tests. Tracer heaters are installed along each section of the test loop to control their temperature and compensate for heat losses. Components of the system in direct contact with the liquid salt (including test loop, pump components and sump tank) are made out of stainless steel Type 316L and are thermally insulated. Operations of the facility, including test preparation, execution, and termination, are automatized and controlled through a programmable logic control (PLC) system interfaced with a data acquisition system (DAQ).
Aim & Objectives of article	Create accurate method for measuring fluid flow and heat distribution parameters in molten salt reactor design.
Novelty/Rationale and Significance:	An experimental test facility has been utilized to characterize the thermal–hydraulic behavior

Why was the research was worth undertaking?	of typical molten salts under steady-state and transient, forced flow conditions, by employing innovative measurement methods to improve measurements which are needed for a permanent molten salt application in smr msrs.
Limitations and Weaknesses What is not understood? What limitations were encountered when performing the experiment for the article, if any mentioned?	Applications of OFDTS (optical fiber distributed temperature sensors) in forced convection molten salt environments present more challenges, and are subsequently not yet fully explored.
Implementation Details/Experimental Setup Dataset [Ref],No of Attributes,, Environment/Tool and Technique, Compared and validated with Techniques [Name and parameters compared]	N/A
Findings and Conclusions	Advanced OFDTS were successfully installed and utilized in combination with conventional K-type thermocouples to study the thermal–hydraulic behavior of the salt by reconstructing two-dimensional temperature fields within the test loop under transient and steady state conditions.
Areas of improvement/ Future Direction	The experimental data produced can support the validation of system-level and computational fluid dynamics (CFD) codes.

3.4. FLiBe Salt

Research Article (Provide proper Reference and Title of published article)	Fusion Blankets and Fluoride-Salt-Cooled HighTemperature Reactors with Flibe Salt Coolant: Common Challenges, Tritium Control, and Opportunities for Synergistic Development Strategies Between Fission, Fusion, and Solar Salt Technologies Charles Forsberg, Guiqiu (Tony) Zheng, Ronald G. Ballinger & Stephen T. Lam Forsberg, Charles, et al. "Fusion Blankets and Fluoride-Salt-Cooled High-Temperature Reactors with Flibe Salt Coolant: Common Challenges, Tritium Control, and Opportunities for Synergistic Development Strategies Between Fission, Fusion, and Solar Salt Technologies." Nuclear Technology, Volume 206, Issue 11, 2020, https://doi.org/10.1080/00295450.2019.1691400.
Problems Addressed / Identified	(1) the characteristics of flibe salts (2) the status of the technology (3) the options for tritium capture and control in the salt, heat exchangers, and secondary heat transfer loops (4) the coupling to power cycles with heat storage - FLiBe shall be constantly moving and stagnation limited. Formation of vortexes in the FLiBe could cause relatively stationary fluid, which could cause rapid local heating ti the boiling point and large variations of FLiBe being tested. - Infrared imaging can detect hotspots associated with the first wall through the flibe. Cherenkov radiation imaging diagnostics from neutron interations with flibe salt may enable direct measurement of fusion power. -The metals of the test loop shall be noble relative to the salt. - Isotopically enriched lithium with 90% Li-6 is used to maximize tritium production. -Part of the blanket structure (FLiBe blanket test concept) includes a diverter that acts as a drain

	to remove high-energy plasma from the system that contains deuterium, tritium, and helium reaction product. This localized area sees much higher heating loads from the plasma but much lower neutron fluxes. -A significant gamma radiation field will be produced from the FLiBe salt flowing outside the reactor and a small amount of decay heat for weeks after shutdown. -The primary limit of any tritium removal from a flibe system is the time it takes the tritium molecules to diffuse from the bulk salt to some surface for removal of tritium. -To prevent corrosion, a reducing agent is required- beryllium shall be introduced. - Figure 8 displays tritium separation technique. -Must decide on gas sparging, vacuum disengager, or permeation (or some combination) to separate gas byproducts from salt initially.
Aim & Objectives of article	Provide high level, conceptual level to the development of FLiBe as a heat transfer fluid and tritium breeding material.
Novelty/Rationale and Significance: Why was the research was worth undertaking?	There is significant advancement in the development of fusion energy. The heat transfer side of this problem has yet to be developed.
Limitations and Weaknesses What is not understood? What limitations were encountered when performing the experiment for the article, if any mentioned?	-The test loop – unlike the arc concept – will be outside the magnetic field of the reactor, but will be in the gauss lines of a significant magnetic field. These will greatly effect the thermal hydraulics via mechanisms such as suppression of turbulence. What is this field strength? - Missing property data includes measurement of radiative heat transfer, and other optical properties as a function of temperature, frequency, and impurity levels. -It is not clear what the online impurity requirements will be for FLiBe.

Implementation Details/Experimental Setup Dataset [Ref],No of Attributes,, Environment/Tool and Technique, Compared and validated with Techniques [Name and parameters compared]	N/A
Findings and Conclusions	Several unknowns currently exist in the development of the ARC FLiBe heat transfer system.
Areas of improvement/ Future Direction	Improvements to nuclear data, corrosion data, and fluid flow are ambiguous currently.

Research Article (Provide proper Reference and Title of published article)	Beryllium Interactions In Molten FliBe https://inldigitallibrary.inl.gov/sites/sti/sti/3303772.pdf Smolik, G.R., et al. "Beryllium Interactions in Molten Flibe." Idaho National Laboratories, INL/CON-05-00927, 2026, https://inldigitallibrary.inl.gov/sites/sti/sti/3303772.pdf.
Problems Addressed / Identified	The paper addresses the issue of controlling hydrogen fluoride (HF) in molten Flibe (2LiF·BeF2) used as a cooling and tritium breeding medium in fusion reactors. It focuses on the effectiveness of beryllium (Be) as a redox control agent to prevent HF and free fluorine ions from reacting with structural materials.
Aim & Objectives of article	The objective is to study the extent and rate of beryllium solubility in molten Flibe during pot-design experiments conducted to suppress continuously supplied HF gas. The paper aims to explore the mechanisms of Be uptake into the Flibe, especially considering the influence of galvanic effects and how Be is partitioned between the salt and container materials.
Novelty/Rationale and Significance: Why was the research was worth undertaking?	The research is motivated by the need to control HF in fusion reactors, where the production of tritium is higher than in earlier applications. If beryllium can effectively control HF in Flibe, it has significant implications for the safety and materials compatibility in future fusion power plants.
Limitations and Weaknesses What limitations were encountered when performing the experiment for the article, if any mentioned?	Uncertainties exist regarding the mechanism of Be uptake into Flibe during experiments. The paper notes that the findings from small-scale crucible tests have limitations in measuring Be solubility limits in Flibe. The extrapolation of behavior from small crucibles to larger pot tests with HF purging is considered precarious.
Implementation Details/Experimental Setup Dataset [Ref],No of Attributes,, Environment/Tool and Technique, Compared and validated with Techniques	Various types of tests were conducted in an inert gas glove box, involving the immersion of Be samples in molten Flibe. Some tests used galvanic coupling with nickel, while others involved electrically insulated Be samples. Samples of salt were removed for analysis, and several analytical methods were used, including scanning electron microscopy (SEM), Auger electron

[Name and parameters compared]	spectroscopy (AES), and X-ray photoelectron spectroscopy (XPS).
Findings and Conclusions	Beryllium acts as a redox control agent in the presence of HF. It undergoes a redox reaction where it reacts with HF, converting it into less corrosive compounds. Beryllium reacts with HF to form beryllium fluoride (BeF2). BeF2 is less corrosive than HF and, therefore, reduces the overall HF concentration in the molten Flibe. Controlling HF concentration through beryllium redox reactions enhances the safety of the fusion reactor, reducing the risk of corrosion-related issues and potential leaks of HF, which can be hazardous to both the system and personnel. Since HF is a precursor to tritium formation, beryllium's role in controlling HF also affects tritium production rates. It allows for more predictable and controlled tritium generation in fusion reactors.
Areas of improvement/ Future Direction	More appropriate measurements can be obtained from hot sampling, which can help evaluate Be uptake for longer exposures and impurity measurements during future corrosion tests. Larger-scale tests could help bridge the gap between laboratory results and practical applications. Continue researching the corrosion behavior of various materials, especially in the presence of HF, to assess their compatibility with fusion reactor components.

Research Article (Provide proper Reference and Title of published article)	Proton Radiation of FLiBe and commercial materials https://doi.org/10.1016/j.jnucmat.2019.151837 Was, B.S., et al. "Materials for Future Nuclear Energy Systems." Journal of Nuclear Materials, Volume 527, 2019, https://doi.org/10.1016/j.jnucmat.2019.151837.
Problems Addressed / Identified	Corrosion of structural materials in molten salt reactors, including corrosion by the salt itself and the potential for high-temperature helium embrittlement. Effects of corrosion in fluoride salt systems, including dissolution of alloying components and the role of impurities in the salt. Consideration of alternative materials like silicon carbide for components with high radiation exposure. Methods to control the fluorine potential in salt systems, including the use of metallic additions, coatings, and other materials.
Aim & Objectives of article	The article aims to address the challenges associated with structural materials in various nuclear reactors, including molten salt reactors and fusion reactors. It investigates the corrosion, radiation damage, and high-temperature embrittlement issues in these systems, and discusses potential materials and strategies to mitigate these problems.
Novelty/Rationale and Significance: Why was the research was worth undertaking?	The findings are significant because they provide insights into the corrosion and radiation-related challenges in different types of nuclear reactors. Understanding these challenges is crucial for improving the safety and efficiency of nuclear energy systems. The research also highlights potential materials and strategies to enhance the performance and longevity of structural components in these reactors.
Limitations and Weaknesses What limitations were encountered when performing the experiment for the article, if any mentioned?	The limitations of the research are not explicitly mentioned in the provided text. However, some potential limitations may include the need for further experimental validation of the proposed materials and strategies, as well as the consideration of

	specific reactor designs and operational conditions.
Implementation Details/Experimental Setup Dataset [Ref],No of Attributes,, Environment/Tool and Technique, Compared and validated with Techniques [Name and parameters compared]	The paper is a meta-study and does not have an experimental setup.
Findings and Conclusions	The dissolution of alloying components in fluoride salts and the role of impurities, especially chromium. The preferential dissolution of chromium over iron and nickel when exposed to fluoride salts. The use of additives and coatings to control the fluorine potential in salt systems. Consideration of alternative materials like silicon carbide for components in fusion reactors. Identification of advanced materials like ODS steels and high-nickel alloys for improved performance in nuclear environments.
Areas of improvement/ Future Direction	Further exploration of materials used for specific, high impact regions of nuclear reactors and additional work for U.S. Regulatory approval for the materials known.

3.5. Filtering

Research Article (Provide proper Reference and Title of published article)	Ceramic Honeycomb Filters and Catalysts Pronob Bardhan Bardhan, Pronob. "Ceramic Honeycomb Filters and Catalysts." Current Opinion in Solid State and Materials Science, Volume 2, Issue 5, Pages 577-583, 1997, https://doi.org/10.1016/S1359-0286(97)80048-4.
Problems Addressed / Identified	-Particulate filtration in diesel and gasoline applications (Information transferable to particulate filtration in other applications) -Optimization of cell wall thickness and cell wall density in ceramic honeycomb filters
Aim & Objectives of article	Discuss hydrocarbon particulate filtration in gasoline and diesel emissions. Lesser focus on ceramic honeycomb filter materials and geometry in both dynamic and static states.
Novelty/Rationale and Significance: Why was the research was worth undertaking?	This research depicts benefits and drawbacks in the use of honeycomb and membrane filter in particulate filtration as a whole, while also discussing possible improvements in the use of ceramics in these filters
Limitations and Weaknesses What limitations were encountered when performing the experiment for the article, if any mentioned?	N/A
Implementation Details/Experimental Setup Dataset [Ref],No of Attributes,, Environment/Tool and Technique, Compared and validated with Techniques [Name and parameters compared]	N/A

Findings and Conclusions	Microporous membrane filters can be processed in such a way as to promote resilience in a hot gas environment. When thin microporous membranes are overlayed between layers of microporous honeycomb filters, pressure drop over the filter can be minimized
Areas of improvement/ Future Direction	Improvements and flexibility and structure of honeycomb filters, possibly through additive manufacturing

Research Article (Provide proper Reference and Title of published article)	Filtration characteristics of polysulfone membrane filters Hsiao-Lin Huang, Shinhao Yang Huang, Hsiao-Lin, et al. "Filtration Characteristics of Polysulfone Membrane Filters." Journal of Aerosol Science, Volume 37, Issue 10, Pages 1198-1208, 2006, https://doi.org/10.1016/j.jaerosci.2005.11.010.
Problems Addressed / Identified	-Aerosol and gas penetration rates through PSF membrane filters -Optimal pore sizes in PSF membrane filters to maximize flow rate
Aim & Objectives of article	Test aerosol penetration rate of PSF filters to determine if they are usable in environments with suspended particles
Novelty/Rationale and Significance: Why was the research was worth undertaking?	Could present a wider range of utility for PSF in a variety of environments
Limitations and Weaknesses What limitations were encountered when performing the experiment for the article, if any mentioned?	N/A
Implementation Details/Experimental Setup Dataset [Ref],No of Attributes,, Environment/Tool and Technique, Compared and validated with Techniques [Name and parameters compared]	Three polysulfone membrane filters were produced at various levels of PSF content and porosity. A polycarbonate filter was included as a control. Polystyrene latex was atomized, neutralized, then passed through each filter in parallel. Penetration through the membrane was measured using a CPC and pressure drop was measured using pressure meters. Humidity and flow rate were held as constants. System efficiency was calculated from these parameters
Findings and Conclusions	Pressure drop decreased with increasing porosity Aerosol penetration decreased with a decrease in porosity Aerosol penetration increases when flow rate increases
Areas of improvement/ Future Direction	N/A

Research Article (Provide proper Reference and Title of published article)	Activation of Sites in MOFs.pdf Akeremale, Olaniran, et al. "Synthesis, Characterization, and Activation of Metal Organic Frameworks (MOFs) for the Removal of Emerging Organic Contaminants through the Adsorption-Oriented Process: A Review." Results in Chemistry, Volume 5, 100866, 2023, https://doi.org/10.1016/j.rechem.2023.100866.
Problems Addressed / Identified	- Contamination of water ways - New types of contaminants being used - Destruction of ecosystems - A need for more efficient and cost-effective remediation techniques to remove EOC's (Emerging organic contaminants)
Aim & Objectives of article	To inform on developments of site activation techniques and synthesis methods used in MOFs
Novelty/Rationale and Significance: Why was the research worth undertaking?	The environment is not getting any better, and while many companies are working to remove trash from waterways, many others are still dumping massive amounts of waste into nearby bodies of water. MOFs, if used correctly, can catch compounds and materials that are too small for basic nets to catch.
Limitations and Weaknesses What is not understood? What limitations were encountered when performing the experiment for the article, if any mentioned?	Currently, there are hundreds of thousands MOFs that theoretically, could be used. However, the techniques necessary to synthesize said MOFs are still unknown, as well their experimental data.
Implementation Details/Experimental Setup Dataset [Ref],No of Attributes,, Environment/Tool and Technique, Compared and validated with Techniques [Name and parameters compared]	N/A

Findings and Conclusions	Several methods of site activation were used and tested to create MOF-74. Many are detrimental to the MOF, which is why techniques like free-drying, supercritical CO2, and solvent exchange with ultra-low surface tension were created.
Areas of improvement/ Future Direction	They required MOFs with larger surface areas and tiny pore diameters with unique pore shapes for quicker transit of MOFs in the aqueous phase. They would also benefit with higher thermal stability and abrasion/moisture resistance before being used in the industry.

Research Article (Provide proper Reference and Title of published article)	Helium_Methane_Separation_Predictions BK.pdf Kadioglu, Ozge, et al. "Efficient Separation of Helium from Methane using MOF Membranes." Separation and Purification Technology, Volume 191, Pages 192-199, 2018, https://doi.org/10.1016/j.seppur.2017.09.031.
Problems Addressed / Identified	- Helium is potentially going to become a scarce material, which is why it is important to develop technologies to capture it from natural gas sources - Few experiments have been done to test MOFs for HE/CH4 separation
Aim & Objectives of article	- to create the first large scale computational study to predict He/CH4 separation of various MOF membranes - to comment/discuss their findings
Novelty/Rationale and Significance: Why was the research was worth undertaking?	Many industries use Helium as a resource for scientific/medical applications, as well as a resource for applications requiring a non-flammable inert gas. Since many industries need it for everyday use, it's abundance is beginning to wane, creating the need for more.
Limitations and Weaknesses What is not understood? What limitations were encountered when performing the experiment for the article, if any mentioned?	Because the number of possible MOFs that could show selectivity of He over CH4 is quite large (139), it is not feasible to fabricate them all and test for selectivity. So, a computational method was used instead. They also limited the types of MOFs used to be those with larger pore diameters than the kinetic diameters of the gases used so they could be large enough to actually capture and store the gases
Implementation Details/Experimental Setup Dataset [Ref],No of Attributes,, Environment/Tool and Technique, Compared and validated with Techniques	- MOF database made by researchers Chung and coworkers (reference 24), as well as the Cambridge Crystallographic Data Centre (CCDC) was used to identify and construct these MOFs - Most of the properties were calculated using the Zeo++ algorithm

[Name and parameters compared]	
Findings and Conclusions	The MOFs GYPCUQ01, HUTZAX01, and PEHBIO showed Helium selectivity as well as high Helium permeability. Also, MOF membranes were predicted to have a higher Helium permeability than polymeric and zeolite membranes.
Areas of improvement/ Future Direction	Later, the use of a larger number of MOFs will be necessary to find future MOFs that can perform better than these. Once those are identified and ran through the system, real-world testing will need to be done to determine further properties of the MOFs.

Research Article (Provide proper Reference and Title of published article)	Possible Tritium Adsorption-H2 and D2 Adsorption through pressure-swing separation.pdf Sharma, Amit, et al. "Hydrogen Uptake on Coordinatively Unsaturated Metal Sites in VSB-5: Strong Binding Affinity Leading to High-Temperature D2/H2 Selectivity." Langmuir 2017, 33, 14586-14591.
Problems Addressed / Identified	➢ The need for tritium and deuterium-selective materials ➢ The problems with current isotopic separation methods ➢ The uses and properties of VSB-5, a nanoporous nickel phosphate
Aim & Objectives of article	The direct objective is to inform not only on the problems associated with Hydrogen-isotope adsorption and removal, but the uses and properties of a Tritium-adsorbing MOF called VSB-5 (a nickel phosphate based nanoporous MOF)
Novelty/Rationale and Significance: Why was the research worth undertaking?	Due to the current usage rates of Tritium and its decay product, Helium, it is important to be able to recycle these materials for repeated use in the many industries that require them. This includes the nuclear, medical, military, and industrial industries.
Limitations and Weaknesses What is not understood? What limitations were encountered when performing the experiment for the article, if any mentioned?	They still do not know why some active sites are not adsorbing more than one hydrogen molecule per site, and they do not know how it would react in an environment enriched with Tritium.
Implementation Details/Experimental Setup Dataset [Ref],No of Attributes,, Environment/Tool and Technique, Compared and validated with Techniques [Name and parameters compared]	- Environment - Activated for 7 days at 563 K under 10^-6 bar - Measurement - All isotherms measured on same sample to eliminate run-to-run variation - Did brief 373K reactivation of sample to ensure empty MOF - Sample loaded at 77K - Machinery

	- Used Micromeritics ASAP 2020 physisorption analyzer with HE cryostat purchased from Cold-Edge Technologies - Used Bomem Da3 spectrometer with quartz halogen source, KBr beam splitter, and mercury cadmium telluride detector for Infrared spectra - Custom-built cryogenic chamber - Techniques - Measurements taken using diffuse reflectance technique
Findings and Conclusions	VSB-5 has one of the highest measured initial heats of adsorption, showing 1.5 kJ/mol more selectivity for Deuterium than Hydrogen, they believe to be one of the highest measured initial D2/H2 selectivity in any material at a temp above 120 K. They believe VSB-5 is an excellent choice for lower cost PSA (pressure-swing adsorption) separations of D2/H2 gas mixtures
Areas of improvement/ Future Direction	I would like to continue this study, but include the next isotope of Hydrogen, Tritium. The gas itself is very expensive, but with the right setup we can reuse tritium for each experiment. I would like to see the selectivity of our MOF for T2/D2, and T2/H2.

Research Article (Provide proper Reference and Title of published article)	Pressure drop in honeycomb adsorption filters filled with granular activated carbon Ruiyan Zhang, Zhenhai Li, Lingjie Zeng, Fei Wang Zhang, Ruiyan, et al. “Pressure Drop in Honeycomb Adsorption Filters Filled with Granular Activated Carbon.” Powder Technology, Volume 393, Pages 550-558, 2021, https://doi.org/10.1016/j.powtec.2021.07.074.
Problems Addressed / Identified	-Pressure drop in filtered material over the length of the filter -Minimization of the friction factor over the length of the filter in both laminar and turbulent airflow patterns
Aim & Objectives of article	Determine pathways to minimize friction factor of the filter, thus minimizing pressure drop
Novelty/Rationale and Significance: Why was the research was worth undertaking?	Less pressure drop over the length of the filter will result in a more stable adsorption rate across the entire length and less impedance of flow withing the filtered area to increase system efficiency
Limitations and Weaknesses What limitations were encountered when performing the experiment for the article, if any mentioned?	Unable to reproduce equal adsorbent distributions between trials consisting of less than 100% adsorbent packing
Implementation Details/Experimental Setup Dataset [Ref],No of Attributes,, Environment/Tool and Technique, Compared and validated with Techniques [Name and parameters compared]	Plastic and aluminum honeycomb skeletons were used with varying hexagonal side lengths. Activated carbon adsorbent was packed into the skeletons to several void ratios. These filters were placed into an apparatus with variable air velocities. Pressure taps were placed in the chambers on either side of the filter. The pressure on each side of the filter was recorded alongside the air velocity. This data was then used to calculate pressure drop over the filter in various scenarios.

Findings and Conclusions	Pressure drop over the filter increases with air velocity and decreases when the void ratio of the adsorbent increases. The plastic skeleton also experience more resistance to flow than the aluminum skeleton
Areas of improvement/ Future Direction	N/A

Research Article (Provide proper Reference and Title of published article)	tritium_Adsorption_Through_Heavily_Tritiated_Water BK.pdf Fu, Xiaolong, et al. "Superhydrophilic Metal-Organic Frameworks Film Modified Surface for Tritium Removal from Tritiated Heavy Water." Microporous and Mesoporous Materials, Volume 348, 112387, 2023, https://doi.org/10.1016/j.micromeso.2022.112387.
Problems Addressed / Identified	- Many gasses exist within liquids that can't be extracted by some MOFs due to their selectivity of their target gasses not being high enough - Safe method of tritium removal from heavy water moderators necessary, since other methods cause possible hydrogen explosions - Dueterons capture neutrons during the use of heavy water reactors, which causes the water to become contaminated with tritium, causing health risks to personnel and the environment
Aim & Objectives of article	To inform on the first attempt at using engineered MOFs to create a detritiation system for heavy water reactors
Novelty/Rationale and Significance: Why was the research was worth undertaking?	"Tritium removal with this distillation system reduces the tritium activity to an acceptable level and extracts valuable concentrated tritium for industrial, medical, and research purposes. Furthermore, this MOFs modified surface strategy holds promise in water distillation systems for nuclear wastewater treatment containing tritium species both for light water systems and heavy water systems."
Limitations and Weaknesses What is not understood? What limitations were encountered when performing the experiment for the article, if any mentioned?	N/A
Implementation Details/Experimental Setup Dataset [Ref],No of Attributes,, Environment/Tool and Technique, Compared and	- Fabrication - Stainless steel spiral prismatic packing was washed with ethanol and deionized water to remove contaminants repeatedly, then treated with diluted hydrochloric acid - For modified packing, the above was modified with polydopamine three times, then immersed

validated with Techniques [Name and parameters compared]	in zirconium tetrachloride and terephthalic acid in N, N-dimethyl formamide, then moved into solvothermal bomb for 24 h at 120 C. - Repeatedly washed with DMF and deionized water 3 times - Dried at 150 C for 6 hours and stored - Simulation Conditions - Above samples was packed with pure heavy water and trace amount of tritium into a water distillation column. - Techniques - Process designed by Chalk River Laboratories - Processes and simulations performed and optimized by Aspen software package - Non-random two-liquid model (NRTL) used for simulation process
Findings and Conclusions	The HETP (height equivalent to a theoretical plate) of this MOF was about 1.53 cm, which is a very good finding as it means better mass transfer, column efficiency, and separation performance. (The lower the HETP, the better)
Areas of improvement/ Future Direction	Since this article describes its selectivity underwater, I would like to use it in an environment riddled with other gasses to simulate the conditions in our salt loop from the nuclear reactor. If it holds up and still shows high selectivity, I would work it in to the mesh for the filter.

Functional Requirements Document (FRD)

University of Cincinnati Molten Salt Test Loop
UC-MSTL

University of Cincinnati
BSME Class of 2024

THIS PAGE PURPOSELY BLANK

1. Introduction

1.1. Purpose of Document

The Functional Requirements Document (FRD) outlines the specifications and expectations for the conceptual heat transfer Molten Salt Test Loop (MSTL) being developed by the University of Cincinnati (UC). The primary objective of this document is to provide a comprehensive understanding of the functional requirements that govern the design, development, and performance of the test loop for implementation in partnership with private fusion enterprises.

1.2. Document Scope

The scope of this document encompasses the functional aspects of the test loop and subsystems, including but not limited to heat dissipation, byproduct removal, thermal regulation, materials selection, safety consideration, and overall system performance on a conceptual basis. The document will be format-limited to the International Council on Systems Engineering (INCOSE) requirement standards.

1.3. Background

The University of Cincinnati senior design group is actively researching open-space and readily available fusion reactor devices, such as those developed by Commonwealth Fusion Systems (CFS) and other fusion energy startups (General Atomics, et al.) [1]. In line with this, the group aims to undertake a conceptual design project focused on a molten salt test loop. This test loop is designed to simulate the nuclear, thermo-fluid, and heat transfer properties of liquid salt, specifically for applications in heat transfer within a fusion device. The project, known as the University of Cincinnati Molten Salt Test Loop (UC-MSTL), seeks to document anticipated engineering challenges, current and required empirical data, and preliminary results derived from heating, fluid flow, and neutronics calculations. Additionally, the team is exploring steady-state solutions for tritium capture and storage. The ultimate objective of this conceptual design is to fulfill graduation requirements for senior mechanical engineering students of the class of 2024, serving as a capstone project.

1.4. System Description

To validate the effectiveness of fusion breeder blankets, fusion enterprises must generate essential experimentally gathered data using a test loop, integrated into operations. This test loop aims to leverage the high neutron flux environment to simulate crucial aspects of fusion device operations, encompassing tritium breeding, heat transfer, thermo-hydraulic flow, and the magnetohydrodynamic aspects of salt. The test loop will feature techniques for real and delayed nuclear data gathering, mechanisms for sampling molten salt and structural materials, and innovative subsystems for byproduct removal. The overarching goal is fusion power plant design and implementation.

1.5. Scope

1.5.1. Users

Users of this Functional Requirement Document include but are not limited to future system designers and engineers, project managers, stakeholders, and regulatory bodies, such as the Department of Energy (DOE) and Nuclear Regulatory Commission (NRC).

1.5.2. Need

The test loop will provide essential experimentally gathered data in order to validate the operational assumptions for fusion powerplants. Data gathered through test loop construction and design will also provide a basis for subsequent fusion device manufacturing and plasma physics research.

1.5.3. Location

The functional requirements in this document are written for a conceptual test loop. The requirements can be transferrable to a physical system given augmentation by future engineering teams.

THIS PAGE PURPOSELY BLANK

2. Functional Requirements

The following objectives are written with the purpose of defining the sub-system architecture of the UC-MSTL, its subsystem purposes, functions, and needs.

2.1. FLiBe Test Loop (System)

A. The FLiBe Test loop shall transfer heat from the tokomak.

Justification: Transfer of heat is essential for the operation of the loop.

B. The FLiBe test loop shall be constructed of compatible materials to the high neutron flux and corrosion environment.

Justification: Compatible materials are required for proper operation and safety of the test loop.

C. The FLiBe test loop shall incorporate passive materials to mitigate effects of corrosion between base materials and FLiBe salt.

Justification: Several studies indicate addition of passively acting materials (such as Beryllium) into the salt reduce overall corrosion levels post operation of FLiBe test loops [4].

D. The FLiBe test loop shall circulate salt.

Justification: Circulation of salt is required for heat distribution.

E. The FLiBe test loop shall remove byproducts from the FLiBe salt.

Justification: Removal of byproducts is essential to maintaining the quality, tritium breeding, and heat transfer properties of the salt.

F. The FLiBe test loop shall connect to balance of plant utilities.

Justification: Connection to balance of plant utilities allows for external and internal functionalities including, but not limited to, real time heat monitoring, powered pumping systems, and cover gas systems.

G. The FLiBe test loop shall incorporate controls to enhance safe operation and real-time monitoring of loop functions.

Justification: Control systems will enhance the functionality of the loop and provide evaluative data for device operations.

H. The FLiBe test loop shall incorporate sampling mechanisms including, but not limited to, sampling ports for FLiBe salt, protected sections of piping, and equipment for loop functionality.

Justification: Sampling mechanisms provide much needed data for device analysis and breeding blanket scale-up.

I. The loop shall incorporate shielding to protect equipment, including, but not limited to, the pump, mechanized valves, sensors, and filters.

Justification: Shielding will protect important control and loop operation equipment from the high neutron flux environment.

J. The loop shall be able to control the pressure and temperature of the system.
Justification: Temperature and pressure of the fluid are critical to the upkeep and reliability of the system.

2.2. FLiBe ($LiF\text{-}BeF_2$, Subsystem)

A. The FLiBe salt shall transfer thermal heat away from the tokomak.
Justification: Transfer of heat is essential for the cooling of the first wall separating the salt from the neutron environment.

B. The FLiBe shall convert high energy neutrons into heat for the system.
Justification: Removal of heat from the plasma is an essential task of the fusion device operation.

C. The FLiBe shall be able to be moved, pumped, transferred, etc. within the loop.
Justification: Transfer of heat from the device is dependent on fluid flow.

D. The FLiBe shall be contained within the loop while in operation.
Justification: Safe and effective functionality of the loop requires all salt to be contained in the loop unless otherwise transferred for re-enrichment outside of device operation or sampled for purity.

E. The FLiBe shall simulate the shielding of magnet components against radiation to prevent quench.
Justification: The magnet components cannot withstand the intense radiation field of the fusion device without additional protection, which is to be provided by the salt.

F. The FLiBe shall maintain a tritium breeding ratio of 1:1.1 tritium atoms.
Justification: A breeding ratio of 1:1.1 can only be maintained given a high enrichment of 6Li and the (n,3H) reaction in the FLiBe salt.

G. The FLiBe salt shall be maintained at a minimum temperature of 500 degrees Celsius and a maximum temperature of 1200 degrees Celsius.
Justification: Melting and boiling points acquired from experimentally derived fluoride salt coolant properties [3] After applying a 10% factor of safety to raise melting limit and lower boiling limit.

H. The FLiBe salt shall be maintained at a specific purity to reduce activation due to trace elements in the salt composition.
Justification: High levels of Fe, Cr, Ni, Mo, Nb and W in the salt prove to be of activation concern in high neutron environments and must be minimized [2].

I. The FLiBe salt shall be maintained at a lithium isotopic enrichment of 90% Li-6 and 10% Li-7.
Justification: Li-6 is the primary isotope of lithium required for tritium production in the neutron environment. The salt must be enriched to maintain the number of tritium production events to sustain the 1:1.1 ratio [5].

2.3. Pump System (Subsystem)

A. The Pump System shall induce the flow of FLiBe salt.
   Justification: Transfer of heat from the device is dependent on fluid flow.

B. The Pump System shall control the flow rate of FLiBe salt.
   Justification: The rate of the transfer of heat from the device is dependent on fluid flow rate.

C. The Pump System shall be able to control the pressure of the fluid.
   Justification: Pressure of the fluid are critical to the upkeep and reliability of the system.

D. The Pump System shall be compatible with the flow of FLiBe molten salt.
   Justification: FLiBe is the primary heat transfer fluid of the system.

E. The Pump System shall be able to tolerate radiation from a high energy neutron environment.
   Justification: Removal of heat from the plasma is in the form of high energy neutrons.

F. The Pump System must be safe to operate.
   Justification: The loop poses a hazard if its subcomponents are not safe for continuous operation.

G. The Pump System shall be able to integrate with the rest of the heat exchange system.
   Justification: The pump subsystem will run in conjunction with all the other subsystems.

H. The Pump System shall be able to undergo scheduled maintenance.
   Justification: The pump system needs to be checked to ensure safe and proper operation.

2.4. Filtering (Subsystem)

A. The filter shall remove tritium, helium, and other semi-particulate gaseous products from the loop.
   Justification: The FLiBe will continue to produce gasses that could lead to critical pressures inside of the loop

B. The filter shall adsorb and be cleaned of gaseous byproducts simultaneously and continuously.
   Justification: Target gasses cannot be adsorbed by porous polymers whose pores are already occupied. A cleansing process is necessary.

C. The filter shall separate Tritium and Helium.
   Justification: Tritium gas and Helium are produced by the FLiBe, however Tritium is of particular interest for use as a fuel source.

D. The filter shall be made of materials capable of withstanding 14.8 MeV neutron Irradiation.

Justification: The filter will be placed some distance from the device.. Without proper shielding, it will be exposed to certain amounts of radiation that some materials cannot handle.

E. The filter shall be mechanized to aid in the removal of byproduct.

Justification: To clean the filter, the contaminated sections must leave the inside of the loop to be cleaned.

F. The filter shall be able to withstand temperatures between 500 C and 1200 C.

Justification: Material should be rated to withstand these temperature ranges with negate thermal shock and maximize the longevity of the filter base within the operating environment.

G. The filter shall be accessible, removable, and replaceable for maintenance, cleaning, and proper operation.

Justification: Ease of maintenance will result in faster, higher quality inspection and failure prevention.

H. The filter shall not significantly impede the flow of gas through the pipe.

Justification: Slowing the flow of the gas could result in buildups, pressure drops, and excessive strain on associated physical and electrical systems.

I. The filter base shall not chemically react with any particulate or gaseous matter within the system.

Justification: Material selection contributes directly to the lifespan and usage conditions of the filter.

2.5. Support Equipment (Balance of Plant, Subsystem)

A. Support Equipment shall connect to the FLiBe test loop while not impeding flow of salt.

Justification: Impeding the flow of salt presents issues surrounding the safety basis of the loop.

B. The FLiBe test loop shall utilize gas lines to supply cover gas, including, but not limited to, helium and argon.

Justification: Cover gas lines are imperative for the removal of gaseous byproducts and prevention of corrosion between salt and loop structure.

C. The FLiBe test loop shall utilize 480 KV and 220KV, and 120 KV power supplies.

Justification: Power supplies are essential for the operation of loop equipment.

D. The FLiBe test loop shall utilize physical infrastructure, including, but not limited to, fasteners, anchors, and stands to maintain its position in the neutron beam and prevent tipping or damage from movement.

Justification: Physical infrastructure is essential for loop operation.

E. The FLiBe test loop shall utilize shielding materials for neutron irradiation sensitive equipment.

Justification: Shielding materials protect balance of plant equipment and provide structural support for the loop.

2.6. Controls (Subsystem)

A. The controls system shall have emergency stops implemented at all potential points of failure.

Justification: Emergency stops are necessary to regulate unforeseen failures and minimize potential damages

B. Emergency stops shall be both visible and easily accessible.

Justification: Emergency stops must be accessible to be operated.

C. Emergency stops shall have their activation reflected on a central control panel.

Justification: Emergency stops must clearly visible to be operated.

D. All controls systems shall be operable in a remote manner.

Justification: Remote controls will enable quick action and minimization of operator exposure to hazardous conditions

E. All controls systems shall be visible from a central control room.

Justification: Utilizing a central viewpoint is useful for ease of system monitoring, minimizing required staff and potential points of failure, and viewing cross-system interactions.

F. The control systems shall be intuitive and simple for operators within a 93rd percentile.

Justification: Intuitive controls will minimize potential points of failure and reduce training times.

G. Real time sensors shall be included in primary control design to measure parameters such as temperature, pressure, and neutron flux.

Justification: Understanding system conditions in a necessity for minimizing risks to the system and ensuring stable operating conditions.

H. Analog (delayed feedback) mechanisms, such as fission chambers, shall be included in primary control design for measure of overall activation.

Justification: Real time measurement of certain parameters is essential for safe operation of test loop.

I. All active systems shall have appropriate sensors for the respective data type.

Justification: Usage of incorrect sensor type or range will result in potential catastrophic oversights in system operations.

- Sensors shall be implemented into the controls system.
- Sensor data shall be reflected within a main control room.

- Large alterations from regular operational data shall be alerted to through an audio or visual cue.

J. A main controls room shall be occupied by a minimum of two qualified operators during all operations.

Justification: A minimum of two operators ensures a division of visual load and restricts the potential oversights a single operator might possess.

K. Control systems shall reflect possible malfunctions of subsystems within the main control room.

Justification: Knowledge of ongoing malfunctions enables a quick response and minimization of possible negative effects.

L. The control system shall halt operations in a safe manner in the event of a critical malfunction.

Justification: Having autonomous coded stops prevents chaining malfunctions, reduces potential human error, and allows for instant system diagnosis based on reason for shutdown.

- Potential malfunctions shall be alerted through use of an obvious visual or audio cue.

M. Control systems shall present feedback from subsystems.

Justification: Understanding how systems are operating in real time allows for small adjustments to be made, potentially further optimizing operations.

- Feedback from these systems shall inform of current operational status and system data from sensors.

N. The control system shall facilitate the operations of all subsystems.

Justification: Having a general control system governing all subsystem controls minimizes risk of a general failure from a single subsystem, while removing the risk of multiple points of failure across the whole system

2.7. Samples (Subsystem)

A. The sampling system shall sample FLiBe salt to detect parameters including, but not limited to, elemental (molar) concentration, elemental composition, activation, viscosity, impurities, particle size, and thermo-physical properties.

Justification: Gathered data will guide Li-6 and Li-7 enrichment protocols to maintain tritium breeding, purity selection, and effect of neutron environment on byproduct production introduced via activation and corrosion.

B. The sampling system shall preserve FLiBe salt and loop component/equipment quality during and post sampling.

Justification: Sampling of salt and componentry should preserve the salt such that it is representative of operational quality.

C. Test loop structural and piping samples should verify the activation of the following elements, including but not limited to: Fe, Cr, Mo, Nb, Ni, W.

Justification: Activation of the listed elements poses a dosage risk during deconstruction and disposition and will guide decommissioning protocols of the test loop, as represented by previous activation studies (see Fig 1.)

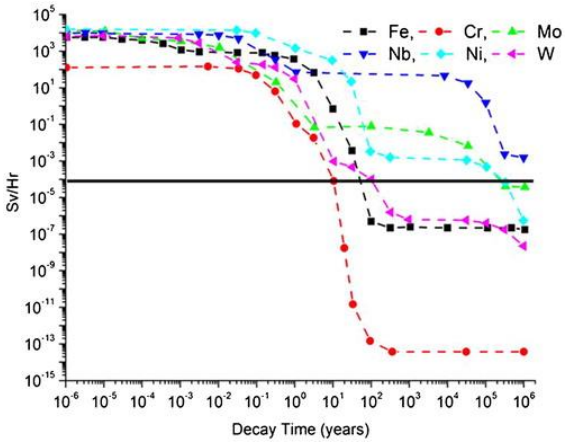

Figure 1 – Level of radioactivity for several elements commonly found in steels (Fe, Cr, Ni, Mo, Nb and W) following the shutdown of a 3·6 GW fusion power, fusion reactor, assuming an anticipated blanket structural materials fusion irradiation flux of ∼1×1019 neutron m−2 s−1 over a 5 year irradiation time; Citation 5 marked on the graph is the ITER administrative limit at 100 μSv/Hr for items available for hands-on maintenance [2].

D. The sampling system shall take samples from equipment including, but not limited to, welds, bends, pump shafts, pipe segments, off-gas and cover gas connection lines, sensor connections, filter material, and ports.

Justification: Sample locations will aid in the determination of corrosion rates, hotspots, and damage caused by test loop operation.

E. The sampling system shall employ devices and mechanisms for the characterization of the neutron flux environment surrounding the MSTL in both operational and decommissioning timelines.

Justification: Charecterization of the neutron flux environment is imperative for the operation of the MSTL and determination of the disposal paths for MSTL equipment.

A. References

[1] A. J. CREELY, “Overview of the SPARC Tokamak,” Cambridge University Press (2020).

[2] Gorley, Mike. “Prospects for Reduced Activation Steel for Fusion Plant.” *Taylor and Francis Online*, Material Science and Technology, Vol. 31, 8 Dec. 2014, www.tandfonline.com/doi/full/10.1179/1743284714Y.0000000732.

[3] R.R. Romatoski, et al. “Fluoride Salt Coolant Properties for Nuclear Reactor Applications: A Review.” Annals of Nuclear Energy, Pergamon, 14 June 2017, www.sciencedirect.com/science/article/pii/S0306454917301391.

[4] Smolik, G. R. “Beryllium Interactions In Molten Flibe- Twelfth International Conference on Fusion Reactor Materials .” *INL/CON-05-00927*, Idaho National Laboratory, Jan. 2006, digital.library.unt.edu/.

[5] Forsberg, Charles, et al. “Fusion Blankets and Fluoride-Salt-Cooled High-Temperature Reactors with Flibe Salt Coolant: Common Challenges, Tritium Control, and Opportunities for Synergistic Development Strategies Between Fission, Fusion, and Solar Salt Technologies.” Nuclear Technology, Volume 206, Issue 11, 2020.

System Design Description

University of Cincinnati Molten Salt Test Loop
UC-MSTL

University of Cincinnati
BSME Class of 2024

THIS PAGE PURPOSELY BLANK

1. Introduction

1.1. Purpose of Document

This document delineates the architecture, functionality, and key components of the proposed conceptual design of the University of Cincinnati Molten Salt Test Loop (UC-MSTL). It aims to offer clarity regarding the conceptual design by leveraging Computer-Aided Design (CAD), simple simulations, explanations of subsystems, interdependencies, requirements, and implementation functions. This document is split into functional sections to highlight the major components of the test loop and their role in the development of the requirements per the UC-MSTL Functional Requirements Document (FRD).

1.2. Document Scope

This document presents the complete conceptual design of the UC-MSTL, building upon the data and analysis produced in other sections of the final report. It leverages the findings from the literature review to draw conclusions on the design of subsystems detailed in the Functional Requirements Document (FRD), with support from the neutronics calculations and filtering experiments.

1.3. Background

The University of Cincinnati senior design group is actively researching open-space and readily available fusion reactor devices, such as those developed by Commonwealth Fusion Systems (CFS) and other fusion energy startups (General Atomics, et al.). In line with this, the group aims to undertake a conceptual design project focused on a molten salt test loop. This test loop is designed to simulate the nuclear, thermo-fluid, and heat transfer properties of liquid salt, specifically for applications in heat transfer within a fusion device. The project, known as the UC Molten Salt Test Loop (UC-MSTL), seeks to document anticipated engineering challenges, current and required empirical data, and preliminary results derived from heating, fluid flow, and neutronics calculations. Additionally, the team is exploring steady-state solutions for tritium capture and storage. The ultimate objective of this conceptual design is to fulfill graduation requirements for senior mechanical engineering students of the class of 2024, serving as a capstone project.

1.4. System Description

To validate the effectiveness of fusion breeder blankets, fusion enterprises must generate essential experimentally gathered data using a test loop, integrated into operations. This test loop aims to leverage the high neutron flux environment to simulate crucial aspects of fusion device operations, encompassing tritium breeding, heat transfer, thermo-hydraulic flow, and the magnetohydrodynamic aspects of salt. The test loop will feature techniques for real and delayed nuclear data gathering, mechanisms for sampling molten salt and structural materials, and innovative subsystems for byproduct removal. The overarching goal is fusion power plant design and implementation.

1.5. Project Scope

1.5.1. Users

Users of this study include future system designers and engineers, project managers, stakeholders, academics, and regulatory bodies, such as the Department of Energy (DOE) and Nuclear Regulatory Commission (NRC).

1.5.2. Need

The test loop will provide essential experimentally gathered data to validate the operational assumptions for fusion power plants. Data gathered through test loop construction and design will also provide a basis for subsequent fusion device manufacturing and plasma physics research.

1.5.3. Location

The designs in this document are composed for a conceptual test loop. The designs can be transferrable to a physical system given augmentation by future engineering teams and the collection of experimental data.

2. Overview of MSTL Design

Nuclear fusion enterprises are maturing at a faster rate than previously anticipated. In December of 2022, a controlled fusion reaction at Lawrence Livermore National Laboratory (LLNL) produced a positive energy output and broke the first barrier of many in fusion energy. Fusion energy, once thought to be decades away, is now at the crest of commercial viability. Currently, the goals of commercial fusion enterprises are complex, yet obtainable: repeat net energy gain, reach magnetic and inertial confinement milestones in fusion output, and devise a path to replace other energy sources.

Although much headway has been made, several technological issues still exist. One of the ongoing issues in the viability of fusion power generation is the heat transfer mechanism by which fusion plasma will be used to produce electricity.

The University of Cincinnati Molten Salt Test Loop (UC-MSTL) is devised to outline much needed experimental data for heat transfer validation. The conceptual design covers several aspects of the test loop and aims to provide a basis for which commercial enterprises will build upon for their own individual needs. The MSTL is composed of six subsystems: The FLiBe (LiF-BeF_2) salt, pump, filtering system, control system, sampling system, and supporting equipment (see Fig. 3 for equipment layout).

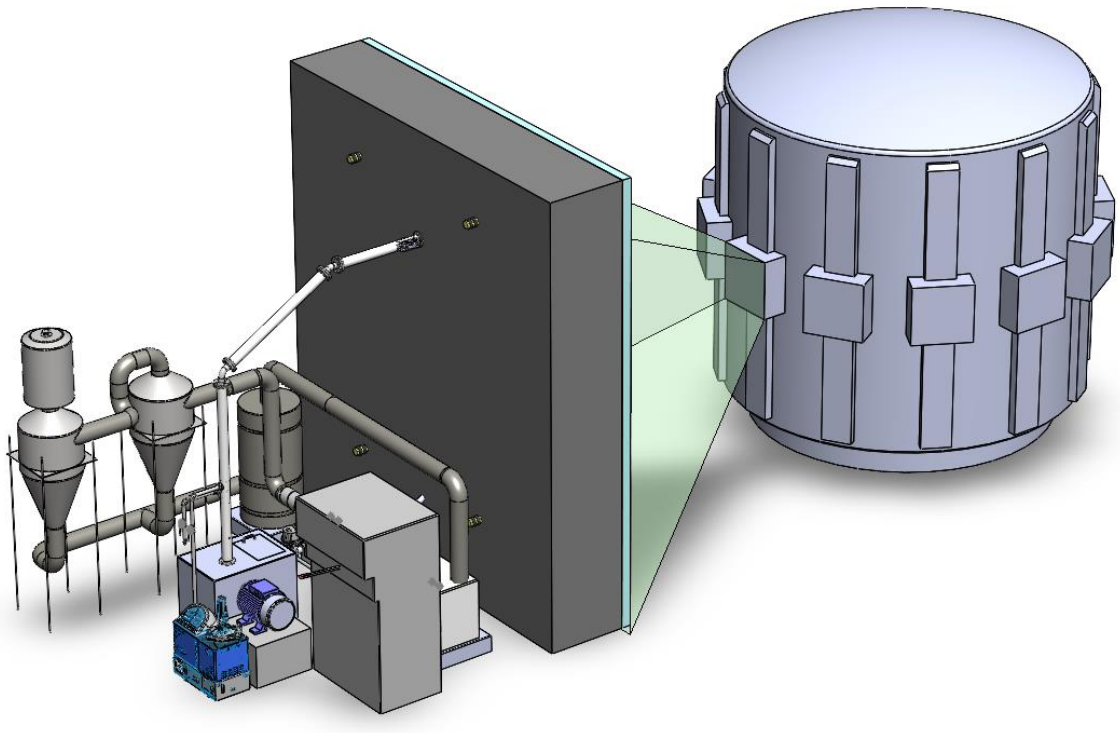

Figure 1 – Isometric View of MSTL with Fictitious Fusion Device with Hypothetical Neutron Beam

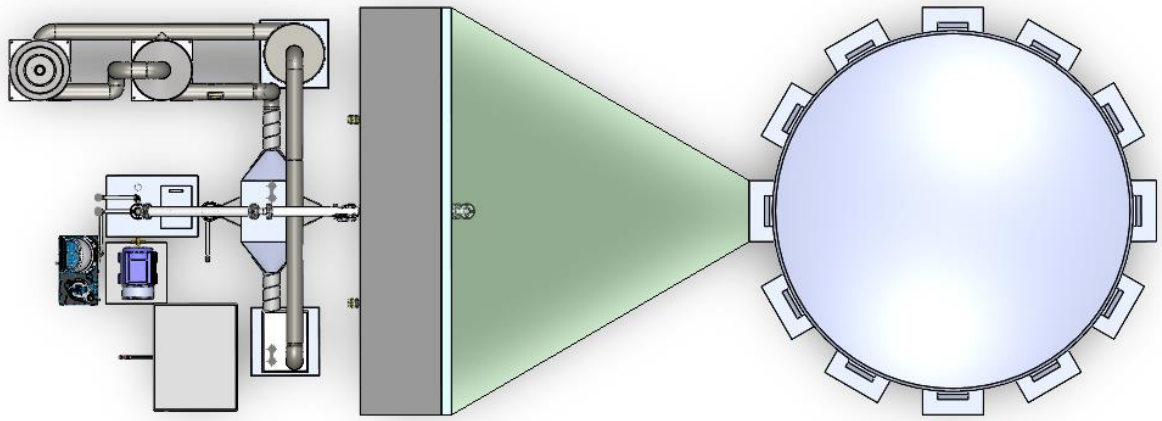

Figure 2 – Top view of MSTL in Relation to Fictitious Fusion Device with Hypothetical Neutron Beam

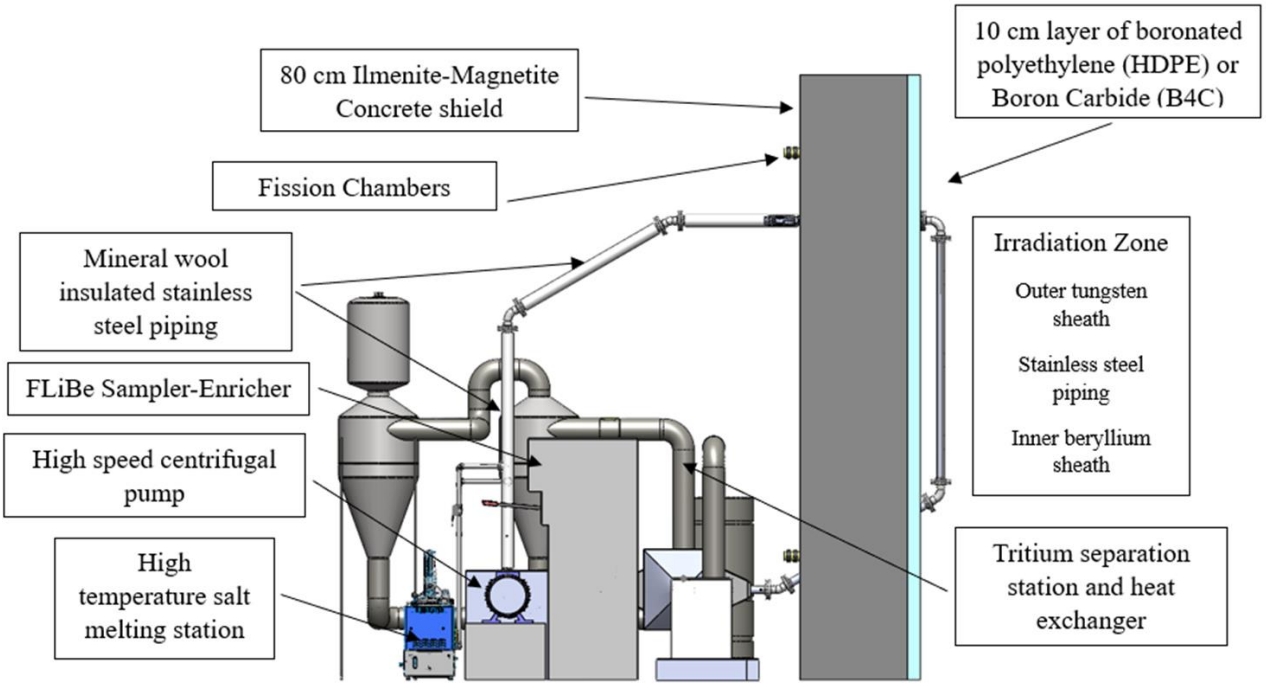

Figure 3 – Detailed View of MSTL (xz plane)

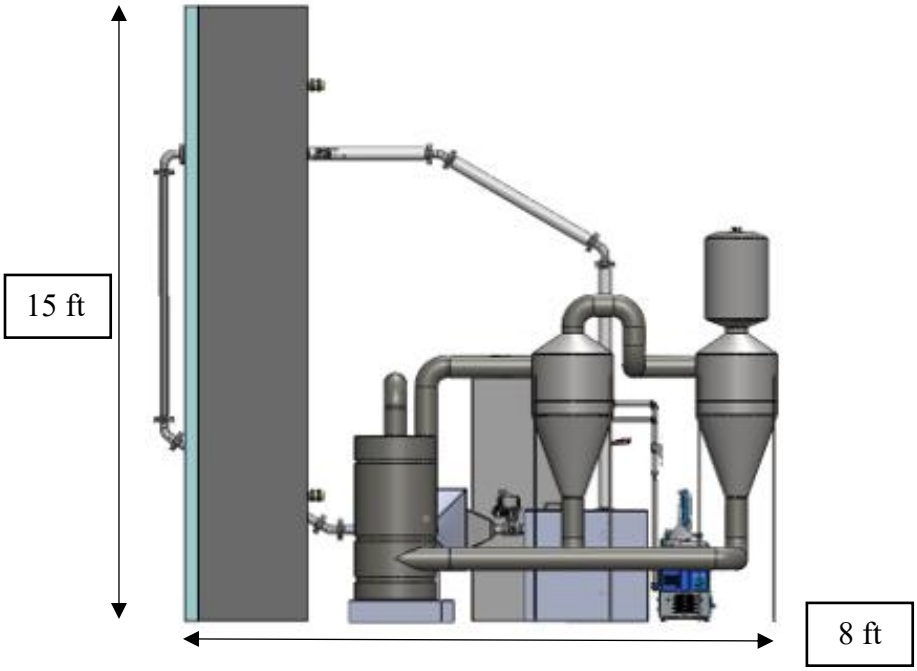

Figure 4 – Detailed View of MSTL (xz plane, reversed)

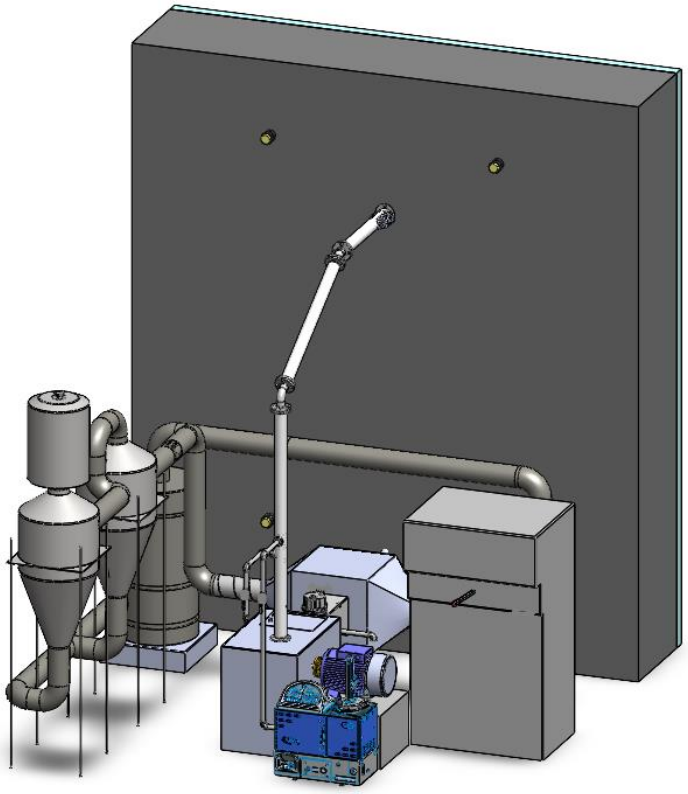

Figure 5 – Reversed Isometric View of MSTL Model

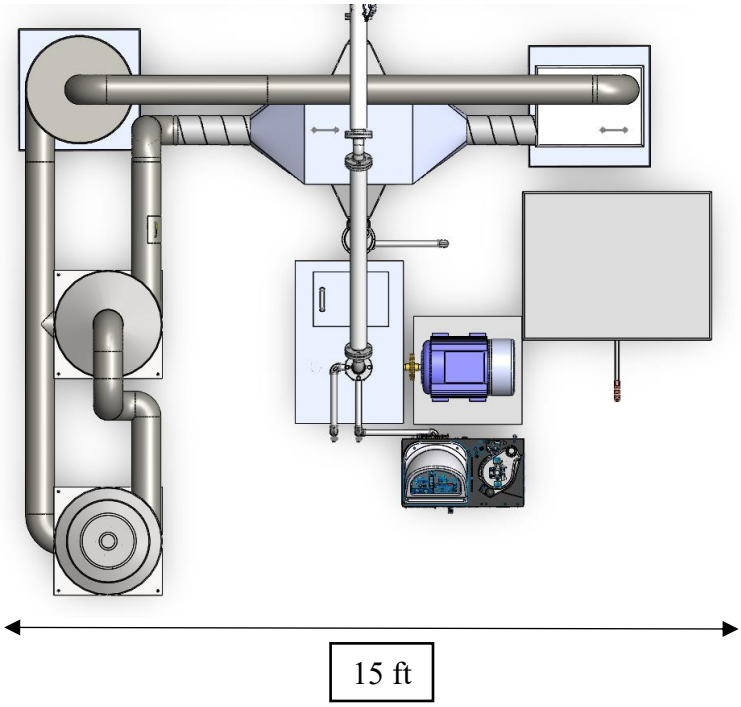

Figure 6 – Top View of MSTL Model

Table 1 –UC-MSTL Specific Parameters for Concept Model

Parameter	Value
UC-MSTL Space Occupation	15 ft x 8 ft x 15 ft
Insulation	Ceramic Fiber Mineral Wool
Cover Gas	High Purity, 99.99% Argon
SS Pipe Dimensions	2in, Schedule 40 316 Stainless Steel
SS Pipe Inner-Coating	TiN (Titanium nitride) or TiC (Titanium Carbide)
SS Pipe Volume	0.0605 m^3
FLiBe Salt Mass	137 kg
FLiBe Flow Rate	0.01 m/sec
Operating Temperature Range	500 C – 1200 C
Shield Block Thickness	80 cm Ilmenite-Magnetite Concrete
Additional Shielding Thickness	Shield Block Thickness + 10 cm Boron Carbide (B4C)

2.1. Heat Transfer

The MSTL will act to simulate heat transfer from the fusion device to a working fluid (FLiBe, LiF-BeF_2) salt. On a host fusion device, a neutron "beam" must be allowed to escape the reactor. This is hypothesized to be aided by the strategic placement of the test loop within the vicinity of an un-occupied port on the side of the reactor and a relocation of shielding elements to allow for streamlined access to fusion neutrons.

The heat is transferred from the fusion reactor to the salt via the kinetic energy transfer between the neutrons through various interactions, such as incident neutron scattering or capture (reference the FLiBe salt subsystem section of this document). In a hypothetical power demonstration scenario, The salt would not connect to a heat sink and would connect to a Rankine cycle, most likely through a protective secondary system.

In the UC-MSTL concept, the salt is heated primarily in the irradiation zone of the loop (see section 2.2 for overview of MSTL zones). As the salt is heated, it is pumped to a heat exchanger. The type of heat exchanger specified in this concept is a simple cross flow heat exchanger utilizing nickel piping for FLiBe flow with a cross flow of forced argon gas. Per the literature review, nickel has shown to have excellent diffusivity properties towards tritium and helium gas, especially in high temperature operations. As such, the gases are hypothesized to be most permeable in the MSTL system during the turbulent flow of the FLiBe through the heat exchanger. The tritium and helium will then be carried by the argon cover gas through the secondary filtering system and separated (see section 3.3 on filtering). Heat will be discharged from the argon gas to a heat sink through radiative fins and a chiller prior to filtering.

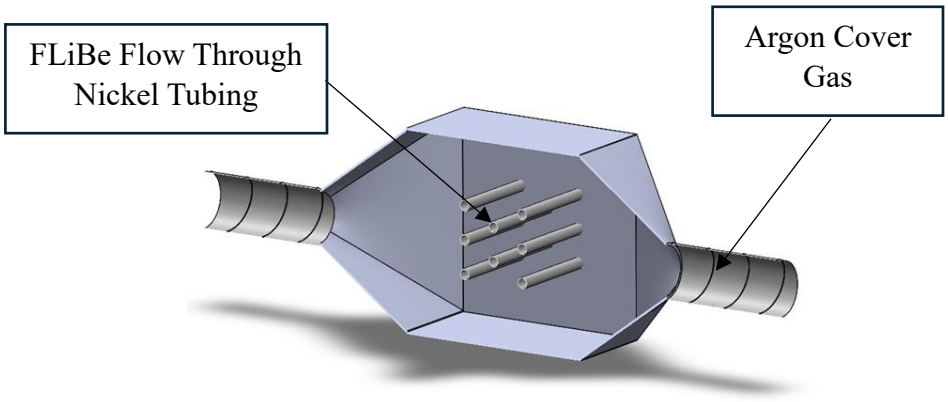

Figure 7 – Cross Flow Heat Exchanger in UC-MSTL

2.2. Irradiation Zone and Non-Irradiation Zone

The MSTL is split into two regions: the non-irradiation zone and irradiation zone (reference Fig. 8). The non-irradiation zone is behind the ilmenite-magnetite shielding block with the additional 10-centimeter shielding configuration to protect sensitive equipment prone to neutron activation and damage. The irradiation zone faces the fusion device and will experience the brunt of the neutron flux. This is highly important for tritium breeding in the salt but will be prone to high flux induced Wigner energy, heating, and material damage.

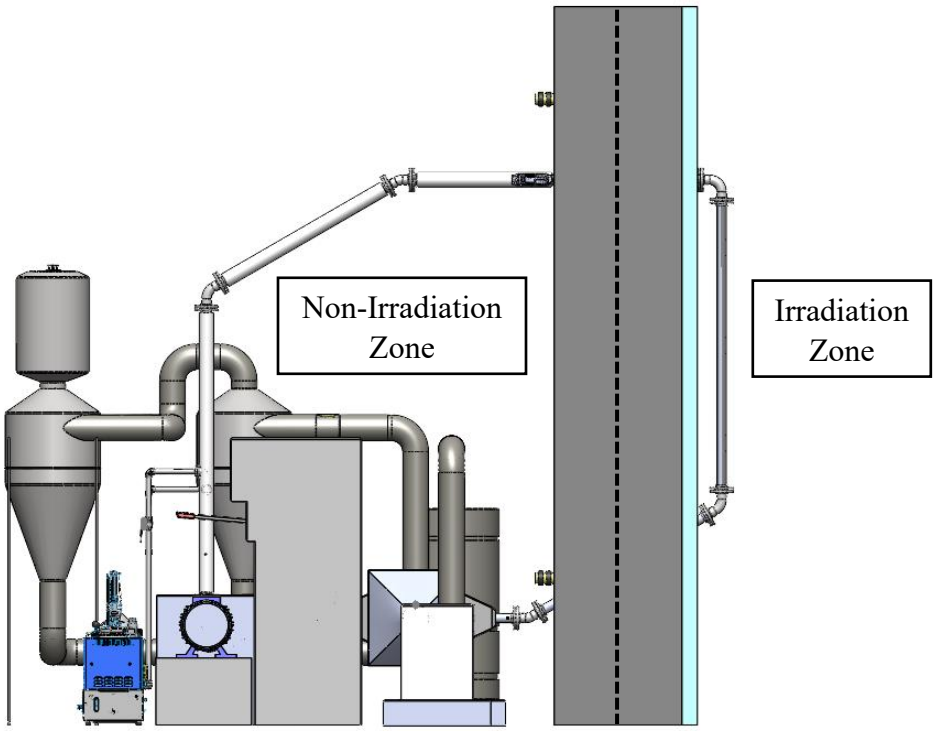

Figure 8 – Side view of MSTL with Irradiation Zone/Non-Irradiation Zone

2.3. Zone Material Selection and Layout

In the irradiation zone, an outer tungsten sheath is present. From the literature review, it was determined that including a thin tungsten boundary later between the fusion neutrons and the salt acts to formulate a hypothetical inner plasma-matter facing wall. The second inner layer is that of the stainless-steel piping, which contains salt. The third layer is an inner sheath of beryllium, which acts to change the neutron spectrum and bring the neutron energies to the thermal region. This also helps in the facilitation of (n,2n) reactions, which further aid in the process of tritium production. Finally, within this beryllium layer is the FLiBe salt, which acts as the heat transfer fluid and tritium production medium.

In the non-irradiation zone, subsystem equipment is shielded from the fast neutron flux environment. The equipment acts to pump and transfer heat from the FLiBe salt, while also filtering and storing the byproducts from salt irradiation.

The piping system is designed to be airtight and not interact with the atmosphere. The piping will also have an interior coated with Titanium Nitride (TiN) or Titanium Carbide (TiC), most likely through chemical vapor deposition. These hard ceramics have been found to prevent tritium diffusion through stainless steel and will aid in the proper processing of tritium [7]. The FLiBe salt also has the potential to pull moisture out of ambient air and could react to further corrode structural components. To prevent this, an inert argon cover gas will be kept at positive pressure inside the loop where salt is not present.

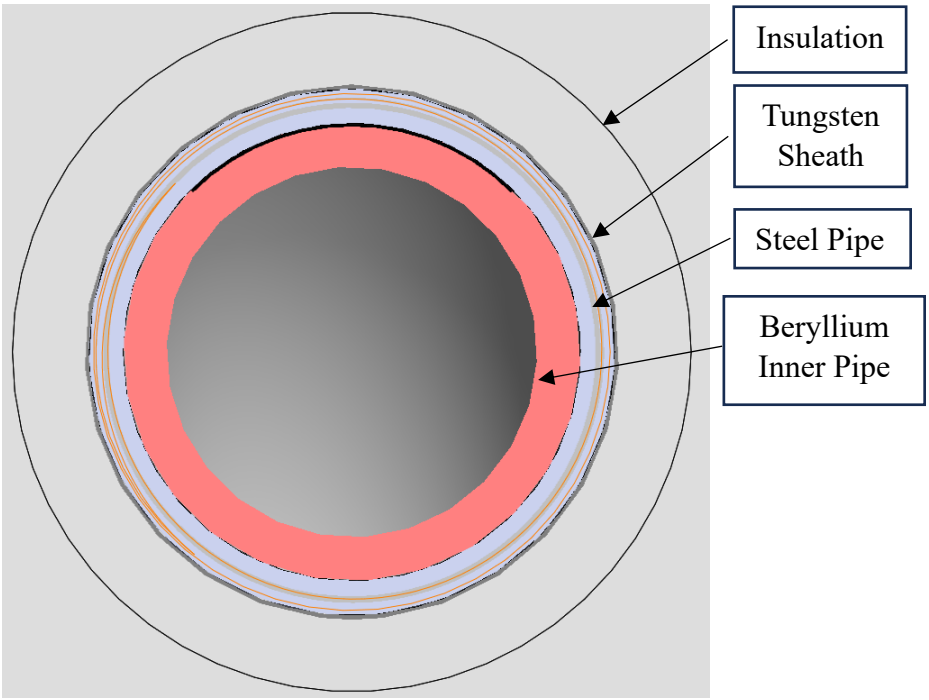

Figure 9 – Close-up Section View of MSTL Irradiation Zone and Layered Piping Scheme

3. Breakdown of Subsystem Design

The comprehensive conceptual design for the UC-MSTL has been finalized and is centered around six key systems crucial to the loop's operation: the FLiBe salt, the pump, filter, control systems, sampling mechanisms, and supporting equipment.

3.1. FLiBe ($LiF\text{-}BeF_2$)

3.1.1. FLiBe Overview

The Molten Salt Test Loop utilizes FLiBe ($LiF\text{-}BeF_2$) salt as its primary working fluid. FLiBe is a very well understood salt and has been studied extensively due to its high thermal heat capacity and ability to breed tritium – a radioactive isotope of hydrogen which is produced via the Li-6 reaction with neutrons [1]. The FLiBe salt also acts to attenuate the high energy neutrons as the primary method of heating occurring in the test loop (reference the Deterministic and Stochastic Calculations for Neutronics Analysis Utilizing CSG Geometry section of the final report for more information on tritium breeding in the MSTL model).

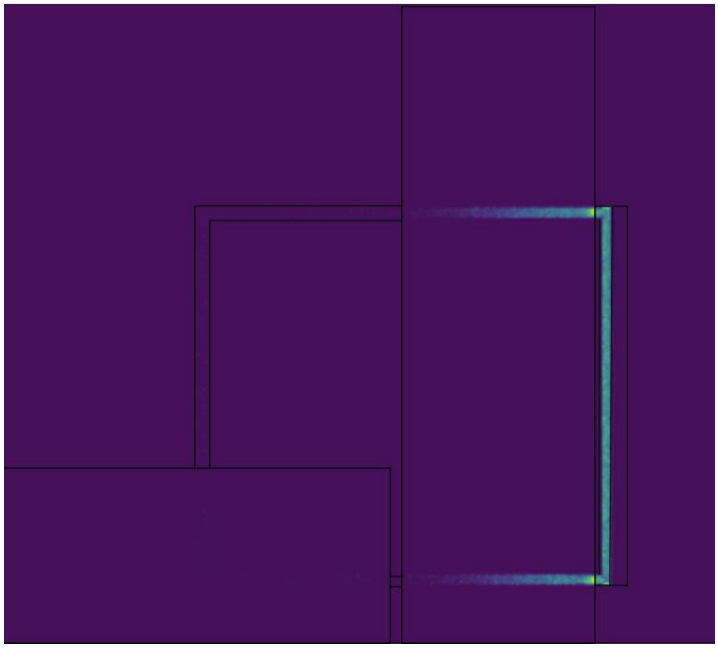

Figure 10 – Cross Section View in xy-Plane of FLiBe Tritium Breeding in MSTL

3.1.2. FLiBe Purity

Numerous experiments have investigated the chemical composition of FLiBe salt for fission and fusion reactor applications. Research on impurity activation remains incomplete and requires documentation via a set of impurity activation experiments utilizing a test loop like the one described herein. The chemical composition of FLiBe salt in the UC-MSTL is detailed in Table 2, where the salt has been theoretically purified to eliminate trace elements or isotopes. Future researchers, operators, and test loop engineers should prioritize elements like K, Na, Mg, Ca, Al, B, and S, which could pose challenges in salt purification [2].

Table 2 – Chemical Composition of $LiF\text{-}BeF_2$ Within UC-MSTL Experiment (ρ = 1.94 g/cm^3)

Isotope	Percent Weight (%)
Li-6	15.03
Li-7	1.67
F-9	67.3
Be-4	16

3.1.3. FLiBe Containment, Loading, and Unloading

The FLiBe salt never exits the containment of the loop during operation, except when being drained for decommissioning activities or sampled through the sampling port or Sampler Enricher (SE). The UC-MSTL team has determined a conceptual process for loading salt into the loop. The FLiBe salt is assumed to be bought and procured – the fusion facility is not assumed to produce or purify their own salt. Heat trace is present along the loop components to maintain the FLiBe at a minimum of 500 C, and a heat sink maintains the FLiBe through the forced cover gas loop such that heat can be dissipated to prevent boiling.

First, salt is received in solid form from a distributor. Second, the solid salt is melted in a high temperature furnace (most likely in batch series) to its baseline operating temperature of 500 C. Simultaneously, the MSTL heat trace operates to heat the loop to operating temperatures. Third, the salt is loaded into the loop. The top purge value of the loop is opened, and a vacuum is drawn. Simultaneous to this operation, the bottom release valve is opened to allow for the FLiBe to leave the furnace and travel through the hard pipe connection to the main loop through a vacuum. This process continues until the FLiBe reaches capacity, or the batch is successfully transferred.

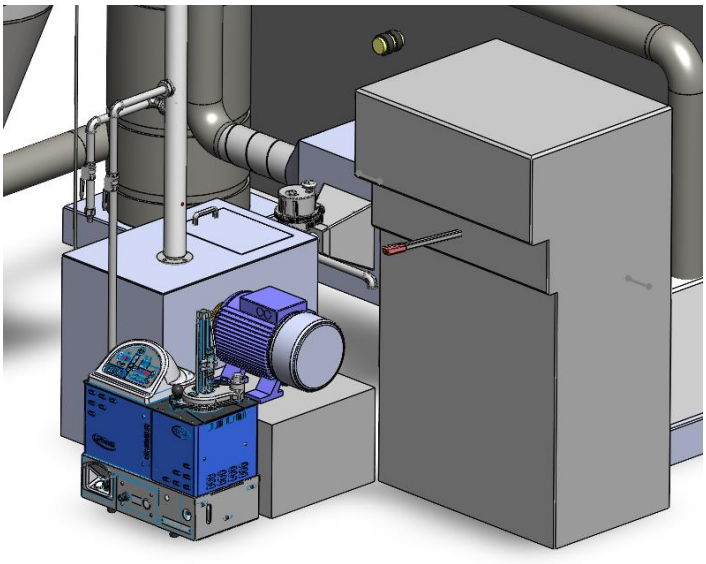

Figure 11 – FLiBe Salt Transfer System to MSTL and Sampler-Enricher (SE)

After operation, the loop will enter a cool-down phase, allowing short half-life activated elements to revert to their ground state. Longer-lived activated elements, potentially present in the FLiBe salt, require proper disposal protocols. The salt must be transferred to a container and kept at its operating temperature until a disposal method is determined. From the literature review, significant gamma ray radiation will be coupled with the alpha particle and tritium production within the FLiBe salt. This must be accounted for in post-operation timing and proper placement of shielding. The salt must be maintained at a molten state while under irradiation, as irradiation of solid FLiBe could release free fluorine gas and pose a health hazard.

3.2. Pump

3.2.1. Pump Material

The compatibility between the pump material and the FLiBe is crucial to the overall performance of the pump, as corrosion-resistant materials must be a primary consideration. Numerous studies have researched the effects of FLiBe on the corrosion-resistance of various materials, including 316 stainless steel and Hastelloy-N. However, Hastelloy-N is not code certified in the ASME Boiler Pressure Vessel Code under sections I, III, B31.1, and B31.3, and therefore cannot presently be used in a commercial reactor without extensive testing [5]. Research was conducted at the University of Wisconsin-Madison on the Fluoride-Salt-Cooled High-Temperature Reactor (FHR) exploring the levels of corrosion of 316 stainless steel in high temperature FLiBe salt. The study concluded that the corrosion attack depth in FLiBe salt was predicted at an acceptable level of 17.1 um/year and 31.2 um/year for 316 stainless steel tested in capsules of 316 stainless steel and graphite, respectively. Tests were performed at temperatures of 700° C for up to 3000 hours [5]. Components that are within the pump do not need to be stainless steel as long as they are not in contact with the FLiBe, but the neutron environment should still be considered.

3.2.2. Pump Location

The pump is to be placed behind the shielding wall and downstream of the tritium filter assemblies, outlines in Section 3.3.

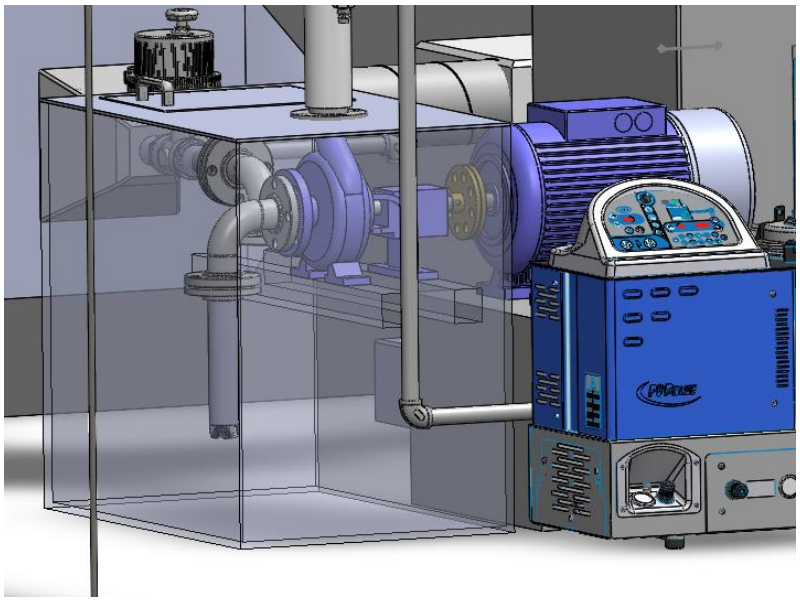

Figure 12 – Pump and Sump Location in MSTL

3.2.3. Pump Design

In designing the circulation system, the pump must be compatible with the viscosity characteristics of the FLiBe salt. A study was performed by MIT to determine the fluid properties of FLiBe for nuclear applications. For a temperature range of 459°C to 1430°C, the viscosity of FLiBe can be defined using the following equation (within 20% uncertainty) [6].

$$\mu\,[\mathrm{Pa}-\mathrm{s}] = 1.164E-4 * \exp\left(\frac{3755}{T[K]}\right)$$

The viscosity when calculated at the baseline temperature of 500°C is as follows.

$$\mu = 1.164E-4 * \exp\left(\frac{3755}{773.15\ \mathrm{K}}\right) = 0.01497\ \mathrm{Pa}-\mathrm{s}$$

Given the low viscosity of FLiBe, a centrifugal pump would be suitable for adequate circulation. The pump size will be a function of the loop size, layout, and required flow rate, as these will affect the head pressure required for the pump. In specific, these parameters will have an effect on the size of the impeller and the number of fins on it which in turn will finalize casing size. The vacuum will need to be verified to make sure that the vacuum pressure from the centrifugal pump is large enough to transport FLiBe and continue the operation of the loop. The vacuum inlet and outlet is theorized to be 2in, Schedule 40- the same size as the rest of the piping in this model.

3.2.4. Pump Shielding

Additional shielding must be considered for protection of pump equipment and electronics. A shielding box or wall could be placed around the outside of the pump. In the case of a box, a door must be considered for maintenance and inspections of the pump system.

3.3. Filter

The transfer of tritium and helium gas produced via the irradiation of the FLiBe salt is imperative to the functionality of the UC-MSTL. The proposed filtering system utilizes a forced argon cover gas system and a coupled nickel-tritium diffusion heat exchanger to extract the tritium from the salt prior to filtering (see section 2.1 for the heat transfer overview of the MSTL). During design development, two methods of filtering were considered for the MSTL- a duct-based system and a centrifugal system.

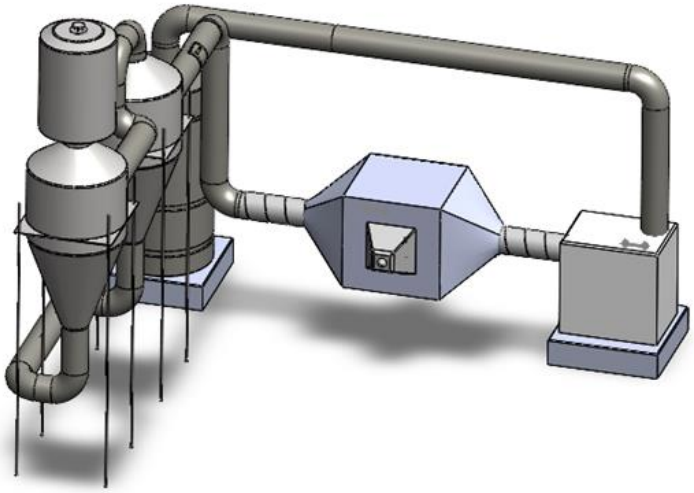

Figure 13 – Forced Argon Cover Gas System Utilizing Centrifugal Tritium separation Unit

The proposed duct-based gas filtration system would consist of a set of 5 ducts and a variable number of filter stacks. These filter stacks could consist of about 10 layers of honeycomb structured rectangular material, staggered by half of a honeycomb's length in a back-and-forth manner. A material that these filter layers could be constructed from is Syndiotactic Polystyrene (SPS) with a 30% glass fiber filament. This material lies within acceptable operating temperatures from –70 C to 200 C, whilst boasting a large thermal shock resistance.

The 5 ducts in the system would be separated into a tritium gas duct, 2 hot gas ducts, and 2 cold gas ducts. The tritium gas duct would be positioned in the center, with the hot gas ducts directly to either side, and the cold gas ducts positioned on the outer edges of the system. An access hatch would be placed along the exterior panel of a single cold air duct to enable the replacement of the filter stacks in a simplified manner. The size of these ducts along with the size of the filter panels are variable and should be adjusted based on calculated optimizations for tritium flow rates.

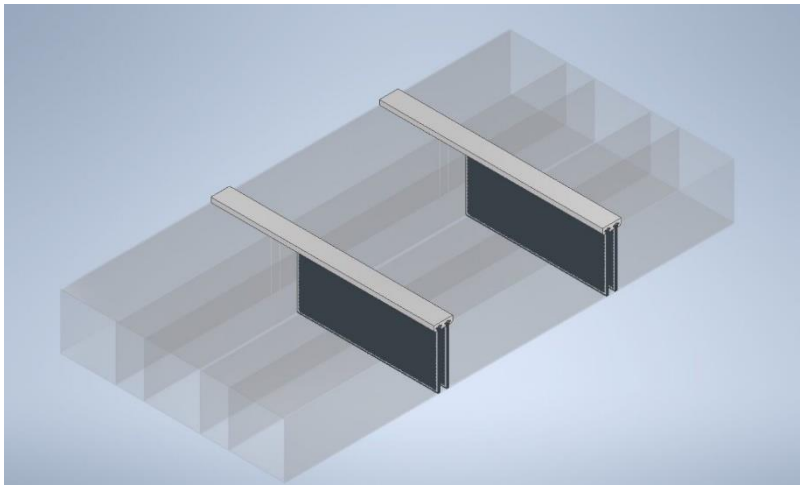

Figure 14 – Variable Duct Filtering Concept

The filter stacks could be placed onto guide rails which would slide the filter panels along the ducts at a regular interval to allow for sustain operation of an applied filter, such as a Metal Organic Framework (MOF). This sliding could be facilitated using magnetic material-based clamps to hold the filter stack together pair with an electromagnetic system to induce the required movement of the filter stacks. The gap between each duct section could be minimized with the addition of a gasket to reduce gas leaks during motion. See the videos below for a visualization of the process.

Sliding Filter Demonstration Isometric

Sliding Filter Assembly Demonstration

Another possibility for the filter system would be a 3-stage filtration approach utilizing a cyclone-style filter. The off gas could be propelled through the filter system at a set flow rate by utilizing an argon purge gas. The purge gas would increase the velocity of the off gas and increase the efficiency of the initial filtration stages. The first stage of filtrations would use an immobile stack of the previously mentioned honeycomb filters, removing most non-particulate debris from the off gas. This filter stack could be maintained or replaced through an access hatch in the intake duct, similar to the access hatch used in the 5-duct system. The second stage of the filter could occur within a cyclone chamber, where the combination of gases would enter the chamber at a specified angle, to maximize centrifugal force on the gases alongside time within the chamber. Due to the difference in mass between the off gas and argon gas, the gases will separate with the of gases rising to the top of the chamber and the argon gas and most remaining contaminants falling to the bottom of the chamber. The centrifugal force applied by the chamber shape would accelerate this process. The third stage of filtration could take place at the top of the chamber, where a membrane filter could be placed across the outlet channel. This membrane filter would have a selectivity leaning towards helium or tritium and serves to further purify the tritium gas. Stages 2 and 3 of the filter system could be iterated as much as necessary to obtain the desired purity of the tritium gas.

Once this purity is obtained, the tritium gas could be collected and stored within a chamber containing a tritium adsorbing MOF. Sections of the MOF could be removed from the chamber's interior to maximize the exposed MOF surface area, thus maximizing potential storage within the chamber. If tritium degrades to helium, the helium gas would escape from the pores of the MOF, so to prevent a pressure buildup within the chamber an exhaust vent could be implemented on the top of the chamber to release any inert gases.

The cyclone filter system was selected in the final model of the UC-MSTL due to the long history of cyclone-based gaseous filtration systems in the nuclear industry and readily available data.

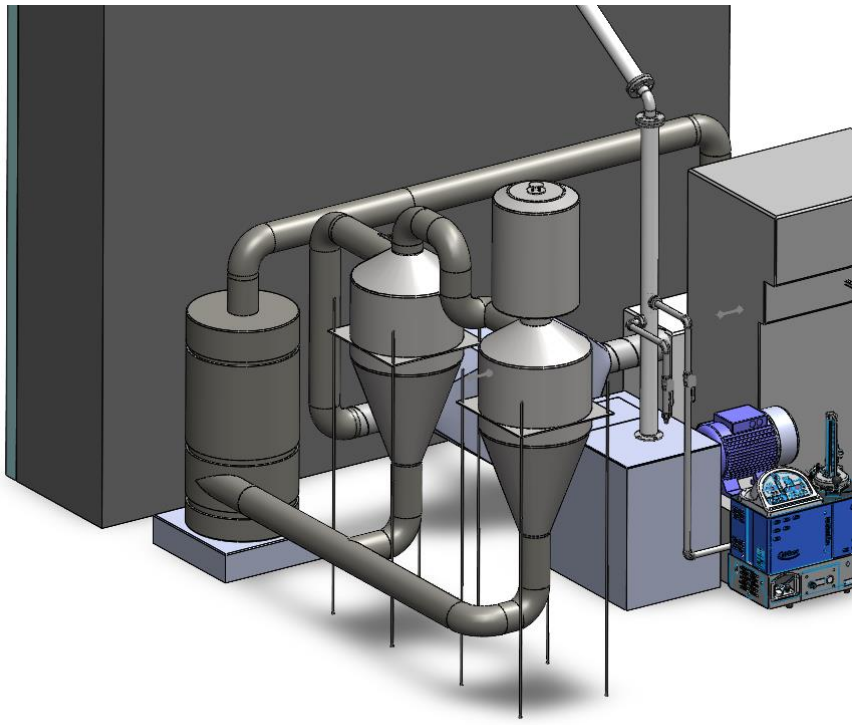

Figure 15 – Centrifugal Filtering Concept Employed in MSTL Model

The proposed Metal-Organic Framework (MOF) solid tritium storage material, namely NU-2100, would be a Cu(I)-based MOF created using a mixture of H2BBTA, Copper Chloride, and Zinc Chloride. The Zinc will act as a catalyst to transform H2BBTA into NU-2100 without allowing Zinc into the final structure. The precipitant would consist of Copper, Hydrogen, Carbon, and Nitrogen atoms chemically bonded. They could be bonded using vacuum heaters, sonicators, and isolated environments such as flasks and glass 3-dram vials. The resultant mixture would be cleaned with DMF to isolate the created NU-2100. The resultant MOF could be analyzed using a single electron microscope by carbon coating the sample, a thermogravimetric analyzer which would heat the sample from room temperature (r.t.) to 600°C at a rate of 10°C/min, and a BET surface area and porosity analyzer using nitrogen gas as the adsorbent at 77K.

The structure created could be viable for Hydrogen and Hydrogen-Isotope capture using various unit cells in the MOF's lattice structure as containment chambers called "activation sites" where functional Nitrogen linkers in the structure could act as nodes for deprotonation-based chemisorption that could target Hydrogen ions. Hydrogen ions could be targeted through physisorption as well, considering the various positive/negative charges of sites along the pores and the diameter of the pores themselves.

When considering the duct based filtering system, the "activation sites" would become primed to capture hydrogen and hydrogen isotopes during the filtering cycle when the gas is cooled to 77 K. When the heating chamber closest to the filter is powered off, the filter system could transport the primed Metal Organic-Framework to the main chamber, where the MOF would capture the Tritium isotopes through physisorption. Once cycled into the next adjacent heating chamber, the activation sites would increase in size due to the heat and will allow the purge gas to carry the captured Tritium away to another chamber.

If the 3-stage cyclone filtration approach is used, then the weight difference between Tritium and Argon would allow for the separation of both gases. The MOF would be stored in a chamber placed at the end of the 3-stage filtration system, just after the membrane filter. The chamber could be kept at 77 K to keep the MOF's activation sites primed to receive the tritium, removing the previous process' need to absorb the MOF. Since the Tritium would be contained within the chamber, after a set maximum storage capacity is reached, the chamber could be replaced by another if more tritium is still being produced. The removed chamber could be isolated and contained to allow the adsorbed tritium to be handed safely.

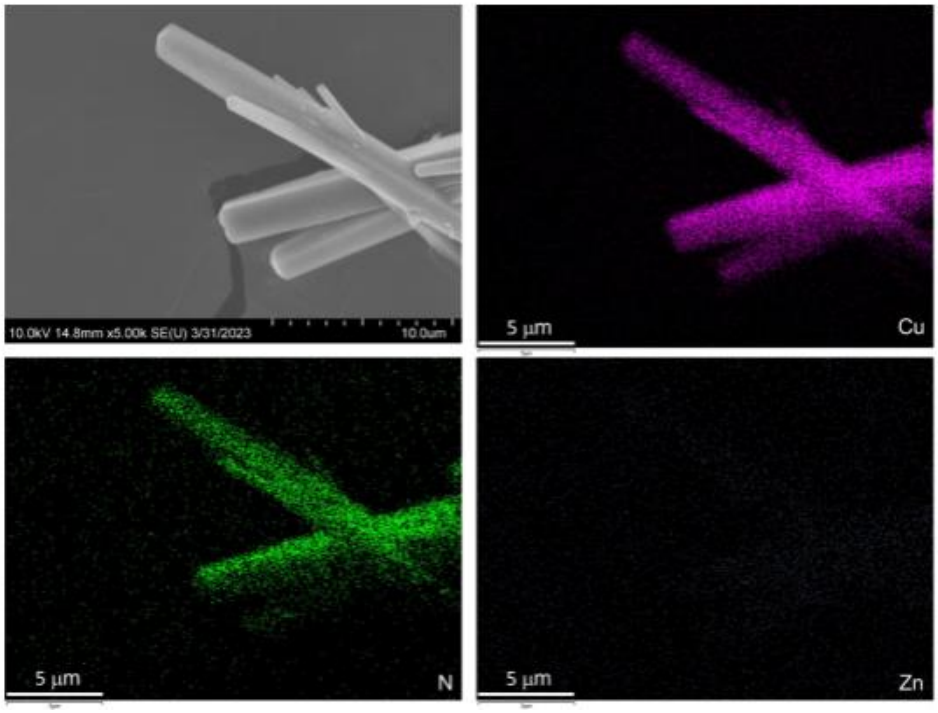

Figure 16 – Scanning electron microscopy (SEM) images of Intermediate and electron

Density mapping analysis of constituent atoms of NU-2100; pink (Cu); green (nitrogen); and red (blue). The amount of zinc is not detectable with respect to copper.

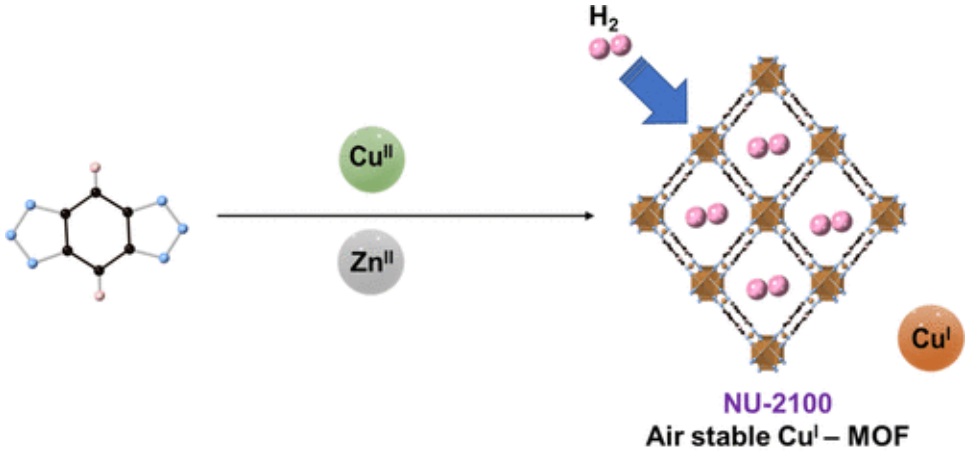

Figure 17 – NU-2100 Molecular Crystalline Structure

3.4. Supporting Equipment

There are three primary groups of support equipment in the UC-MSTL model: connected, structural, and shielding. Each is defined by how it contributes to a key requirement of the loop functionality and/or safety. The support equipment can be passive components that are fully integrated into the loop system to active devices that operate beyond the primary functional areas of the loop.

Connected components are devices or parts fully integrated into the system's functional areas. These connected components are primarily part of the FLiBe loop system in the form of inlet/outlet fittings with valves which can be used to add or remove material from the loop. In the back of the loop, there are three of these: one for the loading of FLiBe, one for the loading of gas, and one for the unloading of FLiBe. The single gas port is designed with a quick disconnect, so that any argon gas canister can be connected to the loop for use as the cover gas. The two FLiBe ports are directly connected to external devices. The FLiBe inlet is connected to an intermediary heater tank, separate from the one integrated into the loop. This allows for material to be added to the loop without directly interacting with the loop. The FLiBe outlet is connected to a sample enricher which will be further discussed in Section 3.6.2.2.

Structural components are devices and assemblies used to physically support the functional areas of the system. All the functional areas of the system have structural components. The ducts and pipe of the loop will be supported by a simple scaffold structure that is capable of holding the mass of both the FLiBe and pipe/duct of the loop. When components cannot be placed on the ground but are too heavy to be suspended, a concrete pad is used to mount the device. This concrete pad would be prefabricated and secured in place on site.

There are many areas of the loop where additional shielding, separate from the primary shielding wall, would be needed to protect the sensors and electrical components. For larger components, such as motors, shielding boxes or walls will need to be built to ensure continued operation of

the loop. These shields would need to be designed with accessibility in mind in case future maintenance requires access to the machinery. For smaller devices, such as flow meters, simple leaded blankets could be used to shield them while also allowing for easy future accessibility.

3.5. Controls

At the most basic level, the control systems presented in this project should ensure safe, intuitive, and accurate assessments of real time system performance. These systems should also allow operators to utilize all crucial controls in real time from a remote location. The first measure that could be taken for the project's safety is implementing emergency stops. These E-stops could be positioned at locations where multiple systems overlap, locations where there is a single point of failure, and locations where operators would have easy access to them. The E-stops could be supplemented by control logic that deactivates select systems in the event of irregularities within system operations. To comply with industry standards, the E-stops should be a bright red color to ensure visibility from a distance. Once pressed, the activation of the E-stop could be reflected in a central operations location.

Another key aspect of the control systems could be the presence of a central location, where all critical systems can be viewed, and any irregularities analyzed promptly. Some of the main features that could be utilized in such a room could be several monitors to display necessary system information and a variety of alarms. The monitors could display exact system information for analysis and operations purposes, whilst the alarms could include audio and visual stimuli to express critical issues or deviations. By setting up such a system, the central controls room would be able to maintain the integrity of all systems with a minimal operations force and minimal chance of error.

Further control systems could be integrated to control flow rates of off-gases, the FLiBe, or other crucial components. This control would enable better planning for tritium filtration purity, total system cooling, sensing accuracy on every part of the system, and allow for optimized operations given a wide variety of circumstances.

3.6. Sampling

3.6.1. Sampling Overview

Sampling is a primary focus of the MSTL and is derived from several resources and texts from previous molten salt experiments. Both real-time sampling and delayed (decommissioning) sampling are to be detailed in this section. Table 3 details the sampling mechanisms, sampling materials, their operation domain, and a brief overview of their usage. Sample amounts, techniques, and methods documented are subject to change per project direction and need.

Table 3 – Sampling Mechanisms in the UC-MSTL

Sampling Equipment	Location	Sampling Properties	Material to be Sampled	Quantity of Material and Tests		Method	In Situ or Decommissioning
Structural Coupons	Inner containment pipe (see fig 17).	Surface degradation, corrosion, and activation	Stainless Steel Piping Material with TiN or TiC coating	All coupons- visual inspection, SEM, XRD, XPS, NAA, presence of oxides, hydrides, discoloration, embrittlement etc.		Physical removal, subsequent analysis	Decomissioning
Magnet Coupon	Inner containment pipe in irradiation zone	Activation	HTS Magnet	All magnet material – visual inspection and NAA		Physical removal, subsequent analysis	Decomissioning
Miscellaneous	Throughout MSTL	Surface degradation, corrosion, and activation	Sensors, cover gas, welds, pipe segments, pump shafts, ports, filter material	Variant material and tests based on sub team requirements		Physical removal, subsequent analysis	Decomissioning
Sampler-Enricher (SE)	Pump well	Li-6 Enrichment, elemental (molar) concentration, elemental composition, activation, viscosity, ICP Spectroscopy, particle size, and	$LiF-BeF_2$ salt	Li-6 enrichment	Varies	Dip sample, operational removal, subsequent analysis	In Situ
				Molar concentration	~ 1g		
				Elemental composition	~ 1g		
				Activation	Varies		
				Viscosity	~ 1g		
				ICP spectroscopy	~ 1g		

		Thermo-physical properties.		Particle size	~ 1g		
				Thermophysical properties	~ 1g		
Salt Drain Container (SDC)	Exterior to MSTL connected to containment pipe	Li-6 Enrichment, elemental (molar) concentration, elemental composition, activation, viscosity, ICP Spectroscopy, particle size, and Thermo-physical properties.	$LiF\text{-}BeF_2$ salt	Li-6 enrichment	Varies	Dip sample, physical removal, subsequent analysis	Decomissioning
				Molar concentration	~ 1g		
				Elemental composition	~ 1g		
				Activation	Varies		
				Viscosity	~ 1g		
				ICP spectroscopy	~ 1g		
				Particle size	~ 1g		
				Thermophysical properties	~ 1g		
Neutron Activation Detector (NAD)	One detector for all equipment	Activation (Bq)	Gamma ray emissions (indirect neutron energy)	All incident particles		Neutron capture followed by gamma ray spectroscopy	Decomissioning
Fission Chamber	Shielding Wall	Neutron flux ($n/cm^2/s$)	Neutrons	All incident particles		Fission event followed by scintillation	In Situ and Decomissioning
Li^6(Eu) Detector	Displaced off shielding wall	Neutron Flux ($n/cm^2/s$)	Neutrons	All incident particles		Li^6 capture event followed by scintillation with Eu dopant	In Situ

3.6.2. FLiBe Sampling

FLiBe salt sampling will be conducted during operation and post operation, with the latter for decommissioning activities and classification.

FLiBe sampling mechanisms will require additional equipment for the proper operation of the MSTL. The two most prominent pieces of equipment include the Sampler-Enricher (SE) and Salt Drain Containers (SDC)s. One of the most influential sources on these systems has been the Molten Salt Reactor Experiment of Oak Ridge National Laboratory (MSRE, ORNL). The experiment involved the implementation of a Sampler-Enricher (SE), which was utilized to sample and enrich the fuel salt in a high radiation environment [3].

3.6.2.1. Salt Drain Container (SDC)

FLiBe sampling post operation will be imperative to direct decommissioning and disposal activities. After a cooldown period, The FLiBe salt must be pumped out of the MSTL into a suitable shielded container, namely the SDC, which isolates the salt while keeping it liquid until removal from the device containment building. The salt will then be sampled from the container to determine final chemical characteristics. Simply stated, the salt will be able to be physically agitated and collected in Salt Sampling Containers (SDCs) before transport for analysis.

3.6.2.2. Sampler-Enricher

An implemented MSTL Sampler-Enricher (SE) would not face nearly the same challenges as the MSRE. The MSTL does not utilize fissile material and will not have nearly the same waste concerns due to the lack of transuranic or actinide material present. The FLiBe, however, will be greatly activated upon sampling. Nonetheless, an implemented SE device in the MSTL would allow for sampling of the salt for the criteria as documented in Table 2 and allow for enrichment of the Li-6 isotope in the salt if needed.

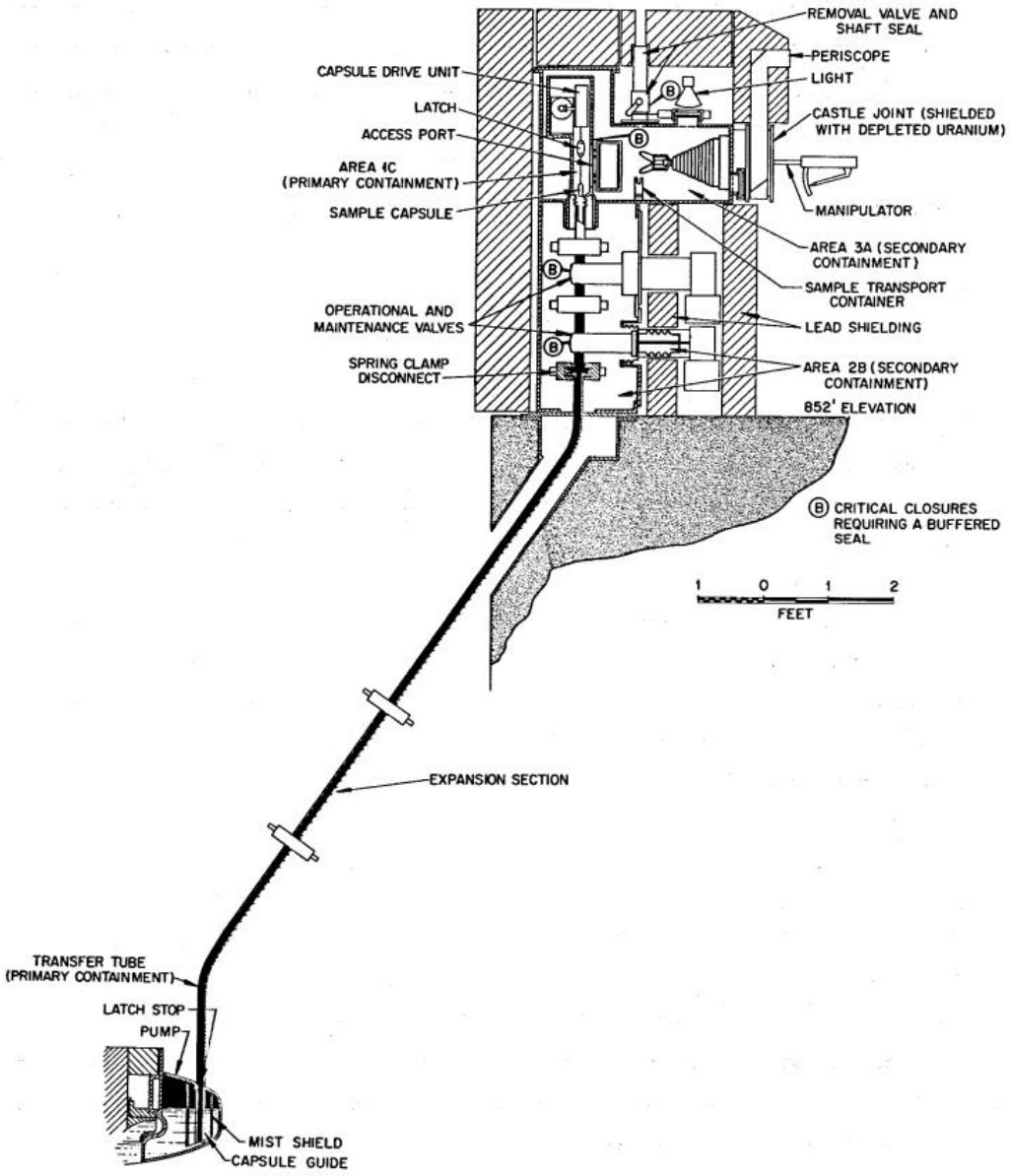

Figure 18 – Molten Salt Reactor Experiment (MSRE) Sampler-Enricher Device [3]

3.6.3. Structural Sampling – Surface Degradation, Corrosion, and Activation

Surface degradation, corrosion, and activation of structural material such as stainless-steel piping must be accounted for in the decommissioning of the MSTL. Nuclear decommissioning is a complicated and time-consuming process. Oftentimes, decommissioning activities must be completed remotely in order to protect rad workers from dosage, and it can be incredibly hard to preserve sampling material without contamination from debris. To remedy this problem, coupons will be added to the inside of the piping and will be removed first in order to preserve the quality of sampling results.

The coupons are proposed to be made of 316 Stainless steel, 4” x 4” in size, and 1/32” thick. They are to be placed along the inside of the piping and bent to the inner radius to conform with

the surface area. Four coupons will be used for the MSTL. They will then be spot welded such that salt cannot ingress between the coupon and the piping. Upon decommissioning, the coupons will be pried off manually to break the welds. The surface of the coupon indicates a change to the structural integrity of the inner surface material or if corrosion occurred during operation. Further, investigation of the TiN or TiC coating on the inner wall of the piping will determine how high operating temperatures affect ceramic degradation. Neutron Activation Analysis (NAA) can determine if the activation of suspect elements for disposal concerns such as Fe, Cr, Mo, Nb, Ni, W are present (see Table 2 for full suite of analysis). Figure 19 shows the location of one of the four coupons in the system.

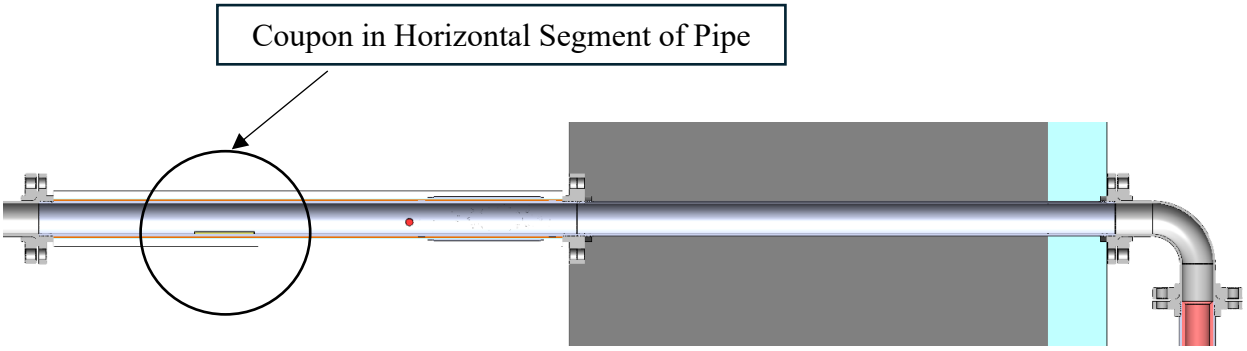

Figure 19 – Coupon present in Horizontal Section of MSTL

3.6.4. Magnet Sampling – Activation

Specialty material compositions are utilized in magnetically confined fusion devices to stabilize plasma for fusion reactions. However, very little data exists on the activation and shielding of this novel magnet material. Current designs of advanced fusion devices look towards the primary working fluid to shield the magnets from the intense neutron radiation produced from the plasma. The MSTL provides this data by including a magnet sample, much like the coupons in the previous section, to gather data on the shielding properties of FLiBe salt. The magnet coupon is present in the irradiation zone facing the neutron irradiation “beam” and is packed in a thin, stainless-steel sheath to protect it from direct FLiBe interaction, as seen in Fig 18. Subsequent measuring devices could be employed to further study the magnetohydrodynamic aspects of FLiBe salt in the magnet coupon region.

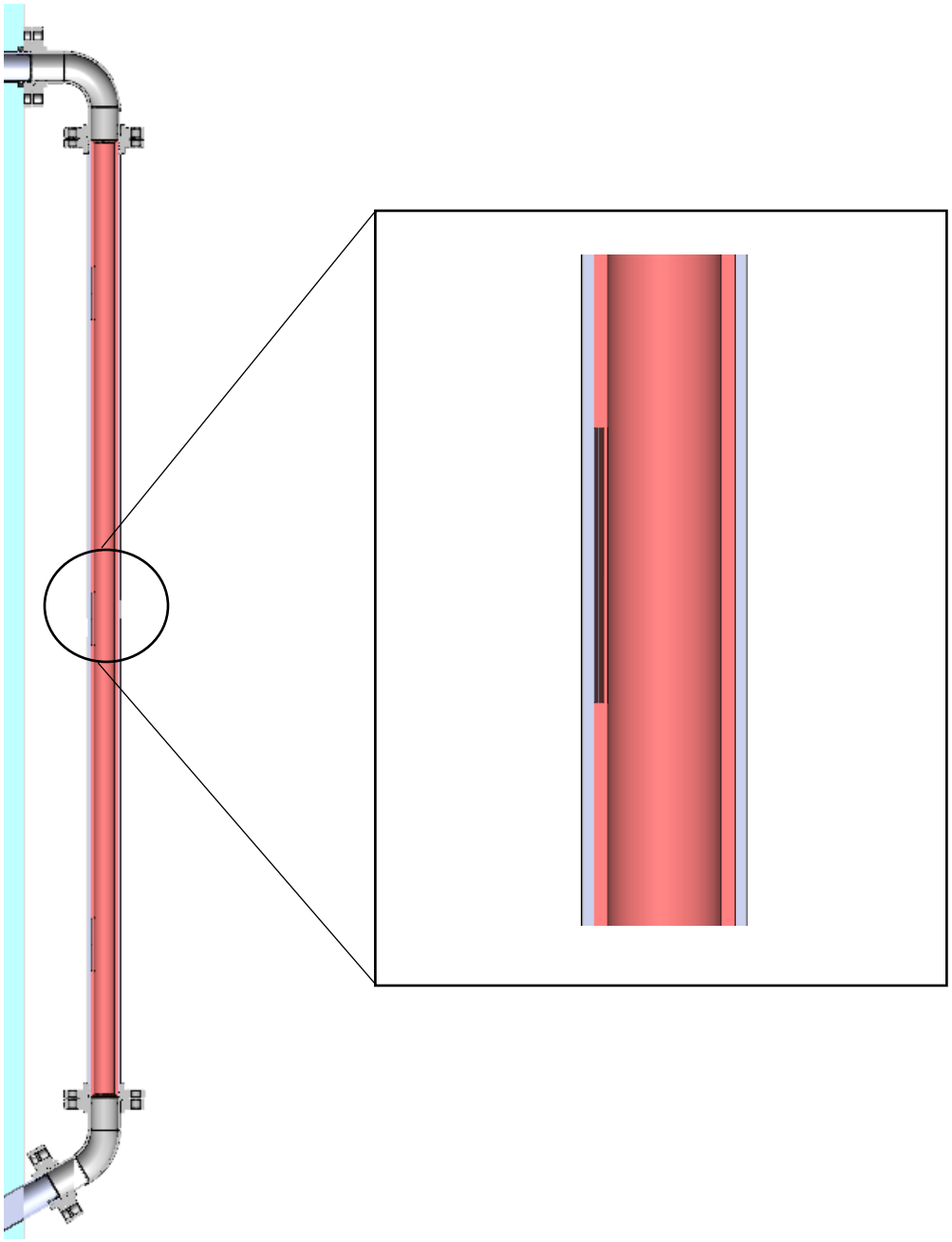

Figure 20 – Magnet Coupon Present in Irradiation Zone of the MSTL

3.6.5. Radiation Environment Sampling

Verification of the MSTL radiation environment is an essential requirement for proper operation. As fusion device operations continue into steady state experiments, activation of salt and equipment will need to be characterized. Shielding simulations and hand calculations will need to be evaluated for their accuracy. Thus, neutron flux measurements will be made using both real time and delayed techniques through fission chambers, Neutron Activation Detectors (NAD)s,

and specialized scintillation devices for fast flux environments, such as those utilizing Li^6Eu. Table 2 highlights the equipment in the MSTL for measurement of the radiation environment.

3.6.5.1. Delayed Measurement Techniques

As part of decommissioning activities, NADs will be used to verify the proper function of the shielding employed by the MSTL and the MCNP simulations conducted on the loop model. Each piece of equipment in the MSTL will have its own NAD. Results of NAA performed on the equipment present in the MSTL will also quantify the radiation environment, such that scattering events can be predicted.

3.6.5.2. Realtime Measurement Techniques

Both fission chambers and the specialized Li^6Eu scintillator will be employed to measure the neutron environment surrounding the MSTL. The Li^6Eu detector was selected for its specialized performance in high neutron energy environments [4]. More suitable detectors may be selected as technology improves. The fission chambers will be used to verify the neutron energy while the scintillator will provide data on the neutron flux present on the opposite (non-irradiation) side of the shielding. The exact number of fission chambers and scintillators for the MSTL will need to be determined at a later date using more complex simulations and sensitivity analysis in order to produce an “adequate” basis for radiation environment validation.

3.6.6. Miscellaneous Equipment Sampling

Upon decommissioning, it will be imperative to preserve certain sections and equipment of the MSTL for activation analysis, visual inspection, material degradation, and many more processes. These equipment types and analyses will be determined by individual needs and project directives.

A. References

[1] Ying, D., Yang, H., Lyu, H., Tan, Y., Jing, F., Li, L., Xiao, F., Liu, J., Zhang, H., Yang, J., & He, T. (2019). Activation of FLiBe coolant in the molten salt reactor. Annals of Nuclear Energy, 129, 62-66, https://doi.org/10.1016/j.anucene.2019.01.038

[2] Carotti, Francesco, et al. “Datasets for Elemental Composition of 2LiF-BEF_2 (Flibe) Salt Purified by Hydro-Fluorination, Analyzed by Inductively Coupled Plasma Mass Spectrometry (ICP-MS) Using Two Digestion Methods.” Data in Brief, Elsevier, 10 Oct. 2018, www.sciencedirect.com/science/article/pii/S2352340918311314.

[3] Gallaher, R. B. “Operation of the Sampler-Enricher in the Molten Salt Reactor Experiment .” ORNL-TM-3524, Oak Ridge National Laboratory - Union Carbide Corporation, 1971, moltensalt.org/references/static/downloads/pdf/ORNL-TM-3524.pdf

[4] Fowler, J.L., et al. “Use of Li6i(Eu) as a Scintillation Detector and Spectrometer for Fast Neutrons.” *Nuclear Instruments*, North-Holland, 30 Oct. 2002, www.sciencedirect.com/science/article/abs/pii/0369643X58900355

[5]Zheng, Guiqiu, et al. “Corrosion of 316 Stainless Steel in High Temperature Molten Li2BeF4 (FLiBe) Salt.” Journal of Nuclear Materials, Volume 461, June 2015, Pages 143-150, https://doi.org/10.1016/j.jnucmat.2015.03.004.

[6] Romatoski, R. R. and L.W. HU. "Fluoride salt coolant properties for nuclear reactor applications: A review." Annals of Nuclear Energy 109 (November 2017): 635-647, http://dx.doi.org/10.1016/j.anucene.2017.05.036.

[7] Changqi, Shan, Aiju, Wu, Yongjing, Li, Ziqiang, Zhao, Qingwang, Chen, Qiurong, Huang, and Suolang, Shi. The behaviour of diffusion and permeation of tritium through 316L stainless steel with coating of TiC and TiN + TiC. Netherlands: N. p., 1992. Web.

Deterministic and Stochastic Calculations Utilizing CSG Geometry for Neutronics Analysis

Austin Michael, Jackson Stanley

University of Cincinnati Molten Salt Test Loop
UC-MSTL

University of Cincinnati
BSME Class of 2024

THIS PAGE PURPOSELY BLANK

1. Introduction

1.1. Purpose of Document

This document is dedicated to exploring and presenting the application of both deterministic and stochastic calculations for neutronics analysis, specifically focusing on the conceptual design of the University of Cincinnati Molten Salt Test Loop (UC-MSTL). By integrating deterministic methods for precise calculations and stochastic approaches to address uncertainties, the document seeks to offer a comprehensive understanding of the intricate interactions within nuclear systems. These systems are instrumental in providing data on various aspects such as shielding, activation of structural and working materials, heat transfer, energy deposition, neutron flux, and tritium breeding. The analysis employs CSG (Constructive Solid Geometry), with the utilization of the OpenMC software, to enhance flexibility and accuracy, providing valuable insights into neutron behavior and distribution across diverse geometrical configurations. Through this exploration, the document aims to contribute significant insights to the field of fusion nuclear science and engineering, facilitating advancements in the operation and testing of fusion devices.

1.2. Document Scope

The scope of this document involves a thorough investigation of neutronics analysis carried out for a Molten Salt Test Loop within the framework of a fusion reactor application. Utilizing the Bateman equations for NAA, straightforward neutron attenuation calculations for shielding design, and sophisticated workflows for stochastic modeling employing OpenMC, the document also incorporates supplemental equations for statistical analysis. It holds significance for material classification, waste disposal, activation, tritium breeding, energy deposition, and project direction. It is important to note that the scope is limited to a conceptual design.

1.3. Background

The University of Cincinnati senior design group is actively researching open-space and readily available fusion reactor devices, such as those developed by Commonwealth Fusion Systems (CFS) and other fusion energy startups (General Atomics, et al.). In line with this, the group aims to undertake a conceptual design project focused on a molten salt test loop. This test loop is designed to simulate the nuclear, thermo-fluid, and heat transfer properties of liquid salt, specifically for applications in heat transfer within a fusion device. The project, known as the UC Molten Salt Test Loop (MSTL), seeks to document anticipated engineering challenges, current and required empirical data, and preliminary results derived from heating, fluid flow, and neutronics calculations. Additionally, the team is exploring steady-state solutions for tritium capture and storage. The ultimate objective of this conceptual design is to fulfill graduation requirements for senior mechanical engineering students of the class of 2024, serving as a capstone project.

1.4. System Description

To validate the effectiveness of fusion breeder blankets, private fusion enterprises must generate essential experimentally gathered data using a test loop, integrated into operations. This test loop

aims to leverage the high neutron flux environment to simulate crucial aspects of fusion device operations, encompassing tritium breeding, heat transfer, thermo-hydraulic flow, and the magnetohydrodynamic aspects of salt. The test loop will feature techniques for real and delayed nuclear data gathering, mechanisms for sampling molten salt and structural materials, and innovative subsystems for byproduct removal. The overarching goal is fusion power plant design and implementation.

1.5. Project Scope

1.5.1. Users

Users of this study include but are not limited to future system designers and engineers, project managers, stakeholders, academics, and regulatory bodies, such as the Department of Energy (DOE) and Nuclear Regulatory Commission (NRC).

1.5.2. Need

The test loop will provide essential experimentally gathered data in order to validate the operational assumptions for fusion powerplants. Data gathered through test loop construction and design will also provide a basis for subsequent fusion device manufacturing and plasma physics research.

1.5.3. Location

The calculations in this document are composed for a conceptual test loop. The calculations can be transferrable to a physical system given augmentation by future engineering teams and the collection of experimental data.

2. Introduction to Neutronics and Nuclear Fusion Engineering

Note: If familiar with the definitions of neutronics, fusion neutronics development, and mathematical concepts behind neutron modeling, proceed to section 3 (three) of this document.

2.1. Simplified Definition of Neutronics

Neutrons are subatomic particles found in the nucleus of atoms. Neutronics, in simple terms, is the study of how neutrons behave in various materials, particularly within the context of nuclear reactions. Understanding the neutron's behavior is crucial for applications ranging from nuclear power to medical imaging.

In the study of neutronics, researchers investigate the interactions, movement, and consequences of neutrons with materials. Neutrons are comparable in size to protons on a macroscopic scale. They also possess a neutral charge which is crucial for stabilizing atomic nuclei. Their energy is determined by velocity, often generated through nuclear reactions, making them integral to nuclear reaction processes. Consequently, neutrons play a vital role in the design and analysis of nuclear systems, particularly reactors, where precise control of neutron behavior is essential for ensuring safe and efficient energy production.

In essence, neutronics provides insights into the intricate dance of neutrons within atoms, helping us harness their power for beneficial purposes while ensuring safety and optimal performance in various technological applications.

2.2. Fusion Energy and the Neutron

In fusion energy, neutrons are primarily generated through the fusion reactions within a fusion reactor's plasma. The most common fusion reaction involves isotopes of hydrogen for fuel—*deuterium*, a hydrogen atom with one neutron, and *tritium*, a hydrogen atom with two neutrons. These isotopes are simply a standard hydrogen nucleus with an additional neutron and two additional neutrons, respectively. When two isotopes undergo fusion, they form helium and release a high-energy neutron.

In a magnetically confined fusion device, such as a tokamak, the process of neutron generation is intricately linked to the complex physics of plasma confinement and fusion reactions. First, deuterium and tritium gas are pumped into the reactor vessel, (deuterium- deuterium reactions can be induced, but will not be covered in this brief section). A high temperature sequence is started to heat up the gas into a plasma state of matter. The device then employs a strong magnetic field to confine the hot, ionized plasma. The magnetic confinement is achieved by shaping the magnetic field into a toroidal configuration, creating a donut-shaped plasma vessel. Within this vessel, the magnetic field lines prevent the hot plasma from touching the walls, maintaining the high temperatures (to the order of $\sim 10^8$ degrees Celsius) necessary for fusion. At these extreme temperatures, the kinetic energy of the particles overcomes the electrostatic repulsion, allowing positively charged nuclei to collide and undergo fusion reactions. A schematic of the tokamak is shown in Figure 1. The green interior is the fusion plasma, while the red and pink rings surrounding the vacuum vessel describe the magnetic field inducing the plasma current [4].

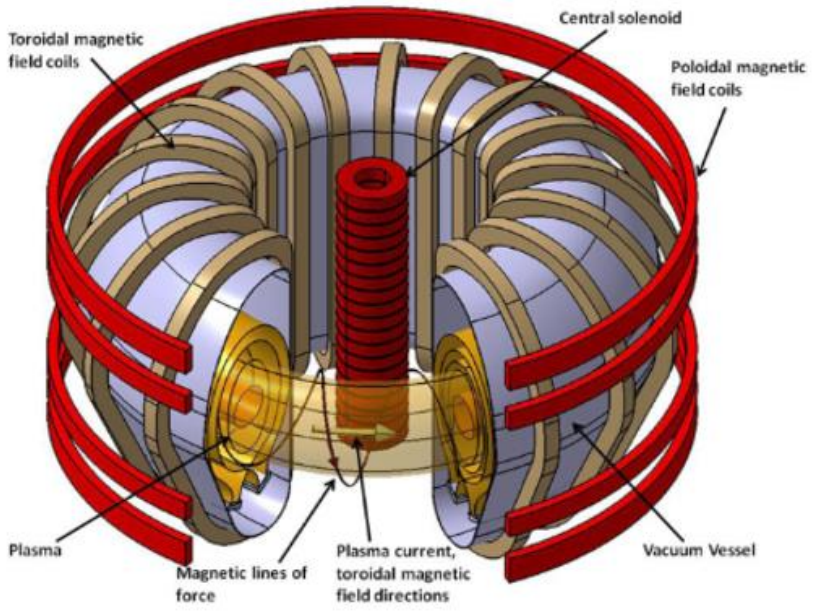

Figure 1 - Tokomak Fusion Reactor Schematic

In the specific case of deuterium-tritium (D-T) fusion, the reaction is as follows:

$$\mathbf{{}_1^2H + {}_1^3H \rightarrow He_2^4 + n_0^1} \qquad \textbf{(Equation 1)}$$

In this equation, a deuterium nucleus collides with a tritium nucleus resulting in the formation of a helium atom and the release of a high energy neutron. The generated neutrons carry a significant portion of the released energy and play a crucial role in sustaining the fusion reaction. However, they also can cause structural damage to reactor components through nuclear reactions and increasing activation, directly contributing to nuclear waste generation. Thus, nuclear engineers must dedicate significant resources to the simulation of these neutrons released through fusion reactions to accurately model power production and limit damage to the fusion device.

Neutrons also play a significant role as a source of isotopes for important functions including medical imaging, cancer treatment, and tritium production. Neutrons generated during fusion reactions can be harnessed to produce tritium through a process involving a lithium breeder blanket. The high-energy neutrons released during fusion reactions interact with lithium isotopes in the breeder blanket. Lithium-6, a specific isotope of lithium, absorbs these neutrons and undergoes a nuclear reaction, converting into tritium and helium. This tritium can then be extracted from the lithium breeder blanket and used as fuel for the fusion device in a self-sustaining cycle. This reaction is described by:

$$\mathbf{{}_3^6Li + n \rightarrow {}_2^4He + {}_1^3H + 4.78\ MeV} \qquad \textbf{(Equation 2)}$$

The energy generated in this intense reaction primarily manifests as the kinetic energy of helium and tritium particles, which dissipates quickly through heat transfer. This temperature rise

establishes the mechanism enabling fusion power plants to function. The downstream aspects of the system eventually include driving steam turbines to generate electricity.

Essentially, the neutrons created during fusion not only contribute to the energy production, but also participate in generating additional fuel, ensuring the continuous operation of the fusion reactor. This process is crucial for achieving a sustainable and efficient fusion energy system.

2.3. Equations for Neutronics Modeling

Two different forms of equations are used to perform analysis in nuclear engineering- deterministic and stochastic.

2.3.1. Deterministic Calculations

Deterministic equations aim to provide exact solutions. These equations are typically used when the system being modeled is assumed to be deterministic, meaning that its future behavior is completely determined by its current state and the governing equations. An example of this is employed in the field of neutronics to perform shielding calculations. Shielding calculations provide exact values for the thickness of material, often called a shield, needed to stop neutrons from activating or damaging equipment, as detailed in the deterministic section of this document.

2.3.2. Stochastic Calculations

Probabilistic or stochastic approaches involve randomness and uncertainty. Stochastic methods are utilized for neutronic simulations that require a high degree of computational power, as inherent in Monte Carlo analysis. Stochastic calculations are used to simulate the behavior of particles or photons by sampling probabilistic events. Monte Carlo simulations are applied in areas such as neutron transport, which provide insights as to how materials behave when interacting with neutrons. The results of stochastic methodologies can inform engineers as to which materials may be damaged by neutron irradiation, how much energy is being deposited into a region, or importantly how much energy is being generated by a particular reaction in the device. Simulations that incorporate Monte Carlo algorithms output important mathematical values including neutron flux and energy deposition to describe how neutrons interact within the test loop, as detailed in the stochastic section of this document.

3. Overview of Loop Conceptual Design

Refer to the System Design Description (SDD) in the final UC-MSTL report for a complete overview of the model.

4. Deterministic Calculations

The deterministic calculations were comprised of a shielding calculation and a neutron activation analysis, as discussed in the following sections.

4.1. Shielding Calculations

Shielding calculations provide more accurate neutronics modeling, especially given simplified geometries. A shielding system was designed under the ALARA (As Low as Reasonably Achievable) principle to protect the equipment from intense neutron irradiation and subsequent activation, as outlined in the functional requirements document.

Shielding material compositions were determined on an element-by-element breakdown and a corresponding atomic weight percent, as determined by the contents of a trusted publication pertaining to the shielding of 14.8 MeV fast neutrons utilizing ilmenite-magnetite concrete [6]. Elemental composition was pre-processed by identifying each element's cross section at 14.8 MeV, and then the atomic weight was applied. The macroscopic cross sections were generated from the total sum of the microscopic, weighted cross sections, and their total macroscopic cross section were used to calculate the mean free path and 50% attenuation thickness of the neutrons.

4.1.1. Derivation of Shielding Calculation

The mean free path of an incident neutron is equal to the reciprocal of the macroscopic cross section of the material. The derivation for the mean free path is as follows:

$$-dI(x) = N\sigma_t I(x)dx = \Sigma_t I(x)dx$$

Substituting gives:

$$-dI(x) = \Sigma_t\, I_o(x)dx$$

$$-\frac{dI(x)}{I_o(x)} = \Sigma_t\, dx$$

The probability that a neutron has not yet collided until x will collide in any next x value is:

$$P(x) = \Sigma_t\, dx = e^{-\Sigma_t x}$$

$$\frac{d}{dx}\big(p(x)\big) = \frac{d}{dx}\left(e^{-\Sigma_t x}\right) = -\Sigma_t e^{-\Sigma_t x}dx$$

The relaxation length is the distance in which the intensity of the neutrons that have not undergone a reaction has decreased by a factor e, as defined by λ:

$$\lambda = \int_0^\infty x\, p(x)dx = \Sigma_t \int_0^\infty x\, e^{-\Sigma_t x}dx$$

Integrating by parts gives the mean free path:

$$v = e^{-\Sigma_t x}, \qquad u = x$$

$$dv = -\Sigma_t e^{-\Sigma_t x}, \qquad du = \frac{x^2}{2}$$

$$\lambda = \Sigma_t \int_0^{\infty} x\, e^{-\Sigma_t x} dx = \boldsymbol{\frac{1}{\Sigma_t}}$$

For a shielding thickness which is a function of probability interaction:

$\lambda_{attenuation} = \frac{\ln(p(x))}{-\Sigma_t}$, where p(x) is a value between (0<p<1], describing the percentage of neutrons attenuated.

4.1.2. Application of Shielding Calculation

The following calculations were performed for each isotope present in each material of the conceptual design to determine its macroscopic cross section. The calculations shown are for C-12, which was calculated to have the greatest macroscopic cross section.

The following parameter inputs were determined for each isotope, as shown below.

Table 1 – Shielding Calculation Inputs

Isotope	C-12
Elemental Weight Fraction	0.07914%
Natural Isotope Abundance	98.9%
Microscopic Cross Section (NNDL at 14.8 MeV)	1.381 barns
Molar Mass	12.01 g/mol
Elemental Density	1.053 g/cm^3

A weighting factor for each isotope is calculated using the following equation. The sum of weighting factors for all isotopes in a material will equal one.

$$Weighting\ Factor = Elemental\ Weight\ Fraction * Natural\ Isotope\ Abundance$$

$$Weighting\ Factor = 0.0007914 * 0.989 = .0007827$$

The microscopic cross section is converted from barns to cm^2.

$$\sigma = 1.381\ barns * \frac{1E-24\ cm^2}{1\ barn} = 1.381E-24\ cm^2$$

The inverse of the molar mass is taken to calculate the mol/g for each isotope, which is multiplied by the elemental density to calculate the molar and atomic density for each isotope. The density is multiplied by the microscopic cross section and the isotope's unique weighting factor to calculate the weighted macroscopic cross section.

$$\frac{1}{M} = \frac{1}{12.01\frac{g}{mol}} = 0.08326\frac{mol}{g}$$

$$\rho_{isotope} = \rho_{element} * \frac{1}{M}$$

$$\rho_{isotope} = 1.053\frac{g}{cm^3} * 0.08326\frac{mol}{g} = 0.08769\frac{mol}{cm^3} * 6.023E23\frac{atoms}{mol} = 5.279E22\frac{atoms}{cm^3}$$

$$\Sigma = \sigma_w * \rho_{isotope}$$

$$\Sigma = 1.381E-24\ cm^2 * 5.279E22\frac{atoms}{cm^3} * 0.0007827 = 5.704E-5\frac{1}{cm}$$

After the calculation is repeated for each isotope, the sum of all microscopic cross sections is used as shown below to calculate the mean free path and shielding thickness. A thickness is calculated to attenuate 50% of all neutrons.

$$Attenuation\ thickness\ for\ 50\%\ of\ neutrons = \frac{\ln(0.50)}{\sum(\Sigma)}$$

$$t = \frac{\ln(0.50)}{-\sum(0.008605\frac{1}{cm})} = 80.55\ cm = \mathbf{31.71\ in}$$

$$mfp = \frac{1}{\Sigma} = \frac{1}{0.008605\frac{1}{cm}} = 116.2\ cm = \mathbf{45.75\ in}$$

4.2. Neutron Activation Analysis (NAA)

The purpose of this activation study is to highlight the potential isotopes present in each material of the conceptual design which pose significant challenges for activation. This study is essential for explaining how key nuclear reactions present in this conceptual model aide in completing the goals of the MSTL such as the production of tritium and limiting the neutron activation in essential structural componentry, (refer to the Functional Requirements Document (FRD) for all conceptual model requirements).

This study derives the neutron activation analysis formula. It then computes the maximum saturation activity in the structural steel, concrete shielding, FLiBe salt, and MOF filter material for select elements (omitting carbon, hydrogen, and other common elements except for the MOF). Saturation activities are compared for the front side of the shield (100% Irradiation Zone) and the back side of the shield (50% Irradiation Zone).

4.2.1. Derivation of Maximum Saturation Activity Formula

The rate of change in neutron density over time equals the product of the neutron flux, the probability of interaction with the material, and the quantity of material present, excluding material decay. The derivation for the maximum saturation activity is determined as follows:

$$\frac{dN}{dt} = \phi\sigma N_T - \lambda N$$

$$\frac{dN}{dt} + \lambda N = \phi\sigma N_T$$

Applying subjective A and B constants gives,

$$N_h(t) = Ae^{-\lambda t}, \quad N_p(t) = B\phi\sigma N_T$$

$$N(t) = N_h(t) + N_p(t) = Ae^{-\lambda t} + B\phi\sigma N_T$$

$$\frac{dN}{dt} = -\lambda Ae^{-\lambda t}$$

$$\frac{dN}{dt} + \lambda N = \phi\sigma N_T = -\lambda Ae^{-\lambda t} + \lambda\left(Ae^{-\lambda t} + B\phi\sigma N_T\right) = \phi\sigma N_T$$

$$\lambda B\phi\sigma N_T = \phi\sigma N_T, \quad B = \frac{1}{\lambda}$$

Assume initial condition of y (0) = 0,

$$\mathrm{A} + B\phi\sigma N_T = 0, \quad A = -\frac{\phi\sigma N_T}{\lambda}$$

$$N(t) = -\frac{\phi\sigma N_T e^{-\lambda t}}{\lambda} + \frac{\phi\sigma N_T}{\lambda} = \phi\sigma N_T \frac{\left(1 - e^{-\lambda t}\right)}{\lambda} = \lambda N(t) = \phi\sigma N_T\left(1 - e^{-\lambda t}\right)$$

Considering the requirement for maximum activation over a time domain, the function's limit is:

$$\lim_{t\to\infty} \phi\sigma N_T\left(1 - e^{-\lambda t}\right) = \phi\sigma N_T(1 - 0) = \boldsymbol{\phi\sigma N_T}$$

$$\boldsymbol{A(Bq) = \lambda N = \phi\sigma N_T}$$

4.2.2. Application of Maximum Saturation Activity Formula

The following calculations were performed for each isotope present in each material of the conceptual design to determine its maximum saturation activity. The calculations shown are for Li-6 in the FLiBe, which was calculated to produce the greatest saturation activity.

Parameter inputs were determined for each isotope, as shown below.

Table 2 – NAA Calculation Inputs

Isotope	Li-6
Elemental Weight Fraction	16.7%
Natural Isotope Abundance	90%
Microscopic Cross Section (NNDL at 14.8 MeV)	1.404 barns
Molar Mass	6.015 g/mol
Elemental Density	0.535 g/cm^3
Material Volume	1228.3 cm^3
Neutron Flux (DT)	1.20E12 neutrons/cm^2/sec
Neutron Flux (DD)	6.09E9 neutrons/cm^2/sec

A weighting factor for each isotope is calculated using the following equation. The sum of weighting factors for all isotopes in a material will equal one.

$$Weighting\ Factor = Elemental\ Weight\ Fraction * Natural\ Isotope\ Abundance$$

$$Weighting\ Factor = 0.167 * 0.90 = 0.1503$$

The microscopic cross section is converted from barns to cm^2.

$$\sigma = 1.404\ barns * \frac{1E-24\ cm^2}{1\ barn} = 1.404E-24\ cm^2$$

The inverse of the molar mass is taken to calculate the mol/g for each isotope, which is multiplied by the elemental density to calculate the molar and atomic density for each isotope. The density is multiplied by the microscopic cross section and the isotope's unique weighting factor to calculate the weighted macroscopic cross section.

$$\frac{1}{M} = \frac{1}{6.015\frac{g}{mol}} = 0.1663\frac{mol}{g}$$

$$\rho_{isotope} = \rho_{element} * \frac{1}{M}$$

$$\rho_{isotope} = 0.535\frac{g}{cm^3} * 0.1663\frac{mol}{g} = 0.08894\frac{mol}{cm^3} * 6.023E23\frac{atoms}{mol} = 5.354E22\frac{atoms}{cm^3}$$

$$\Sigma = \sigma_w * \rho_{isotope}$$

$$\Sigma = 1.404E-24\ cm^2 * 5.354E22\frac{atoms}{cm^3} = 0.07518\frac{1}{cm}$$

$$V_{isotope} = V * Weighted\ Factor$$

$$V_{isotope} = 1228.3\ cm^3 * 0.1503 = 184.6\ cm^3$$

$$M_{isotope} = V_{isotope} * \rho_{element}$$

$$M_{isotope} = 184.6\ cm^3 * 0.535 \frac{g}{cm^3} = 98.77\ g$$

The saturation activities are calculated using the equation derived in the section above.

$$A(Bq) = \lambda N = \phi \sigma N_T$$

$$N_T = \rho_{isotope} * V_{isotope}$$

$$A_{DT} = 1.20E12 \frac{neutrons}{cm^2 * sec} * 0.07518 \frac{1}{cm} * 184.6\ cm^3 = 1.66E13\ Bq$$

$$A_{DD} = 6.09E9 \frac{neutrons}{cm^2 * sec} * 0.07518 \frac{1}{cm} * 184.6\ cm^3 = 8.46E10\ Bq$$

The maximum saturation activity was calculated in the irradiation zone (before the shield), which receives the full neutron flux, and behind the shield, where only 50% of the neutron flux is received. The following percentages were applied to certain inputs for each case.

Table 3 - Multiplication Factors for NAA Cases

Input	Before Shield	After Shield
Neutron Flux	100%	50%
Concrete Volume	100%	0%
Steel Volume	25%	75%
FLiBe Volume	25%	75%
MOF Volume	0%	100%

The following calculations were performed to convert the activity into Bq/g and consider the weighting factors for FLiBe volume and Neutron Flux in both cases mentioned above.

$$\boldsymbol{A_{DT.before} = \frac{1.66E13\ Bq}{98.77\ g} * 1.00 * 0.25 = 4.21E10\ \frac{Bq}{g}}$$

$$\boldsymbol{A_{DT.after} = \frac{1.66E13\ Bq}{98.77\ g} * 0.50 * 0.75 = 6.32E10\ \frac{Bq}{g}}$$

$$\boldsymbol{A_{DD.before} = \frac{8.46E10\ Bq}{98.77\ g} * 1.00 * 0.25 = 2.14E8\ \frac{Bq}{g}}$$

$$A_{DD.after} = \frac{8.46E10\ Bq}{98.77\ g} * 0.50 * 0.75 = 3.21E8\ \frac{Bq}{g}$$

4.2.3. Maximum Saturation Activity Results

The table below outlines the maximum saturation activity for each isotope in the model, categorized by their materials. Notably, certain isotopes such as hydrogen, oxygen, and carbon were omitted from the material composition models, except for the MOF. It's important to emphasize that the data presented in this table could be potentially misleading. While some isotopes may initially display high activation levels, they might subsequently transmute into isotopes with shorter half-lives. As a result, they may not present significant engineering challenges for future projects. On the other hand, certain isotopes with lower activation levels could pose considerable challenges.

Table 4 - Summary of Neutron Activation Analysis Results for Each Isotope

			Before Shield (100% Irradiated)		After Shield (50% Irradiated)	
Material	Isotopes	Mass (g)	Bq/g (DD)	Bq/g (DT)	Bq/g (DD)	Bq/g (DT)
FLIBE	F-19	1.38	8.64E+07	1.70E+10	1.30E+08	2.55E+10
	Li-6	98.77	2.14E+08	4.21E+10	3.21E+08	6.32E+10
	Li-7	10.97	1.83E+08	3.61E+10	2.75E+08	5.41E+10
	Be-9	363.58	1.51E+08	2.97E+10	2.26E+08	4.45E+10
NU-2100 MOF	H-1	1.59E+00	0.00E+00	0.00E+00	5.91E+08	1.16E+11
	H-2	1.59E+00	0.00E+00	0.00E+00	3.55E+08	6.99E+10
	C-12	1.43E+06	0.00E+00	0.00E+00	1.06E+08	2.08E+10
	C-13	1.43E+06	0.00E+00	0.00E+00	1.02E+08	2.01E+10
	N-14	920.84	0.00E+00	0.00E+00	1.04E+08	2.04E+10
	N-15	920.84	0.00E+00	0.00E+00	9.89E+07	1.95E+10
	Cu-63	9.98E+06	0.00E+00	0.00E+00	4.14E+07	8.15E+09
	Cu-65	9.98E+06	0.00E+00	0.00E+00	4.08E+07	8.04E+09
	Si-28	2.79E+05	5.76E+07	1.13E+10	8.63E+07	1.70E+10
	Si-29	1.41E+04	5.56E+07	1.09E+10	8.34E+07	1.64E+10
	Si-30	9.38E+03	5.37E+07	1.06E+10	8.06E+07	1.59E+10
	Mn-55	6.04E+04	4.05E+07	7.97E+09	6.07E+07	1.20E+10

STEEL	Cr-50	2.94E+02	4.37E+07	8.60E+09	6.56E+07	1.29E+10
	Cr-52	5.66E+03	4.21E+07	8.29E+09	6.32E+07	1.24E+10
	Cr-53	6.41E+02	4.13E+07	8.14E+09	6.20E+07	1.22E+10
	Cr-54	1.60E+02	4.06E+07	7.99E+09	6.09E+07	1.20E+10
	Ni-58	7.01E+03	4.11E+07	8.09E+09	6.17E+07	1.21E+10
	Ni-60	2.70E+03	4.11E+07	8.09E+09	6.17E+07	1.21E+10
	Ni-61	1.17E+02	4.04E+07	7.95E+09	6.06E+07	1.19E+10
	Ni-62	3.74E+02	3.95E+07	7.78E+09	5.93E+07	1.17E+10
	Ni-64	9.53E+01	3.85E+07	7.58E+09	5.78E+07	1.14E+10
	Fe-54	3.46E+05	4.13E+07	8.12E+09	6.19E+07	1.22E+10
	Fe-56	5.47E+06	4.12E+07	8.11E+09	6.18E+07	1.22E+10
	Fe-57	1.31E+05	4.05E+07	7.97E+09	6.07E+07	1.20E+10
	Fe-58	1.67E+04	3.98E+07	7.83E+09	5.97E+07	1.17E+10
CONCRETE	Mg-24	1.94E+05	2.76E+08	5.43E+10	0.00E+00	0.00E+00
	Mg-25	1.94E+05	2.67E+08	5.26E+10	0.00E+00	0.00E+00
	Mg-26	1.94E+05	2.60E+08	5.13E+10	0.00E+00	0.00E+00
	Al-27	1.48E+05	2.38E+08	4.68E+10	0.00E+00	0.00E+00
	Si-28	3.46E+05	2.30E+08	4.53E+10	0.00E+00	0.00E+00
	Si-29	3.46E+05	2.22E+08	4.37E+10	0.00E+00	0.00E+00
	Si-30	3.46E+05	2.15E+08	4.23E+10	0.00E+00	0.00E+00
	Ti-46	1.77E+06	1.77E+08	3.48E+10	0.00E+00	0.00E+00
	Ti-47	1.77E+06	1.75E+08	3.44E+10	0.00E+00	0.00E+00
	Ti-48	1.77E+06	1.73E+08	3.40E+10	0.00E+00	0.00E+00
	Ti-49	1.77E+06	1.71E+08	3.37E+10	0.00E+00	0.00E+00
	Ti-50	1.77E+06	1.69E+08	3.33E+10	0.00E+00	0.00E+00
	V-50	1.41E+04	1.69E+08	3.33E+10	0.00E+00	0.00E+00
	V-51	1.41E+04	1.65E+08	3.25E+10	0.00E+00	0.00E+00

	Cr-50	7.71E+03	1.75E+08	3.44E+10	0.00E+00	0.00E+00
	Cr-52	7.71E+03	1.69E+08	3.32E+10	0.00E+00	0.00E+00
	Cr-53	7.71E+03	1.65E+08	3.25E+10	0.00E+00	0.00E+00
	Cr-54	7.71E+03	1.62E+08	3.19E+10	0.00E+00	0.00E+00
	Mn-55	6.90E+04	1.62E+08	3.19E+10	0.00E+00	0.00E+00
	Fe-54	6.81E+06	1.65E+08	3.25E+10	0.00E+00	0.00E+00
	Fe-56	6.81E+06	1.65E+08	3.24E+10	0.00E+00	0.00E+00
	Fe-57	6.81E+06	1.62E+08	3.19E+10	0.00E+00	0.00E+00
	Fe-58	6.81E+06	1.59E+08	3.13E+10	0.00E+00	0.00E+00
	Ni-58	1.18E+04	1.64E+08	3.24E+10	0.00E+00	0.00E+00
	Ni-60	1.18E+04	1.64E+08	3.24E+10	0.00E+00	0.00E+00
	Ni-61	1.18E+04	1.62E+08	3.18E+10	0.00E+00	0.00E+00
	Ni-62	1.18E+04	1.58E+08	3.11E+10	0.00E+00	0.00E+00
	Ni-64	1.18E+04	1.54E+08	3.03E+10	0.00E+00	0.00E+00

The ranking of isotopes in order of maximum saturation activity is shown below.

Table 5 - Ranking of Isotopes by Maximum Saturation Activity

	Before Shield		After Shield	
Ranking	Isotope	Bq/g (DT)	Isotope	Bq/g (DT)
1	Mg-24	5.43E+10	Li-6	6.32E+10
2	Mg-25	5.26E+10	Li-7	5.41E+10
3	Mg-26	5.13E+10	Be-9	4.45E+10
4	Al-27	4.68E+10	N-15	1.95E+10
5	Si-28	4.53E+10	Si-28	1.70E+10
6	Si-29	4.37E+10	Si-29	1.64E+10
7	Si-30	4.23E+10	Si-30	1.59E+10
8	Li-6	4.21E+10	Cr-50	1.29E+10

9	Li-7	3.61E+10	Cr-52	1.24E+10
10	Ti-46	3.48E+10	Cr-53	1.22E+10
11	Ti-47	3.44E+10	Fe-54	1.22E+10
12	Cr-50	3.44E+10	Fe-56	1.22E+10
13	Ti-48	3.40E+10	Ni-58	1.21E+10
14	Ti-49	3.37E+10	Ni-60	1.21E+10
15	Ti-50	3.33E+10	Cr-54	1.20E+10
16	V-50	3.33E+10	Mn-55	1.20E+10
17	Cr-52	3.32E+10	Fe-57	1.20E+10
18	Cr-53	3.25E+10	Ni-61	1.19E+10
19	Fe-54	3.25E+10	Fe-58	1.17E+10
20	V-51	3.25E+10	Ni-62	1.17E+10
21	Fe-56	3.24E+10	Ni-64	1.14E+10
22	Ni-58	3.24E+10	Cu-63	8.15E+09
23	Ni-60	3.24E+10	Cu-65	8.04E+09
24	Cr-54	3.19E+10		
25	Mn-55	3.19E+10		
26	Fe-57	3.19E+10	Common Elements	
27	Ni-61	3.18E+10	H-1	1.16E+11
28	Fe-58	3.13E+10	H-2	6.99E+10
29	Ni-62	3.11E+10	C-12	2.08E+10
30	Ni-64	3.03E+10	N-14	2.04E+10
31	Be-9	2.97E+10	C-13	2.01E+10
32	F-19	1.70E+10	N-15	1.95E+10
33	Si-28	1.13E+10		
34	Si-29	1.09E+10		
35	Si-30	1.06E+10		

36	Cr-50	8.60E+09		
37	Cr-52	8.29E+09		
38	Cr-53	8.14E+09		
39	Fe-54	8.12E+09		
40	Fe-56	8.11E+09		
41	Ni-58	8.09E+09		
42	Ni-60	8.09E+09		
43	Cr-54	7.99E+09		
44	Mn-55	7.97E+09		
45	Fe-57	7.97E+09		
46	Ni-61	7.95E+09		
47	Fe-58	7.83E+09		
48	Ni-62	7.78E+09		

The top three isotopes present in the 100% irradiation zone (Mg-24, Mg-25, and Mg-26) are from the concrete shielding block. This is due to their relatively high cross sections through (n, α) reactions. Absorption is a desirable quality in shielding as the shielding acts to attenuate neutrons. The byproduct of this reaction is the thermal heating of the shielding material. Subsequent Al and Si isotopes further provide the effectiveness of the shielding material, whereas steel isotopes such as Fe, Ni, and Cr are spared activation.

The top three isotopes present in the 50% irradiation zone (Li-6, Li-7, Be-9) are from the FLiBe salt. This is due to the relatively high cross sections for a multifold of reactions including (n,α) and (n,T) in Lithium and (n,2n) in Beryllium. Of utmost importance is the (n,T) reaction for the production of tritium as a usable byproduct in further fusion reactions. To aide in this process, the (n,2n) reactions further multiply the neutrons within the salt, allowing for lucrative tritium production from thermal neutron interaction. Refer to section 5 for the MSTL tritium production values.

It is important to note the presence of gamma rays with the release of alpha particles will cause associated decay heat from the salt. These results indicate that the high activity of the salt must be mitigated post operation. Additional shielding might need to be employed around the loop post operation to mitigate and attenuate these gamma rays.

This computation also proved the effectiveness of the shielding of the MOF filter, as the Cu isotopes present in its material composition were the lowest in the ranking.

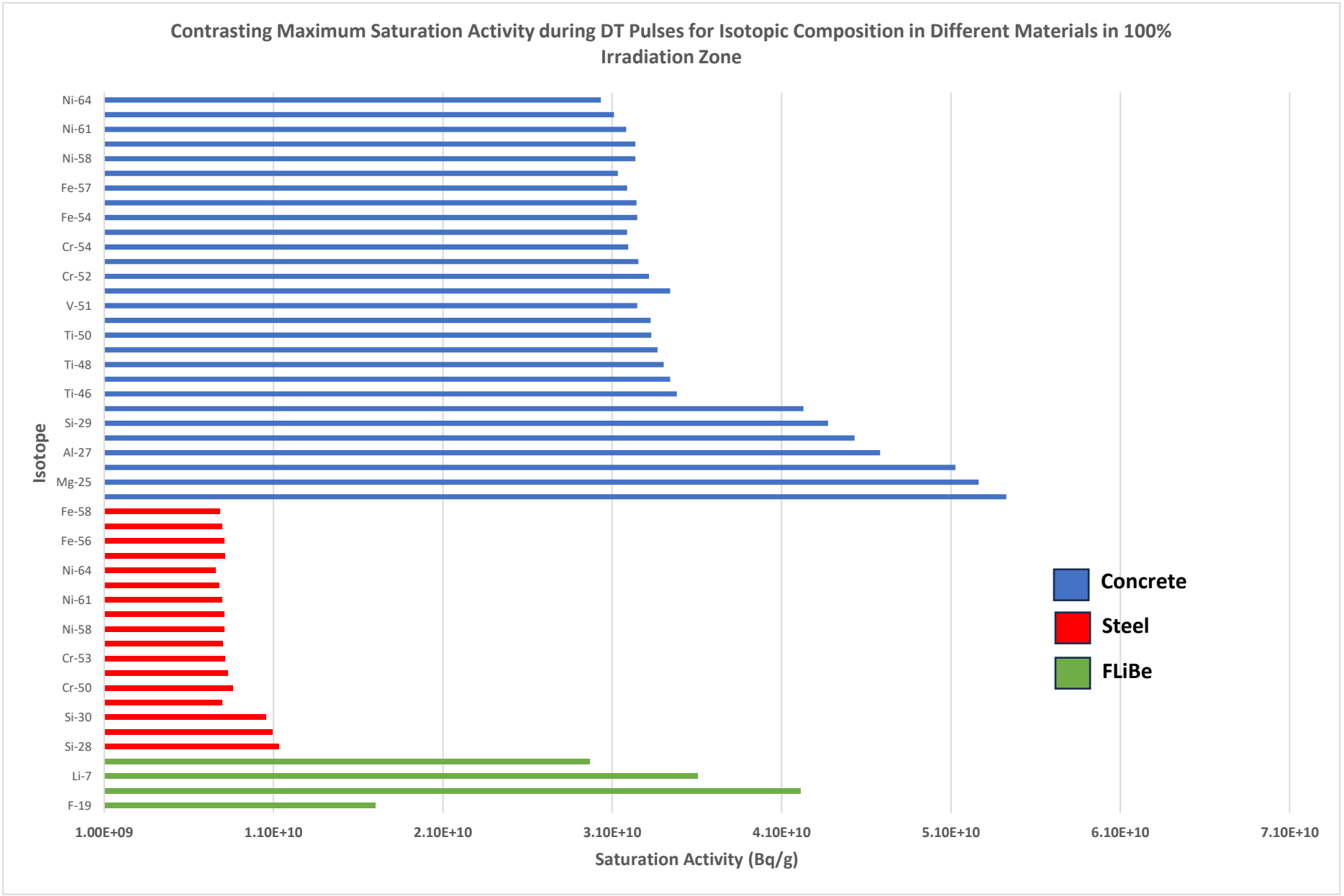

Figure 2 – Summary of Neutron Activation Analysis Results for DT Pulses in 100% Irradiation Zone

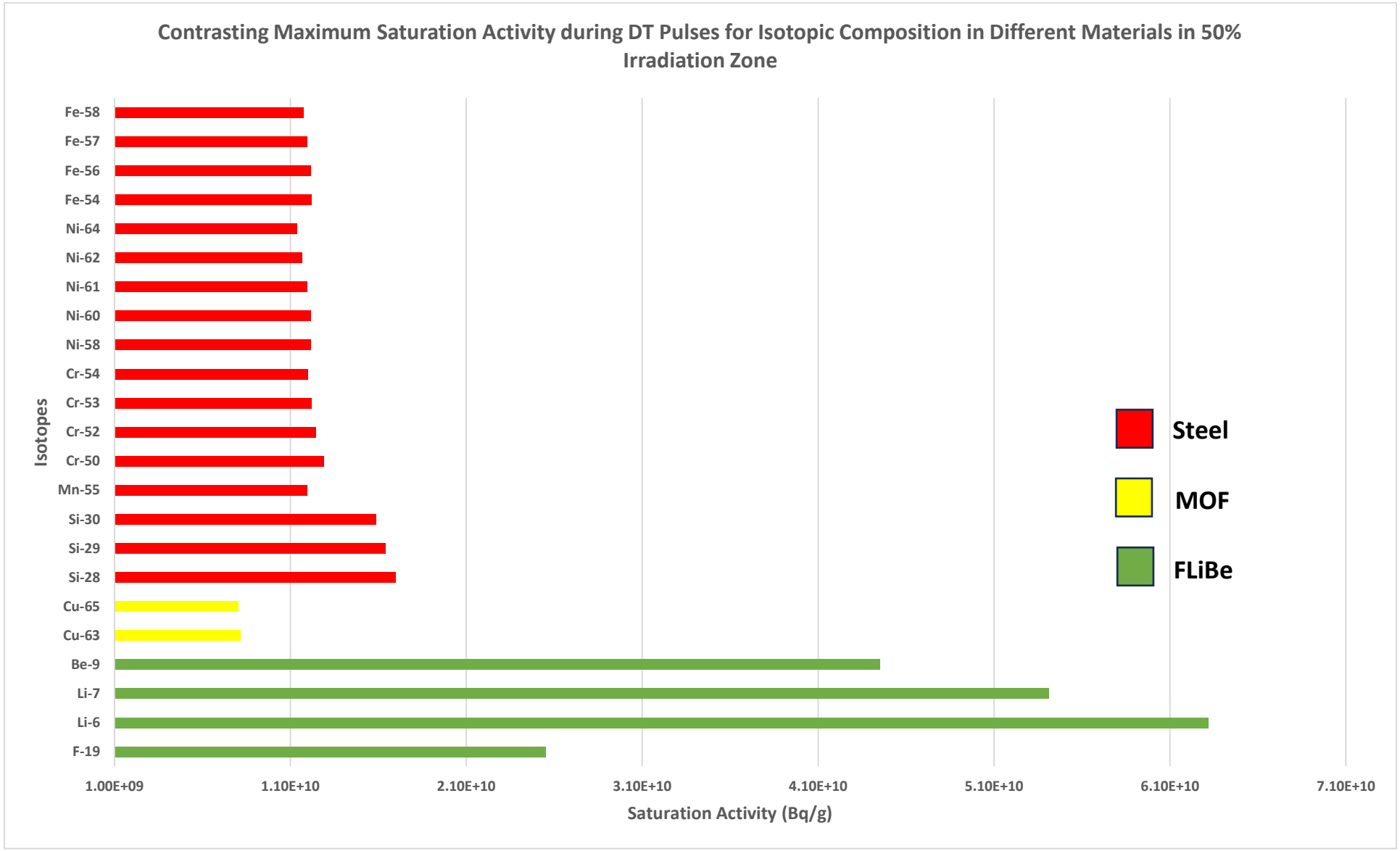

Figure 3 – Summary of Neutron Activation Analysis Results for DT Pulses in 50% Irradiation Zone

5. Stochastic Calculations

The use of stochastic modeling techniques is essential for accurately predicting and assessing MSTL behavior in a fusion environment. This section of the report introduces a stochastic model of the MSTL, utilizing the capabilities of the OpenMC software. The topics addressed in this section include:

1. Constructing the MSTL model to accurately reflect real-world conditions encountered in a fast neutron flux environment.
2. Identifying effective shielding applications for the MSTL.
3. Implementing measures to minimize heat deposition and protect equipment in the MSTL.
4. Exploring methods to increase tritium production in the MSTL.

Driven by the literature review, the nuclear engineering team of the UC-MSTL worked to provide results focused on these topics through three experiments: a convergence study, shielding sensitivity study, and a tritium production experimental study (see Appendix B for raw code and results). The tally results from the simulations previously described will be left in terms of source particle (denotated as sp). This is due to a lack of a specific neutron fluence rate (n/s) for the ITER DT spectra, and allows for individual fusion entities to apply the results of these computations to their particular use case.

Unlike other Finite Element Analysis (FEA) tools like COMSOL Multiphysics or ANSYS, neutronics software's such as OpenMC are not inherently tailored for time-domain analysis, structural assessments, or fluid flow simulations. OpenMC's primary focus lies in modeling the intricate behavior of neutrons as they interact with materials and move through predefined geometries. Realistic aspects, such as concerns about structural stability or salt flow rate are not directly addressed within the scope of OpenMC's capabilities.

Initially, the aim of this section of the MSTL project was to employ unstructured mesh geometry. However, due to project constraints, utilizing unstructured mesh was not feasible and fell beyond the scope of the UC-MSTL project. Consequently, geometry for this model had to be developed using Constructive Solid Geometry (CSG).

5.1. Constructing the Model

The stochastic MSTL model was designed using CSG as the primary geometry tool. This model was de-featured such that components of the MSTL which provide little data as to the performance of the loop were removed. Removed components include flanges, nuts, bolts, excess piping, electrical components, and sensors, as well as unnecessary structural components. Simplifying the geometry of the model allows for a faster iteration through analysis versions. Some simplifications include the pump, which is modeled as a solid stainless-steel block. Similarly, the filtering system is modeled as a solid block of filter material. The most detail is given to the piping system, FLiBe salt and shielding, as these are imperative for the effectiveness of the concept goals.

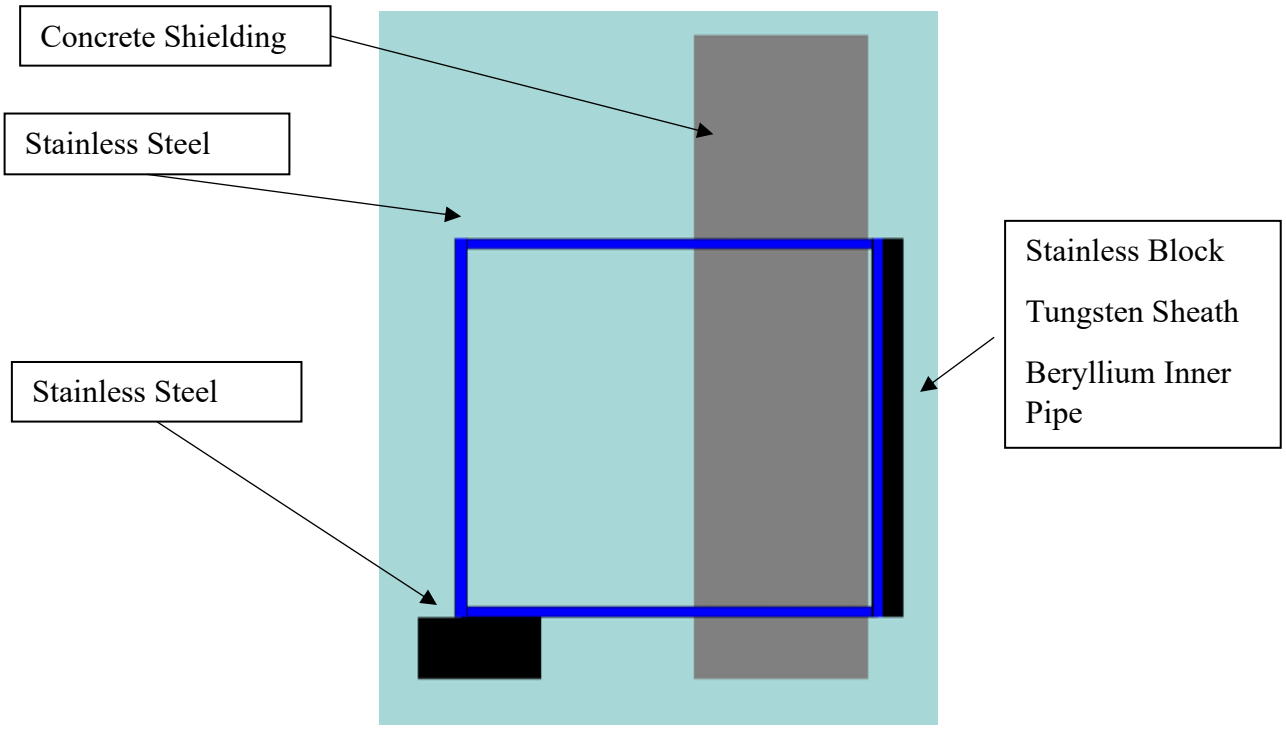

Figure 4 – Side View of MSTL as Modeled in CSG

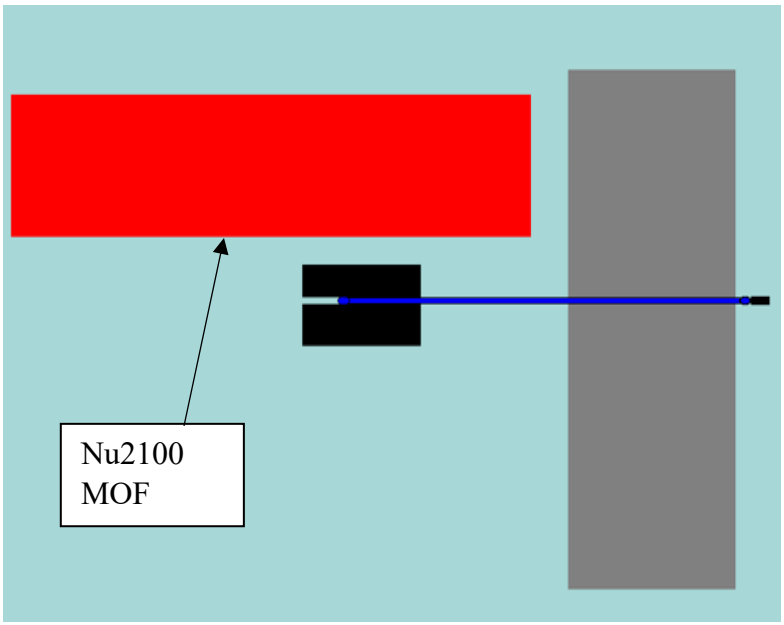

Figure 5 –Top View of MSTL as Modeled in CSG

Much of the detail and functionality of the MSTL has been preserved for effectiveness of OpenMC utilization as described in section 3 of this document. Within the MSTL irradiation zone, the stainless-steel block, beryllium inner piping segment, and tungsten sheath are featured in Figure 6.

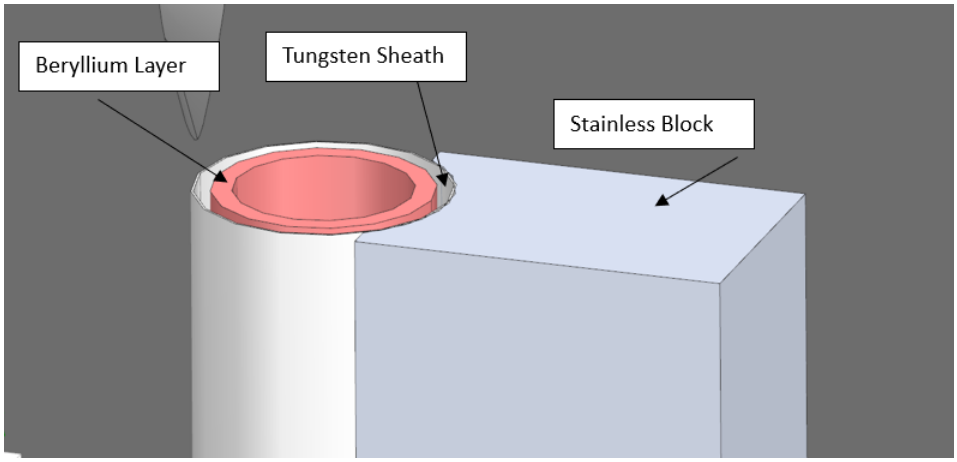

Figure 6 – Detailed view of tungsten sheath, beryllium inner layer, and stainless-steel block in irradiation zone of MSTL with FLiBe salt and steel pipe removed for detail.

All structures in the model were subsequently constructed using basic boolean geometry, including spheres, rectangular prisms, and cylinders, following standard Constructive Solid Geometry (CSG) processes. Figure 7 provides an illustrative example of how geometry is constructed in OpenMC. The shielding block is modeled as a three-dimensional rectangular prism and is assigned a material composition.

```
#CONCRETE
x0_Concrete=107.805  #cm
y0_Concrete=-203.2 #cm
z0_Concrete=0      #cm

# Define dimensions of the concrete slab
#length_x_Concrete = 20.955   #cm
length_x_Concrete = 80.55   #cm
length_y_Concrete = 365.76   #cm
length_z_Concrete = 365.76    #cm

# Create the concrete slab
concrete_slab = openmc.model.RectangularParallelepiped(xmin=x0_Concrete,
xmax=x0_Concrete + length_x_Concrete, ymin=y0_Concrete, ymax=y0_Concrete +
length_y_Concrete,zmin=z0_Concrete, zmax=z0_Concrete + length_z_Concrete)

concrete_slab_region = -concrete_slab & +pipe_cylinder_steel_3 &
+pipe_cylinder_steel_4

concrete_slab = openmc.Cell(12, name = 'concrete_shielding_slab')
concrete_slab.fill = concrete
concrete_slab.region = concrete_slab_region
```

Figure 7 – Construction of Shielding (Concrete Slab) Geometry in OpenMC Assigning Materials in the Model

Material assignment in OpenMC holds paramount significance in establishing a stable model. Within the MSTL framework, all materials are formed using an elemental breakdown determined by weight percent. Certain material compositions, like FLiBe salt, necessitate an isotopic breakdown to account for unnatural or enriched isotopic abundance. For instance, Figure 8 provides an example of a material composition, as configured for the concrete shielding slab.

```
#Concrete
concrete = openmc.Material(name='Concrete')
concrete.set_density('g/cm3', 2.232)
concrete.add_element('H', 0.56478, percent_type='wo')
concrete.add_element('C', 0.079137, percent_type='wo')
concrete.add_element('O', 38.565616, percent_type='wo')
concrete.add_element('Mg', 3.647482, percent_type='wo')
concrete.add_element('Al', 1.78777, percent_type='wo')
concrete.add_element('Si', 4.852518, percent_type='wo')
concrete.add_element('P', 0.007194, percent_type='wo')
concrete.add_element('S', 0.057554, percent_type='wo')
concrete.add_element('Ca', 8.881295, percent_type='wo')
concrete.add_element('Ti', 12.816547, percent_type='wo')
concrete.add_element('V', 0.07554, percent_type='wo')
concrete.add_element('Cr', 0.035071, percent_type='wo')
concrete.add_element('Mn', 0.302158, percent_type='wo')
concrete.add_element('Fe', 28.284173, percent_type='wo')
concrete.add_element('Ni', 0.043165, percent_type='wo')
```

Figure 8 – Construction of Shielding (Concrete Slab) material composition in OpenMC.

5.2. Assumptions

The following assumptions were determined for the MSTL OpenMC model:

5.2.1. Geometry

1. The pump is modeled as a single, stainless-steel elemental composition block.
2. The MOF filter is modeled as a single, nu2100 elemental composition block.
3. The Shielding segment is modeled as a single, concrete elemental composition block.
4. The loop sections are modeled as four cylindrical stainless-steel pipes filled with FLiBe salt.
5. The irradiation zone contains the beryllium inner layer, tungsten sheath, and stainless steel containing the FLiBe salt.

5.2.2. Material

1. The FLiBe salt material composition is 90% enriched with Li-6 all other elements in the salt have a standard elemental composition without specified isotopic breakdown (see System Design Description (SDD) for salt material composition).
2. All materials are modeled initially at room temperature.
3. All materials unless otherwise specified have material compositions pulled from the OpenMC example library, as specified by the BWR.ipyb example on the OpenMC website.

5.2.3. Nuclear Data

1. The MSTL is simulated during operation – not showdown.
2. All materials utilize the ENDF/B-VII.1 (Evaluated Nuclear Data File, version VII.1) nuclear data library for cross section specification at room temperature.
3. All tally results are left in terms of source particle (sp) due to a lack of a specific neutron fluence rate (n/s).
4. The source term for this model is the 175-group ITER DT neutron spectra, as seen in Figure 9. The energy bins and corresponding flux spectra values can be found in Appendix B and online through FISPACT [5]. The source geometry is a unidirectional planar source of dimensions equal to the shielding block.

5.2.4. Source Selection

The ITER DT spectra-based unidirectional planar source demonstrated the lowest neutron leakage rate and best reflected the loop's behavior in a fast neutron flux "beam" environment. Multiple sources were evaluated, including a point source positioned outside the loop and an isotropic point source, both based on the ITER DT spectra. However, the isotropic point source resulted in excessive neutron leakage (upwards of 90%). The OpenMC openmc-plasma-source [7], incorporating a fusion point source, offered a slightly lower neutron leakage rate and produced neutron flux tally values similar to a unidirectional source based on the ITER DT spectra. However, it simulated conditions beyond the scope of the MSTL model, such as plasma-facing scenarios with elevated temperatures.

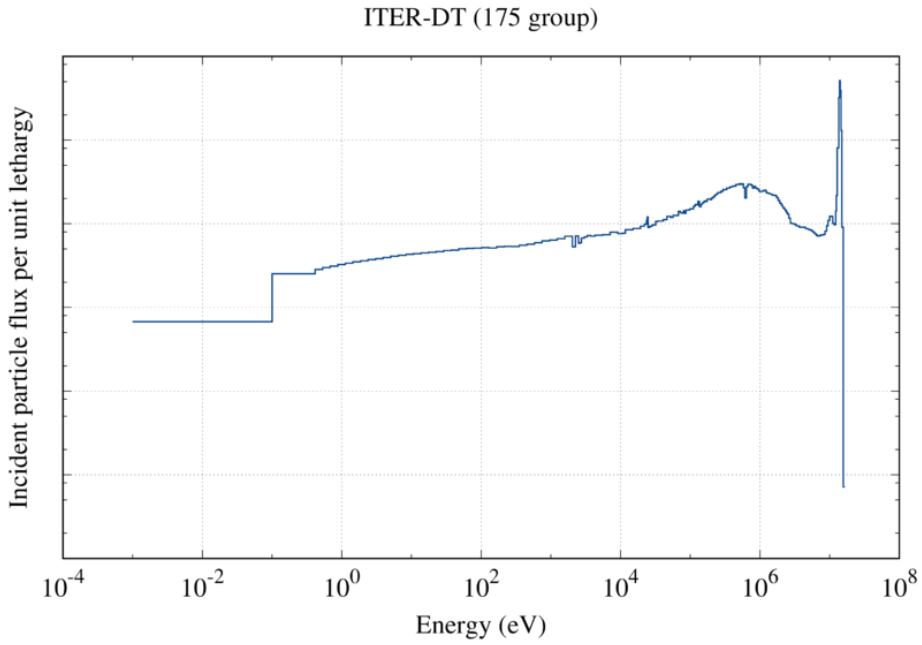

Figure 9 – ITER DT Spectra

5.3. Requested Data

The following tallies and requested data were specified for the OpenMC simulation. The appendix to this report contains all requested data for a variety of simulations utilizing shielding sensitivity study and tritium experimental study results.

Table 6 – OpenMC Tallies and Requested Data

Score	Description	Location
flux	Total flux	Total Geometries
absorption	Total absorption rate. For incident neutrons, this accounts for all reactions that do not produce secondary neutrons as well as fission.	Total Geometries
Elastic	Elastic scattering rate	Irradiation Zone and Shielding
Scatter	Total scattering rate	Irradiation Zone and Shielding
(n,a)	(n, α) reaction	Salt Zones
(n,gamma)	(n,gamma) reaction	Salt Zones and Filter
(n,t)	Tritium production from (n,t)	Salt Zones
Heating	Total nuclear heating in units of eV per source particle. For neutrons this corresponds to MT = 301 produced by NJOY's HEATR.module while from photons, this is tallied from direct photon energy deposition.	Total Geometries

5.4. Convergence Study

Assessing the quality of data generated by a model is crucial before investing resources and time into its enhancement. Through this convergence study, neutron flux, total heating, and tritium production underwent systematic testing to ascertain the optimal number of particles and batches needed for thorough model characterization and the attainment of satisfactory results.

5.4.1. Assumptions and Methodology

The following assumptions and methodology were made for this convergence study.

1. The model used for this study is the UC-MSTL model with a unidirectional planar source term (see section 5.3.1)
2. The model is augmented with 10 cm of boronated polyethylene to reduce leakage in the model and conserve time resources (see section 5.4.3).
3. Total reaction rate values were produced via the summation of individual flux, heating, and (n,t) tally results from all 17 cells specified in the model.

5.4.2. Results

Table 7 – Summary of Starting Particles and Neutron Flux Reaction Rate

Starting Particles	Time (sec)	Neutron Flux Reaction rate (n-cm^2/sp)
10	8.6	1.32E+02
25	5.5	1.30E+02
50	5.9	1.29E+02
75	6.4	1.28E+02
100	6.4	1.30E+02
1000	15.8	1.28E+02
5000	55	1.28E+02
10000	1058.4	1.28E+02
100000	1419.5	1.28E+02
1000000	7281.9	1.28E+02

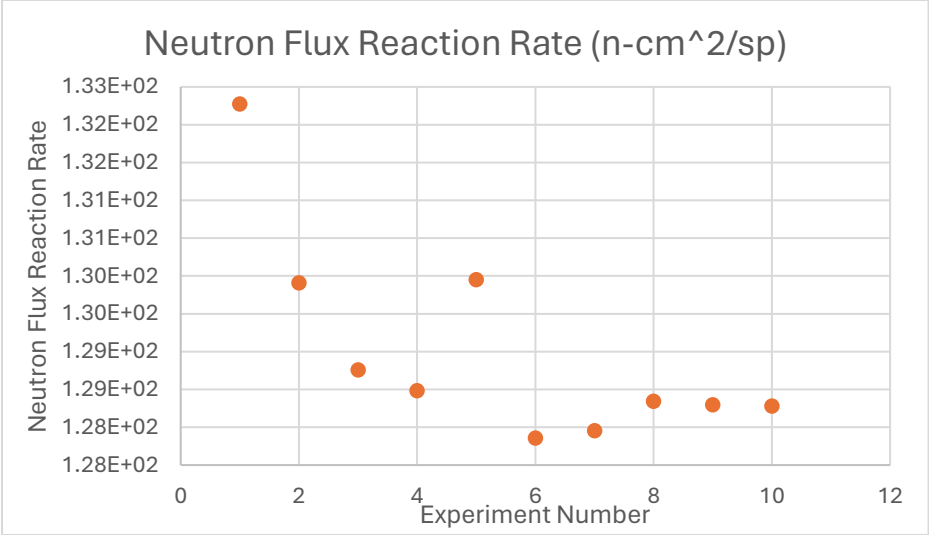

Figure 10 – Starting Particles Versus Neutron Flux Reaction Rate

Table 8 – Summary of Starting Particles and Heating Reaction Rate

Starting Particles	Time (sec)	Heating Reaction Rate (ev/sp)
10	8.6	3.43E+06
25	5.5	3.41E+06
50	5.9	3.82E+06
75	6.4	3.45E+06
100	6.4	2.78E+06
1000	15.8	2.79E+06
5000	55	2.77E+06
10000	1058.4	2.76E+06
100000	1419.5	2.77E+06
1000000	7281.9	2.76E+06

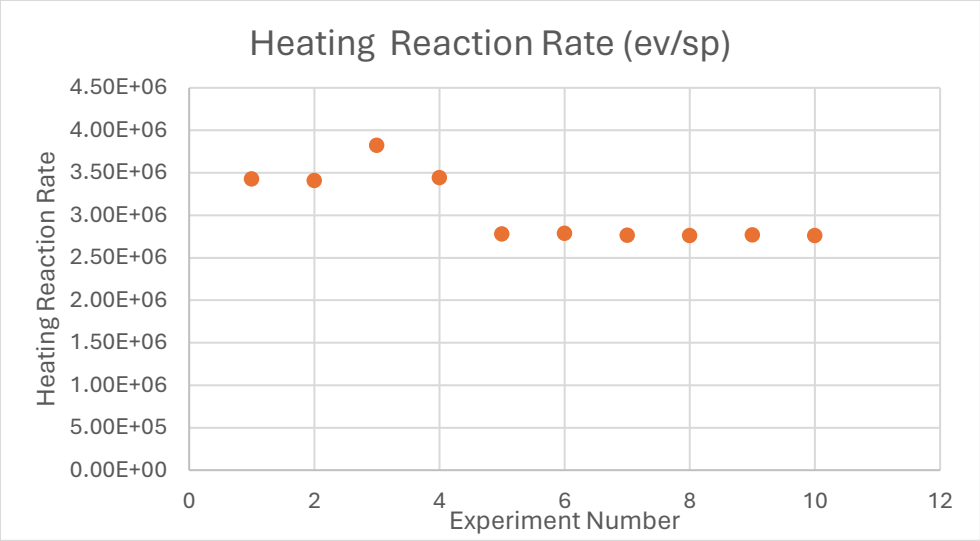

Figure 11 – Starting Particles Versus Heating Reaction Rate

Table 9 – Summary of Starting Particles and Tritium Reaction Rate

Starting Particles	Time (sec)	Reaction rate (n,t) reactions/source particle)
10	5.2	4.36E-04
25	5.2	8.10E-04
50	5.8	1.32E-03
75	5.6	1.48E-03
100	6.4	1.48E-03
1000	27.1	1.25E-03
5000	47.7	1.24E-03
10000	128.1	1.21E-03
100000	1419.5	1.20E-03
1000000	7281.9	1.21E-03

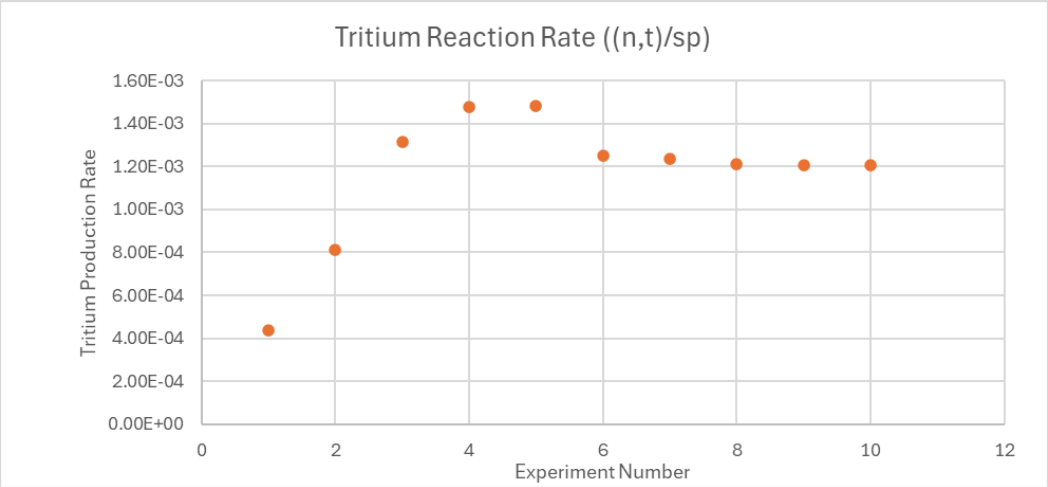

Figure 12 – Starting Particles Versus Tritium Production Reaction Rate

Accurate values for preliminary work were defined as having a coefficient of variation which is no more than 10%. Accurate values for analytical work or further experimentation must have coefficient of variations below 1% of the estimate. Through the convergence study, a starting particle value of 10,000 produces accurate data across most primary tallies and can be used for preliminary analysis. Time estimates to complete a 10,000-particle computation vary between three minutes and 10 minutes, depending on the number of tallies specified and complexity of the geometry. Table 10 highlights the results from a 10,000 particle for the neutron flux rate. Standard deviations vary depending on location in the model and distance from the source term, as well as the volume of material present. The Beryllium inner sheath is of particular concern given the high standard deviation relative to the mean. Thus, to further analyze this material, it would be necessary to isolate this tally and run a 100,000 particle or 1-million particle run.

Two regions of the model with some of the lowest coefficient of variations include the shield/polyethylene layer and the irradiation zone steel block. Given the accuracy across these model regions, these were selected for further experimentation.

It is important to note that as the starting number of particles increases, the time dedication increases exponentially. Time estimates for 1-million particle runs vary between two to seven hours, depending on the number of runs. It is imperative to plan and estimate time dedication accordingly before computing.

Table 10 – Summary of Neutron Flux Rate in 10,000 Particle Run Across All Geometries

Cell Name	Mean Neutron Flux Reaction Rate (n-cm^2/sp)	Neutron Flux Standard Deviation	Coefficient of Variation $\left(\frac{\sigma}{\mu}\right)$
TALLY 16: POLY	10.2051	0.00356461	0.03%

TALLY 11: STEEL BLOCK IRRADIATION ZONE	0.110957	0.000544017	0.49%
TALLY 13: STEEL PUMP	0.00179144	0.000199717	11.15%
TALLY 15: AIR	98.5822	0.0717322	0.07%
TALLY 3: STEEL PIPING IRRADIATION ZONE	0.0118412	9.28E-05	0.78%
TALLY 5: VERTICAL STEEL PIPING NON-IRRADIATION ZONE	4.01E-05	3.76E-06	9.38%
TALLY 7: TOP HORIZONTAL STEEL PIPING	1.07E-03	2.49E-05	2.33%
TALLY 9: BOTTOM HORIZONTAL STEEL PIPING	9.97E-04	2.30E-05	2.31%
TALLY 14: NU2100 FILTER	1.89E-02	0.000580311	3.07%
TALLY 12: CONCRETE SHIELDING	18.4025	0.0223906	0.12%
TALLY 2: BERYLLIUM INNER SHEATH IRRADIATION ZONE	8.98E-20	8.98E-20	100.00%

TALLY 4: TUNGSTEN OUTER SHEATH IRRADIATION ZONE	7.49E-04	6.73E-06	0.90%
TALLY 1: FLIBE IRRADIATION ZONE	1.00E-02	0.000112858	1.13%
TALLY 6: VERTICAL FLIBE NON-IRRADIATION ZONE	0.000105906	1.30E-05	12.28%
TALLY 8: TOP HORIZONTAL FLIBE	2.58E-03	7.03E-05	2.72%
TALLY 10: BOTTOM HORIZONTAL FLIBE	2.45E-03	6.84E-05	2.79%

5.5. Shielding Sensitivity Study

It is crucial to minimize heating and neutron flux to protect equipment, filtering mechanisms, and electronics against harmful radiation within the non-irradiation zone of the MSTL. This study documents a comparative analysis between three distinct shielding configurations for the MSTL within the demanding conditions of a fast neutron environment produced via a fusion device. Specifically, we scrutinize the efficacy of a conventional ilmenite-magnetite concrete shielding block against an enhanced configuration incorporating the same concrete block augmented with a 10 cm layer of boronated polyethylene or a 10-cm layer of boron carbide. This comparison is done in order to determine if shielding augmentation can minimize heat deposition and neutron flux in the non-irradiation zone. Attention will also be paid to whether geometric changes to the model improve model fidelity.

The confidence study mentioned in the preceding section of this report underscores the shield's capability to consistently generate converged tally data across neutron flux and heating. This reliability facilitates robust experimentation with the tallies, fostering high confidence in the produced results.

The ilmenite- magnetite shielding material selected has significantly higher fast neutron attenuating properties comparable to standard concrete compositions. However, in a fast neutron flux application, a pure concrete shield wall could act much like a large scattering plane- causing neutrons to activate and impact other materials in the fusion device. The goal of shielding in neutronic applications is to attenuate and thermalize neutrons as fast as possible, while

containing any emission of accompanying radiation (such as gamma rays). Typically, hydrogenous material is best for thermalization. Thus, polyethylene was selected with a boron dopant, due to boron's ability to absorb and attenuate neutrons.

Theory indicates that as the intense neutron flux impacts the shield wall, significant heating will occur. It is possible that this heating will melt the boronated polyethylene. In order to address this, boron carbide was selected as a secondary shielding option. Boron carbide is a ceramic with an extremely high hardness, in addition to a high neutron absorption cross section.

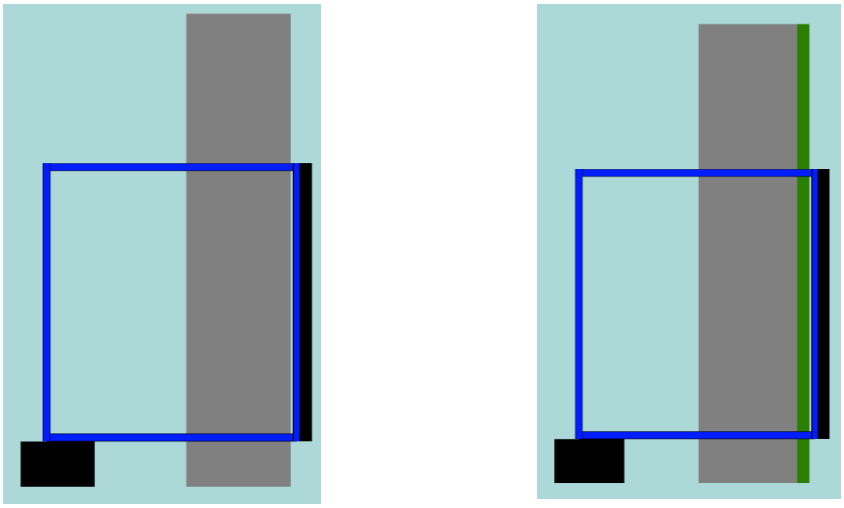

Figure 13 – Comparison of MSTL CSG model utilizing ilmenite-magnetite concrete (left) and same concrete shield with an additional 10 cm of boronated polyethylene or boron carbide (right).

The chemical composition of boronated polyethylene was established using information sourced from a publication concerning fast neutrons produced in linear accelerators for medical radiotherapy, considering the energy spectrum of neutrons involved in both settings (14 to 18 MeV) [8]. The boron carbide material selected is of standard elemental composition per the Royal Society of Chemistry [9].

```
#Parafin, High Density Polyethylene (HDPE)
poly.set_density('g/cm3', 0.92)
poly.add_element('H', 11.60, percent_type='wo')
poly.add_element('C', 61.20, percent_type='wo')
poly.add_element('O', 22.20, percent_type='wo')
poly.add_nuclide('B10', 1, percent_type='wo')
poly.add_nuclide('B11', 4, percent_type='wo')

#Boron Carbide
B4C = openmc.Material(name='B4C')
B4C.set_density('g/cm3', 2.52)
B4C.add_element('C', 0.217390, percent_type='wo')
B4C.add_element('B', 0.782610, percent_type='wo')
```

Figure 14 – Material compositions of boronated polyethylene and boron carbide for use in MSTL shielding

5.5.1. Addition of Boronated Polyethylene to Model

The addition of boronated polyethylene reduced overall heating in the componentry of the non-irradiated zone. A summary of model results can be seen in Table 11.

Table 11 – Summary of Results with Addition of Boronated Polyethylene

Simulation parameter	**Basic, Non-augmented Model Computation**	**Polyethylene Computation**
Starting Particles	1,000,000	1,000,000
Batches	500	500
Computation Time (sec)	19456.5 (5.404 hours)	7281.9 (2.02 hours)
Neutron Leakage	0.59874	0.2507

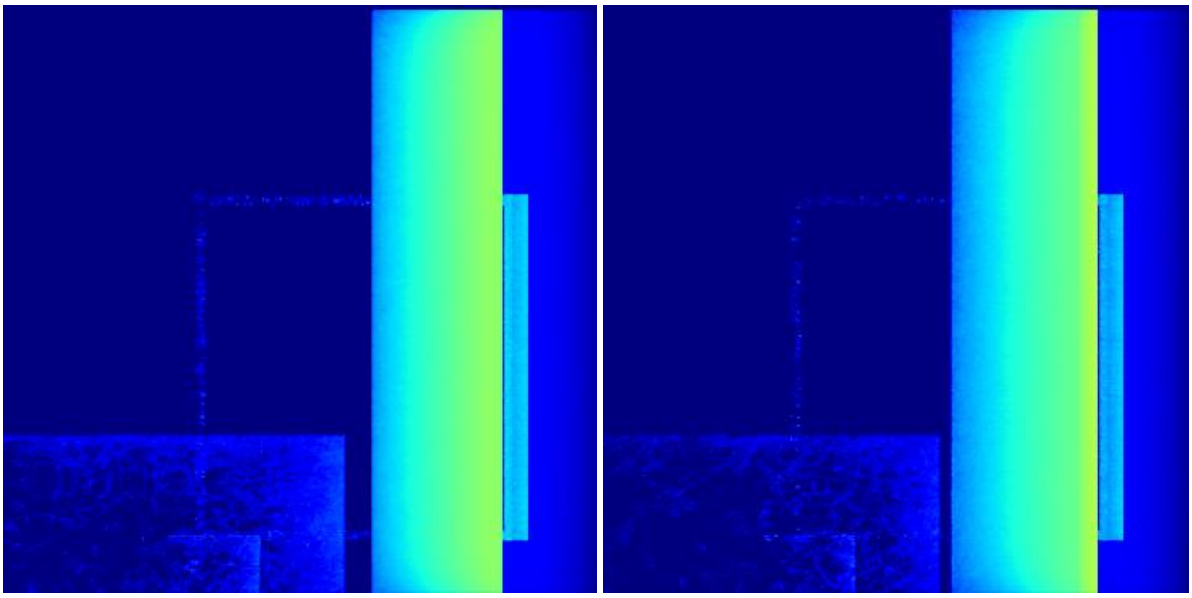

Figure 15 – *Heating of MSTL with (right) and without (left) boronated polyethylene shielding added to the model

Blue indicates heating values of 3E-4 ev/sp, white indicates values of 1.5E6 ev/sp, and yellow indicates values of 3E6 ev/sp. Values were assigned to a log scale before plotting.

Table 12 – Comparative Results from Shielding Sensitivity Study Between Boronated Polyethylene and Bare Concrete.

Tally	Location	Flux (percent change)	Flux Reaction rate (n-cm^2/sp) Relative Change	Heating (percent change)	Heating Reaction Rate (ev/sp) Relative Change

11	Steel Block Irradiation Zone	-27.13%	-4.11E-02	-5.55%	-159.01
13	Steel Pump	-49.23%	-1.83E-03	-49.71%	-18.87
15	Air	-53.19%	-1.12E+02	-41.62%	-1483.26
3	Steel Piping Irradiation Zone	-53.21%	-1.35E-02	-16.63%	-54.73
5	Vertical Steel Piping Non-Irradiation Zone	-49.00%	-3.79E-05	-49.35%	-1.12033
7	Top Horizontal Steel Piping	-51.37%	-1.09E-03	-16.20%	-3.79
9	Bottom Horizontal Steel Piping	-51.42%	-1.07E-03	-15.71%	-3.6367
14	NU2100 Filter	-49.92%	-1.97E-02	-49.19%	-522.002
12	Concrete Shielding	-69.26%	-4.15E+01	-49.03%	-641055
2	Beryllium Inner Sheath Irradiation Zone	15.37%	9.60E-21	-59.75%	-3.344E-15
4	Tungsten Outer Sheath Irradiation Zone	-55.51%	-9.38E-04	-26.96%	-2.083
1	FLiBe Irradiation Zone	-50.64%	-1.01E-02	-54.36%	-5242.54
6	Vertical FLiBe Non-Irradiation Zone	-47.32%	-9.42E-05	-52.14%	-48.80
8	Top Horizontal FLiBe	-47.09%	-2.28E-03	-59.88%	-1787.99
10	Bottom Horizontal FLiBe	-46.81%	-2.22E-03	-59.94%	-1747.8

The components within the non-irradiation zone, including the pump, Nu2100 filter, piping, and concrete shielding, exhibit heating percentage reductions ranging from 5% to nearly 60%.

The addition of boronated polyethylene in the shielding composition also decreased neutron leakage by improving the fidelity of the model, as seen in the model parameters. This is due to a decrease in the number of scattering events occurring between the fast neutron interaction with

the concrete shielding. Scattering events with the concrete shield cause particles to exit the space of the model and terminate before contributing to useful tallies such as flux and heating. Instead, the polyethylene shield layer attenuates the neutrons and allows them to deposit their energy as quickly as possible. This is demonstrated in Figure 15 and Figure 16, where visualizations of the data were computed in electron-volts per source particle (ev/sp).

It is important to note that the improved fidelity of the model increased neutron flux in the beryllium inner pipe, as the number of flux interactions increased. This does not signify that adding boronated polyethylene increases neutron flux, but rather indirectly improved the performance of the model. Furthermore, the hydrogenous material acts to attenuate gamma rays and secondary forms of radiation from neutron-material interactions. This attenuation, coupled with thermalization, decreases the available neutron population which decreases flux and heating events, even in regions upstream of the shielding.

5.5.2. Addition of Boron Carbide to Model

From a holistic engineering perspective, there is a possibility that the boronated polyethylene will melt due to the intense neutron flux and heating during irradiation. The purpose of the boron carbide (B4C) study is to explore a shielding augmentation for the purposes of the MSTL while accounting for these engineering challenges. In this study, the 10-cm layer of boronated polyethylene in the stochastic model was changed to B4C [9]. All other assumptions are held constant.

Table 13 – Summary of Results with Addition of Boron Carbide

Simulation parameter	**Basic, Non-augmented Model Computation**	**Boron Carbide Computation**
Starting Particles	1,000,000	1,000,000
Batches	500	500
Computation Time (sec)	19456.5 sec (5.404 hours)	5258.6 sec (1.46 hours)
Neutron Leakage	0.59874	0.33541

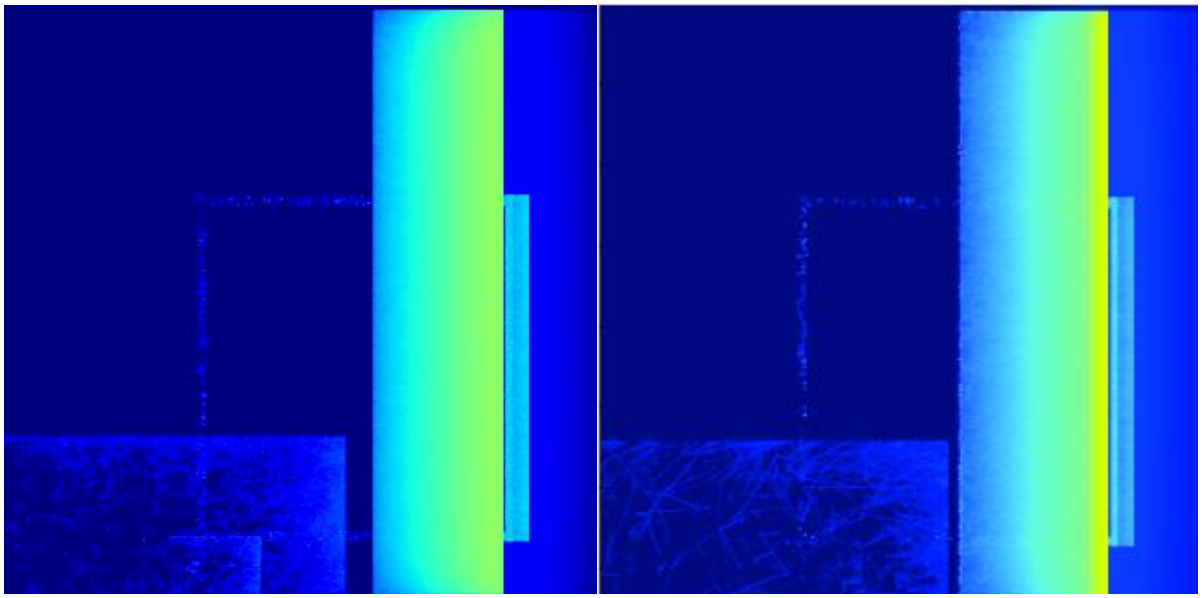

Figure 16 – *Heating of MSTL with (right) and without (left) boron carbide shielding added to the model

Blue indicates heating values of 3E-4 ev/sp, white indicates values of 1.5E6 ev/sp, and yellow indicates values of 3E6 ev/sp. Values were assigned to a log scale before plotting.

Table 14 – Comparative Results from Shielding Sensitivity Study Between Boron Carbide and Bare Concrete.

Tally	Location	Flux (percent change)	Flux Reaction rate (n-cm^2/sp)	Heating (percent change)	Heating Reaction Rate (ev/sp)
11	Steel Block Irradiation Zone	-14.71%	-2.23E-02	3.00%	8.60E+01
13	Steel Pump	-67.44%	-2.51E-03	-71.97%	-2.73E+01
15	Air	-41.11%	-8.65E+01	-17.22%	-6.14E+02
3	Steel Piping Irradiation Zone	-26.99%	-6.83E-03	7.24%	2.38E+01
5	Vertical Steel Piping Non-Irradiation Zone	-68.33%	-5.28E-05	-70.65%	-1.60E+00

7	Top Horizontal Steel Piping	-47.81%	-1.01E-03	-19.21%	-4.50E+00
9	Bottom Horizontal Steel Piping	-47.33%	-9.84E-04	-18.15%	-4.20E+00
14	NU2100 Filter	-68.63%	-2.71E-02	-70.67%	-7.50E+02
12	Concrete Shielding	-73.10%	-4.38E+01	-65.05%	-8.51E+05
2	Beryllium Inner Sheath Irradiation Zone	178.61%	1.12E-19	36.39%	2.04E-15
4	Tungsten Outer Sheath Irradiation Zone	-32.57%	-5.51E-04	9.46%	7.31E-01
1	FLiBe Irradiation Zone	-12.09%	-2.42E-03	-67.31%	-6.49E+03
6	Vertical FLiBe Non-Irradiation Zone	-67.83%	-1.35E-04	-70.36%	-6.59E+01
8	Top Horizontal FLiBe	-38.24%	-1.85E-03	-68.61%	-2.05E+03
10	Bottom Horizontal FLiBe	-37.68%	-1.79E-03	-68.97%	-2.01E+03

Boron carbide offers a balanced solution between the bare concrete shielding block and the boronated polyethylene trial. Similar to the polyethylene setup, scattering events are minimized with the introduction of boron carbide. Although neutron leakage sees a slight

increase in the boron carbide simulation to 33%, up from the 25% observed in the polyethylene trial, the overall model performance is enhanced compared to the 60% neutron leakage rate in the standard model.

Neutron flux decreases across all cells in the model, ranging from 12% to over 70%, except for the beryllium inner sheath, which experiences a 178% increase. This pattern, akin to the polyethylene trial, indicates superior performance across the cell and greater accuracy. However, boron carbide's neutron attenuation and thermalization properties are inferior to those of polyethylene. This leads to reduced initial thermalization and moderation of neutrons, resulting in more prevalent subsequent secondary reactions and radiation forms such as gamma rays.

Consequently, cells upstream of the boron carbide, such as the steel block, steel piping, tungsten, etc., in the irradiation zone, experience an increase in heating alongside a decrease in neutron flux. Despite this, the balance achieved between reducing neutron flux and heating behind the shield wall while preserving heating in the irradiation zone, coupled with the overall improved model performance, indicates a well-designed shielding simulation.

5.6. Tritium Production Experimental Study

One of the primary objectives of the UC-MSTL is to demonstrate tritium breeding through interactions between fast neutrons and FLiBe salt. Initially, it was believed that the incident neutrons required thermalization because their energies from the neutron "beam" were too high to generate tritium, given the low (n,t) cross-section value of Li-6 of the FLiBe salt in the fast neutron energy range (refer to Figure 17). To address this, it was proposed to add a steel block to the front of the loop to thermalize the neutrons before interacting with the salt (see Figure 6 for detailed view of irradiation zone). This study examines how altering the thickness of the steel block at the forefront of the loop affects tritium breeding in the salt of the UC-MSTL.

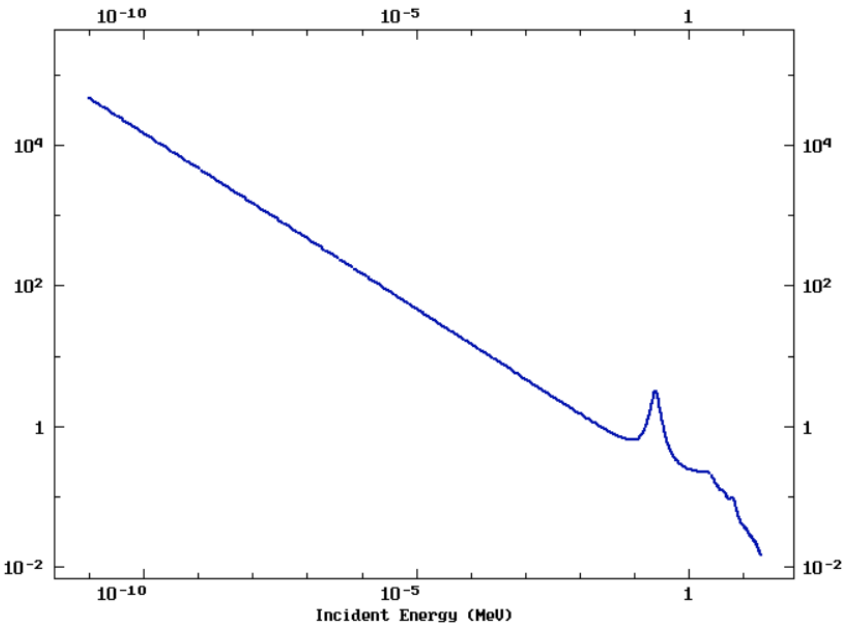

Figure 17 – (n,t) Cross section of primary tritium producing isotope (Li-6) in FLiBe salt

5.6.1. Assumptions

The following assumptions were made to the tritium production experimental study:

1. All computational runs utilized the same geometry excluding the block.
2. Each run utilized 100,000 particles and the same source value (see section 5.2.4).
3. Each run shortened the block by 1 centimeter.
4. Only Li-6 contributed to the production of tritium as a conservative underestimate.

5.6.2. Results

It was quickly determined that increasing the thickness of the steel block decreased the number of (n,t) events occurring within the FLiBe salt. Figure 18 highlights the summated number of (n,t) events occurring within the FLiBe salt from the four sections of FLiBe defined in the model with each subsequent shortening of the block. Figure 19 illustrates the visual aspects of the FLiBe salt with four select runs at 9-cm, 6-cm, 3-cm, and 0-cm of block thickness respectively.

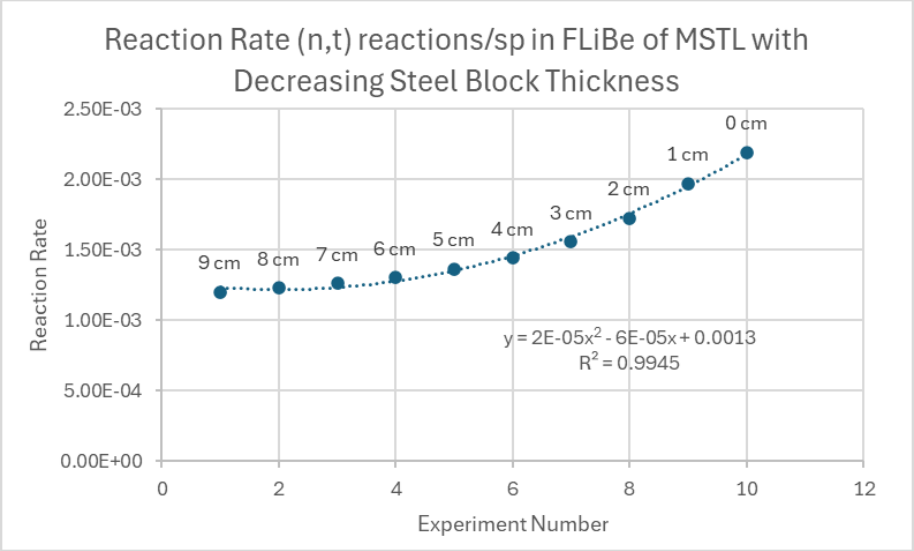

Figure 18 – (n,t) Reactions/sp of FLiBe of MSTL with decreasing block thickness

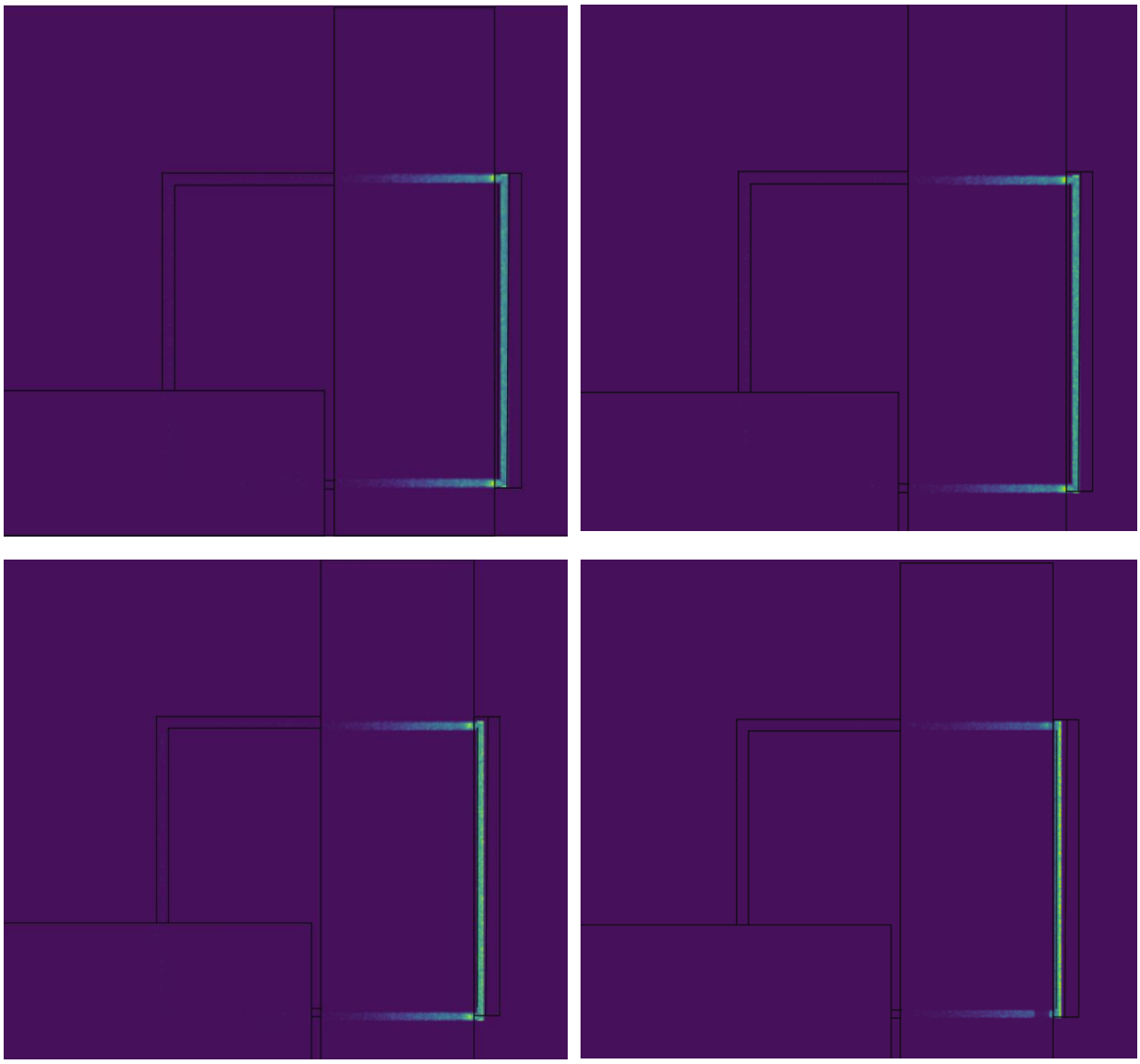

Figure 19 – (n,t) Reactions/sp of FLiBe of MSTL with decreasing block thickness (9cm – top left; 6cm – top right; 3 cm – bottom left; 0 cm – bottom right)

Blue values indicate a value of zero, while tallies were plotted on a logarithmic scale with light blue representing 8e-06 and bright yellow representing 8e-04.

After completely removing the block, the number of (n,t) events increased by nearly a factor of two, as highlighted by Table 15.

Table 15 – Results from removal of steel block from UC-MSTL and impact on FLiBe salt (n,t) reactions. Positive values indicate an increase in (n,t) reactions following removal of the block.

Location	8-cm Block (n,t) Reactions/sp	Std. Deviation	No Block (n,t) Reactions/sp	Std. Deviation	Relative Change	Percent change
Vertical section irradiation zone	0.000764279	4.39552e-06	0.00180193	6.99547e-06	0.001037651	57.59%
Vertical section non-irradiation zone	7.25517e-06	4.76585e-07	7.43099e-06	4.82201e-07	1.76E-07	2.37%
Horizontal top section	0.000167093	2.23421e-06	0.000220045	2.53195e-06	0.000052952	24.06%
Horizontal bottom section	0.000180809	2.33169e-06	0.000163352	2.13123e-06	-0.000017457	-10.69%

It can be determined that removal of the steel block positively impacts the production of tritium in the model. The number of tritium atoms produced per simulation is highlighted in Table 16.

Table 16 – Number of tritium atoms produced per reaction with decreasing block thickness.

experiment number	Thickness of Steel Block (cm)	Reaction rate ((n,t) reactions/source particle) in FLiBe of MSTL
1	9 cm	1.20E-03
2	8 cm	1.23E-03
3	7 cm	1.26E-03
4	6 cm	1.30E-03
5	5 cm	1.36E-03
6	4 cm	1.44E-03
7	3 cm	1.56E-03
8	2 cm	1.73E-03
9	1 cm	1.97E-03
10	0 cm	2.19E-03

The results of this experiment recommend the removal of the steel block from the final model. The results coincide with current literature on the concept models of breeder blankets for fusion

applications, as seen in Figure 20 of a conceptual breeder blanket for an ARC-like fusion power plant [10].

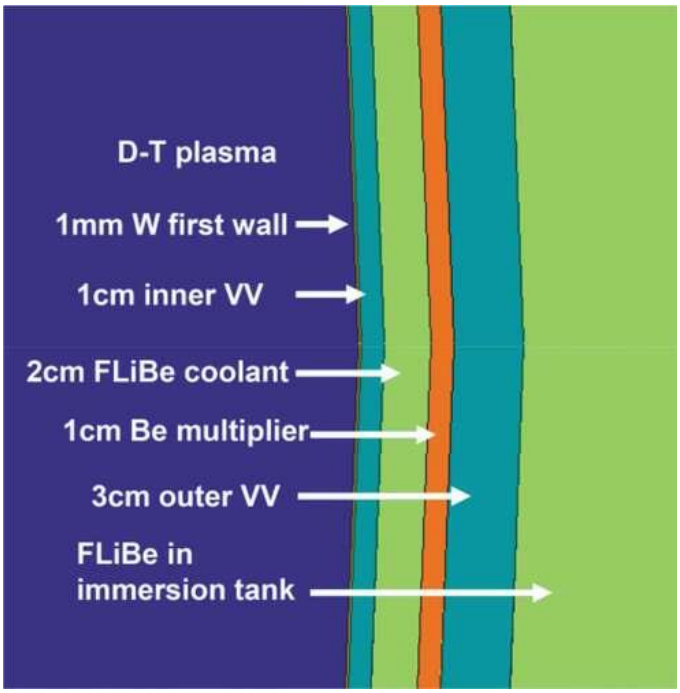

Figure 20 – ARC vacuum vessel design displaying section view of tokomak and proposed FLiBe coolant. A total of 1.1 cm of material separates the plasma from FLiBe location

6. Future Work

The three experiments performed utilizing the stochastic simulator OpenMC provide several avenues for future work including:

1. Application of neutron spectra and neutron fluence rate for particular reactor design in MSTL model, such as that being pioneered by Commonwealth Fusion Systems, General Atomics, etc.
2. Determination of standardized (utilizing particular fluence rate) operating temperatures, flux values, heating values, and total number of tritium atoms produced in model.
3. Verification of 1:1.1 or greater tritium breeding ratio utilizing test loop or greater scaleup.
4. Additional complexity in stochastic model to more accurately reflect MSTL geometry.
5. A FISPACT or activation study to determine post-operation decay schemes for activated elements in the MSTL structure and FLiBe salt.

A. References

This document benefited from AI in its generation.

[1] OpenAI. (2024). ChatGPT: Language Model by OpenAI. Retrieved January 20th, 2024 https://www.openai.com/

[2] Adams, Marvin L. (2009). Introduction to Nuclear Reactor Theory. Texas A&M University.

[3] "The OpenMC Monte Carlo Code." The OpenMC Monte Carlo Code - OpenMC Documentation, 2011 The OpenMC Monte Carlo Code — OpenMC Documentation

[4] Kikuchi, M.; Lackner, K.; Tran, M.Q. (Eds.) Fusion Physics; International Atomic Energy Agency: Vienna, Austria, 2012.

[5] "Reference Input Spectra - Magnetic Confined ITER DT Neutron Spectra." FISPACT, UKAEA, 30 Jan. 2018, fispact.ukaea.uk/wiki/Reference_input_spectra.

[6] Sahadath, Hossain, et al. "Calculation of Gamma Ray Attenuation Parameters for Locally Developed Ilmenite-Magnetite Concrete." Journal of Bangladesh Academy of Sciences, 40(1), 11-21, June 2016, http://dx.doi.org/10.3329/jbas.v40i1.28321.

[7] Delaporte-Mathurin, R., Shimwell, J., Pattinson, L., Pranto, A. I., & Faisal, M. (2023). OpenMC Plasma Source (Version 0.3.0) [Computer software]. https://github.com/fusion-energy/openmc-plasma-source

[8] Rebello, W. F. "Multileaf Shielding Design against Neutrons Produced by Medical Linear Accelerators." ResearchGate, Journal of Radiation Protection Dosimetry , Feb. 2008, www.researchgate.net/publication/6266884_Multileaf_shielding_design_against_neutrons_produced_by_medical_linear_accelerators.

[9] "Reference Tables | the Merck Index Online." *Boron Carbide*, Royal Society of Chemistry, 2024, merckindex.rsc.org/reference.

[10] Charles Forsberg, Guiqiu (Tony) Zheng, Ronald G. Ballinger & Stephen T. Lam (2020) Fusion Blankets and Fluoride-Salt-Cooled High-Temperature Reactors with Flibe Salt Coolant: Common Challenges, Tritium Control, and Opportunities for Synergistic Development Strategies Between Fission, Fusion, and Solar Salt Technologies, Nuclear Technology, 206:11, 1778-1801, DOI: 10.1080/00295450.2019.1691400,https://www.tandfonline.com/doi/citedby/10.1080/00295450.2019.1691400?scroll=top&needAccess=true

B. Code Sets and Analytical Results

Deterministic

Shielding Calculation

	B	C	D
1	**DATA**		
2	**Given nuclear data**		
3	Neutron energy (MeV)	14.8	
4			
5			
6	**Sheilding Data**		
7	Material	air (stp)	
8	density (g/cm^3)	0.0013	
9			
10	Material	concrete	
11	density (g/cm^3)	2.78	
12			
13	Material	Enhanced B4C conrete	
14	density (g/cm^3), table 3	2.232	
15			
16			
17	**RANGE**		
18		**cm**	
19	Range of neutron in air	=(530*C3-106)/C8	
20	Range of neutron in concrete (std portland cement)	=(530*C3-106)/C11	
21	Range of neutron in B4C	=(530*C3-106)/C14	
22			
23			
24			
25	**SHIELD THICKNESS**	**(from online source, found to be 0.22 - unverified)**	
26			
27			
28	Mean free path of ilmenite-magnetite concrete:		
29	macroscopic XS of concrete:	0.22	
30	mean free path	=LN(0.01)/-C29	
31			
32	Calculation of Macroscopic capture XS of ilmenite magnetite concrete-		

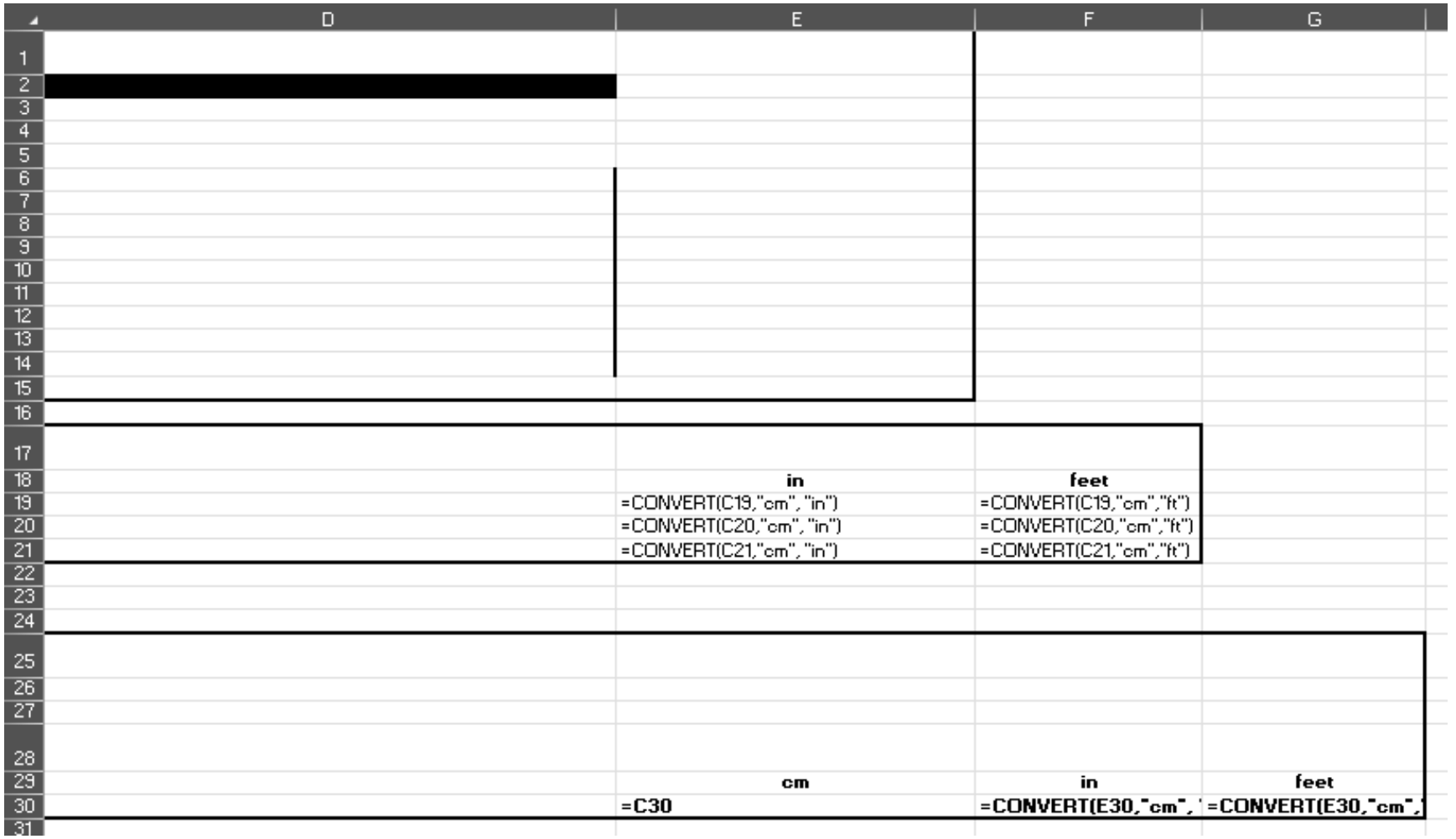

	D	E	F	G
1				
2				
3				
4				
5				
6				
7				
8				
9				
10				
11				
12				
13				
14				
15				
16				
17				
18		in	feet	
19		=CONVERT(C19,"cm","in")	=CONVERT(C19,"cm","ft")	
20		=CONVERT(C20,"cm","in")	=CONVERT(C20,"cm","ft")	
21		=CONVERT(C21,"cm","in")	=CONVERT(C21,"cm","ft")	
22				
23				
24				
25				
26				
27				
28				
29		cm	in	feet
30		=C30	=CONVERT(E30,"cm",	=CONVERT(E30,"cm",
31				

	C	D	E	F	G	H	I	J	K	L	M	N	
32													
33													
34	Elemental Weight Fraction	Natural Abundance	Weighting Factor	Microscopic Cross Section value (NNDL) (barns)	Microscopic Cross Section (cm^2)	g/mol	mol/g	elemental density (g/cm^3)	mol/cm^3	atms/cm^3	Macroscopic XS	Weighted Macroscopic XS	
35													
36	0.0056478	0.99985	=C36*D36	0.65	=F36*1E-24	1.00794	=1/H36	0.0157	=J36*I36	=K36*6.02E+23	=L36*G36	=M36*E36	
37	0.0056478	0.00015	=C37*D37	0.78	=F37*1E-24	2.01588	=1/H37	0.0157	=J37*I37	=K37*6.02E+23	=L37*G37	=M37*E37	
38	0.00079137	0.989	=C38*D38	1.38056	=F38*1E-24	12.0107	=1/H38	1.0532	=J38*I38	=K38*6.02E+23	=L38*G38	=M38*E38	**Pulle**
39	0.00079137	0.011	=C39*D39	1.45022	=F39*1E-24	13.0107	=1/H39	1.0532	=J39*I39	=K39*6.02E+23	=L39*G39	=M39*E39	**Pulle**
40	0.37852518	0.99762	=C40*D40	1.747	=F40*1E-24	15.994	=1/H40	0.0022	=J40*I40	=K40*6.02E+23	=L40*G40	=M40*E40	
41	0.37852518	0.00038	=C41*D41	1.708	=F41*1E-24	16.9991315	=1/H41	0.0022	=J41*I41	=K41*6.02E+23	=L41*G41	=M41*E41	
42	0.37852518	0.002	=C42*D42	1.24022	=F42*1E-24	17.999161	=1/H42	0.0022	=J42*I42	=K42*6.02E+23	=L42*G42	=M42*E42	**Pulle**
43	0.03647482	0.7899	=C43*D43	1.803	=F43*1E-24	23.985	=1/H43	0.1014	=J43*I43	=K43*6.02E+23	=L43*G43	=M43*E43	
44	0.03647482	0.1	=C44*D44	1.822	=F44*1E-24	24.985	=1/H44	0.1014	=J44*I44	=K44*6.02E+23	=L44*G44	=M44*E44	
45	0.03647482	0.1101	=C45*D45	1.845	=F45*1E-24	25.982	=1/H45	0.1014	=J45*I45	=K45*6.02E+23	=L45*G45	=M45*E45	
46	0.0178777	1	=C46*D46	1.75	=F46*1E-24	26.9815	=1/H46	0.0497	=J46*I46	=K46*6.02E+23	=L46*G46	=M46*E46	
47	0.04852518	0.9223	=C47*D47	1.756	=F47*1E-24	27.97692	=1/H47	0.1349	=J47*I47	=K47*6.02E+23	=L47*G47	=M47*E47	
48	0.04852518	0.0467	=C48*D48	1.756	=F48*1E-24	28.97649	=1/H48	0.1349	=J48*I48	=K48*6.02E+23	=L48*G48	=M48*E48	
49	0.04852518	0.031	=C49*D49	1.756	=F49*1E-24	29.97377	=1/H49	0.1349	=J49*I49	=K49*6.02E+23	=L49*G49	=M49*E49	
50	0.00007194	1	=C50*D50	1.85579	=F50*1E-24	30.973762	=1/H50	0.0002	=J50*I50	=K50*6.02E+23	=L50*G50	=M50*E50	
51	0.00057554	0.9502	=C51*D51	1.723	=F51*1E-24	31.97207	=1/H51	0.0016	=J51*I51	=K51*6.02E+23	=L51*G51	=M51*E51	
52	0.00057554	0.0075	=C52*D52	1.746	=F52*1E-24	32.97145	=1/H52	0.0016	=J52*I52	=K52*6.02E+23	=L52*G52	=M52*E52	
53	0.00057554	0.0421	=C53*D53	1.761	=F53*1E-24	33.96786	=1/H53	0.0016	=J53*I53	=K53*6.02E+23	=L53*G53	=M53*E53	
54	0.00057554	0.0002	=C54*D54	1.804	=F54*1E-24	35.96708	=1/H54	0.0016	=J54*I54	=K54*6.02E+23	=L54*G54	=M54*E54	
55	0.08881295	0.96941	=C55*D55	2.125	=F55*1E-24	39.96259	=1/H55	0.2469	=J55*I55	=K55*6.02E+23	=L55*G55	=M55*E55	
56	0.08881295	0.00647	=C56*D56	2.127	=F56*1E-24	41.95861	=1/H56	0.2469	=J56*I56	=K56*6.02E+23	=L56*G56	=M56*E56	
57	0.08881295	0.00135	=C57*D57	2.147	=F57*1E-24	42.95876	=1/H57	0.2469	=J57*I57	=K57*6.02E+23	=L57*G57	=M57*E57	
58	0.08881295	0.02086	=C58*D58	2.169	=F58*1E-24	43.95548	=1/H58	0.2469	=J58*I58	=K58*6.02E+23	=L58*G58	=M58*E58	
59	0.08881295	0.00004	=C59*D59	2.211	=F59*1E-24	45.95368	=1/H59	0.2469	=J59*I59	=K59*6.02E+23	=L59*G59	=M59*E59	
60	0.08881295	0.00187	=C60*D60	2.255	=F60*1E-24	47.95252	=1/H60	0.2469	=J60*I60	=K60*6.02E+23	=L60*G60	=M60*E60	
61	0.12816547	0.08	=C61*D61	2.21644	=F61*1E-24	45.95263	=1/H61	0.3563	=J61*I61	=K61*6.02E+23	=L61*G61	=M61*E61	
62	0.12816547	0.073	=C62*D62	2.23848	=F62*1E-24	46.95176	=1/H62	0.3563	=J62*I62	=K62*6.02E+23	=L62*G62	=M62*E62	
63	0.12816547	0.738	=C63*D63	2.2606	=F63*1E-24	47.94794	=1/H63	0.3563	=J63*I63	=K63*6.02E+23	=L63*G63	=M63*E63	
64	0.12816547	0.055	=C64*D64	2.28316	=F64*1E-24	48.94787	=1/H64	0.3563	=J64*I64	=K64*6.02E+23	=L64*G64	=M64*E64	
65	0.12816547	0.054	=C65*D65	2.30401	=F65*1E-24	49.94479	=1/H65	0.3563	=J65*I65	=K65*6.02E+23	=L65*G65	=M65*E65	
66	0.0007554	0.0025	=C66*D66	2.30149	=F66*1E-24	49.94715	=1/H66	0.0021	=J66*I66	=K66*6.02E+23	=L66*G66	=M66*E66	
67	0.0007554	0.9975	=C67*D67	2.29132	=F67*1E-24	50.94395	=1/H67	0.0021	=J67*I67	=K67*6.02E+23	=L67*G67	=M67*E67	
68	0.00035071	0.0435	=C68*D68	2.38104	=F68*1E-24	49.94604	=1/H68	0.001	=J68*I68	=K68*6.02E+23	=L68*G68	=M68*E68	
69	0.00035071	0.83789	=C69*D69	2.38652	=F69*1E-24	51.9405	=1/H69	0.001	=J69*I69	=K69*6.02E+23	=L69*G69	=M69*E69	
70	0.00035071	0.09501	=C70*D70	2.38692	=F70*1E-24	52.94064	=1/H70	0.001	=J70*I70	=K70*6.02E+23	=L70*G70	=M70*E70	
71	0.00035071	0.02365	=C71*D71	2.38652	=F71*1E-24	53.93888	=1/H71	0.001	=J71*I71	=K71*6.02E+23	=L71*G71	=M71*E71	
72	0.00302158	1	=C72*D72	2.4262	=F72*1E-24	54.94083	=1/H72	0.0084	=J72*I72	=K72*6.02E+23	=L72*G72	=M72*E72	
73	0.28284173	0.058	=C73*D73	2.427	=F73*1E-24	53.9396	=1/H73	0.7863	=J73*I73	=K73*6.02E+23	=L73*G73	=M73*E73	
74	0.28284173	0.9172	=C74*D74	2.513	=F74*1E-24	55.93493	=1/H74	0.7863	=J74*I74	=K74*6.02E+23	=L74*G74	=M74*E74	
75	0.28284173	0.022	=C75*D75	2.514	=F75*1E-24	56.93539	=1/H75	0.7863	=J75*I75	=K75*6.02E+23	=L75*G75	=M75*E75	
76	0.28284173	0.0028	=C76*D76	2.514	=F76*1E-24	57.93327	=1/H76	0.7863	=J76*I76	=K76*6.02E+23	=L76*G76	=M76*E76	
77	0.00043165	0.68077	=C77*D77	2.598	=F77*1E-24	57.93534	=1/H77	0.0012	=J77*I77	=K77*6.02E+23	=L77*G77	=M77*E77	
78	0.00043165	0.26223	=C78*D78	2.6875	=F78*1E-24	59.93078	=1/H78	0.0012	=J78*I78	=K78*6.02E+23	=L78*G78	=M78*E78	
79	0.00043165	0.0114	=C79*D79	2.68541	=F79*1E-24	60.93105	=1/H79	0.0012	=J79*I79	=K79*6.02E+23	=L79*G79	=M79*E79	
80	0.00043165	0.03634	=C80*D80	2.66847	=F80*1E-24	61.92834	=1/H80	0.0012	=J80*I80	=K80*6.02E+23	=L80*G80	=M80*E80	
81	0.00043165	0.00926	=C81*D81	2.68555	=F81*1E-24	63.92796	=1/H81	0.0012	=J81*I81	=K81*6.02E+23	=L81*G81	=M81*E81	
82													
83											**Total Macr**	=SUM(N36:N81)	1/cm
84													
85											**50% Attenu**	=LN(0.5)/-N83	cm
86												=CONVERT(N85,"cm","in"	in
87													
88											**Mean free p**	=1/N83	cm
89												=CONVERT(N88,"cm","in"	in
90													

NAA – Neutron Flux Calculations

	A	B	C	D	E	F
1						
2	DD_Flux			DT_Flux		
3						
4	**Sum Flux Values:**		**=SUM(A7:A181)**	**Sum Flux Values:**		**=SUM(E7:E181)**
5	**Average Flux:**		**=C4/COUNT(A7:A181)**	**Average Flux:**		**=F4/COUNT(E7:E181)**
6	Flux	Energy			Flux	Energy
7	0	19640000			0	19640000
8	0	17332000			0	17332000
9	0	16905000			0	16905000
10	0	16487000			359020000	16487000
11	0	15683000			456260000000	15683000
12	0	14918000			3242400000000	14918000
13	0	14550000			9775500000000	14550000
14	5588300000	14191000			12871000000000	14191000
15	219420000	13840000			8051100000000	13840000
16	253010000	13499000			4046900000000	13499000
17	54487000	12840000			540330000000	12840000
18	39982000	12523000			355200000000	12523000
19	53732000	12214000			487870000000	12214000
20	62379000	11618000			505020000000	11618000
21	71404000	11052000			611200000000	11052000
22	68383000	10513000			616300000000	10513000
23	63709000	10000000			548400000000	10000000
24	67356000	9512300			473610000000	9512300
25	63431000	9048400			408210000000	9048400
26	54287000	8607100			373070000000	8607100

NAA – Maximum Saturation Activity - Steel

	A	B	C	D	E	F	G
1							
2							
3							
4	**STEEL**						
5	Element	Isotopes	Elemental Weight Fraction	Natural Abundance	Weighted Factor	Microscopic Cross Section value (NNDL)	Microscopic Cross Section (cm^2)
6		Si-28	0.04852518	0.9223	=C6*D6	1.756	=F6*1E-24
7	Si (1%)	Si-29	0.04852518	0.0467	=C7*D7	1.756	=F7*1E-24
8		Si-30	0.04852518	0.031	=C8*D8	1.756	=F8*1E-24
9	Mn (2%)	Mn-55	0.00302158	1	=C9*D9	2.4262	=F9*1E-24
10	Cr (20%)	Cr-50	0.00035071	0.0435	=C10*D10	2.38104	=F10*1E-24
11		Cr-52	0.00035071	0.83789	=C11*D11	2.38652	=F11*1E-24
12		Cr-53	0.00035071	0.09501	=C12*D12	2.38692	=F12*1E-24
13		Cr-54	0.00035071	0.02365	=C13*D13	2.38652	=F13*1E-24
14	Ni (11%)	Ni-58	0.00043165	0.68077	=C14*D14	2.598	=F14*1E-24
15		Ni-60	0.00043165	0.26223	=C15*D15	2.6875	=F15*1E-24
16		Ni-61	0.00043165	0.0114	=C16*D16	2.68541	=F16*1E-24
17		Ni-62	0.00043165	0.03634	=C17*D17	2.66847	=F17*1E-24
18		Ni-64	0.00043165	0.00926	=C18*D18	2.68555	=F18*1E-24
19	Fe (65.845%)	Fe-54	0.28284173	0.058	=C19*D19	2.427	=F19*1E-24
20		Fe-56	0.28284173	0.9172	=C20*D20	2.513	=F20*1E-24
21		Fe-57	0.28284173	0.022	=C21*D21	2.514	=F21*1E-24
22		Fe-58	0.28284173	0.0028	=C22*D22	2.514	=F22*1E-24
23						brookhaven	

	H	I	J	K	L	M
1						
2		Volume (cm^3):	2676600			
3		Accounts for Basin, pump, MOF, Pipe, and barrier				
4						
5	g/mol	mol/g	elemental density (g/cm^3)	mol/cm^3	atms/cm^3	Macroscopic XS
6	27.977	=1/H6	2.33	=I6*J6	=K6*6.02E+23	=L6*G6
7	28.976	=1/H7	2.33	=I7*J7	=K7*6.02E+23	=L7*G7
8	29.974	=1/H8	2.33	=I8*J8	=K8*6.02E+23	=L8*G8
9	54.938	=1/H9	7.47	=I9*J9	=K9*6.02E+23	=L9*G9
10	49.946	=1/H10	7.19	=I10*J10	=K10*6.02E+23	=L10*G10
11	51.941	=1/H11	7.19	=I11*J11	=K11*6.02E+23	=L11*G11
12	52.941	=1/H12	7.19	=I12*J12	=K12*6.02E+23	=L12*G12
13	53.939	=1/H13	7.19	=I13*J13	=K13*6.02E+23	=L13*G13
14	57.935	=1/H14	8.908	=I14*J14	=K14*6.02E+23	=L14*G14
15	59.931	=1/H15	8.908	=I15*J15	=K15*6.02E+23	=L15*G15
16	60.931	=1/H16	8.908	=I16*J16	=K16*6.02E+23	=L16*G16
17	61.928	=1/H17	8.908	=I17*J17	=K17*6.02E+23	=L17*G17
18	63.928	=1/H18	8.908	=I18*J18	=K18*6.02E+23	=L18*G18
19	53.94	=1/H19	7.875	=I19*J19	=K19*6.02E+23	=L19*G19
20	55.935	=1/H20	7.875	=I20*J20	=K20*6.02E+23	=L20*G20
21	56.935	=1/H21	7.875	=I21*J21	=K21*6.02E+23	=L21*G21
22	57.933	=1/H22	7.875	=I22*J22	=K22*6.02E+23	=L22*G22
23	ChemCAD		ChemCAD			
24						

	N	O	P	Q
1				
2	Maximum saturation activity (atms/sec) = flux (n/cm^2/s)*microscopic xs (cm^2)*N(#of atms)			
3				
4				
5	Neutron Flux (DT)	Neutron Flux (DD)	Volume (cm^3)	mass (g)
6	=Neutron_Flux_Values_ITER!$F$5	=Neutron_Flux_Values_ITER!$C$5	=$J$2*E6	=J6*P6
7	=Neutron_Flux_Values_ITER!$F$5	=Neutron_Flux_Values_ITER!$C$5	=$J$2*E7	=J7*P7
8	=Neutron_Flux_Values_ITER!$F$5	=Neutron_Flux_Values_ITER!$C$5	=$J$2*E8	=J8*P8
9	=Neutron_Flux_Values_ITER!$F$5	=Neutron_Flux_Values_ITER!$C$5	=$J$2*E9	=J9*P9
10	=Neutron_Flux_Values_ITER!$F$5	=Neutron_Flux_Values_ITER!$C$5	=$J$2*E10	=J10*P10
11	=Neutron_Flux_Values_ITER!$F$5	=Neutron_Flux_Values_ITER!$C$5	=$J$2*E11	=J11*P11
12	=Neutron_Flux_Values_ITER!$F$5	=Neutron_Flux_Values_ITER!$C$5	=$J$2*E12	=J12*P12
13	=Neutron_Flux_Values_ITER!$F$5	=Neutron_Flux_Values_ITER!$C$5	=$J$2*E13	=J13*P13
14	=Neutron_Flux_Values_ITER!$F$5	=Neutron_Flux_Values_ITER!$C$5	=$J$2*E14	=J14*P14
15	=Neutron_Flux_Values_ITER!$F$5	=Neutron_Flux_Values_ITER!$C$5	=$J$2*E15	=J15*P15
16	=Neutron_Flux_Values_ITER!$F$5	=Neutron_Flux_Values_ITER!$C$5	=$J$2*E16	=J16*P16
17	=Neutron_Flux_Values_ITER!$F$5	=Neutron_Flux_Values_ITER!$C$5	=$J$2*E17	=J17*P17
18	=Neutron_Flux_Values_ITER!$F$5	=Neutron_Flux_Values_ITER!$C$5	=$J$2*E18	=J18*P18
19	=Neutron_Flux_Values_ITER!$F$5	=Neutron_Flux_Values_ITER!$C$5	=$J$2*E19	=J19*P19
20	=Neutron_Flux_Values_ITER!$F$5	=Neutron_Flux_Values_ITER!$C$5	=$J$2*E20	=J20*P20
21	=Neutron_Flux_Values_ITER!$F$5	=Neutron_Flux_Values_ITER!$C$5	=$J$2*E21	=J21*P21
22	=Neutron_Flux_Values_ITER!$F$5	=Neutron_Flux_Values_ITER!$C$5	=$J$2*E22	=J22*P22
23				

	R	S	T	U	V	W
1						
2						
3						
4			Before Shield - 25% Volume		After Shield - 75% Volume, 50% Flux	
5	DT Activity (Bq)	DD Activity (Bq)	Bq/g (DD)	Bq/g (DT)	Bq/g (DD)	Bq/g (DT)
6	=P6*L6*N6*G6	=O6*G6*L6*P6	=S6/Q6*0.25	=R6/Q6*0.25	=S6/Q6*0.75*0.5	=R6/Q6*0.75*0.5
7	=P7*L7*N7*G7	=O7*G7*L7*P7	=S7/Q7*0.25	=R7/Q7*0.25	=S7/Q7*0.75*0.5	=R7/Q7*0.75*0.5
8	=P8*L8*N8*G8	=O8*G8*L8*P8	=S8/Q8*0.25	=R8/Q8*0.25	=S8/Q8*0.75*0.5	=R8/Q8*0.75*0.5
9	=P9*L9*N9*G9	=O9*G9*L9*P9	=S9/Q9*0.25	=R9/Q9*0.25	=S9/Q9*0.75*0.5	=R9/Q9*0.75*0.5
10	=P10*L10*N10*G10	=O10*G10*L10*P10	=S10/Q10*0.25	=R10/Q10*0.25	=S10/Q10*0.75*0.5	=R10/Q10*0.75*0.5
11	=P11*L11*N11*G11	=O11*G11*L11*P11	=S11/Q11*0.25	=R11/Q11*0.25	=S11/Q11*0.75*0.5	=R11/Q11*0.75*0.5
12	=P12*L12*N12*G12	=O12*G12*L12*P12	=S12/Q12*0.25	=R12/Q12*0.25	=S12/Q12*0.75*0.5	=R12/Q12*0.75*0.5
13	=P13*L13*N13*G13	=O13*G13*L13*P13	=S13/Q13*0.25	=R13/Q13*0.25	=S13/Q13*0.75*0.5	=R13/Q13*0.75*0.5
14	=P14*L14*N14*G14	=O14*G14*L14*P14	=S14/Q14*0.25	=R14/Q14*0.25	=S14/Q14*0.75*0.5	=R14/Q14*0.75*0.5
15	=P15*L15*N15*G15	=O15*G15*L15*P15	=S15/Q15*0.25	=R15/Q15*0.25	=S15/Q15*0.75*0.5	=R15/Q15*0.75*0.5
16	=P16*L16*N16*G16	=O16*G16*L16*P16	=S16/Q16*0.25	=R16/Q16*0.25	=S16/Q16*0.75*0.5	=R16/Q16*0.75*0.5
17	=P17*L17*N17*G17	=O17*G17*L17*P17	=S17/Q17*0.25	=R17/Q17*0.25	=S17/Q17*0.75*0.5	=R17/Q17*0.75*0.5
18	=P18*L18*N18*G18	=O18*G18*L18*P18	=S18/Q18*0.25	=R18/Q18*0.25	=S18/Q18*0.75*0.5	=R18/Q18*0.75*0.5
19	=P19*L19*N19*G19	=O19*G19*L19*P19	=S19/Q19*0.25	=R19/Q19*0.25	=S19/Q19*0.75*0.5	=R19/Q19*0.75*0.5
20	=P20*L20*N20*G20	=O20*G20*L20*P20	=S20/Q20*0.25	=R20/Q20*0.25	=S20/Q20*0.75*0.5	=R20/Q20*0.75*0.5
21	=P21*L21*N21*G21	=O21*G21*L21*P21	=S21/Q21*0.25	=R21/Q21*0.25	=S21/Q21*0.75*0.5	=R21/Q21*0.75*0.5
22	=P22*L22*N22*G22	=O22*G22*L22*P22	=S22/Q22*0.25	=R22/Q22*0.25	=S22/Q22*0.75*0.5	=R22/Q22*0.75*0.5

NAA – Maximum Saturation Activity – Concrete

	A	B	C	D	E	F	G	H	I	J	K	L	M	N
1														
2			CONCRETE						source	14.8 MeV	Volume	10770000	cm^3	
3			Isotopes	Elemental Weight Fraction	Natural Abundance	Weighted Factor	Microscopic Cross Section value (NNDL)	Weighted Microscopic Cross Section (cm^2)	g/mol	mol/g weighted	elemental density (g/cm^3)	mol/cm^3	atms/cm^3	Macroscopic XS
4			Mg-24	0.03647482	0.7899	=D4*E4	1.803	=G4*1E-24	23.985	=1/I4	1.74	=J4*K4	=L4*6.02E+23	=M4*H4
5			Mg-25	0.03647482	0.1	=D5*E5	1.822	=G5*1E-24	24.986	=1/I5	1.74	=J5*K5	=L5*6.02E+23	=M5*H5
6			Mg-26	0.03647482	0.1101	=D6*E6	1.845	=G6*1E-24	25.983	=1/I6	1.74	=J6*K6	=L6*6.02E+23	=M6*H6
7			Al-27	0.0178777	1	=D7*E7	1.75	=G7*1E-24	26.981	=1/I7	2.7	=J7*K7	=L7*6.02E+23	=M7*H7
8			Si-28	0.04852518	0.9223	=D8*E8	1.756	=G8*1E-24	27.977	=1/I8	2.33	=J8*K8	=L8*6.02E+23	=M8*H8
9			Si-29	0.04852518	0.0467	=D9*E9	1.756	=G9*1E-24	28.976	=1/I9	2.33	=J9*K9	=L9*6.02E+23	=M9*H9
10			Si-30	0.04852518	0.031	=D10*E10	1.756	=G10*1E-24	29.974	=1/I10	2.33	=J10*K10	=L10*6.02E+23	=M10*H10
11			Ti-46	0.12816547	0.08	=D11*E11	2.21644	=G11*1E-24	45.953	=1/I11	4.507	=J11*K11	=L11*6.02E+23	=M11*H11
12			Ti-47	0.12816547	0.073	=D12*E12	2.23848	=G12*1E-24	46.952	=1/I12	4.507	=J12*K12	=L12*6.02E+23	=M12*H12
13			Ti-48	0.12816547	0.738	=D13*E13	2.2606	=G13*1E-24	47.948	=1/I13	4.507	=J13*K13	=L13*6.02E+23	=M13*H13
14			Ti-49	0.12816547	0.055	=D14*E14	2.28316	=G14*1E-24	48.948	=1/I14	4.507	=J14*K14	=L14*6.02E+23	=M14*H14
15			Ti-50	0.12816547	0.054	=D15*E15	2.30401	=G15*1E-24	49.945	=1/I15	4.507	=J15*K15	=L15*6.02E+23	=M15*H15
16			V-50	0.0007554	0.0025	=D16*E16	2.30149	=G16*1E-24	49.947	=1/I16	6.11	=J16*K16	=L16*6.02E+23	=M16*H16
17			V-51	0.0007554	0.9975	=D17*E17	2.29132	=G17*1E-24	50.944	=1/I17	6.11	=J17*K17	=L17*6.02E+23	=M17*H17
18			Cr-50	0.00035071	0.0435	=D18*E18	2.38104	=G18*1E-24	49.946	=1/I18	7.19	=J18*K18	=L18*6.02E+23	=M18*H18
19			Cr-52	0.00035071	0.83789	=D19*E19	2.38652	=G19*1E-24	51.941	=1/I19	7.19	=J19*K19	=L19*6.02E+23	=M19*H19
20			Cr-53	0.00035071	0.09501	=D20*E20	2.38692	=G20*1E-24	52.941	=1/I20	7.19	=J20*K20	=L20*6.02E+23	=M20*H20
21			Cr-54	0.00035071	0.02365	=D21*E21	2.38652	=G21*1E-24	53.939	=1/I21	7.19	=J21*K21	=L21*6.02E+23	=M21*H21
22			Mn-55	0.00302158	1	=D22*E22	2.4262	=G22*1E-24	54.938	=1/I22	7.47	=J22*K22	=L22*6.02E+23	=M22*H22
23			Fe-54	0.28284173	0.058	=D23*E23	2.427	=G23*1E-24	53.94	=1/I23	7.875	=J23*K23	=L23*6.02E+23	=M23*H23
24			Fe-56	0.28284173	0.9172	=D24*E24	2.513	=G24*1E-24	55.935	=1/I24	7.875	=J24*K24	=L24*6.02E+23	=M24*H24
25			Fe-57	0.28284173	0.022	=D25*E25	2.514	=G25*1E-24	56.935	=1/I25	7.875	=J25*K25	=L25*6.02E+23	=M25*H25
26			Fe-58	0.28284173	0.0028	=D26*E26	2.514	=G26*1E-24	57.933	=1/I26	7.875	=J26*K26	=L26*6.02E+23	=M26*H26
27			Ni-58	0.00043165	0.68077	=D27*E27	2.598	=G27*1E-24	57.935	=1/I27	8.908	=J27*K27	=L27*6.02E+23	=M27*H27
28			Ni-60	0.00043165	0.26223	=D28*E28	2.6875	=G28*1E-24	59.931	=1/I28	8.908	=J28*K28	=L28*6.02E+23	=M28*H28
29			Ni-61	0.00043165	0.0114	=D29*E29	2.68541	=G29*1E-24	60.931	=1/I29	8.908	=J29*K29	=L29*6.02E+23	=M29*H29
30			Ni-62	0.00043165	0.03634	=D30*E30	2.66847	=G30*1E-24	61.928	=1/I30	8.908	=J30*K30	=L30*6.02E+23	=M30*H30
31			Ni-64	0.00043165	0.00926	=D31*E31	2.68555	=G31*1E-24	63.928	=1/I31	8.908	=J31*K31	=L31*6.02E+23	=M31*H31

	O	P	Q	R	S	T	U	V	W	X
1			Maximum saturation activity (atms/sec) = flux							
2			(n/cm^2/s)*microscopic xs (cm^2)*N(#of atms)				Before Shield		After Shield - 0% Volume	
3	Neutron Flux (DT)	Neutron Flux (DD)	Volume of mat'l (cm^3)	Mass of mat'l (g)	DD Activity (Bq)	DT Activity (Bq)	Bq/g (DD)	Bq/g (DT)	Bq/g (DD)	Bq/g (DT)
4	=Neutron_Flux_Values_ITER!$F$5	=Neutron_Flux_Values_ITER!$C$5	=$L$2*D4	=K4*Q4	=H4*M4*Q4*P4	=H4*M4*Q4*O4	=S4/R4	=T4/R4	=S4/R4*0	=T4/R4*0
5	=Neutron_Flux_Values_ITER!$F$5	=Neutron_Flux_Values_ITER!$C$5	=$L$2*D5	=K5*Q5	=H5*M5*Q5*P5	=H5*M5*Q5*O5	=S5/R5	=T5/R5	=S5/R5*0	=T5/R5*0
6	=Neutron_Flux_Values_ITER!$F$5	=Neutron_Flux_Values_ITER!$C$5	=$L$2*D6	=K6*Q6	=H6*M6*Q6*P6	=H6*M6*Q6*O6	=S6/R6	=T6/R6	=S6/R6*0	=T6/R6*0
7	=Neutron_Flux_Values_ITER!$F$5	=Neutron_Flux_Values_ITER!$C$5	=$L$2*D7	=K7*Q7	=H7*M7*Q7*P7	=H7*M7*Q7*O7	=S7/R7	=T7/R7	=S7/R7*0	=T7/R7*0
8	=Neutron_Flux_Values_ITER!$F$5	=Neutron_Flux_Values_ITER!$C$5	=$L$2*D8	=K8*Q8	=H8*M8*Q8*P8	=H8*M8*Q8*O8	=S8/R8	=T8/R8	=S8/R8*0	=T8/R8*0
9	=Neutron_Flux_Values_ITER!$F$5	=Neutron_Flux_Values_ITER!$C$5	=$L$2*D9	=K9*Q9	=H9*M9*Q9*P9	=H9*M9*Q9*O9	=S9/R9	=T9/R9	=S9/R9*0	=T9/R9*0
10	=Neutron_Flux_Values_ITER!$F$5	=Neutron_Flux_Values_ITER!$C$5	=$L$2*D10	=K10*Q10	=H10*M10*Q10*P10	=H10*M10*Q10*O10	=S10/R10	=T10/R10	=S10/R10*0	=T10/R10*0
11	=Neutron_Flux_Values_ITER!$F$5	=Neutron_Flux_Values_ITER!$C$5	=$L$2*D11	=K11*Q11	=H11*M11*Q11*P11	=H11*M11*Q11*O11	=S11/R11	=T11/R11	=S11/R11*0	=T11/R11*0
12	=Neutron_Flux_Values_ITER!$F$5	=Neutron_Flux_Values_ITER!$C$5	=$L$2*D12	=K12*Q12	=H12*M12*Q12*P12	=H12*M12*Q12*O12	=S12/R12	=T12/R12	=S12/R12*0	=T12/R12*0
13	=Neutron_Flux_Values_ITER!$F$5	=Neutron_Flux_Values_ITER!$C$5	=$L$2*D13	=K13*Q13	=H13*M13*Q13*P13	=H13*M13*Q13*O13	=S13/R13	=T13/R13	=S13/R13*0	=T13/R13*0
14	=Neutron_Flux_Values_ITER!$F$5	=Neutron_Flux_Values_ITER!$C$5	=$L$2*D14	=K14*Q14	=H14*M14*Q14*P14	=H14*M14*Q14*O14	=S14/R14	=T14/R14	=S14/R14*0	=T14/R14*0
15	=Neutron_Flux_Values_ITER!$F$5	=Neutron_Flux_Values_ITER!$C$5	=$L$2*D15	=K15*Q15	=H15*M15*Q15*P15	=H15*M15*Q15*O15	=S15/R15	=T15/R15	=S15/R15*0	=T15/R15*0
16	=Neutron_Flux_Values_ITER!$F$5	=Neutron_Flux_Values_ITER!$C$5	=$L$2*D16	=K16*Q16	=H16*M16*Q16*P16	=H16*M16*Q16*O16	=S16/R16	=T16/R16	=S16/R16*0	=T16/R16*0
17	=Neutron_Flux_Values_ITER!$F$5	=Neutron_Flux_Values_ITER!$C$5	=$L$2*D17	=K17*Q17	=H17*M17*Q17*P17	=H17*M17*Q17*O17	=S17/R17	=T17/R17	=S17/R17*0	=T17/R17*0
18	=Neutron_Flux_Values_ITER!$F$5	=Neutron_Flux_Values_ITER!$C$5	=$L$2*D18	=K18*Q18	=H18*M18*Q18*P18	=H18*M18*Q18*O18	=S18/R18	=T18/R18	=S18/R18*0	=T18/R18*0
19	=Neutron_Flux_Values_ITER!$F$5	=Neutron_Flux_Values_ITER!$C$5	=$L$2*D19	=K19*Q19	=H19*M19*Q19*P19	=H19*M19*Q19*O19	=S19/R19	=T19/R19	=S19/R19*0	=T19/R19*0
20	=Neutron_Flux_Values_ITER!$F$5	=Neutron_Flux_Values_ITER!$C$5	=$L$2*D20	=K20*Q20	=H20*M20*Q20*P20	=H20*M20*Q20*O20	=S20/R20	=T20/R20	=S20/R20*0	=T20/R20*0
21	=Neutron_Flux_Values_ITER!$F$5	=Neutron_Flux_Values_ITER!$C$5	=$L$2*D21	=K21*Q21	=H21*M21*Q21*P21	=H21*M21*Q21*O21	=S21/R21	=T21/R21	=S21/R21*0	=T21/R21*0
22	=Neutron_Flux_Values_ITER!$F$5	=Neutron_Flux_Values_ITER!$C$5	=$L$2*D22	=K22*Q22	=H22*M22*Q22*P22	=H22*M22*Q22*O22	=S22/R22	=T22/R22	=S22/R22*0	=T22/R22*0
23	=Neutron_Flux_Values_ITER!$F$5	=Neutron_Flux_Values_ITER!$C$5	=$L$2*D23	=K23*Q23	=H23*M23*Q23*P23	=H23*M23*Q23*O23	=S23/R23	=T23/R23	=S23/R23*0	=T23/R23*0
24	=Neutron_Flux_Values_ITER!$F$5	=Neutron_Flux_Values_ITER!$C$5	=$L$2*D24	=K24*Q24	=H24*M24*Q24*P24	=H24*M24*Q24*O24	=S24/R24	=T24/R24	=S24/R24*0	=T24/R24*0
25	=Neutron_Flux_Values_ITER!$F$5	=Neutron_Flux_Values_ITER!$C$5	=$L$2*D25	=K25*Q25	=H25*M25*Q25*P25	=H25*M25*Q25*O25	=S25/R25	=T25/R25	=S25/R25*0	=T25/R25*0
26	=Neutron_Flux_Values_ITER!$F$5	=Neutron_Flux_Values_ITER!$C$5	=$L$2*D26	=K26*Q26	=H26*M26*Q26*P26	=H26*M26*Q26*O26	=S26/R26	=T26/R26	=S26/R26*0	=T26/R26*0
27	=Neutron_Flux_Values_ITER!$F$5	=Neutron_Flux_Values_ITER!$C$5	=$L$2*D27	=K27*Q27	=H27*M27*Q27*P27	=H27*M27*Q27*O27	=S27/R27	=T27/R27	=S27/R27*0	=T27/R27*0
28	=Neutron_Flux_Values_ITER!$F$5	=Neutron_Flux_Values_ITER!$C$5	=$L$2*D28	=K28*Q28	=H28*M28*Q28*P28	=H28*M28*Q28*O28	=S28/R28	=T28/R28	=S28/R28*0	=T28/R28*0
29	=Neutron_Flux_Values_ITER!$F$5	=Neutron_Flux_Values_ITER!$C$5	=$L$2*D29	=K29*Q29	=H29*M29*Q29*P29	=H29*M29*Q29*O29	=S29/R29	=T29/R29	=S29/R29*0	=T29/R29*0
30	=Neutron_Flux_Values_ITER!$F$5	=Neutron_Flux_Values_ITER!$C$5	=$L$2*D30	=K30*Q30	=H30*M30*Q30*P30	=H30*M30*Q30*O30	=S30/R30	=T30/R30	=S30/R30*0	=T30/R30*0
31	=Neutron_Flux_Values_ITER!$F$5	=Neutron_Flux_Values_ITER!$C$5	=$L$2*D31	=K31*Q31	=H31*M31*Q31*P31	=H31*M31*Q31*O31	=S31/R31	=T31/R31	=S31/R31*0	=T31/R31*0
32										
33										
34						Min :	=MIN(U4:U31)	=MIN(V4:V31)	=MIN(W4:W31)	=MIN(X4:X31)
35						Max:	=MAX(U4:U31)	=MAX(V4:V31)	=MAX(W4:W31)	=MAX(X4:X31)
36										
37										
38										

NAA – Maximum Saturation Activity – MOF

	A	B	C	D	E	F	G	H	I	J
1								Volume	2500000	cm^3
2	Element	Isotopes	Elemental Weight Fraction	Natural Abundance	Weighted Factor	Microscopic Cross Section value (NNDL)	Weighted Microscopic Cross Section (cm^2)	g/mol	mol/g weighted	elemental density (g/cm^3)
3	H	H-1	0.007068	=0.99985	=C3*D3	0.65	=F3*1E-24	1.008	=1/H3	0.0000899
4		H-2	0.007068	0.00015	=C4*D4	0.78	=F4*1E-24	2.014	=1/H4	0.0000899
5	C	C-12	0.252662	0.989	=C5*D5	1.381	=F5*1E-24	12	=1/H5	2.26
6		C-13	0.252662	0.011	=C6*D6	1.45	=F6*1E-24	13.003	=1/H6	2.26
7	N	N-14	0.29467	0.99634	=C7*D7	1.583	=F7*1E-24	14.003	=1/H7	0.00125
8		N-15	0.29467	0.00366	=C8*D8	1.618	=F8*1E-24	15	=1/H8	0.00125
9	Cu	Cu-63	0.4456	0.3083	=D9*C9	2.843	=F9*1E-24	62.93	=1/H9	8.96
10		Cu-65	0.4456	0.6917	=D10*C10	2.891	=F10*1E-24	64.928	=1/H10	8.96

	K	L	M	N	O	P	Q
1				=Neutron_Flux_Values_ITER!$F$5	=Neutron_Flux_Values_ITER!$C$5		
2	mol/cm^3	atms/cm^3	Macroscopic XS	Neutron Flux (DT)	Neutron Flux (DD)	Volume of mat'l (cm^3)	Mass of mat'l (g)
3	=I3*J3	=K3*6.02E+23	=L3*G3	=$N$1/2	=$O$1/2	=$I$1*C3	=J3*P3
4	=I4*J4	=K4*6.02E+23	=L4*G4	=$N$1/2	=$O$1/2	=$I$1*C4	=J4*P4
5	=I5*J5	=K5*6.02E+23	=L5*G5	=$N$1/2	=$O$1/2	=$I$1*C5	=J5*P5
6	=I6*J6	=K6*6.02E+23	=L6*G6	=$N$1/2	=$O$1/2	=$I$1*C6	=J6*P6
7	=I7*J7	=K7*6.02E+23	=L7*G7	=$N$1/2	=$O$1/2	=$I$1*C7	=J7*P7
8	=I8*J8	=K8*6.02E+23	=L8*G8	=$N$1/2	=$O$1/2	=$I$1*C8	=J8*P8
9	=I9*J9	=K9*6.02E+23	=L9*G9	=$N$1/2	=$O$1/2	=$I$1*C9	=J9*P9
10	=I10*J10	=K10*6.02E+23	=L10*G10	=$N$1/2	=$O$1/2	=$I$1*C10	=J10*P10

	R	S	T	U	V	W
1			Before Shield (0% volume)		After Shield (50% Flux)	
2	DT Activity (Bq)	DD Activity (Bq)	Bq/g (DD)	Bq/g (DT)	Bq/g (DD)	Bq/g (DT)
3	=G3*L3*P3*N3	=G3*L3*P3*O3	0	0	=S3/Q3*0.5	=R3/Q3*0.5
4	=G4*L4*P4*N4	=G4*L4*P4*O4	0	0	=S4/Q4*0.5	=R4/Q4*0.5
5	=G5*L5*P5*N5	=G5*L5*P5*O5	0	0	=S5/Q5*0.5	=R5/Q5*0.5
6	=G6*L6*P6*N6	=G6*L6*P6*O6	0	0	=S6/Q6*0.5	=R6/Q6*0.5
7	=G7*L7*P7*N7	=G7*L7*P7*O7	0	0	=S7/Q7*0.5	=R7/Q7*0.5
8	=G8*L8*P8*N8	=G8*L8*P8*O8	0	0	=S8/Q8*0.5	=R8/Q8*0.5
9	=G9*L9*P9*N9	=G9*L9*P9*O9	0	0	=S9/Q9*0.5	=R9/Q9*0.5
10	=G10*L10*P10*N10	=G10*L10*P10*O10	0	0	=S10/Q10*0.5	=R10/Q10*0.5
11						
12				Min:	=MIN(V3:V10)	=MIN(W3:W10)
13				Max:	=MAX(V3:V10)	=MAX(W3:W10)
14						

NAA – Maximum Saturation Activity – FLiBe

	A	B	C	D	E
1		**FLiBe**			
2					
3	Notes	Element	Isotopes	Elemental Weight Fraction	Abundance (stable isotopes only- Li-6 Enriched
4		F (67.3%)	F-19	0.673	1
5	Li-6 Must be enruched by 90% by weight	Li (16.7%)	Li-6	0.167	0.9
6			Li-7	0.167	0.1
7	**Link to g/mol values:**	Be (16%)	Be-9	0.16	1
8	https://pubchem.ncbi.nlm.nih.gov/				
9	**Link to density values:**				
10	Density of All Elements in g/cm3 (Complete Chart Inside) (periodictableguide.				
11					

	F	G	H	I	J	K	L	M	N	O	P
1		**Volume:**	1228.31514	**cm^3**		Maximum saturation activity (atms/sec) = flux (r					
2											
3	Weighted Factor	Microscopic Cross Section value	Microscopic Cross Section (cm^2)	g/mol	mol/g	elemental density (g/cm^3)	mol/cm^3	atms/cm^3	Macroscopic XS	Volume of mat'l (cm^3)	mass of mat'l (grams)
4	=D4*E4	1.79	=G4*1E-24	18.998	=1/I4	0.00167	=J4*K4	=L4*6.02E+23	=M4*H4	=$H$1*F4	=K4*O4
5	=D5*E5	1.404	=G5*1E-24	6.015	=1/I5	0.535	=J5*K5	=L5*6.02E+23	=M5*H5	=$H$1*F5	=K5*O5
6	=D6*E6	1.402	=G6*1E-24	7.016	=1/I6	0.535	=J6*K6	=L6*6.02E+23	=M6*H6	=$H$1*F6	=K6*O6
7	=D7*E7	1.482	=G7*1E-24	9.012	=1/I7	1.85	=J7*K7	=L7*6.02E+23	=M7*H7	=$H$1*F7	=K7*O7
8											

	Q	R	S	T
1	n/cm^2/s)*microscopic xs (cm^2)*N(#of atms)			
2				
3	Neutron Flux (DT)	Neutron Flux (DD)	DT Activity (Bq)	DD Activity (Bq)
4	=Neutron_Flux_Values_ITER!$F$5	=Neutron_Flux_Values_ITER!$C$5	=Q4*H4*M4*O4	=R4*H4*M4*O4
5	=Neutron_Flux_Values_ITER!$F$5	=Neutron_Flux_Values_ITER!$C$5	=Q5*H5*M5*O5	=R5*H5*M5*O5
6	=Neutron_Flux_Values_ITER!$F$5	=Neutron_Flux_Values_ITER!$C$5	=Q6*H6*M6*O6	=R6*H6*M6*O6
7	=Neutron_Flux_Values_ITER!$F$5	=Neutron_Flux_Values_ITER!$C$5	=Q7*H7*M7*O7	=R7*H7*M7*O7
8				
9				Min:
10				Max:
11				

	U	V	W	X
1				
2	Before Shield - 25% Volume		After Shield - 75% Volume, 50% Flux	
3	Bq/g (DD)	Bq/g (DT)	Bq/g (DD)	Bq/g (DT)
4	=T4/P4*0.25	=S4/P4*0.25	=T4/P4*0.75*0.5	=S4/P4*0.75*0.5
5	=T5/P5*0.25	=S5/P5*0.25	=T5/P5*0.75*0.5	=S5/P5*0.75*0.5
6	=T6/P6*0.25	=S6/P6*0.25	=T6/P6*0.75*0.5	=S6/P6*0.75*0.5
7	=T7/P7*0.25	=S7/P7*0.25	=T7/P7*0.75*0.5	=S7/P7*0.75*0.5
8				
9	=MIN(U4:U7)	=MIN(V4:V7)	=MIN(W4:W7)	=MIN(X4:X7)
10	=MAX(U4:U7)	=MAX(V4:V7)	=MAX(W4:W7)	=MAX(X4:X7)

NAA – Display of Results

				Before Shield (100% Irradiated)		After Shield (50% Irradiated)	
Material	Isotopes	Mass of each Isotope in Model (g)		Bq/g (DD)	Bq/g (DT)	Bq/g (DD)	Bq/g (DT)
FLIBE	F-19	1.3805156689374		=FLiBe!U4	=FLiBe!V4	=FLiBe!W4	=FLiBe!X4
	Li-6	38.76943456497		=FLiBe!U5	=FLiBe!V5	=FLiBe!W5	=FLiBe!X5
	Li-7	10.97438161833		=FLiBe!U6	=FLiBe!V6	=FLiBe!W6	=FLiBe!X6
	Be-9	363.58128144		=FLiBe!U7	=FLiBe!V7	=FLiBe!W7	=FLiBe!X7
NU-2100 MOF	H-1	1.588533		=MOF!T3	=MOF!U3	=MOF!V3	=MOF!W3
	H-2	1.588533		=MOF!T4	=MOF!U4	=MOF!V4	=MOF!W4
	C-12	1427540.3		=MOF!T5	=MOF!U5	=MOF!V5	=MOF!W5
	C-13	1427540.3		=MOF!T6	=MOF!U6	=MOF!V6	=MOF!W6
	N-14	920.84375		=MOF!T7	=MOF!U7	=MOF!V7	=MOF!W7
	N-15	920.84375		=MOF!T8	=MOF!U8	=MOF!V8	=MOF!W8
	Cu-63	9381440		=MOF!T9	=MOF!U9	=MOF!V9	=MOF!W9
	Cu-65	9381440		=MOF!T10	=MOF!U10	=MOF!V10	=MOF!W10
STEEL	Si-28	279112.160415044		=Steel!T6	=Steel!U6	=Steel!V6	=Steel!W6
	Si-29	14132.6443579931		=Steel!T7	=Steel!U7	=Steel!V7	=Steel!W7
	Si-30	9381.41274239724		=Steel!T8	=Steel!U8	=Steel!V8	=Steel!W8
	Mn-55	60414.08087916		=Steel!T9	=Steel!U9	=Steel!V9	=Steel!W9
	Cr-50	293.59575387729		=Steel!T10	=Steel!U10	=Steel!V10	=Steel!W10
	Cr-52	5655.19416589063		=Steel!T11	=Steel!U11	=Steel!V11	=Steel!W11
	Cr-53	641.253622434053		=Steel!T12	=Steel!U12	=Steel!V12	=Steel!W12
	Cr-54	159.621539521791		=Steel!T13	=Steel!U13	=Steel!V13	=Steel!W13
	Ni-58	7006.41465677931		=Steel!T14	=Steel!U14	=Steel!V14	=Steel!W14
	Ni-60	2698.84412563185		=Steel!T15	=Steel!U15	=Steel!V15	=Steel!W15
	Ni-61	117.327624729768		=Steel!T16	=Steel!U16	=Steel!V16	=Steel!W16
	Ni-62	374.007533568401		=Steel!T17	=Steel!U17	=Steel!V17	=Steel!W17
	Ni-64	95.3029653506712		=Steel!T18	=Steel!U18	=Steel!V18	=Steel!W18
	Fe-54	345784.494211096		=Steel!T19	=Steel!U19	=Steel!V19	=Steel!W19
	Fe-56	5468164.44983479		=Steel!T20	=Steel!U20	=Steel!V20	=Steel!W20
	Fe-57	131159.635735244		=Steel!T21	=Steel!U21	=Steel!V21	=Steel!W21
	Fe-58	16693.0445481219		=Steel!T22	=Steel!U22	=Steel!V22	=Steel!W22
CONCRETE	Mg-24	194003.43981024		='Concrete '!U4	='Concrete '!V4	='Concrete '!W4	='Concrete '!X4
	Mg-25	194003.43981024		='Concrete '!U5	='Concrete '!V5	='Concrete '!W5	='Concrete '!X5
	Mg-26	194003.43981024		='Concrete '!U6	='Concrete '!V6	='Concrete '!W6	='Concrete '!X6
	Al-27	147551.094072		='Concrete '!U7	='Concrete '!V7	='Concrete '!W7	='Concrete '!X7
	Si-28	345613.02462192		='Concrete '!U8	='Concrete '!V8	='Concrete '!W8	='Concrete '!X8
	Si-29	345613.02462192		='Concrete '!U9	='Concrete '!V9	='Concrete '!W9	='Concrete '!X9
	Si-30	345613.02462192		='Concrete '!U10	='Concrete '!V10	='Concrete '!W10	='Concrete '!X10
	Ti-46	1765735.37259287		='Concrete '!U11	='Concrete '!V11	='Concrete '!W11	='Concrete '!X11
	Ti-47	1765735.37259287		='Concrete '!U12	='Concrete '!V12	='Concrete '!W12	='Concrete '!X12
	Ti-48	1765735.37259287		='Concrete '!U13	='Concrete '!V13	='Concrete '!W13	='Concrete '!X13
	Ti-49	1765735.37259287		='Concrete '!U14	='Concrete '!V14	='Concrete '!W14	='Concrete '!X14
	Ti-50	1765735.37259287		='Concrete '!U15	='Concrete '!V15	='Concrete '!W15	='Concrete '!X15
	V-50	14108.6420592		='Concrete '!U16	='Concrete '!V16	='Concrete '!W16	='Concrete '!X16
	V-51	14108.6420592		='Concrete '!U17	='Concrete '!V17	='Concrete '!W17	='Concrete '!X17
	Cr-50	7708.04185832		='Concrete '!U18	='Concrete '!V18	='Concrete '!W18	='Concrete '!X18
	Cr-52	7708.04185832		='Concrete '!U19	='Concrete '!V19	='Concrete '!W19	='Concrete '!X19
	Cr-53	7708.04185832		='Concrete '!U20	='Concrete '!V20	='Concrete '!W20	='Concrete '!X20
	Cr-54	7708.04185832		='Concrete '!U21	='Concrete '!V21	='Concrete '!W21	='Concrete '!X21
	Mn-55	68995.65210768		='Concrete '!U22	='Concrete '!V22	='Concrete '!W22	='Concrete '!X22
	Fe-54	6808650.377079		='Concrete '!U23	='Concrete '!V23	='Concrete '!W23	='Concrete '!X23
	Fe-56	6808650.377079		='Concrete '!U24	='Concrete '!V24	='Concrete '!W24	='Concrete '!X24
	Fe-57	6808650.377079		='Concrete '!U25	='Concrete '!V25	='Concrete '!W25	='Concrete '!X25
	Fe-58	6808650.377079		='Concrete '!U26	='Concrete '!V26	='Concrete '!W26	='Concrete '!X26
	Ni-58	11753.81844976		='Concrete '!U27	='Concrete '!V27	='Concrete '!W27	='Concrete '!X27
	Ni-60	11753.81844976		='Concrete '!U28	='Concrete '!V28	='Concrete '!W28	='Concrete '!X28
	Ni-61	11753.81844976		='Concrete '!U29	='Concrete '!V29	='Concrete '!W29	='Concrete '!X29
	Ni-62	11753.81844976		='Concrete '!U30	='Concrete '!V30	='Concrete '!W30	='Concrete '!X30
	Ni-64	11753.81844976		='Concrete '!U31	='Concrete '!V31	='Concrete '!W31	='Concrete '!X31

NAA – Ranking of Isotopes by Activity

	C	D	E	F	G
61					
62		Before Shield		After Shield	
63	Ranking	Isotope	Bq/g (DT)	Isotope	Bq/g (DT)
64	1	=INDEX($C$4:$C$60,MATCH(E64,$F$4:$F$60,0))	=LARGE($F$4:$F$60,C64)	=INDEX($C$4:$C$60,MATCH(G64,$H$4:$H$60,0))	=LARGE($H$4:$H$60,C66)
65	2	=INDEX($C$4:$C$60,MATCH(E65,$F$4:$F$60,0))	=LARGE($F$4:$F$60,C65)	=INDEX($C$4:$C$60,MATCH(G65,$H$4:$H$60,0))	=LARGE($H$4:$H$60,C67)
66	3	=INDEX($C$4:$C$60,MATCH(E66,$F$4:$F$60,0))	=LARGE($F$4:$F$60,C66)	=INDEX($C$4:$C$60,MATCH(G66,$H$4:$H$60,0))	=LARGE($H$4:$H$60,C68)
67	4	=INDEX($C$4:$C$60,MATCH(E67,$F$4:$F$60,0))	=LARGE($F$4:$F$60,C67)	=INDEX($C$4:$C$60,MATCH(G67,$H$4:$H$60,0))	=LARGE($H$4:$H$60,C73)
68	5	=INDEX($C$4:$C$60,MATCH(E68,$F$4:$F$60,0))	=LARGE($F$4:$F$60,C68)	=INDEX($C$4:$C$60,MATCH(G68,$H$4:$H$60,0))	=LARGE($H$4:$H$60,C74)
69	6	=INDEX($C$4:$C$60,MATCH(E69,$F$4:$F$60,0))	=LARGE($F$4:$F$60,C69)	=INDEX($C$4:$C$60,MATCH(G69,$H$4:$H$60,0))	=LARGE($H$4:$H$60,C75)
70	7	=INDEX($C$4:$C$60,MATCH(E70,$F$4:$F$60,0))	=LARGE($F$4:$F$60,C70)	=INDEX($C$4:$C$60,MATCH(G70,$H$4:$H$60,0))	=LARGE($H$4:$H$60,C76)
71	8	=INDEX($C$4:$C$60,MATCH(E71,$F$4:$F$60,0))	=LARGE($F$4:$F$60,C71)	=INDEX($C$4:$C$60,MATCH(G71,$H$4:$H$60,0))	=LARGE($H$4:$H$60,C77)
72	9	=INDEX($C$4:$C$60,MATCH(E72,$F$4:$F$60,0))	=LARGE($F$4:$F$60,C72)	=INDEX($C$4:$C$60,MATCH(G72,$H$4:$H$60,0))	=LARGE($H$4:$H$60,C78)
73	10	=INDEX($C$4:$C$60,MATCH(E73,$F$4:$F$60,0))	=LARGE($F$4:$F$60,C73)	=INDEX($C$4:$C$60,MATCH(G73,$H$4:$H$60,0))	=LARGE($H$4:$H$60,C79)
74	11	=INDEX($C$4:$C$60,MATCH(E74,$F$4:$F$60,0))	=LARGE($F$4:$F$60,C74)	=INDEX($C$4:$C$60,MATCH(G74,$H$4:$H$60,0))	=LARGE($H$4:$H$60,C80)
75	12	=INDEX($C$4:$C$60,MATCH(E75,$F$4:$F$60,0))	=LARGE($F$4:$F$60,C75)	=INDEX($C$4:$C$60,MATCH(G75,$H$4:$H$60,0))	=LARGE($H$4:$H$60,C81)
76	13	=INDEX($C$4:$C$60,MATCH(E76,$F$4:$F$60,0))	=LARGE($F$4:$F$60,C76)	=INDEX($C$4:$C$60,MATCH(G76,$H$4:$H$60,0))	=LARGE($H$4:$H$60,C82)
77	14	=INDEX($C$4:$C$60,MATCH(E77,$F$4:$F$60,0))	=LARGE($F$4:$F$60,C77)	=INDEX($C$4:$C$60,MATCH(G77,$H$4:$H$60,0))	=LARGE($H$4:$H$60,C83)
78	15	=INDEX($C$4:$C$60,MATCH(E78,$F$4:$F$60,0))	=LARGE($F$4:$F$60,C78)	=INDEX($C$4:$C$60,MATCH(G78,$H$4:$H$60,0))	=LARGE($H$4:$H$60,C84)
79	16	=INDEX($C$4:$C$60,MATCH(E79,$F$4:$F$60,0))	=LARGE($F$4:$F$60,C79)	=INDEX($C$4:$C$60,MATCH(G79,$H$4:$H$60,0))	=LARGE($H$4:$H$60,C85)
80	17	=INDEX($C$4:$C$60,MATCH(E80,$F$4:$F$60,0))	=LARGE($F$4:$F$60,C80)	=INDEX($C$4:$C$60,MATCH(G80,$H$4:$H$60,0))	=LARGE($H$4:$H$60,C86)
81	18	=INDEX($C$4:$C$60,MATCH(E81,$F$4:$F$60,0))	=LARGE($F$4:$F$60,C81)	=INDEX($C$4:$C$60,MATCH(G81,$H$4:$H$60,0))	=LARGE($H$4:$H$60,C87)
82	19	=INDEX($C$4:$C$60,MATCH(E82,$F$4:$F$60,0))	=LARGE($F$4:$F$60,C82)	=INDEX($C$4:$C$60,MATCH(G82,$H$4:$H$60,0))	=LARGE($H$4:$H$60,C88)
83	20	=INDEX($C$4:$C$60,MATCH(E83,$F$4:$F$60,0))	=LARGE($F$4:$F$60,C83)	=INDEX($C$4:$C$60,MATCH(G83,$H$4:$H$60,0))	=LARGE($H$4:$H$60,C89)
84	21	=INDEX($C$4:$C$60,MATCH(E84,$F$4:$F$60,0))	=LARGE($F$4:$F$60,C84)	=INDEX($C$4:$C$60,MATCH(G84,$H$4:$H$60,0))	=LARGE($H$4:$H$60,C90)
85	22	=INDEX($C$4:$C$60,MATCH(E85,$F$4:$F$60,0))	=LARGE($F$4:$F$60,C85)	=INDEX($C$4:$C$60,MATCH(G85,$H$4:$H$60,0))	=LARGE($H$4:$H$60,C91)
86	23	=INDEX($C$4:$C$60,MATCH(E86,$F$4:$F$60,0))	=LARGE($F$4:$F$60,C86)	=INDEX($C$4:$C$60,MATCH(G86,$H$4:$H$60,0))	=LARGE($H$4:$H$60,C92)
87	24	=INDEX($C$4:$C$60,MATCH(E87,$F$4:$F$60,0))	=LARGE($F$4:$F$60,C87)		
88	25	=INDEX($C$4:$C$60,MATCH(E88,$F$4:$F$60,0))	=LARGE($F$4:$F$60,C88)		
89	26	=INDEX($C$4:$C$60,MATCH(E89,$F$4:$F$60,0))	=LARGE($F$4:$F$60,C89)	**Common Elements**	
90	27	=INDEX($C$4:$C$60,MATCH(E90,$F$4:$F$60,0))	=LARGE($F$4:$F$60,C90)	H-1	116380710537.877
91	28	=INDEX($C$4:$C$60,MATCH(E91,$F$4:$F$60,0))	=LARGE($F$4:$F$60,C91)	H-2	63897769347.8729
92	29	=INDEX($C$4:$C$60,MATCH(E92,$F$4:$F$60,0))	=LARGE($F$4:$F$60,C92)	C-12	20770196838.8244
93	30	=INDEX($C$4:$C$60,MATCH(E93,$F$4:$F$60,0))	=LARGE($F$4:$F$60,C93)	N-14	20402717011.1581
94	31	=INDEX($C$4:$C$60,MATCH(E94,$F$4:$F$60,0))	=LARGE($F$4:$F$60,C94)	C-13	20125775297.0807
95	32	=INDEX($C$4:$C$60,MATCH(E95,$F$4:$F$60,0))	=LARGE($F$4:$F$60,C95)	N-15	19467735545.3833
96	33	=INDEX($C$4:$C$60,MATCH(E96,$F$4:$F$60,0))	=LARGE($F$4:$F$60,C96)		
97	34	=INDEX($C$4:$C$60,MATCH(E97,$F$4:$F$60,0))	=LARGE($F$4:$F$60,C97)		
98	35	=INDEX($C$4:$C$60,MATCH(E98,$F$4:$F$60,0))	=LARGE($F$4:$F$60,C98)		
99	36	=INDEX($C$4:$C$60,MATCH(E99,$F$4:$F$60,0))	=LARGE($F$4:$F$60,C99)		
100	37	=INDEX($C$4:$C$60,MATCH(E100,$F$4:$F$60,0))	=LARGE($F$4:$F$60,C100)		
101	38	=INDEX($C$4:$C$60,MATCH(E101,$F$4:$F$60,0))	=LARGE($F$4:$F$60,C101)		
102	39	=INDEX($C$4:$C$60,MATCH(E102,$F$4:$F$60,0))	=LARGE($F$4:$F$60,C102)		
103	40	=INDEX($C$4:$C$60,MATCH(E103,$F$4:$F$60,0))	=LARGE($F$4:$F$60,C103)		
104	41	=INDEX($C$4:$C$60,MATCH(E104,$F$4:$F$60,0))	=LARGE($F$4:$F$60,C104)		
105	42	=INDEX($C$4:$C$60,MATCH(E105,$F$4:$F$60,0))	=LARGE($F$4:$F$60,C105)		
106	43	=INDEX($C$4:$C$60,MATCH(E106,$F$4:$F$60,0))	=LARGE($F$4:$F$60,C106)		
107	44	=INDEX($C$4:$C$60,MATCH(E107,$F$4:$F$60,0))	=LARGE($F$4:$F$60,C107)		
108	45	=INDEX($C$4:$C$60,MATCH(E108,$F$4:$F$60,0))	=LARGE($F$4:$F$60,C108)		
109	46	=INDEX($C$4:$C$60,MATCH(E109,$F$4:$F$60,0))	=LARGE($F$4:$F$60,C109)		
110	47	=INDEX($C$4:$C$60,MATCH(E110,$F$4:$F$60,0))	=LARGE($F$4:$F$60,C110)		
111	48	=INDEX($C$4:$C$60,MATCH(E111,$F$4:$F$60,0))	=LARGE($F$4:$F$60,C111)		

Stochastic

***Note:* stochastic results are based on a 100,000-particle run with all pre-defined tallies specified for all cells.**

UC-MSTL Model (Basic, no Boronated Polyethelene)

```
# Molten Salt Test Loop MCNP Computation - All Tallies
#University of Cincinnati, Class of 2024 Senior Design Group

import openmc
import math
import numpy as np
from matplotlib import pyplot as plt
#Add in cross_sections.xml file in
!echo $OPENMC_CROSS_SECTIONS

#Steel
steel = openmc.Material(name='Stainless Steel')
steel.set_density('g/cm3', 8.00)
steel.add_element('C', 0.08, percent_type='wo')
steel.add_element('Si', 1.00, percent_type='wo')
steel.add_element('Mn', 2.00, percent_type='wo')
steel.add_element('P', 0.045, percent_type='wo')
steel.add_element('S', 0.030, percent_type='wo')
steel.add_element('Cr', 20.0, percent_type='wo')
steel.add_element('Ni', 11.0, percent_type='wo')
steel.add_element('Fe', 65.845, percent_type='wo')

#Tungsten
tungsten = openmc.Material(name='Tungsten')
tungsten.set_density('g/cm3', 19.3)
```

```
tungsten.add_element('W', 100, percent_type='wo')

#FLiBe with Li-6 enriched to account for 90% of Li weight %
flibe = openmc.Material(name='FLiBe')
flibe.set_density('g/cm3', 1.94)
flibe.add_element('F', 67.3, percent_type='wo')
flibe.add_nuclide('Li6', 15.03, percent_type='wo')
flibe.add_nuclide('Li7', 1.67, percent_type='wo')
flibe.add_element('Be', 16, percent_type='wo')

#Concrete
concrete = openmc.Material(name='Concrete')
concrete.set_density('g/cm3', 2.232)
concrete.add_element('H', 0.56478, percent_type='wo')
concrete.add_element('C', 0.079137, percent_type='wo')
concrete.add_element('O', 38.565616, percent_type='wo')
concrete.add_element('Mg', 3.647482, percent_type='wo')
concrete.add_element('Al', 1.78777, percent_type='wo')
concrete.add_element('Si', 4.852518, percent_type='wo')
concrete.add_element('P', 0.007194, percent_type='wo')
concrete.add_element('S', 0.057554, percent_type='wo')
concrete.add_element('Ca', 8.881295, percent_type='wo')
concrete.add_element('Ti', 12.816547, percent_type='wo')
concrete.add_element('V', 0.07554, percent_type='wo')
concrete.add_element('Cr', 0.035071, percent_type='wo')
concrete.add_element('Mn', 0.302158, percent_type='wo')
concrete.add_element('Fe', 28.284173, percent_type='wo')
concrete.add_element('Ni', 0.043165, percent_type='wo')
```

```
#Beryllium
beryllium = openmc.Material(name='Beryllium')
beryllium.set_density('g/cm3', 1.85)
beryllium.add_element('Be', 100, percent_type='wo')

#NU-2100 Filter material
nu2100 = openmc.Material(name='NU-2100')
nu2100.set_density('g/cm3', 1.66)
nu2100.add_element('C', 25.2662, percent_type='wo')
nu2100.add_element('H', 0.7068, percent_type='wo')
nu2100.add_element('Cu', 44.56, percent_type='wo')
nu2100.add_element('N', 29.467, percent_type='wo')

#air
air = openmc.Material(name='air')
air.set_density('g/cm3', 0.00129)
air.add_element('O', 20.95, percent_type='wo')
air.add_element('Ar', 0.97, percent_type='wo')
air.add_element('N', 78.08, percent_type='wo')

materials = openmc.Materials([steel,tungsten,flibe,concrete,beryllium,nu2100,air])
materials.export_to_xml()

#Geometry definitions and Visualization

#Void space
void_cell = openmc.Cell(16, 'void')
```

```
void_surf = openmc.Sphere(r=500, boundary_type= "vacuum")
void_region = +void_surf
#void_cell.fill = void
void_cell.region = void_region

# Define a cell for the pipe sections

#PIPING
#Volume of FLiBe in model is 1.762252E4 cm
#to get number of t atms, multiply volume x total (n,t) production rates x time or simulation x number of source particles

#Bottom pipe (horizontal)
x0_cylinder4=0     #cm
y0_cylinder4=0     #cm
z0_cylinder4=38.1  #cm

#Top pipe (horizontal)
x0_cylinder3=0       #cm
y0_cylinder3=0       #cm
#z0_cylinder3=231.13   #cm
z0_cylinder3=247.13   #cm

#Left pipe (vertical)
x0_cylinder2=0       #cm
y0_cylinder2=0       #cm
z0_cylinder2=38.1    #cm

#Right pipe (vertical)
```

```
x0_cylinder1=193.04     #cm
y0_cylinder1=0          #cm
z0_cylinder1=38.1       #cm

length_x = 193.04       #cm
length_z = 213.36       #cm

#STEEL (piping)
S_max_dia = 6.0325      #cm
S_max_rad = S_max_dia/2    #cm

#FLIBE (irradiation zone)
F_max_dia_irr = 4.244           #cm
F_max_rad_irr = F_max_dia_irr/2    #cm

#FLIBE (non-irradiation zone)
F_max_dia = 5.2451      #cm
F_max_rad = F_max_dia/2    #cm

#BERYLLIUM

x0_Beryllium=193.04  #cm
y0_Beryllium=0       #cm
z0_Beryllium=68.58   #cm

B_max_rad = 2.62255   #cm
B_min_rad = 2.122   #cm
B_length = 152.4    #cm
```

```
#TUNGSTEN

x0_Tungsten=193.04   #cm
y0_Tungsten=0        #cm
z0_Tungsten=68.58    #cm

T_max_rad = 3.06628    #cm
T_min_rad = 3.01625    #cm
T_length = 152.4       #cm

left = openmc.XPlane(x0=0)
right = openmc.XPlane(x0=193.04)
bottom = openmc.ZPlane(z0=35.1)
top = openmc.ZPlane(z0=250.46)
#length of horizontal pipes is 215.36 cm
#length of vertical pipes is 193.04 cm

#Irradiation zone section (designated 1)

# Create the outer tungsten pipe section as cylinder
pipe_cylinder_tungsten_1 = openmc.ZCylinder(x0 = x0_cylinder1, y0=y0_cylinder1,
r=T_max_rad)
# Create the steel pipe section as cylinder
pipe_cylinder_steel_1 = openmc.ZCylinder(x0 = x0_cylinder1, y0=y0_cylinder1, r=S_max_rad)
# Create the inner beryllium pipe section as cylinder
pipe_cylinder_beryllium_1 = openmc.ZCylinder(x0 = x0_cylinder1, y0=y0_cylinder1,
r=B_min_rad)
# Create the innermost flibe pipe section as cylinder
```

```
pipe_cylinder_flibe_1 = openmc.ZCylinder(x0 = x0_cylinder1, y0=y0_cylinder1,
r=F_max_rad_irr)

flibe_region_1 = -pipe_cylinder_flibe_1 & +bottom & -top
beryllium_region_1 = +pipe_cylinder_flibe_1 & -pipe_cylinder_beryllium_1 & +bottom & -top
steel_region_1 = +pipe_cylinder_beryllium_1 & -pipe_cylinder_steel_1 & +bottom & -top
tungsten_region_1 = +pipe_cylinder_steel_1 & -pipe_cylinder_tungsten_1 & +bottom & -top

flibe_1 = openmc.Cell(1, name = 'flibe_irradiation_section')
flibe_1.fill = flibe
flibe_1.region = flibe_region_1

beryllium_1 = openmc.Cell(2, name = 'beryllium_irradiation_section')
beryllium_1.fill = beryllium
beryllium_1.region = beryllium_region_1

steel_1 = openmc.Cell(3, name = 'steel_irradiation_section')
steel_1.fill = steel
steel_1.region = steel_region_1

tungsten_1 = openmc.Cell(4, name = 'tungsten_irradiation_section')
tungsten_1.fill = tungsten
tungsten_1.region = tungsten_region_1

#Vertical_steel_section_non_irradiation

# Create the innermost flibe pipe section as cylinder
pipe_cylinder_flibe_2 = openmc.ZCylinder(x0 = x0_cylinder2, y0=y0_cylinder2, r=F_max_rad)
# Create the steel pipe section as cylinder
```

```
pipe_cylinder_steel_2 = openmc.ZCylinder(x0 = x0_cylinder2, y0=y0_cylinder2, r=S_max_rad)

flibe_region_2 = -pipe_cylinder_flibe_2 & +bottom & -top
steel_region_2 = +pipe_cylinder_flibe_2 & -pipe_cylinder_steel_2 & +bottom & -top

steel_2 = openmc.Cell(5, name = 'vertical_steel_section_non_irradiation')
steel_2.fill = steel
steel_2.region = steel_region_2

flibe_2 = openmc.Cell(6, name = 'vertical_flibe_section_non_irradiation')
flibe_2.fill = flibe
flibe_2.region = flibe_region_2

#Top horizontal section

# Create the innermost flibe pipe section as cylinder
pipe_cylinder_flibe_3 = openmc.XCylinder(z0 = z0_cylinder3, y0=y0_cylinder3, r=F_max_rad)
# Create the steel pipe section as cylinder
pipe_cylinder_steel_3 = openmc.XCylinder(z0 = z0_cylinder3, y0=y0_cylinder3, r=S_max_rad)

flibe_region_3 = -pipe_cylinder_flibe_3 & +left & -right
steel_region_3 = +pipe_cylinder_flibe_3 & -pipe_cylinder_steel_3 & +left & -right

steel_3 = openmc.Cell(7, name = 'top_horizontal_steel_section')
steel_3.fill = steel
steel_3.region = steel_region_3

flibe_3 = openmc.Cell(8, name = 'top_horizontal_flibe_section')
```

```
flibe_3.fill = flibe
flibe_3.region = flibe_region_3

#Bottom horizontal section

# Create the innermost flibe pipe section as cylinder
pipe_cylinder_flibe_4 = openmc.XCylinder(z0 = z0_cylinder4, y0=y0_cylinder4, r=F_max_rad)
# Create the steel pipe section as cylinder
pipe_cylinder_steel_4 = openmc.XCylinder(z0 = z0_cylinder4, y0=y0_cylinder4, r=S_max_rad)

flibe_region_4 = -pipe_cylinder_flibe_4 & +left & -right
steel_region_4 = +pipe_cylinder_flibe_4 & -pipe_cylinder_steel_4 & +left & -right

steel_4 = openmc.Cell(9, name = 'bottom_horizontal_steel_section')
steel_4.fill = steel
steel_4.region = steel_region_4

flibe_4 = openmc.Cell(10, name = 'bottom_horizontal_flibe_section')
flibe_4.fill = flibe
flibe_4.region =flibe_region_4

#STEEL BLOCK

x0_Steel= 195.8632 #cm
y0_Steel=-3.066    #cm
z0_Steel= 35.1     #cm

length_x_Steel = 8.89      #cm
```

```
length_y_Steel = 6.132576  #cm
length_z_Steel = 223.04    #cm

steel_block = openmc.model.RectangularParallelepiped(xmin=x0_Steel, xmax=x0_Steel + length_x_Steel, ymin=y0_Steel, ymax=y0_Steel + length_y_Steel,zmin=z0_Steel, zmax=z0_Steel + length_z_Steel)

steel_block_region = -steel_block & -top

steel_block = openmc.Cell(11, name = 'irradiation_zone_steel_block')
steel_block.fill = steel
steel_block.region = steel_block_region

#CONCRETE
x0_Concrete=107.805  #cm
y0_Concrete=-203.2 #cm
z0_Concrete=0      #cm

# Define dimensions of the concrete slab
#length_x_Concrete = 20.955   #cm
length_x_Concrete = 80.55   #cm
length_y_Concrete = 365.76   #cm
length_z_Concrete = 365.76    #cm

# Create the concrete slab
concrete_slab = openmc.model.RectangularParallelepiped(xmin=x0_Concrete, xmax=x0_Concrete + length_x_Concrete, ymin=y0_Concrete, ymax=y0_Concrete + length_y_Concrete,zmin=z0_Concrete, zmax=z0_Concrete + length_z_Concrete)

concrete_slab_region = -concrete_slab & +pipe_cylinder_steel_3 & +pipe_cylinder_steel_4
```

```
concrete_slab = openmc.Cell(12, name = 'concrete_shielding_slab')
concrete_slab.fill = concrete
concrete_slab.region = concrete_slab_region

#PUMP

x0_Pump=-20    #cm
y0_Pump=-31.75 #cm
z0_Pump= 0     #cm

# Define dimensions of the pump
length_x_Pump = 57.15   #cm
length_y_Pump = 57.15   #cm
length_z_Pump = 38.1    #cm

# Create the pump
pump = openmc.model.RectangularParallelepiped(xmin=x0_Pump, xmax=x0_Pump +
length_x_Pump, ymin=y0_Pump, ymax=y0_Pump + length_y_Pump,zmin=z0_Pump,
zmax=z0_Pump + length_z_Pump)

pump_region = -pump & +pipe_cylinder_steel_4

pump = openmc.Cell(13, name = 'pump')
pump.fill = steel
pump.region = pump_region

#nu2100
```

```
x0_nu2100=-160     #cm
y0_nu2100= 45.0    #cm
z0_nu2100=0        #cm

# Define dimensions of the nu2100filter
length_x_nu2100 = 250.068   #cm
length_y_nu2100 = 100       #cm
length_z_nu2100 = 100       #cm

# Create the nu2100filter
nu2100_filter = openmc.model.RectangularParallelepiped(xmin=x0_nu2100, xmax=x0_nu2100
+ length_x_nu2100, ymin=y0_nu2100, ymax=y0_nu2100 + length_y_nu2100,zmin=z0_nu2100,
zmax=z0_nu2100 + length_z_nu2100)

nu2100_region = -nu2100_filter

nu2100_filter = openmc.Cell(14, name = 'nu2100_filter')
nu2100_filter.fill = nu2100
nu2100_filter.region = nu2100_region

#air

air_region = -void_surf & ~tungsten_region_1 & ~steel_region_1 & ~steel_region_2 &
~steel_region_3 & ~steel_region_4 & ~beryllium_region_1 & ~flibe_region_1 &
~flibe_region_2 & ~flibe_region_3 & ~flibe_region_4 & ~steel_block_region &
~concrete_slab_region & ~pump_region & ~nu2100_region

air_cell = openmc.Cell(15, name = 'air')
air_cell.fill = air
air_cell.region = air_region
```

```
# Create a universe
universe = openmc.Universe(cells=[air_cell,void_cell,nu2100_filter,pump,concrete_slab,steel_block,flibe_4,flibe_3,flibe_2,flibe_1,steel_4,steel_3,steel_2,steel_1,beryllium_1,tungsten_1])

# Create a geometry and set the root universe
geometry = openmc.Geometry()
geometry.root_universe = universe

# Export the geometry to XML
geometry.export_to_xml()
# Read neutron flux spectrum from a .txt file
# Assume the file has two columns: energy (MeV) and flux (neutrons/cm^2/s/MeV)
data = np.loadtxt('ITER_DT.txt')

energies = data[:, 0]  # Neutron energies (MeV)
fluxes = data[:, 1]    # Neutron fluxes (neutrons/cm^2/s/MeV)

# Define energy distribution based on neutron flux spectrum
energy_distribution = openmc.stats.Discrete(energies, fluxes)

# Define spatial distribution (e.g., point source at coordinates)
# original x coordiante was 210
#spatial_distribution = openmc.stats.Point(xyz=(210, 0, 182.88))  # Coordinates (x, y, z)

plane_x_min = 205.0  # Define minimum x-coordinate of the plane
plane_x_max = 205.1  # Define maximum x-coordinate of the plane
plane_y_min = -203.2  # Define minimum y-coordinate of the plane
```

```
plane_y_max = 162.56   # Define maximum y-coordinate of the plane
plane_z_min = 0  # Define minimum z-coordinate of the plane
plane_z_max = 365.76  # Define maximum z-coordinate of the plane

spatial_distribution = openmc.stats.Box((plane_x_min, plane_y_min, plane_z_min),
(plane_x_max, plane_y_max, plane_z_max))

#angular_distribution = openmc.stats.isotropic
angular_distribution = openmc.stats.Monodirectional([-1.0, 0.0, 0.0])

# Create neutron source with energy and spatial distributions
neutron_source = openmc.Source(space=spatial_distribution, energy=energy_distribution,
angle=angular_distribution)

# Assign the source to the settings
settings = openmc.Settings()
settings.source = neutron_source
settings.run_mode = 'fixed source'
settings.particles = 10000
#Set number of starting particles above
settings.generations_per_batch = 10
settings.batches = 500
settings.inactive = 5
#Tallies

flibe_1_filter = openmc.CellFilter([1])
flibe_1_tally = openmc.Tally(name='flibe irradiation zone')
flibe_1_tally.filters = [flibe_1_filter]
flibe_1_tally.scores = ['flux','heating' ,'heating-local','absorption', '(n,a)', '(n,gamma)', '(n,t)']
```

```
beryllium_1_filter = openmc.CellFilter([2])
beryllium_1_tally = openmc.Tally(name = 'beryllium inner sheath irradiation zone')
beryllium_1_tally.filters = [beryllium_1_filter]
beryllium_1_tally.scores = ['flux','heating' ,'heating-local','absorption', '(n,a)', '(n,gamma)', '(n,t)']

steel_1_filter = openmc.CellFilter([3])
steel_1_tally = openmc.Tally(name = 'steel piping irradiation zone')
steel_1_tally.filters = [steel_1_filter]
steel_1_tally.scores = ['flux','heating' ,'heating-local','absorption', '(n,a)', '(n,gamma)', '(n,t)']

tungsten_1_filter = openmc.CellFilter([4])
tungsten_1_tally = openmc.Tally(name = 'tungsten outer sheath irradiation zone')
tungsten_1_tally.filters = [tungsten_1_filter]
tungsten_1_tally.scores = ['flux','heating' ,'heating-local','absorption', '(n,a)', '(n,gamma)', '(n,t)']

steel_2_filter = openmc.CellFilter([5])
steel_2_tally = openmc.Tally(name = 'vertical steel piping non-irradiation zone' )
steel_2_tally.filters = [steel_2_filter]
steel_2_tally.scores = ['flux','heating' ,'heating-local','absorption', '(n,a)', '(n,gamma)', '(n,t)']

flibe_2_filter = openmc.CellFilter([6])
flibe_2_tally = openmc.Tally(name = 'vertical flibe non-irradiation zone')
flibe_2_tally.filters = [flibe_2_filter]
flibe_2_tally.scores = ['flux','heating' ,'heating-local','absorption', '(n,a)', '(n,gamma)', '(n,t)']

steel_3_filter = openmc.CellFilter([7])
steel_3_tally = openmc.Tally(name = 'top horizontal steel piping')
```

```
steel_3_tally.filters = [steel_3_filter]
steel_3_tally.scores = ['flux','heating' ,'heating-local','absorption', '(n,a)', '(n,gamma)', '(n,t)']

flibe_3_filter = openmc.CellFilter([8])
flibe_3_tally = openmc.Tally(name = 'top horizontal flibe')
flibe_3_tally.filters = [flibe_3_filter]
flibe_3_tally.scores = ['flux','heating' ,'heating-local','absorption', '(n,a)', '(n,gamma)', '(n,t)']

steel_4_filter = openmc.CellFilter([9])
steel_4_tally = openmc.Tally(name = 'bottom horizontal steel piping')
steel_4_tally.filters = [steel_4_filter]
steel_4_tally.scores = ['flux','heating' ,'heating-local','absorption', '(n,a)', '(n,gamma)', '(n,t)']

flibe_4_filter = openmc.CellFilter([10])
flibe_4_tally = openmc.Tally(name = 'bottom horizontal flibe')
flibe_4_tally.filters = [flibe_4_filter]
flibe_4_tally.scores = ['flux','heating' ,'heating-local','absorption', '(n,a)', '(n,gamma)', '(n,t)']

steel_block_filter = openmc.CellFilter([11])
steel_block_tally = openmc.Tally(name = 'steel block irradiation zone')
steel_block_tally.filters = [steel_block_filter]
steel_block_tally.scores = ['flux','heating' ,'heating-local','absorption', '(n,a)', '(n,gamma)', '(n,t)']

concrete_filter = openmc.CellFilter([12])
concrete_tally = openmc.Tally(name = 'concrete shielding')
concrete_tally.filters = [concrete_filter]
concrete_tally.scores = ['flux','heating' ,'heating-local','absorption', '(n,a)', '(n,gamma)', '(n,t)']
```

```
steel_pump_filter = openmc.CellFilter([13])
steel_pump_tally = openmc.Tally(name = 'steel pump')
steel_pump_tally.filters = [steel_pump_filter]
steel_pump_tally.scores = ['flux','heating' ,'heating-local','absorption', '(n,a)', '(n,gamma)', '(n,t)']

nu2100_filter = openmc.CellFilter([14])
nu2100_tally = openmc.Tally(name = 'nu2100 filter')
nu2100_tally.filters = [nu2100_filter]
nu2100_tally.scores = ['flux','heating' ,'heating-local','absorption', '(n,a)', '(n,gamma)', '(n,t)']

air_filter = openmc.CellFilter([15])
air_tally = openmc.Tally(name = 'air')
air_tally.filters = [air_filter]
air_tally.scores = ['flux','heating' ,'heating-local','absorption', '(n,a)', '(n,gamma)', '(n,t)']

tallies = openmc.Tallies([steel_block_tally, steel_pump_tally, air_tally, steel_1_tally,
steel_2_tally, steel_3_tally, steel_4_tally, nu2100_tally, concrete_tally, beryllium_1_tally,
tungsten_1_tally, flibe_1_tally, flibe_2_tally, flibe_3_tally, flibe_4_tally])
tallies.export_to_xml()

model = openmc.Model(materials=materials, geometry=geometry, settings=settings,
tallies=tallies)
model.export_to_model_xml()
openmc.run()
```

UC-MSTL Results (Basic, no Boronated Polyethylene)

Leakage Rate: 0.59868

Time to complete: 3131 seconds.

==========> TALLY 11: STEEL BLOCK IRRADIATION ZONE<==========

Cell 11

Total Material

Flux	0.151767 +/- 0.000200615
heating	2871.11 +/- 8.47098
heating-local	22510.7 +/- 53.1456
Absorption Rate	0.00135015 +/- 4.29698e-06
(n,a)	5.47837e-05 +/- 1.87544e-07
(n,gamma)	0.00111722 +/- 4.21201e-06
(n,t)	7.07866e-09 +/- 4.42422e-11

=====================> TALLY 13: STEEL PUMP <=====================

Cell 13

Total Material

Flux	0.00352947 +/- 8.45957e-05
heating	36.1257 +/- 1.25772
heating-local	348.352 +/- 9.04231
Absorption Rate	2.28627e-05 +/- 7.03757e-07
(n,a)	5.45599e-07 +/- 2.6946e-08
(n,gamma)	2.01753e-05 +/- 6.87914e-07
(n,t)	3.33698e-11 +/- 4.13158e-12

=========================> TALLY 15: AIR <=========================

Cell 15

Total Material

Flux	210.44 +/- 0.0276291
heating	3562.93 +/- 1.23573
heating-local	5100.26 +/- 1.92571
Absorption Rate	0.00165591 +/- 7.76169e-07
(n,a)	0.000163217 +/- 9.62715e-08
(n,gamma)	5.56297e-05 +/- 3.15534e-08

(n,t) 1.11907e-05 +/- 8.50014e-09

==========> TALLY 3: STEEL PIPING IRRADIATION ZONE <==========

Cell 3

Total Material

Flux 0.0253778 +/- 4.74476e-05

heating 331.104 +/- 1.54479

heating-local 3844.72 +/- 13.5096

Absorption Rate 0.000298868 +/- 1.38734e-06

(n,a) 5.88407e-06 +/- 3.47381e-08

(n,gamma) 0.000272451 +/- 1.38442e-06

(n,t) 6.09868e-10 +/- 7.6797e-12

======> TALLY 5: VERTICAL STEEL PIPING NON-IRRADIATION ZONE <======

Cell 5

Total Material

Flux 7.82087e-05 +/- 1.61735e-06

heating 2.34367 +/- 0.0972864

heating-local 22.2465 +/- 0.807328

Absorption Rate 1.36256e-06 +/- 7.89757e-08

(n,a) 4.48208e-08 +/- 2.24979e-09

(n,gamma) 1.15317e-06 +/- 7.87872e-08

(n,t) 2.48333e-12 +/- 2.91925e-13

==========> TALLY 7: TOP HORIZONTAL STEEL PIPING <==========

Cell 7

Total Material

Flux 0.00210887 +/- 1.14326e-05

heating 23.0533 +/- 0.389348

heating-local 432.292 +/- 4.15349

Absorption Rate 3.9557e-05 +/- 4.3622e-07

(n,a) 3.84614e-07 +/- 8.91194e-09

(n,gamma) 3.76591e-05 +/- 4.32814e-07

(n,t) 1.93242e-11 +/- 1.48891e-12

==========> TALLY 9: BOTTOM HORIZONTAL STEEL PIPING<==========

Cell 9

Total Material

Flux 0.00207771 +/- 1.0495e-05

heating 22.55 +/- 0.362685

heating-local 424.87 +/- 3.93215

Absorption Rate 3.89751e-05 +/- 4.25417e-07

(n,a) 3.71858e-07 +/- 8.51146e-09

(n,gamma) 3.71286e-05 +/- 4.24989e-07

(n,t) 1.91403e-11 +/- 1.37424e-12

==========> TALLY 14: NU2100 FILTER <==========

Cell 14

Total Material

Flux 0.0394765 +/- 0.000275041

heating 1052.85 +/- 9.72988

heating-local 2584.16 +/- 20.7481

Absorption Rate 0.000357118 +/- 3.37217e-06

(n,a) 2.91077e-05 +/- 3.39219e-07

(n,gamma) 0.00014231 +/- 1.49007e-06

(n,t) 1.91892e-06 +/- 3.12022e-08

==========> TALLY 12: CONCRETE SHIELDING <==========

Cell 12

Total Material

Flux 59.8486 +/- 0.00908836

heating 1.30727e+06 +/- 364.128

heating-local 5.10818e+06 +/- 1107.35

Absorption Rate 0.409568 +/- 0.00010168

(n,a) 0.0346687 +/- 1.30348e-05

(n,gamma) 0.349404 +/- 9.80233e-05

(n,t) 5.84789e-06 +/- 2.50835e-09

=======> TALLY 2: BERYLLIUM INNER SHEATH IRRADIATION ZONE<========

Cell 2

Total Material

Flux 8.98436e-21 +/- 8.98436e-21

heating 2.98943e-15 +/- 2.98943e-15

heating-local 2.98946e-15 +/- 2.98946e-15

Absorption Rate 1.58193e-23 +/- 1.58193e-23

(n,a) 1.55646e-23 +/- 1.55646e-23

(n,gamma) 1.84902e-27 +/- 1.84902e-27

(n,t) 2.52811e-25 +/- 2.52811e-25

========>TALLY 4: TUNGSTEN OUTER SHEATH IRRADIATION ZONE<========

Cell 4

Total Material

Flux 0.00169172 +/- 3.43303e-06

heating 7.74256 +/- 0.0397575

heating-local 1750.3 +/- 9.83217

Absorption Rate 0.000319761 +/- 1.85106e-06

(n,a) 3.03979e-09 +/- 2.94781e-11

(n,gamma) 0.000319749 +/- 1.85105e-06

(n,t) 0 +/- 0

================> TALLY 1: FLIBE IRRADIATION ZONE <===============

Cell 1

Total Material

Flux 0.0200524 +/- 5.33487e-05

heating 9686.01 +/- 34.2156

heating-local 9852.85 +/- 34.3639

Absorption Rate 0.00184398 +/- 7.06943e-06

(n,a) 8.44905e-06 +/- 6.07788e-08

(n,gamma) 5.59123e-07 +/- 3.90397e-09

(n,t) 0.00183151 +/- 7.06602e-06

=========> TALLY 6: VERTICAL FLIBE NON-IRRADIATION ZONE <=========

Cell 6

Total Material

Flux 0.00019944 +/- 5.12948e-06

heating 89.8616 +/- 3.33863

heating-local 93.251 +/- 3.35562

Absorption Rate 1.53092e-05 +/- 6.87512e-07

(n,a) 2.37802e-07 +/- 1.0828e-08

(n,gamma) 3.45986e-09 +/- 2.32157e-10

(n,t) 1.49851e-05 +/- 6.8798e-07

================> TALLY 8: TOP HORIZONTAL FLIBE<================

Cell 8

Total Material

Flux 0.00483279 +/- 3.21121e-05

heating 3020.92 +/- 20.6245

heating-local 3062.47 +/- 20.7108

Absorption Rate 0.000591705 +/- 4.23546e-06

(n,a) 2.47904e-06 +/- 3.77496e-08

(n,gamma) 1.41284e-07 +/- 2.19086e-09

(n,t) 0.000588323 +/- 4.23425e-06

==============> TALLY 10: BOTTOM HORIZONTAL FLIBE<==============

Cell 10

Total Material

Flux	0.00473424 +/- 3.0693e-05
heating	2916.46 +/- 21.8219
heating-local	2956.98 +/- 21.9114
Absorption Rate	0.000570881 +/- 4.49038e-06
(n,a)	2.41598e-06 +/- 4.06256e-08
(n,gamma)	1.39916e-07 +/- 2.19874e-09
(n,t)	0.000567582 +/- 4.48835e-06

UC-MSTL Model (Advanced, Added Boronated PolyEthylene, Removed Steel Block)

```
# Molten Salt Test Loop MCNP Computation - All Tallies
#University of Cincinnati, Class of 2024 Senior Design Group
#matplotlib inline
import openmc
import math
import numpy as np
from matplotlib import pyplot as plt
!echo $OPENMC_CROSS_SECTIONS

#Steel
steel = openmc.Material(name='Stainless Steel')
steel.set_density('g/cm3', 8.00)
steel.add_element('C', 0.08, percent_type='wo')
steel.add_element('Si', 1.00, percent_type='wo')
steel.add_element('Mn', 2.00, percent_type='wo')
steel.add_element('P', 0.045, percent_type='wo')
steel.add_element('S', 0.030, percent_type='wo')
```

```
steel.add_element('Cr', 20.0, percent_type='wo')
steel.add_element('Ni', 11.0, percent_type='wo')
steel.add_element('Fe', 65.845, percent_type='wo')

#Tungsten
tungsten = openmc.Material(name='Tungsten')
tungsten.set_density('g/cm3', 19.3)
tungsten.add_element('W', 100, percent_type='wo')

#FLiBe with Li-6 enriched to account for 90% of Li weight %
flibe = openmc.Material(name='FLiBe')
flibe.set_density('g/cm3', 1.94)
flibe.add_element('F', 67.3, percent_type='wo')
flibe.add_nuclide('Li6', 15.03, percent_type='wo')
flibe.add_nuclide('Li7', 1.67, percent_type='wo')
flibe.add_element('Be', 16, percent_type='wo')

#Concrete
concrete = openmc.Material(name='Concrete')
concrete.set_density('g/cm3', 2.232)
concrete.add_element('H', 0.56478, percent_type='wo')
concrete.add_element('C', 0.079137, percent_type='wo')
concrete.add_element('O', 38.565616, percent_type='wo')
concrete.add_element('Mg', 3.647482, percent_type='wo')
concrete.add_element('Al', 1.78777, percent_type='wo')
concrete.add_element('Si', 4.852518, percent_type='wo')
concrete.add_element('P', 0.007194, percent_type='wo')
concrete.add_element('S', 0.057554, percent_type='wo')
```

```
concrete.add_element('Ca', 8.881295, percent_type='wo')
concrete.add_element('Ti', 12.816547, percent_type='wo')
concrete.add_element('V', 0.07554, percent_type='wo')
concrete.add_element('Cr', 0.035071, percent_type='wo')
concrete.add_element('Mn', 0.302158, percent_type='wo')
concrete.add_element('Fe', 28.284173, percent_type='wo')
concrete.add_element('Ni', 0.043165, percent_type='wo')

#Beryllium
beryllium = openmc.Material(name='Beryllium')
beryllium.set_density('g/cm3', 1.85)
beryllium.add_element('Be', 100, percent_type='wo')

#NU-2100 Filter material
nu2100 = openmc.Material(name='NU-2100')
nu2100.set_density('g/cm3', 1.66)
nu2100.add_element('C', 25.2662, percent_type='wo')
nu2100.add_element('H', 0.7068, percent_type='wo')
nu2100.add_element('Cu', 44.56, percent_type='wo')
nu2100.add_element('N', 29.467, percent_type='wo')

#air
air = openmc.Material(name='air')
air.set_density('g/cm3', 0.00129)
air.add_element('O', 20.95, percent_type='wo')
air.add_element('Ar', 0.97, percent_type='wo')
air.add_element('N', 78.08, percent_type='wo')
```

```
#Poly
#Parafiin, High Density Polyethylene (HDPE)
poly = openmc.Material(name='poly')
poly.set_density('g/cm3', 0.92)
poly.add_element('H', 11.60, percent_type='wo')
poly.add_element('C', 61.20, percent_type='wo')
poly.add_element('O', 22.20, percent_type='wo')
poly.add_nuclide('B10', 1, percent_type='wo')
poly.add_nuclide('B11', 4, percent_type='wo')

materials = openmc.Materials([steel,tungsten,flibe,concrete,beryllium,nu2100,air,poly])
materials.export_to_xml()
#Geometry definitions and Visualization

#Void space
void_cell = openmc.Cell(16, 'void')
void_surf = openmc.Sphere(r=500, boundary_type= "vacuum")
void_region = +void_surf
#void_cell.fill = void
void_cell.region = void_region

# Define a cell for the pipe sections

#PIPING
#Volume of FLiBe in model is 1.762252E4 cm
#to get number of t atms, multiply volume x total (n,t) production rates x time or simulation x number of source particles

#Bottom pipe (horizontal)
```

```
x0_cylinder4=0     #cm
y0_cylinder4=0     #cm
z0_cylinder4=38.1  #cm

#Top pipe (horizontal)
x0_cylinder3=0       #cm
y0_cylinder3=0       #cm
z0_cylinder3=247.13   #cm

#Left pipe (vertical)
x0_cylinder2=0       #cm
y0_cylinder2=0       #cm
z0_cylinder2=38.1    #cm

#Right pipe (vertical)
x0_cylinder1=193.04     #cm
y0_cylinder1=0          #cm
z0_cylinder1=38.1       #cm

length_x = 193.04      #cm
length_z = 213.36      #cm

#STEEL (piping)
S_max_dia = 6.0325       #cm
S_max_rad = S_max_dia/2    #cm

#FLIBE (irradiation zone)
F_max_dia_irr = 4.244             #cm
```

```
F_max_rad_irr = F_max_dia_irr/2    #cm

#FLIBE
F_max_dia = 5.2451       #cm
F_max_rad = F_max_dia/2    #cm

#BERYLLIUM

x0_Beryllium=193.04  #cm
y0_Beryllium=0       #cm
z0_Beryllium=68.58   #cm

B_max_rad = 2.62255   #cm
B_min_rad = 2.122   #cm
B_length = 152.4    #cm

#TUNGSTEN

x0_Tungsten=193.04   #cm
y0_Tungsten=0        #cm
z0_Tungsten=68.58    #cm

T_max_rad = 3.06628    #cm
T_min_rad = 3.01625    #cm
T_length = 152.4       #cm

left = openmc.XPlane(x0=0)
right = openmc.XPlane(x0=193.04)
```

```
bottom = openmc.ZPlane(z0=35.1)
top = openmc.ZPlane(z0=250.46)

#Irradiation zone section (designated 1)

# Create the outer tungsten pipe section as cylinder
pipe_cylinder_tungsten_1 = openmc.ZCylinder(x0 = x0_cylinder1, y0=y0_cylinder1, r=T_max_rad)
# Create the steel pipe section as cylinder
pipe_cylinder_steel_1 = openmc.ZCylinder(x0 = x0_cylinder1, y0=y0_cylinder1, r=S_max_rad)
# Create the inner beryllium pipe section as cylinder
pipe_cylinder_beryllium_1 = openmc.ZCylinder(x0 = x0_cylinder1, y0=y0_cylinder1, r=B_min_rad)
# Create the innermost flibe pipe section as cylinder
pipe_cylinder_flibe_1 = openmc.ZCylinder(x0 = x0_cylinder1, y0=y0_cylinder1, r=F_max_rad_irr)

flibe_region_1 = -pipe_cylinder_flibe_1 & +bottom & -top
beryllium_region_1 = +pipe_cylinder_flibe_1 & -pipe_cylinder_beryllium_1 & +bottom & -top
steel_region_1 = +pipe_cylinder_beryllium_1 & -pipe_cylinder_steel_1 & +bottom & -top
tungsten_region_1 = +pipe_cylinder_steel_1 & -pipe_cylinder_tungsten_1 & +bottom & -top

flibe_1 = openmc.Cell(1, name = 'flibe_irradiation_section')
flibe_1.fill = flibe
flibe_1.region = flibe_region_1

beryllium_1 = openmc.Cell(2, name = 'beryllium_irradiation_section')
beryllium_1.fill = beryllium
beryllium_1.region = beryllium_region_1
```

```
steel_1 = openmc.Cell(3, name = 'steel_irradiation_section')
steel_1.fill = steel
steel_1.region = steel_region_1

tungsten_1 = openmc.Cell(4, name = 'tungsten_irradiation_section')
tungsten_1.fill = tungsten
tungsten_1.region = tungsten_region_1

#Vertical_steel_section_non_irradiation

# Create the innermost flibe pipe section as cylinder
pipe_cylinder_flibe_2 = openmc.ZCylinder(x0 = x0_cylinder2, y0=y0_cylinder2, r=F_max_rad)
# Create the steel pipe section as cylinder
pipe_cylinder_steel_2 = openmc.ZCylinder(x0 = x0_cylinder2, y0=y0_cylinder2, r=S_max_rad)

flibe_region_2 = -pipe_cylinder_flibe_2 & +bottom & -top
steel_region_2 = +pipe_cylinder_flibe_2 & -pipe_cylinder_steel_2 & +bottom & -top

steel_2 = openmc.Cell(5, name = 'vertical_steel_section_non_irradiation')
steel_2.fill = steel
steel_2.region = steel_region_2

flibe_2 = openmc.Cell(6, name = 'vertical_flibe_section_non_irradiation')
flibe_2.fill = flibe
flibe_2.region = flibe_region_2

#Top horizontal section
```

```
# Create the innermost flibe pipe section as cylinder
pipe_cylinder_flibe_3 = openmc.XCylinder(z0 = z0_cylinder3, y0=y0_cylinder3, r=F_max_rad)
# Create the steel pipe section as cylinder
pipe_cylinder_steel_3 = openmc.XCylinder(z0 = z0_cylinder3, y0=y0_cylinder3, r=S_max_rad)

flibe_region_3 = -pipe_cylinder_flibe_3 & +left & -right
steel_region_3 = +pipe_cylinder_flibe_3 & -pipe_cylinder_steel_3 & +left & -right

steel_3 = openmc.Cell(7, name = 'top_horizontal_steel_section')
steel_3.fill = steel
steel_3.region = steel_region_3

flibe_3 = openmc.Cell(8, name = 'top_horizontal_flibe_section')
flibe_3.fill = flibe
flibe_3.region = flibe_region_3

#Bottom horizontal section

# Create the innermost flibe pipe section as cylinder
pipe_cylinder_flibe_4 = openmc.XCylinder(z0 = z0_cylinder4, y0=y0_cylinder4, r=F_max_rad)
# Create the steel pipe section as cylinder
pipe_cylinder_steel_4 = openmc.XCylinder(z0 = z0_cylinder4, y0=y0_cylinder4, r=S_max_rad)

flibe_region_4 = -pipe_cylinder_flibe_4 & +left & -right
steel_region_4 = +pipe_cylinder_flibe_4 & -pipe_cylinder_steel_4 & +left & -right

steel_4 = openmc.Cell(9, name = 'bottom_horizontal_steel_section')
```

```
steel_4.fill = steel
steel_4.region = steel_region_4

flibe_4 = openmc.Cell(10, name = 'bottom_horizontal_flibe_section')
flibe_4.fill = flibe
flibe_4.region =flibe_region_4

#STEEL BLOCK

x0_Steel= 195.8632 #cm
y0_Steel=-3.066    #cm
z0_Steel= 35.1     #cm

length_x_Steel = 1     #cm
length_y_Steel = 6.132576  #cm
length_z_Steel = 223.04    #cm

#steel_block = openmc.model.RectangularParallelepiped(xmin=x0_Steel, xmax=x0_Steel +
length_x_Steel, ymin=y0_Steel, ymax=y0_Steel + length_y_Steel,zmin=z0_Steel,
zmax=z0_Steel + length_z_Steel)

#steel_block_region = -steel_block & -top

#steel_block = openmc.Cell(11, name = 'irradiation_zone_steel_block')
#steel_block.fill = steel
#steel_block.region = steel_block_region

#CONCRETE
x0_Concrete=97.805  #cm
```

```
y0_Concrete=-203.2 #cm
z0_Concrete=0      #cm

# Define dimensions of the concrete slab
length_x_Concrete = 80.55   #cm
length_y_Concrete = 365.76   #cm
length_z_Concrete = 365.76    #cm

# Create the concrete slab
concrete_slab = openmc.model.RectangularParallelepiped(xmin=x0_Concrete,
xmax=x0_Concrete + length_x_Concrete, ymin=y0_Concrete, ymax=y0_Concrete +
length_y_Concrete,zmin=z0_Concrete, zmax=z0_Concrete + length_z_Concrete)

concrete_slab_region = -concrete_slab & +pipe_cylinder_steel_3 & +pipe_cylinder_steel_4

concrete_slab = openmc.Cell(12, name = 'concrete_shielding_slab')
concrete_slab.fill = concrete
concrete_slab.region = concrete_slab_region

#POLY LAYER

x0_poly= 178.355  #cm
#x0_poly= 179      #cm
y0_poly=-203.2    #cm
z0_poly=0         #cm

# Define dimensions of the poly layer
length_x_poly = 10       #cm
length_y_poly = 365.76    #cm
```

```
length_z_poly = 365.76    #cm


# Create the poly banket
poly_blanket = openmc.model.RectangularParallelepiped(xmin=x0_poly, xmax=x0_poly + length_x_poly, ymin=y0_poly, ymax=y0_poly + length_y_poly,zmin=z0_poly, zmax=z0_poly + length_z_poly)


poly_region = -poly_blanket | concrete_slab_region & +pipe_cylinder_steel_3 & +pipe_cylinder_steel_4


poly_blanket = openmc.Cell(17, name = 'poly_blanket')
poly_blanket.fill = poly
poly_blanket.region = poly_region


#PUMP


x0_Pump=-20    #cm
y0_Pump=-31.75 #cm
z0_Pump= 0     #cm


# Define dimensions of the pump
length_x_Pump = 57.15   #cm
length_y_Pump = 57.15   #cm
length_z_Pump = 38.1  #cm


# Create the pump
pump = openmc.model.RectangularParallelepiped(xmin=x0_Pump, xmax=x0_Pump + length_x_Pump, ymin=y0_Pump, ymax=y0_Pump + length_y_Pump,zmin=z0_Pump, zmax=z0_Pump + length_z_Pump)
```

```
pump_region = -pump & +pipe_cylinder_steel_4


pump = openmc.Cell(13, name = 'pump')
pump.fill = steel
pump.region = pump_region


#nu2100


#x0_nu2100=-101.6   #cm
x0_nu2100=-160     #cm
y0_nu2100= 45.0    #cm
z0_nu2100=0        #cm


# Define dimensions of the nu2100filter
length_x_nu2100 = 250.068   #cm
length_y_nu2100 = 100       #cm
length_z_nu2100 = 100       #cm


# Create the nu2100filter
nu2100_filter = openmc.model.RectangularParallelepiped(xmin=x0_nu2100, xmax=x0_nu2100
+ length_x_nu2100, ymin=y0_nu2100, ymax=y0_nu2100 + length_y_nu2100,zmin=z0_nu2100,
zmax=z0_nu2100 + length_z_nu2100)


nu2100_region = -nu2100_filter


nu2100_filter = openmc.Cell(14, name = 'nu2100_filter')
nu2100_filter.fill = nu2100
nu2100_filter.region = nu2100_region
```

```
#air


air_region = -void_surf & ~tungsten_region_1 & ~steel_region_1 & ~steel_region_2 &
~steel_region_3 & ~steel_region_4 & ~beryllium_region_1 & ~flibe_region_1 &
~flibe_region_2 & ~flibe_region_3 & ~flibe_region_4 & ~concrete_slab_region &
~pump_region & ~nu2100_region & ~poly_region

#~steel_block_region &

air_cell = openmc.Cell(15, name = 'air')

air_cell.fill = air

air_cell.region = air_region


# Create a universe

universe =
openmc.Universe(cells=[air_cell,void_cell,nu2100_filter,pump,poly_blanket,concrete_slab,flibe
_4,flibe_3,flibe_2,flibe_1,steel_4,steel_3,steel_2,steel_1,beryllium_1,tungsten_1])

#steel_block


# Create a geometry and set the root universe

geometry = openmc.Geometry()

geometry.root_universe = universe


# Export the geometry to XML

geometry.export_to_xml()
```

Source term and tallies are same in both models.

UC-MSTL Results (Advanced, added Boronated Polyethelene, Removed Steel Block)

Leakage Rate: 25.071%

Time to complete: 1419.5 seconds

```
=========================>     TALLY 15: POLY     <=========================

 Cell 17
```

Total Material

Flux	10.2292 +/- 0.00114775
heating	2.76587e+06 +/- 364.721
heating-local	3.17268e+06 +/- 419.879
Absorption Rate	0.637145 +/- 0.000120838
(n,a)	0.629787 +/- 0.000119679
(n,gamma)	0.00633376 +/- 1.21755e-06
(n,t)	4.21007e-05 +/- 1.42891e-08

=====================> TALLY 12: STEEL PUMP <=====================

Cell 13

Total Material

Flux	0.00180425 +/- 6.23708e-05
heating	18.1534 +/- 0.792506
heating-local	168.155 +/- 5.96814
Absorption Rate	1.05497e-05 +/- 5.12214e-07
(n,a)	2.74564e-07 +/- 1.68435e-08
(n,gamma)	9.19414e-06 +/- 5.06696e-07
(n,t)	1.61117e-11 +/- 2.53857e-12

=========================> TALLY 14: AIR <=========================

Cell 15

Total Material

Flux	98.0986 +/- 0.023147
heating	2080.93 +/- 1.01884
heating-local	3086.08 +/- 1.63018
Absorption Rate	0.000543978 +/- 3.22261e-07
(n,a)	0.000109184 +/- 7.36259e-08
(n,gamma)	1.45584e-05 +/- 1.2299e-08
(n,t)	9.89083e-06 +/- 7.50936e-09

============> TALLY 3: STEEL PIPING IRRADIATION ZONE <============

Cell 3

Total Material

Flux	0.0305329 +/- 4.75193e-05
heating	934.498 +/- 3.09154
heating-local	5663.95 +/- 16.0736
Absorption Rate	0.000234902 +/- 8.26452e-07
(n,a)	1.90616e-05 +/- 7.04897e-08
(n,gamma)	0.000155565 +/- 7.69004e-07
(n,t)	2.51228e-09 +/- 1.56763e-11

======> TALLY 5: VERTICAL STEEL PIPING NON-IRRADIATION ZONE <======

Cell 5

Total Material

Flux	4.01353e-05 +/- 1.17655e-06
heating	1.19839 +/- 0.0722479
heating-local	10.8424 +/- 0.513398
Absorption Rate	5.92137e-07 +/- 3.99874e-08
(n,a)	2.30429e-08 +/- 1.70482e-09
(n,gamma)	4.82243e-07 +/- 3.97357e-08
(n,t)	1.04815e-12 +/- 1.95984e-13

============> TALLY 7: TOP HORIZONTAL STEEL PIPING <============

Cell 7

Total Material

Flux	0.00111611 +/- 7.90273e-06
heating	27.0568 +/- 0.564682
heating-local	236.329 +/- 3.18699
Absorption Rate	1.29427e-05 +/- 2.155e-07
(n,a)	5.17365e-07 +/- 1.29706e-08

(n,gamma) 1.05128e-05 +/- 2.10871e-07

(n,t) 3.40367e-11 +/- 2.38691e-12

==========> TALLY 9: BOTTOM HORIZONTAL STEEL PIPING <==========

Cell 9

Total Material

Flux 0.00103021 +/- 7.55305e-06

heating 27.0842 +/- 0.565921

heating-local 229.428 +/- 3.20616

Absorption Rate 1.21285e-05 +/- 2.1978e-07

(n,a) 5.24971e-07 +/- 1.29695e-08

(n,gamma) 9.67915e-06 +/- 2.13471e-07

(n,t) 3.45593e-11 +/- 2.55693e-12

==========> TALLY 13: NU2100 FILTER <==========

Cell 14

Total Material

Flux 0.0198442 +/- 0.000205038

heating 543.66 +/- 7.53702

heating-local 1283.37 +/- 15.8467

Absorption Rate 0.000168985 +/- 2.30687e-06

(n,a) 1.55164e-05 +/- 2.5436e-07

(n,gamma) 6.63158e-05 +/- 9.98278e-07

(n,t) 9.86002e-07 +/- 2.17992e-08

==========> TALLY 11: CONCRETE SHIELDING <==========

Cell 12

Total Material

Flux 18.4171 +/- 0.00732436

heating 668414 +/- 292.682

heating-local 1.94935e+06 +/- 836.852

Absorption Rate 0.117624 +/- 6.0005e-05

(n,a) 0.0203783 +/- 1.02531e-05

(n,gamma) 0.0828086 +/- 5.25495e-05

(n,t) 2.76046e-06 +/- 1.9164e-09

=======> TALLY 2: BERYLLIUM INNER SHEATH IRRADIATION ZONE <========

Cell 2

Total Material

Flux 5.41179e-20 +/- 3.82868e-20

heating 3.08849e-15 +/- 2.20841e-15

heating-local 3.08862e-15 +/- 2.2085e-15

Absorption Rate 4.83658e-24 +/- 4.78734e-24

(n,a) 4.81996e-24 +/- 4.779e-24

(n,gamma) 1.66224e-26 +/- 1.17421e-26

(n,t) 0 +/- 0

========> TALLY 4: TUNGSTEN OUTER SHEATH IRRADIATION ZONE <========

Cell 4

Total Material

Flux 0.00206072 +/- 3.52716e-06

heating 19.9415 +/- 0.0672853

heating-local 1970.02 +/- 11.2409

Absorption Rate 0.000315038 +/- 2.02605e-06

(n,a) 1.40523e-08 +/- 6.78465e-11

(n,gamma) 0.000314981 +/- 2.02606e-06

(n,t) 0 +/- 0

================> TALLY 1: FLIBE IRRADIATION ZONE <================

Cell 1

Total Material

Flux	0.0263179 +/- 5.57942e-05
heating	10725.6 +/- 34.4793
heating-local	11048.3 +/- 34.7294
Absorption Rate	0.0018295 +/- 7.00014e-06
(n,a)	1.72467e-05 +/- 7.65213e-08
(n,gamma)	6.0946e-07 +/- 4.38821e-09
(n,t)	0.00180193 +/- 6.99547e-06

=========> TALLY 6: VERTICAL FLIBE NON-IRRADIATION ZONE <==========

Cell 6

Total Material

Flux	0.00010649 +/- 3.8258e-06
heating	45.373 +/- 2.36872
heating-local	47.2176 +/- 2.3891
Absorption Rate	7.60879e-06 +/- 4.82247e-07
(n,a)	1.28623e-07 +/- 7.70633e-09
(n,gamma)	1.83347e-09 +/- 2.05142e-10
(n,t)	7.43099e-06 +/- 4.82201e-07

=================> TALLY 8: TOP HORIZONTAL FLIBE <=================

Cell 8

Total Material

Flux	0.00282325 +/- 2.22045e-05
heating	1277.4 +/- 12.6347
heating-local	1318.25 +/- 12.787
Absorption Rate	0.000223965 +/- 2.53356e-06
(n,a)	2.80351e-06 +/- 4.34165e-08
(n,gamma)	5.86937e-08 +/- 1.26727e-09
(n,t)	0.000220045 +/- 2.53195e-06

==========> TALLY 10: BOTTOM HORIZONTAL FLIBE
<==========

Cell 10

Total Material

Flux	0.00224058 +/- 1.98833e-05
heating	977.81 +/- 10.7553
heating-local	1012.82 +/- 10.9165
Absorption Rate	0.000166733 +/- 2.13496e-06
(n,a)	2.39963e-06 +/- 3.88515e-08
(n,gamma)	4.48367e-08 +/- 1.13642e-09
(n,t)	0.000163352 +/- 2.13123e-06

UC-MSTL Results (Advanced, added Boron Carbide)

Leakage Rate: 33.541%

Time to complete: 5258.6 seconds

=========================> TALLY 16: B4C <=========================

Cell 17

Total Material

Flux 10.9151 +/- 0.000562042

heating 2.36642e+06 +/- 99.2305

============> TALLY 11: STEEL BLOCK IRRADIATION ZONE <============

Cell 11

Total Material

Flux 0.129205 +/- 6.06544e-05

heating 2949.61 +/- 2.5824

====================> TALLY 13: STEEL PUMP <====================

Cell 13

Total Material

Flux 0.00121073 +/- 1.64311e-05

heating 10.6425 +/- 0.1864

=========================> TALLY 15: AIR <=========================

Cell 15

Total Material

Flux 123.922 +/- 0.00730871

heating 2950.46 +/- 0.364096

============> TALLY 3: STEEL PIPING IRRADIATION ZONE <============

Cell 3

Total Material

Flux 0.0184765 +/- 1.42151e-05

heating 352.912 +/- 0.51794

======> TALLY 5: VERTICAL STEEL PIPING NON-IRRADIATION ZONE <======

Cell 5

Total Material

Flux 2.44901e-05 +/- 2.93561e-07

heating 0.666295 +/- 0.0166527

=============> TALLY 7: TOP HORIZONTAL STEEL PIPING <==============

Cell 7

Total Material

Flux 0.00110626 +/- 2.45246e-06

heating 18.9077 +/- 0.106362

============> TALLY 9: BOTTOM HORIZONTAL STEEL PIPING
<============

Cell 9

Total Material

Flux 0.00109496 +/- 2.42e-06

heating 18.9491 +/- 0.107867

====================> TALLY 14: NU2100 FILTER <====================

Cell 14

Total Material

Flux 0.0123944 +/- 4.98984e-05

heating 311.197 +/- 1.82458

==========> TALLY 12: CONCRETE SHIELDING <==========

Cell 12

Total Material

Flux 16.0982 +/- 0.00210669

heating 457025 +/- 73.613

=======> TALLY 2: BERYLLIUM INNER SHEATH IRRADIATION ZONE <========

Cell 2

Total Material

Flux 1.73974e-19 +/- 9.71355e-20

heating 7.63379e-15 +/- 3.54854e-15

========> TALLY 4: TUNGSTEN OUTER SHEATH IRRADIATION ZONE <========

Cell 4

Total Material

Flux 0.00113976 +/- 9.74577e-07

heating 8.45691 +/- 0.0128818

==========> TALLY 1: FLIBE IRRADIATION ZONE <==========

Cell 1

Total Material

Flux 0.0175729 +/- 1.65648e-05

heating 3152.79 +/- 3.8018

=========> TALLY 6: VERTICAL FLIBE NON-IRRADIATION ZONE <==========

Cell 6

Total Material

Flux 6.4016e-05 +/- 9.66922e-07

heating 27.7458 +/- 0.562801

==========> TALLY 8: TOP HORIZONTAL FLIBE <==========

Cell 8

Total Material

Flux 0.00298562 +/- 7.47448e-06

heating 937.182 +/- 3.21246

==========> TALLY 10: BOTTOM HORIZONTAL FLIBE
<==========

Cell 10

Total Material

Flux 0.00295647 +/- 7.35463e-06

heating 904.648 +/- 3.12108

C. Glossary of Terms

Fusion: The process by which two light atomic nuclei combine to form a heavier nucleus, releasing a large amount of energy in the process.

Plasma: A state of matter consisting of charged particles, such as ions and electrons, where the gas is heated to extremely high temperatures and becomes ionized.

Tokamak: A toroidal (doughnut-shaped) device used to confine and control plasma for fusion reactions through the use of magnetic fields.

Neutron Activation: The process by which materials exposed to neutron flux become radioactive through neutron capture reactions.

Neutron Flux: The rate of neutrons passing through a unit area per unit time, often measured in neutrons per square centimeter per second.

Breeding: The process of creating additional fusion fuel, such as tritium, within the fusion reactor itself.

Blanket: A region surrounding the fusion core where breeding and energy extraction occur, often composed of lithium to breed tritium and extract heat.

Radiation Shielding: Protective barriers surrounding the fusion reactor to absorb and attenuate harmful radiation emitted during fusion reactions.

(n,γ): Neutron capture reaction, where a neutron is absorbed by a nucleus, resulting in the emission of a gamma ray.

(n,α): Neutron-alpha reaction, where a neutron is captured by a nucleus, producing an alpha particle (helium-4 nucleus) and emitting other particles or radiation.

(n,t): Neutron-tritium reaction, where a neutron is captured by a nucleus, producing an tritium particle (Hydrogen-3 nucleus) and emitting other particles of radiation.

(n,n): Neutron-neutron elastic reaction, where a neutron is elastically scattered off the nucleus of the atom, causing little change to the original target nucleus.

(n,n'): Neutron-neutron inelastic reaction, where a neutron collides with a target nucleus, resulting in the excitation of the target nucleus to a higher energy state without changing its identity.

(n,α)t: Neutron-alpha-tritium reaction, where a neutron is captured by a nucleus, producing an alpha particle (helium-4 nucleus) and a tritium particle (a hydrogen-3 particle).

(n,2n): Neutron-two-neutron reaction, where a neutron is absorbed by a nucleus, causing it to emit two neutrons.

(n,3n): Neutron-three-neutron reaction, where a neutron is absorbed by a nucleus, causing it to emit three neutrons.

(n,α): Neutron-alpha reaction, where a neutron is absorbed by a nucleus, resulting in the emission of an alpha particle.

(n,β-): Neutron-beta-minus reaction, where a neutron is captured by a nucleus, resulting in the emission of a beta particle (an electron) and an antineutrino.

(n,γ): Neutron-gamma reaction, where a neutron is absorbed by a nucleus, leading to the emission of one or more gamma rays.

Filtering Mechanism Theory, Experimental Plan, and Analysis

Benjamin L. Kraus

University of Cincinnati Molten Salt Test Loop

UC-MSTL

University of Cincinnati

BSME Class of 2024

THIS PAGE PURPOSELY BLANK

1. Introduction

1.1. Purpose of Document

The purpose of this procedure and analysis is to provide information and analysis of our existing procedures and data concerning the purity, viability, and experimentation of MOFs (Metal Organic Frameworks) for the solid-state storage of Tritium. The document will focus on describing MOFs, the current techniques used to synthesize and analyze them, informing on the currently accepted procedures to create our chosen MOF, NU-2100, and sharing data obtained through scanning electron microscopy, energy dispersive x-ray spectroscopy, surface area and porosity analysis, and thermogravimetric analysis. For ease of access, the name and model of each machine used will be included in a list below the procedure. Each section will contain a figure displaying the data collected from the respective machine. The surface area and porosity analysis section will describe the levels of Nitrogen adsorbed by the MOF at varying levels of pressure. The scanning electron microscopy section will provide imaging and analysis of the MOF at microscopic levels. The energy dispersive x-ray spectroscopy section will provide energy signatures obtained from the sample and cross-reference those signatures with currently known values of elements. Finally, the conclusion section will provide an overall analysis of the MOF, regarding the feasibility of the intended use.

1.2. Document Scope

This report's scope includes a thorough examination of NU-2100's capabilities of adsorbing isotopes of Hydrogen. A thorough investigation of proper synthesis and procedure to create NU-2100 will be conducted. Utilizing sonicating therapy, stoichiometry, Energy Dispersive X-ray Spectroscopy, Scanning Electron Microscopy, Brauer-Emmett-Teller Porosity Analysis, this document will analyze NU-2100 and inform on the capabilities of NU-2100 to adsorb Tritium and act as a storage unit to allow the Tritium to degrade to Helium.

1.3. Background

The University of Cincinnati senior design group is conducting research into the open space and readily available fusion reactor devices such as those being produced by Commonwealth Fusion Systems (CFS) and other Fusion energy start-ups (General Atomics, et. al). As such, the group would like to complete a conceptual design on a molten salt test loop, which simulates the nuclear, thermo-fluid, and heat transfer properties of liquid salt for the purposes of heat transfer in a fusion device. The concept under development is the Molten Salt Test Loop (MSTL). The goal of the conceptual design is to document expected engineering challenges, current and needed empirical data, and preliminary results from heating, fluid flow, and neutronics calculations. This is to be completed by senior mechanical engineering students of the class of 2024 to satisfy graduation requirements per a capstone project.

1.4. Scope

1.4.1. Users

Users of this report include future system designers and engineers, project managers, stakeholders, and regulatory bodies, such as the Department of Energy (DOE) and the Nuclear Regulatory Commission (NRC).

1.4.2. Need

The report will provide essential research to validate the operational assumptions for fusion power plants. Previously published results and data provide a basis for the procedures and analysis methods.

2. Introduction to Metal-Organic Frameworks

***Note:** If familiar with the definitions of metal organic frameworks, adsorption, physisorption, TGA, SEM, ASAP, and porosity, proceed to the section titled "Experimental Instructions" of this document.*

2.1. Reticular Chemistry

In the past 30 years, a growing branch of inorganic chemistry has been capturing researcher's interests, called Reticular Chemistry. The premise is to pair various kinds of materials together to allow target molecules within the chemicals to create strong bonds to form crystalline structures. By experimenting with various types of chemicals, researchers have made many discoveries in how different bonds can result in wildly new geometries within the structure of the materials.

However, not only did they discover new geometries, or "frameworks," but they began to realize some of these new materials had interesting characteristics that set them apart from other materials of their class. Due to their crystallinity and the geometric structure of the framework, these materials adopted porous-like structures (like sponges on a microscopic level) that could act as cages for specific types of atoms. This was due to an interplay of forces (Van der Waals forces) between the molecules encompassing the pores and the targeted molecule, physically and magnetically keeping atoms contained within certain sections of the framework. This is called "adsorption." The atoms involved are mostly hydrogen, nitrogen, and water vapor. As they continued to discover new frameworks more gaseous atoms became possible to capture.

2.2. Metal-Organic Frameworks

Metal-Organic Frameworks (MOFs) fall under reticular chemistry due to the nature of how they are created: bonding metal ions with organic linkers. These can include basic metals like copper, iron, and zinc, along with ligands such as amine's, carbazoles, and pyridines. The organic ligands are necessary for the framework due to their ability to serve as connections between metal nodes and clusters of Hydrogen, Nitrogen, Oxygen, and Carbon atoms. They can be Nitrogen or Oxygen donors, which is especially important when attempting to bond with these clusters of atoms. Whereas the metal nodes are important since they are the main factor in creating the crystalline structure of the MOF. Different metal ions, since they have many types of molecular geometries when bonding with other atoms, can be used to change the geometrical characteristics of MOFs.

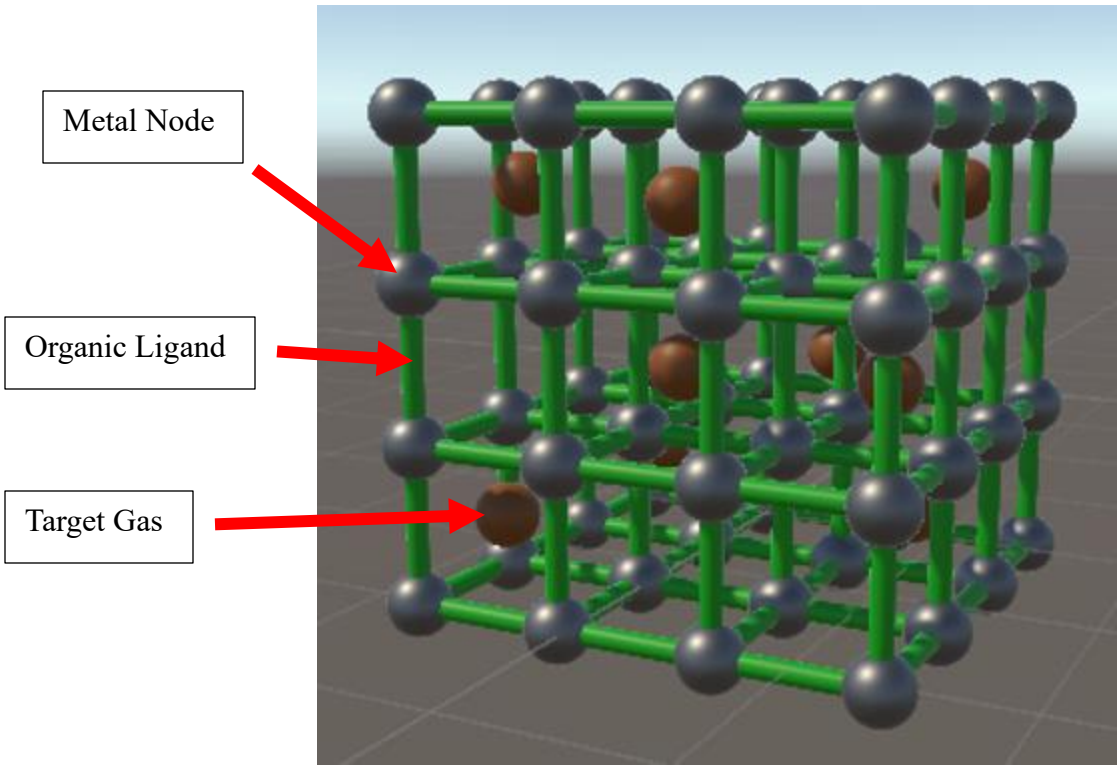

Figure 1: A basic labeled representation of an MOF containing a target gas

MOFs have become an important material due to their average number of pores (porosity) being much higher than other porous structures of their class. Also, due to their framework, they are known to have high surface areas, having as much as 1000-10000 m^2 (about half the size of a block in Manhattan) of surface area within a single gram of MOF. This can be attributed to the high number of pores within a particle of MOF micrometers long, the pores ranging between 0 and 10 nm in diameter. Due to these properties, MOFs have become an attractive material used for catalysis, chemical sensing, and gas storage.

2.3. MOF Decision Matrix

In the class of Metal-Organic Frameworks, many stood out as great contenders. In the beginning, MOFs that seemed ideal were simply ones that could adsorb Hydrogen isotopes, specifically Tritium. However, after careful consideration of the environmental factors that allowed each MOF to adsorb Hydrogen, as well as how much it could adsorb, it came down to a few choices.

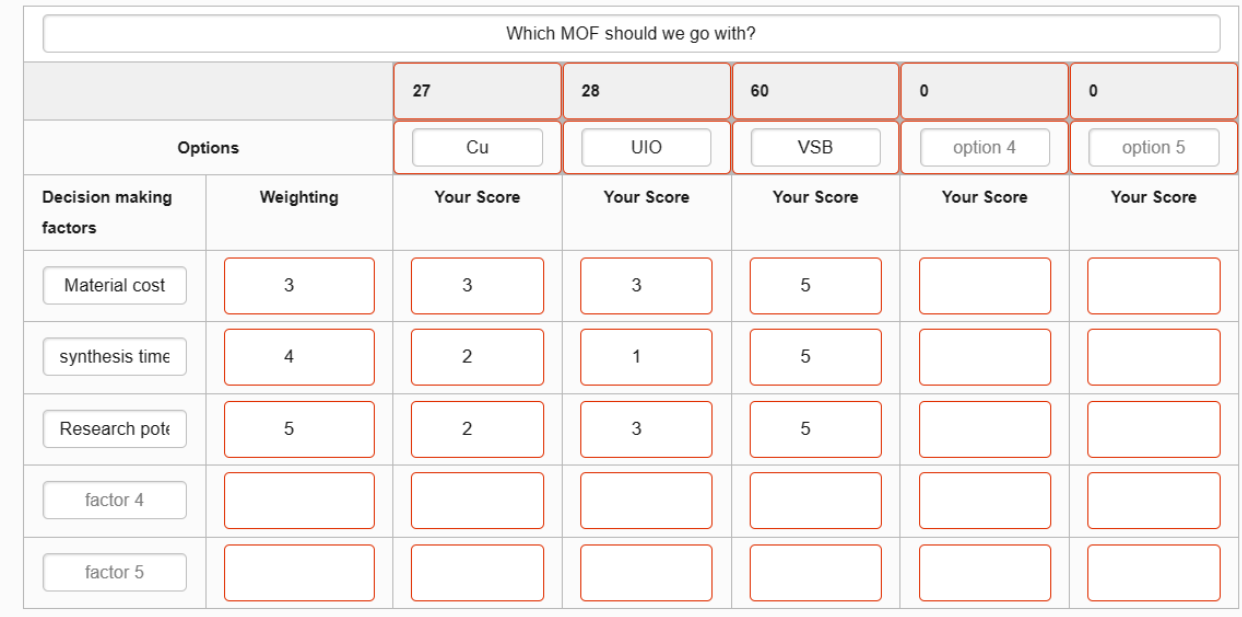

Which MOF should we go with?

		27	28	60	0	0
Options		Cu	UIO	VSB	option 4	option 5
Decision making factors	Weighting	Your Score	Your Score	Your Score	Your Score	Your Score
Material cost	3	3	3	5		
synthesis time	4	2	1	5		
Research pote	5	2	3	5		
factor 4						
factor 5						

Figure 2: MOF Decision Matrix

As you can see in the above decision matrix, we decided there were three constraints that truly limited our decision of the ideal MOF more than the surface area it possesses or its thermal stability. Due to our constraints on costs for equipment and resources, the cost of our supplies was considered our major constraint in the project. The second most important was the synthesis time due to our constrained period for research and development, and the third most important was research potential. Working on an MOF where all the answers are already readily available would not seem worth performing an experiment for.

The MOFs decided upon were UiO-66, VSB-5, and Cu(I)-MFU-4l. UiO-66 is a Zirconium-based MOF with high thermal stability and a large surface area, allowing for considerable amounts of adsorption while also remaining stable at higher temperatures. The synthesis time is about a day, and the cost of materials was around $400. The problem with this material, however, was the amount of research associated with each alternative of the material. Radiation trials, graphs of the various gas adsorption rates, there was nothing new to learn from the material. This was a similar problem we had with VSB-5, the Nickel-based MOF. Not only is there a lot of research, however, but the cost of materials came out to around $700, and the synthesis time came out to around 1 week. Therefore, this MOF was not ideal. In the end, the copper-based MOF, NU-2100, was the ideal MOF due not only to its thermal stability and high surface area, but the low cost of materials, the high research potential, and the 2-day synthesis period.

Other materials were explored as well, such as Silicon and Polyimides. However, with the amount of radiation expected from the reactor, a concern rose regarding their structural stability in radioactive environments. Due to the considerable amounts of research done previously explaining the effects of radiation on these materials, these materials were rejected in favor of the MOF.

2.4. Methods of Analysis

Many methods exist to characterize and measure the capacity of MOFs. Some, such as scanning electron microscopy (SEM), are to confirm the physical characteristics of MOFs at the microscopic level. This includes density, crystal shape, and external damage. Some, such as thermogravimetric analysis (TGA) and Energy Dispersive X-Ray Spectroscopy (EDS), are to confirm the molecular makeup of the MOF and compare the collected data to other samples to help correctly identify the MOF. Finally, there are methods such as surface area and porosity analysis (ASAP). This method first clears the MOF of any remaining molecules within the pores and introduces various gases to test how well the MOF can adsorb these gases at various pressures. The act of clearing the initial molecules within the MOF is called “activation” and is particularly important when planning to use the MOF to adsorb gases, especially during these methods of testing.

2.4.1. Brauer-Emmett-Teller Surface Area and Porosity Analysis

When it comes to porous materials, it is necessary to have some way to calculate their ability to adsorb various gases, which can be done through various methods. The one used here is the Brauer-Emmett-Teller Surface Area and Porosity Analysis (BET). The goal of BET is to measure the surface area of a material through gas adsorption. This often refers to porous materials since those structures usually require advanced methods to calculate the surface area.

Figure 3: Example of a BET Machine

After determining a sample’s properties and pore diameter, the user would choose a gas they would like the material to adsorb. After preparations are made to activate the MOF within a sample tube, the sample tube is purged of all gases and dipped in liquid nitrogen. While in the liquid nitrogen, the sample tube is filled with the target gas to allow the MOF time to try to adsorb it. After a while, the tube is removed from the liquid nitrogen. As the sample heats up, it begins to release the adsorbed target gases back into the tube/machine. The released gas molecules are then quantified, and from that data the surface area/porosity is calculated.

2.4.2. Scanning Electron Microscopy

Think of scanning electron microscopy like a powerful microscope that uses electrons rather than light. Where a microscope lets you see objects up to about 500 nanometers in length (some bacteria), scanning electron microscopes allow you to see objects closer to 1 nanometer in length. This is done by encasing the sample in a vacuum chamber to not have any gaseous atoms interfere, then firing electrons at your sample and analyzing the results. However, if your sample is not conductive, this can cause problems with both the resultant image and the sample. The sample could catch and trap electrons, causing white spots in the image due to no data being recorded. On top of that, built up charges from the electrons can cause the sample to overheat and deteriorate. This is why for samples that are non-conductive, they first must be coated with a conductive material that can keep the shape of the sample without allowing it to burn up. These types of coatings range from carbon particles to gold particles.

Many laboratories use these SEM machines not only to see CNTs (carbon nanotubes) or the individual fibers of graphene, but under SEM you can see the physical shape of MOFs. MOFs can typically range from 3-50 microns thick, and to get good characterizations of the MOF, SEM analysis is necessary.

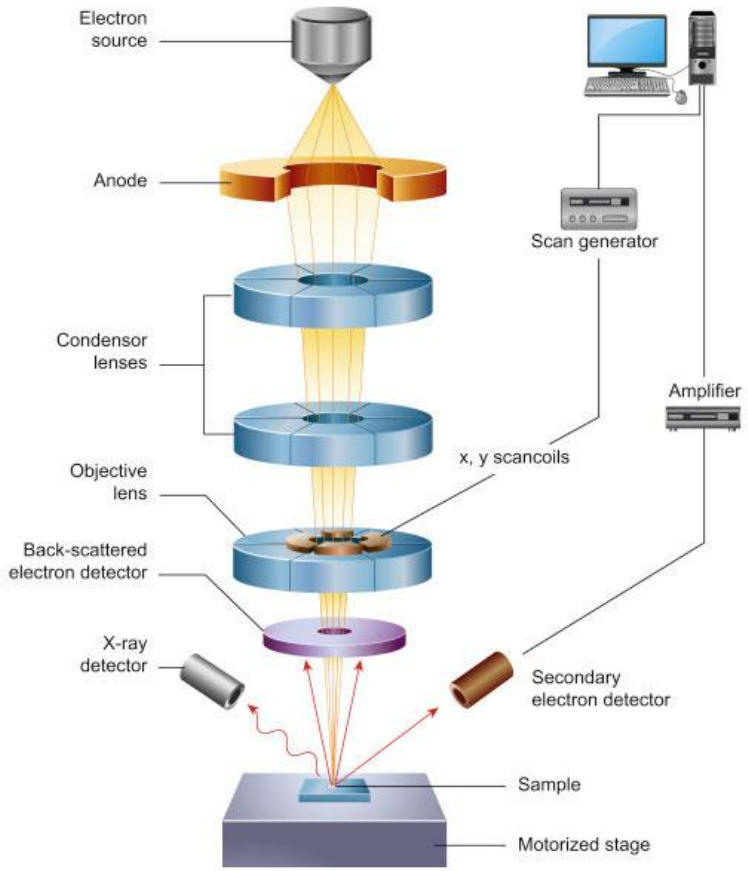

[2]Figure 4: Diagram of the Operating Mechanisms within a Scanning-Electron Microscope

To pick up those images, SEM machines fire electrons at your sample to attempt to either replace the sample's electrons, knock them off, or bounce off the sample. If any of those instances occur, it provides several types of data, which portrays a picture to be viewed for analysis. Any replaced electron is called secondary electrons, which help provide a topographical image of the material. Any electrons that bounce off are called backscatter electrons and depending on the number that bounce off/the intensity of the movement/the angle of return can help identify the type of material interacted with. Finally, any electrons that knock off an electron can be used for a different type of analysis, called energy dispersive x-ray spectroscopy (EDS).

2.4.3. Energy Dispersive X-ray Spectroscopy

Within most SEM machines exists another form of analysis, depending on the accuracy of the electron source and the sensors that exist within the machine. Energy Dispersive X-ray Spectroscopy (EDS) utilizes many of the same principles that allow SEM machines to obtain their imaging, however the result is quite different. Whereas SEM utilizes the electron to simply map out an image of the sample using the same electrons shot at the sample, EDS utilizes the x-ray photons created as a result of the electron configurations of elements in the sample being effectively altered.

A key component to obtaining an x-ray photon from an element is the valence electrons. When an electron from the SEM machine is fired, 1 of 4 things happens: either the electron misses, the electron hits a sample and bounces off, it hits the sample in an elastic collision and replaces the electron, or it hits the sample in an inelastic collision and both electrons fly away. In the last case, the hole left behind cannot exist within the lower levels of the electron configuration, requiring electrons from outer shells to jump a shell and replace the hole. This jump in shells produces enough energy to create an x-ray photon, one unique to the element hit. Once this photon flies away, x-ray detectors on the SEM machine can analyze those photons and produce a graph representing the energy signatures of the various photons analyzed.

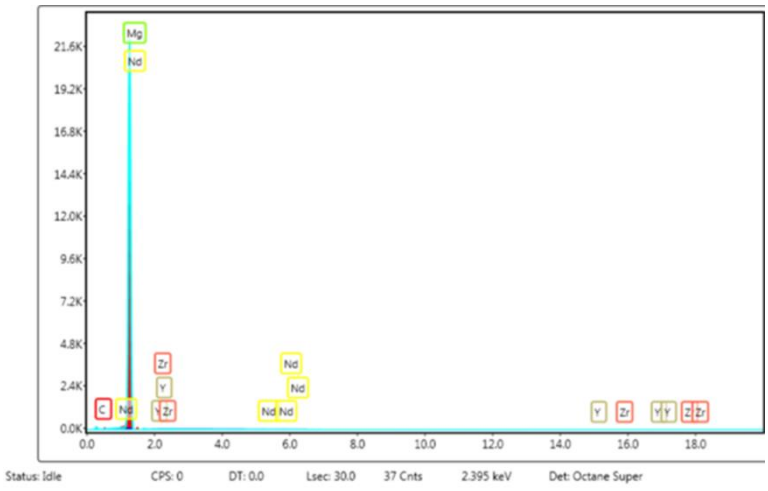

Figure 5:EDS Analysis of WE43 Magnesium

The system will then cross-reference the energy signature obtained from the photon and compare it to currently known values for existing elements and provide the closest element it could be from. After a few seconds, you will begin to see peaks in the graph where the system analyzed the most common type of photon present, and an analysis can be made. This type of analysis could confirm every element present, and comparisons can be made to confirm the ratios of elements to each other. You couldn't confirm specific chemicals in a mixture, but if you know only one type of chemical is present, then you will see a ratio similar to the mol ratios from the mass balance equation.

2.4.4. Thermogravimetric Analysis

Thermogravimetric analysis can be described as creating the thermal footprint of a material. Not only that but running a material through thermogravimetric analysis can show a material's thermal stability over a range of temperatures. After placing the material within a crucible, the material is then placed in a furnace capable of temperatures up to 1700°C. To achieve different results, the chamber is then filled with purge gases to analyze several types of combustion or ignition in the sample. These gases include Nitrogen, Oxygen, Argon, or regular air. While the furnace slowly heats up the sample, there is a precision weight balance underneath the furnace that tracks any weight loss within the sample as the temperature increases.

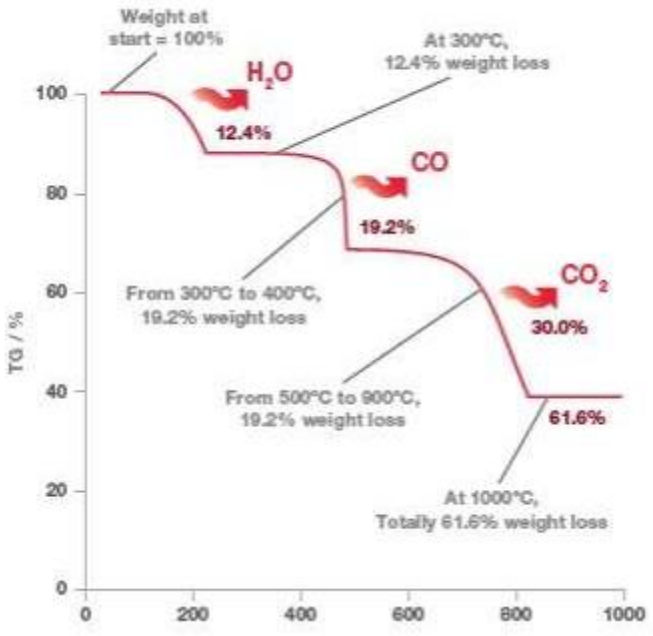

Figure 6: Thermogravimetric Analysis of a sample Material

As you can expect, as the temperature rises the sample begins to lose mass due to aspects of the sample being lost to elevated temperatures. This is a result of the loss of substantial amounts of mass, or large decomposition. At various stages of the temperature range, several aspects of the sample experience this decomposition. As seen in Figure 6, around 50°C-150°C, you can expect

to see a drop in mass due to the loss of absorbed moisture. Beyond that range, between 200°C-800°C it is expected to see drops in mass related to elements within the material.

2.5. Stoichiometric Calculations

Before producing the theoretical amount of product from the reagents, balancing out the mass equation of the chemicals must be performed to have an expected amount of moles of NU-2100. When balancing equations for MOFs, the goal is to make sure the number of electrons and protons on both sides of the equation end up equal to each other.

$$ZnCl_2 + CuCl_2 + C_6H_4N_6 \Rightarrow C_6H_2Cu_2N_6 + Zn^{+2} + HCL + Cl_2$$

Here, none of the compounds have an identified number of moles, making the equation easier to manipulate to find the correct molar amounts of each compound.

First, compare the intended product with the reagents. Notice how 2 Copper atoms are required to create NU-2100. Therefore, there must always be two moles of $CuCl_2$ for every one mole of $C_6H_2Cu_2N_6$.

$$ZnCl_2 + 2\,CuCl_2 + C_6H_4N_6 \Rightarrow 1\,C_6H_2Cu_2N_6 + Zn^{+2} + HCL + Cl_2$$

Second, compare the first element of NU-2100 with the left side to determine if there are any other compounds that require more than one mole. Since there are 6 carbon atoms on both the left and right sides (6 with $C_6H_4N_6$ and 6 with $C_6H_2Cu_2N_6$), no manipulation is necessary in this regard. Therefore, in terms of carbon:

$$ZnCl_2 + 2\,CuCl_2 + 1\,C_6H_4N_6 \Rightarrow 1\,C_6H_2Cu_2N_6 + Zn^{+2} + HCL + Cl_2$$

In the procedure, it is expected to always use a ratio of 3 Zn atoms for every 2 Cu atoms. After balancing out both sides with that knowledge, the equation comes out to:

$$3\,ZnCl_2 + 2\,CuCl_2 + 1\,C_6H_4N_6 \Rightarrow 1\,C_6H_2Cu_2N_6 + 3\,Zn^{+2} + HCL + Cl_2$$

Then, after calculating out the number of Cl and H atoms on the left side (10 Cl, 4 H), and knowing that NU-2100 only needs 2 H atoms per compound, we can assume that HCL will be 2 mols since there are 2 H atoms left to balance with, and there will be 4 mols of Cl_2 since 8 are left over, making the equation:

$$3\,ZnCl_2 + 2\,CuCl_2 + 1\,C_6H_4N_6 \Rightarrow 1\,C_6H_2Cu_2N_6 + 3\,Zn^{+2} + 2\,HCL + 4\,Cl_2$$

Therefore, this is the final mass balance equation, and what is used to calculate the expected yield of NU-2100. If we were to simplify the equation to just the compounds reacting in the mixture, it would become:

$$2\,CuCl_2 + 1\,C_6H_4N_6 \Rightarrow 1\,C_6H_2Cu_2N_6 + 2\,HCL + 1\,Cl_2$$

2.5.1. Chemical Specs and Calculated Yield

Table 1: Values of Chemical Weights Obtained from Stoichiometric Calculations

	Empirical Formula	**Molar Mass (g/mol)**	**Mols**	**Calculated Weight (g)**
Zinc Chloride	$ZnCl_2$	136.286	3	408.858
Copper Chloride	$CuCl_2$	134.45	2	268.900
H_2BBTA	$C_6H_4N_6$	160.14	1	160.140
NU-2100	$C_6H_2Cu_2N_6$	285.22	1	285.220

This was determined by taking the molar masses of each compound and multiplying them by the calculated number of moles in the balanced equation. For example, Copper chloride was:

$$2\ CuCl_2 = 134.45\frac{g}{mol} * 2\ mols = 268.900\ g$$

However, due to our restrictions on chemicals and tests, H_2BBTA is limited to 100 mg for 3 samples. Therefore, to attempt to reduce the amount of reagent used, the number of mols used will be reduced to mmols:

$$1\ mol = \ 1000\ mmol => 1\ mmol\ H_2BBTA = 160.14\frac{g}{mol} * \frac{1}{1000}\frac{mol}{mmol} = 0.16014\frac{g}{mmol}$$

Since 0.16014 g/mmol is still 60 mg above the intended amount, the goal will be to reduce the amount of reagent to 33 mg to avoid wasting the material. Therefore, the multiplier needed to reduce the amount of H_2BBTA and the reciprocal of the smallest number of mmols in the balanced equation is:

$$H_2BBTA = \frac{0.16014\frac{g}{mmol}}{0.033\ g} = 4.8527\ mmol^{-1} = 0.206071\ mmol$$

Table 2: Stoichiometric calculations of amount of chemical necessary per sample

	Empirical Formula	**Molar Mass (g/mol)**	**mMolar Mass (g/mmol)**	**Mmol**	Weight (g)	Weight (mg)
Zinc Chloride	$ZnCl_2$	136.286	0.136286	$0.6183 = 3 * 0.2061$	0.0842656	84.266
Copper Chloride	$CuCl_2$	134.45	0.134450	$0.4122 = 2 * 0.2061$	0.0554203	55.420
H_2BBTA	$C_6H_4N_{64}H_4$	160.14	0.160140	0.2061	0.0330049	33.005
NU-2100	$C_6H_2Cu_2N_6$	285.22	0.285220	0.2061	0.0587838	58.784

Therefore, with these adjusted amounts, the theoretical amount of NU-2100 per sample is 58.784 mg.

2.5.2. Precipitants

As a result of our procedure, 2 products of our experiment are unnecessary to our final experiment and are deemed “precipitants”, or extra materials. These are Zn {+2} particles and Cl_2 gas.

During the initial mixing and sonicating phase, the purpose is to create a material that creates a crystalline framework based around the Zinc ions. Due to this, it is expected chlorine gas will be released from the compound $ZnCl_2$ during the mixing process while the Zinc bonds with the $C_6H_4N_6$.

Afterwards, during the heating process, based on the provided paper, the Zinc ions will eventually be displaced by the Copper ions from $CuCl_2$, resulting in more chlorine gas as the copper ions are displaced. This will also cause solid Zinc {2+} particles to appear as the ions are replaced by copper ions in the framework. After heating, the sample must be washed with DMF to remove any Zinc particles left in the mixture.

THIS PAGE PURPOSELY BLANK

3. Background

In this experiment, NU-2100 will be produced in three 3-dram vials as a powder made of brown crystals. The procedure requires processing in solution. Zinc Chloride, Copper Chloride, and H_2BBTA are mixed in a solvent (DMF) under sonication to break the weaker bonds in the compounds and mix the solutes. This will cause the zinc to mix with the H_2BBTA to create a zinc-based MOF to initialize a framework called Zn-MFU-4l. Any positive changes in the solution can be observed by a color change from green to a solid brown. After placing in the oven, the zinc ions will be replaced by the copper ions still within the mixture. If the displacement is successful, a caked brown substance may appear at the bottom of the vial. After washing out with DMF and air drying to remove any precipitants such as Zinc, the sample will be broken apart to create the brown powder-like substance known as NU-2100.

4. Experimental Instructions

1. Pour 10 mL of DMF solution into a 100 mL eggplant flask
    a. Use a Graduated Cylinder no smaller than 15 mL
2. Carefully setup the eggplant flask above a magnetic stirring plate using a chemical stand
    a. Add the magnetic stirrer to the flask
    b. Turn on the magnetic stirring plate, do not heat the sample (set speed to 2-4)

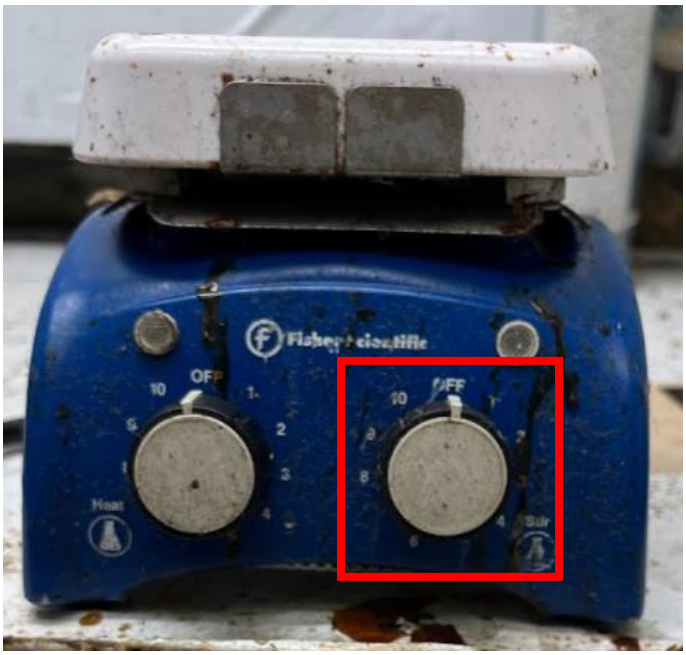

Figure 7: Dr. Iroh's Provided Magnetic Stirring Plate

3. Using a Laboratory Balance Scale, add 252.798 mg of $ZnCl_2$, 166.26 mg of $CuCl_2$, and 99.015 mg of H_2BBTA to the eggplant flask

a. Add each chemical to the flask separately, waiting 1-5 minutes between each one

Figure 8: Dri. Iroh's Laboratory Balance Scale

4. Once the mixture is fully homogenous, turn off the magnetic stirring plate
    a. First, weigh each vial and record initial weights
        i. Label one vial as “24 Hour”, one as “36 Hour”, and one as “48 Hour”

Figure 9: Three Provided 3-Dram Vials

5. Place the 100mL flask within the sonicator and mix it for 10 minutes

a. Support the flask using a chemical stand and clamps
b. There is no reducing of power, just a dial to set time for sonication

Figure 10: Experimental Setup for Dr. Iroh's Sonicator

6. Once the sample has been sonicated, carefully pour the contents of the flask into the three 3-dram vials
    a. Each vial should contain the same amount of mixture

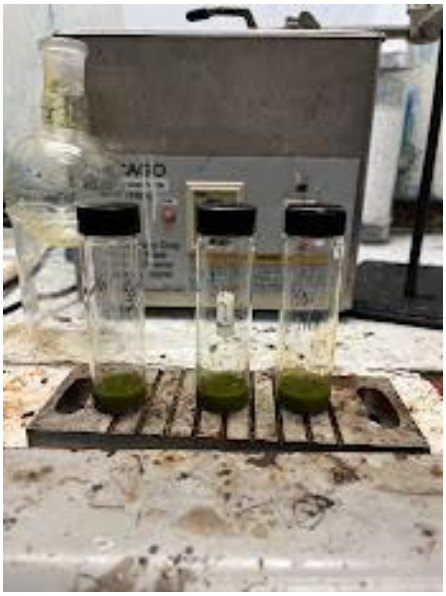

Figure 11: (LEFT SAMPLE) "24 hour", (MIDDLE SAMPLE) "36 hour", (RIGHT SAMPLE) "48 hour"

7. Next, set each within the vacuum oven

a. Set the oven to 413 K, and keep each sample in overnight
b. DO NOT leave the lid on the vial; it will melt

Figure 12: Dr. Iroh's Vacuum Oven

8. Remove “24 Hour” sample once 24 hours has passed
    a. Remove with tongs and allow vial to cool down
    b. Mix with 10-15 mL of DMF until a homogeneous solution
    c. Pour 5mL DMF into the sample vial
    d. Shake for 1 min, attempting to pick up Zinc particles not stuck to the surface
    e. Allow to settle to reduce MOF in DMF, use pipette to remove DMF
    f. Pour final 5mL into sample vial
    g. Shake until all particles have been picked up
    h. Heat hot plate to 100C and place sample on hot plate for 6 hours
    i. Once DMF has dried, remove samples from hot plate and allow to sit and air-dry
9. Remove “36 Hour” sample once 36 hours has passed
    a. Repeat steps 8a-8i for the second sample
10. Remove “48 Hour” sample once 48 hours has passed
    a. Turn off oven
    b. Repeat steps 8a-8i for the third sample
11. For SEM and EDS analysis:
    a. Prepare three 0.5 cm long strips of carbon tape on a provided stainless-steel plate
    b. Label each strip with their corresponding oven time (24, 36, 48)
    c. Place a small spoonful of MOF on each corresponding strip

i. Make sure to blow off any excess MOF not sticking to the carbon tape using a balloon-type blower

d. Using the AMCC's proper procedure and machinery, coat the MOF in a gold-based coating
    i. Since the MOF is not inherently conductive, this is a necessary step
    ii. Seek the assistance of lab personnel
e. After the coating is finished and approval has been given by personnel, turn on SEM machine
    i. Power on computer
    ii. Open program for SEM machine
    iii. Fill SEM chamber with gas
    iv. Once finished, place sample plate within chamber
    v. Close chamber, then purge gas from chamber
    vi. Follow proper protocol listed at the SEM machine for preparing sample for analysis
    vii. Take images at the appropriate locations and magnifications
        0. Two locations should be picked showing interesting MOF topography, crystal growth, or ideal crystals
        1. At each location, take 3 pictures: one at 2000x magnification, one at 5000x, and one at 10000x. If other magnifications are more ideal, then alter magnifications as necessary
    viii. Once finished, perform EDS as well
        0. Do not perform yourself: ask personnel
    ix. Once finished, save sample pictures and data to OneDrive while filling chamber with air
    x. Once chamber is full, remove sample and purge chamber of air
    xi. Turn off computer
f. This is a destructive analysis; you will not be able to salvage the sample

12. For BET analysis:
    a. Prepare a bulb-shaped sample tube for the procedure
        i. Clean with methanol or use specified cleaning procedure in laboratory
    b. Prepare 10-20 mg of sample using a laboratory scale and square weighing paper
    c. Degas empty sample tube using BET machine (reach maximum temperature of 120°C
        i. After removing the sample tube from the BET machine, allow the tube to cool down to room temperature before moving on
        ii. DO NOT OPEN THE TUBE
    d. Next, weigh the sample tube on a laboratory scale
        i. The initial weight of the tube before adding the sample is required for the ASAP machine to properly analyze the sample

e. After weighing the sample tube, open it up and pour the measured sample in the tube
f. Repeat steps c and d
g. Afterwards, inform personnel at the laboratory you are ready to run the analysis
h. This is NOT a destructive analysis; you may salvage the sample if necessary.
i. After the personnel perform the analysis, if necessary, remove the sample tube from the machine and pour the sample into a clean 1-dram vial
    i. Be sure to label the vial with the type of sample used and that it has been used for BET analysis

4.1. Safety

Chemical gloves

Wear eye protection

4.2. Materials:

4.2.1. Chemicals Used

- N-N-Dimethylformamide, ACE Reagent, ≥99.8%
- Copper (II) Chloride, anhydrous, powder, ≥99.995% trace metals basis
- Zinc Chloride, Granular, USP, 97-100.5%, Spectrum™ Chemical
- 1,5-Dihydrobenzo[1,2-d:4,5-d']bis([1,2,3]triazole)

4.2.2. Equipment:

- 100 mL Eggplant flask
- ≥15 mL Graduated cylinder
- 3x 3-dram vials
- 2x Centrifuge-grade vials
- 3x 1-dram vials
- 1 magnetic stirrer
- Fisher Scientific Magnetic Stirring Plate
- Chicago Industrial 1.5 Quart Heavy Duty Stainless Steel Ultrasonic Cleaner Model No. 91957
- Isotemp Vacuum Oven Model 281A
- TGA Machine
- SEM Machine with X-ray photon Sensors
- BET Surface Area and Porosity Analysis Machine

THIS PAGE PURPOSELY BLANK

5. MOF Results and Analysis

After performing Scanning Electron Microscopy, Energy Dispersive X-ray Spectroscopy, and Brauer-Emmett-Teller Surface Area and Porosity Analysis, the MOF has been confirmed to be NU-2100. SEM images were taken of each sample at magnitudes of 800x, 1000x, 1500x, 2500x, 3500x, 5000x, 8000x, and 10,000x. Not every sample needed each magnitude, and all the images for each sample will be listed below.

The EDS reports were printed and will be listed below as well, but each will display the weight percentages of each prominent element present in the sample. There will also be a graph displaying the intensity of each element present in the sample, with labels at each peak signifying the chemical formula.

The BET analysis was printed as well, showing a low measured surface area, but a high calculated surface area. This could be the result of insufficient resources, since the BET analysis requires at least 200 mg of sample to get accurate measurements. However, the sample supplied could only amount to between 50 and 70 mg. Therefore, the calculated analysis will be used for our results while future work will include creating more samples for a better measured analysis.

5.1. Porosity

The surface area of NU-2100 was found in two ways: measurements and calculations. In the former, nitrogen gas was exposed to the NU-2100 while in a vacuum-like environment. The ASAP machine then recorded the amount of nitrogen adsorbed by the MOF at each relative pressure. Nitrogen is used due to its small atomic radius, allowing it to pass between most pores, cracks, and surface roughness, and the experiment is set to 77K since MOFs are activated at very low temperatures. The results obtained were then compared to the results obtained from the researchers at Northwestern University.

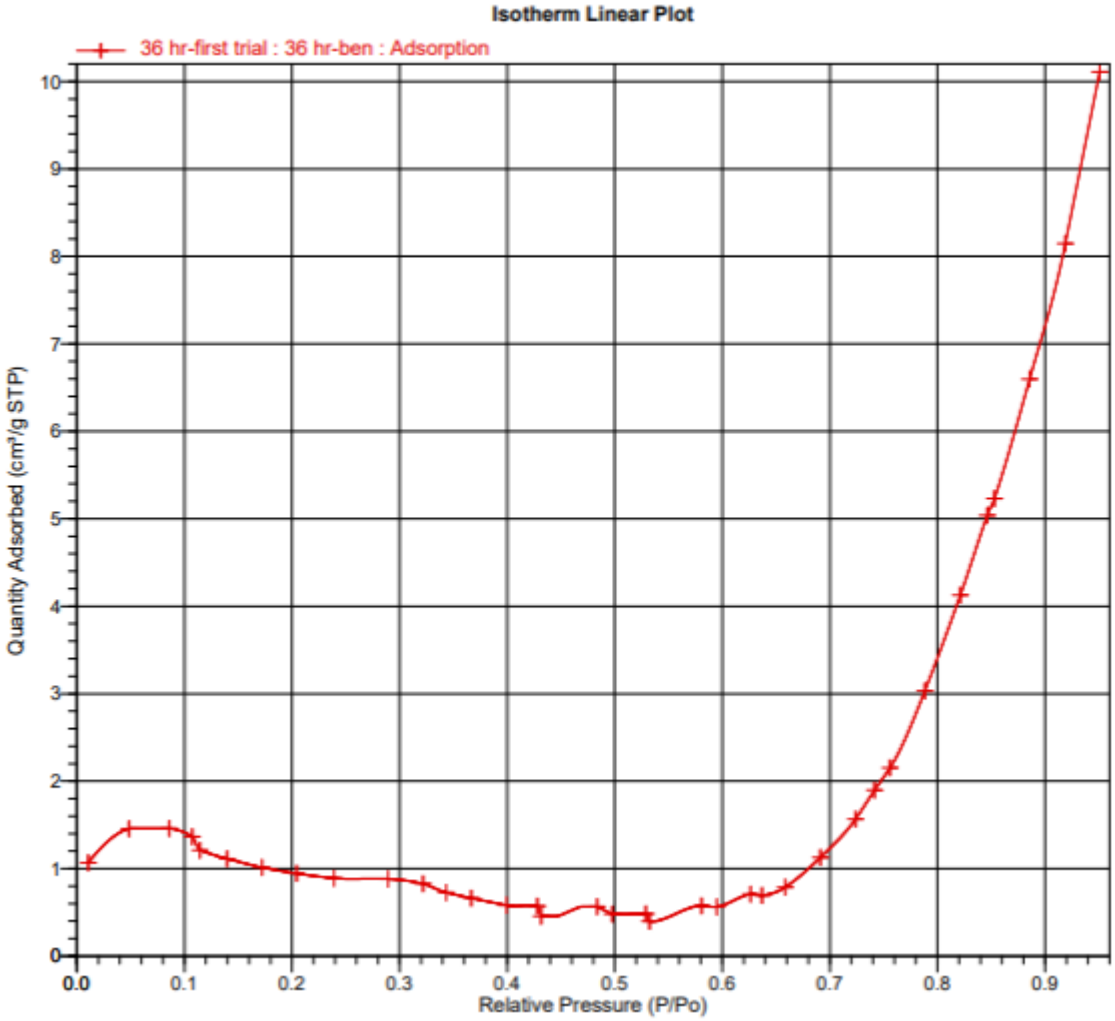

Figure 13: Quantity of N2 Adsorbed vs Relative Pressure in the "36 Hour" sample measured

Due to the types of adsorption and measurements taken of each sample, it is difficult to accurately compare the results obtained in this experiment to the results obtained by Northwestern University. The surface areas can be compared however, and the results obtained show the measured adsorption rate/surface area are much lower than the compared results. This can be attributed to the low number of samples used for the BET analysis, due to insufficient resources and project managerial issues. However, the calculated surface area/adsorption rate of each sample was shown to not only meet expectation but exceed them. It is believed that for future work, if an appropriate amount of sample is created, then accurate measurements can be made regarding the surface area, porosity, and adsorption rate of the samples.

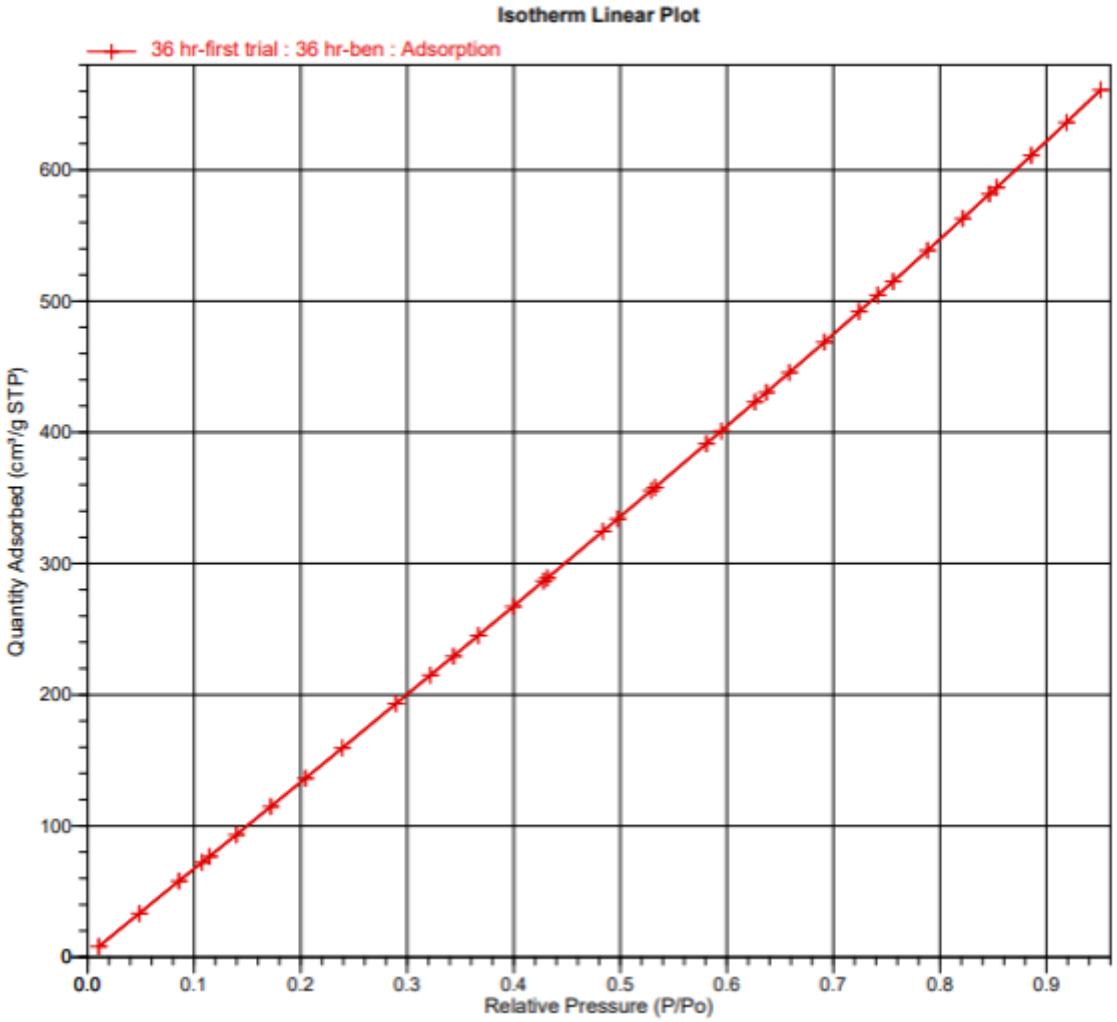

Figure 14: Quantity of N2 Adsorbed vs Relative Pressure in the "36 Hour" sample calculated

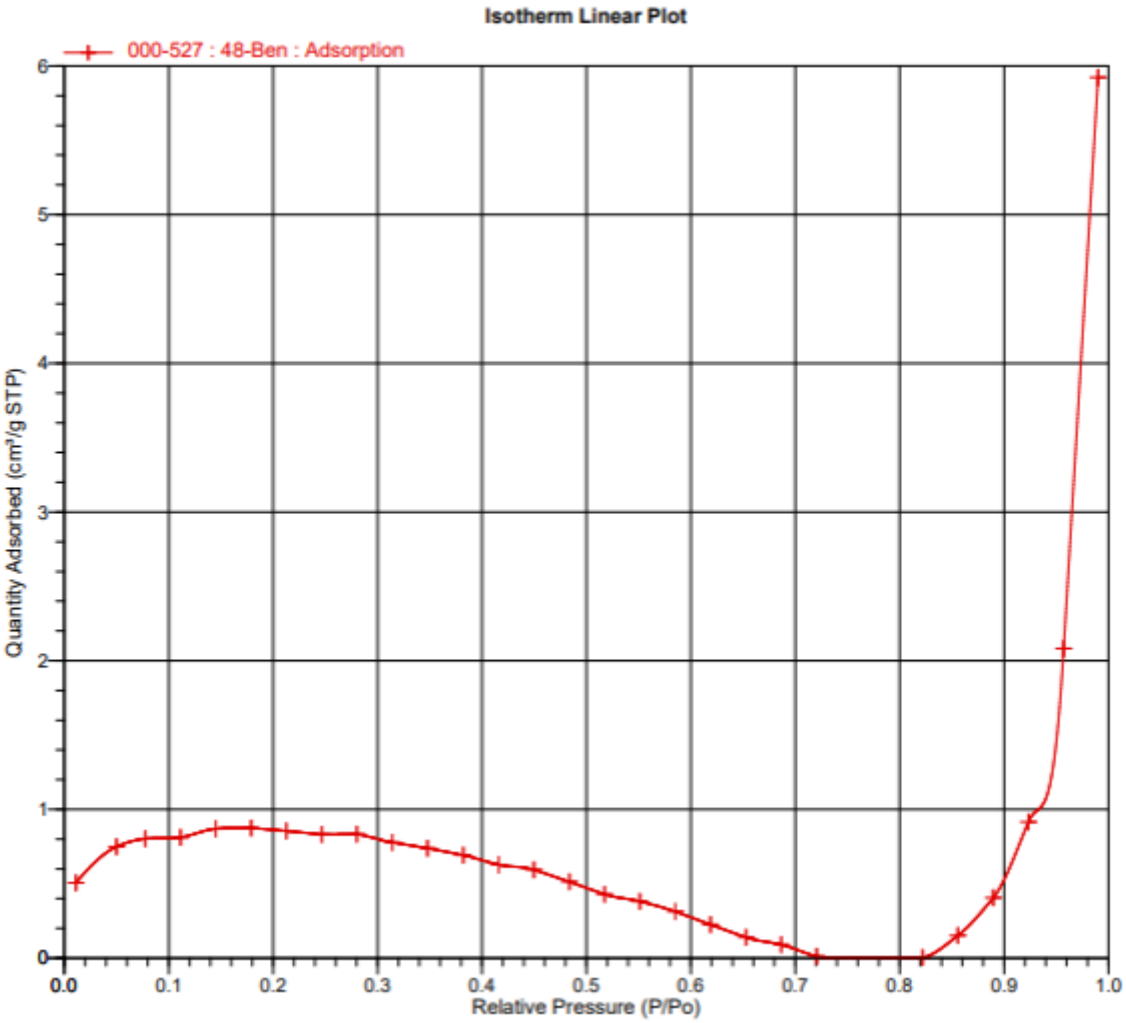

Figure 15: Quantity of N2 Adsorbed vs Relative Pressure in the "48 Hour" sample measured

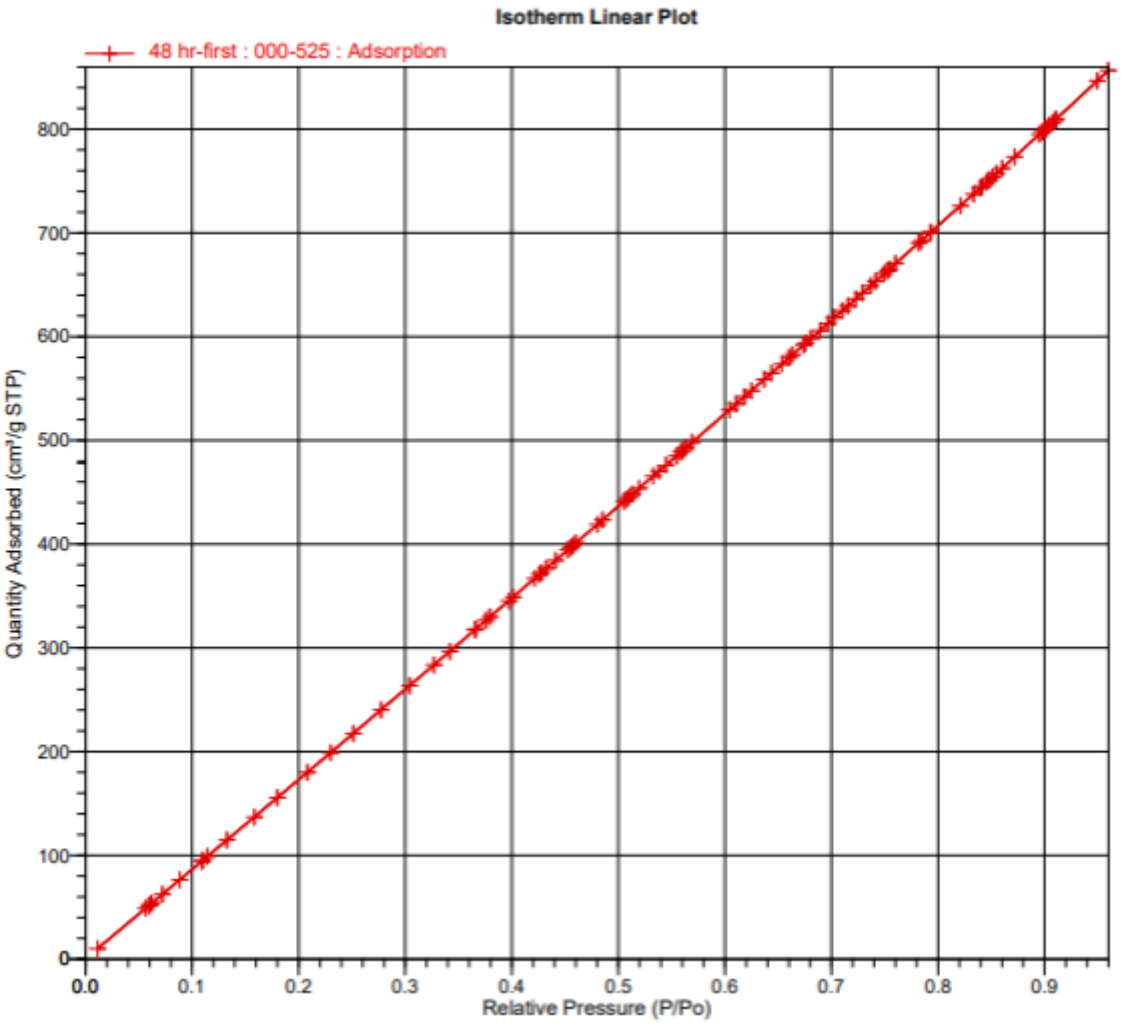

Figure 16: Quantity of N2 Adsorbed vs Relative Pressure in the "48 Hour" sample calculated

5.2. Imaging

In terms of the imagery, I planned on comparing the geometric shape of the sample with those presented by the reference paper.

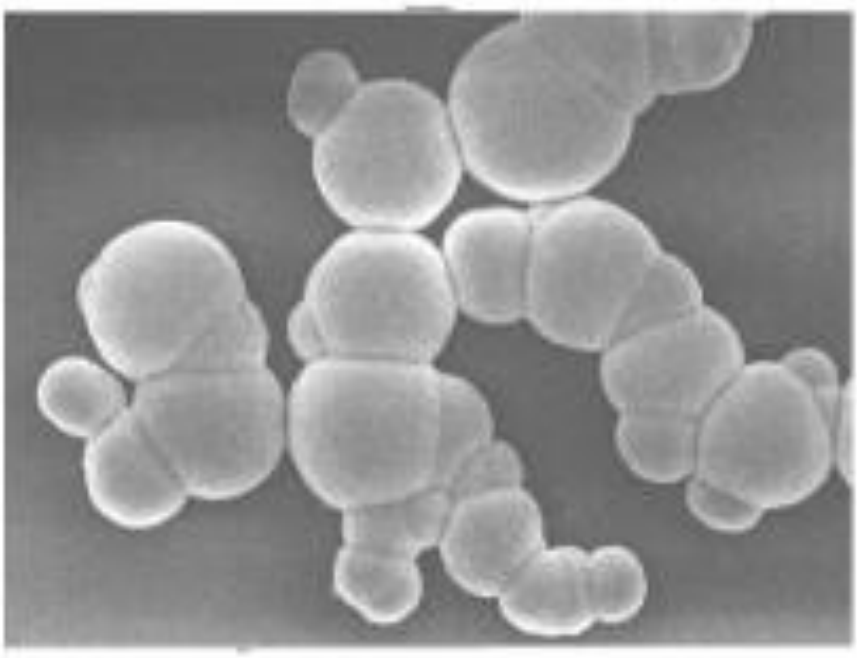

Figure 17 Scanning electron microscopic (SEM) images of Zn-MFU-4l before the Cu and Zn displacement to create NU-2100

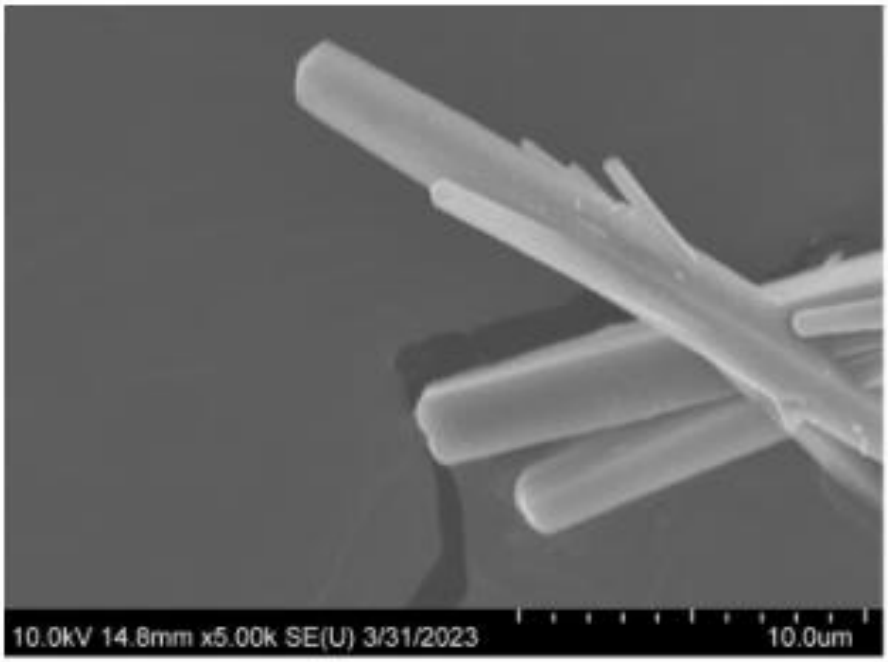

Figure 18: Scanning electron microscopic (SEM) images of NU-2100 in the completed form

To get an accurate analysis of NU-2100, the MOF was made to represent each stage of the process that represented the switch from the mixed sample to NU-2100. In Figure 17, the image shows the MOF before the transition to NU-2100, an intermediate step just before the copper ions begin to replace the zinc ions within the sample. “Clusters” of MOF can be seen, being a physical characteristic of the initial form of MOF. In Figure 18, the final MOF is shown, solid bars protruding to form clusters of rods. This physical representation is an important geometric indicator of the NU-2100 MOF.

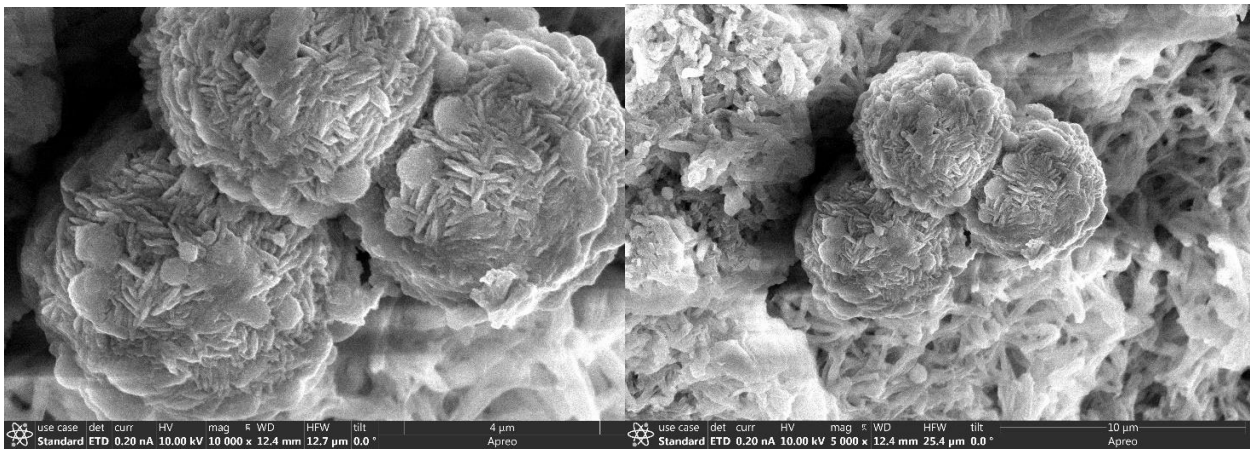

Figure 19: "24 Hour" Sample at (Left) 10000x magnification and (Right) 5000x magnification. These clusters are the intermediate form of th eNU-21000 MOF.

In Figure 21, the initial intermediate form can be seen, with a ball of various particles bound together to form a cluster of MOF. Compared to Figure 19, the MOF seen here could be compared to the MOF created by previous researchers, however more data should be obtained for a more accurate conclusion. Furthermore, in this form, while it would be able to adsorb MOF, it would pale in comparison to NU-2100's ability to adsorb gases.

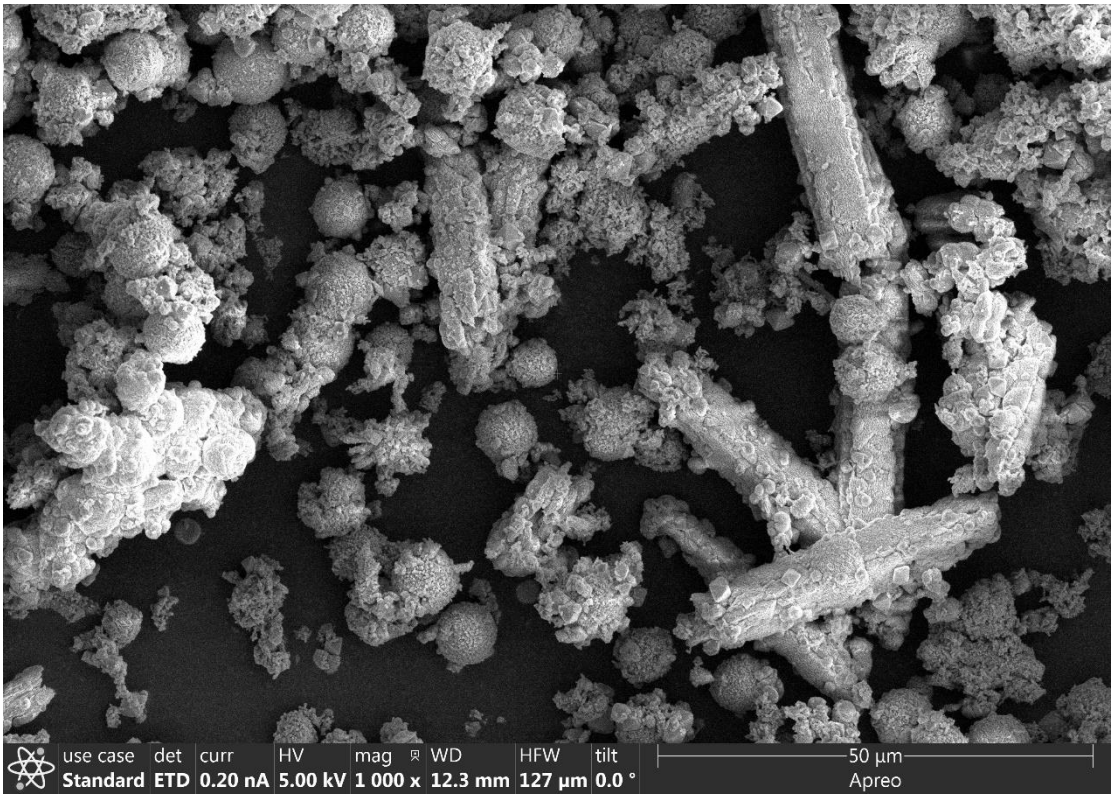

Figure 20: The "36 Hour" Sample taken at 1000x magnification. It can be seen both the clusters and a new rod is formed, showing both the intermediate and final forms of NU-2100

In Figure 20, a transition can be seen occurring within the sample. Rods have started growing among the clusters of MOF, showing a growing leap towards the final form of NU-2100.

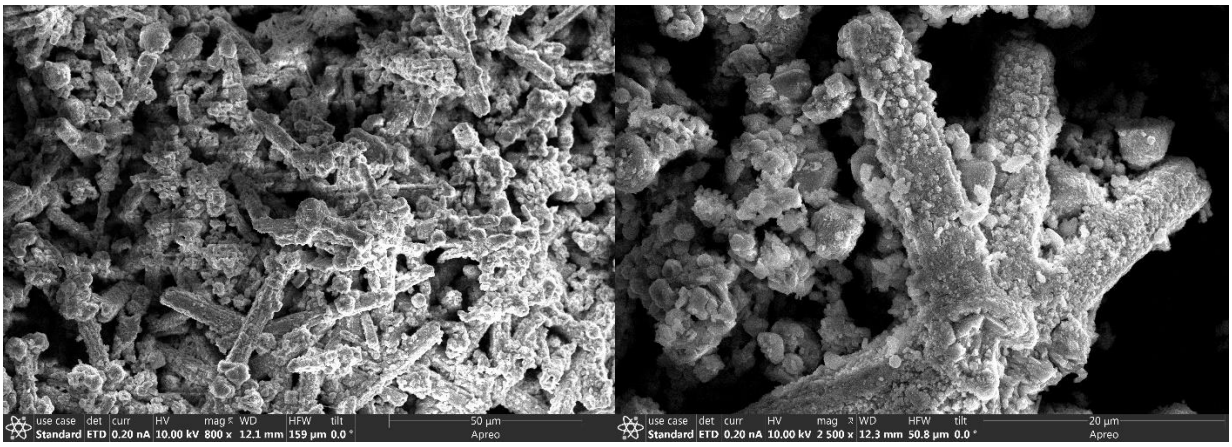

Figure 21: The "48 Hour" sample, showing the final form of the NU-2100. Very few clusters now exist, having been replaced by the rods representative of NU-2100

In Figure 21, the final MOF can be seen. The physical representation of cluster of rods is quite similar to the representation in Figure 18. This allows for the assumption that physically, the MOF created by our procedure is quite similar, if not the same as the NU-2100 created previously by researchers in Northwestern University.

5.3. Energy Signatures

To confirm the chemicals involved in each sample, an EDS spectrum was made to confirm each.

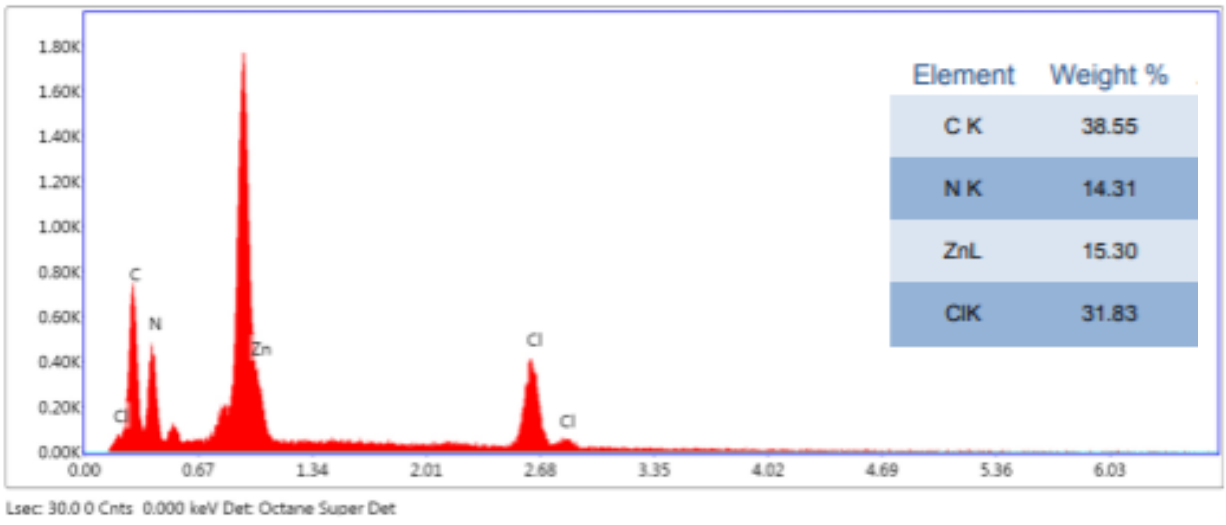

Figure 22 :EDS Spectrum of "24 Hour" Sample

In the first sample, it was expected to see only Zinc, Nitrogen, Carbon, etc. due to the MOF not undergoing the metal ion displacement yet. Copper has not yet been introduced into the sample; therefore, it did not register within the sample.

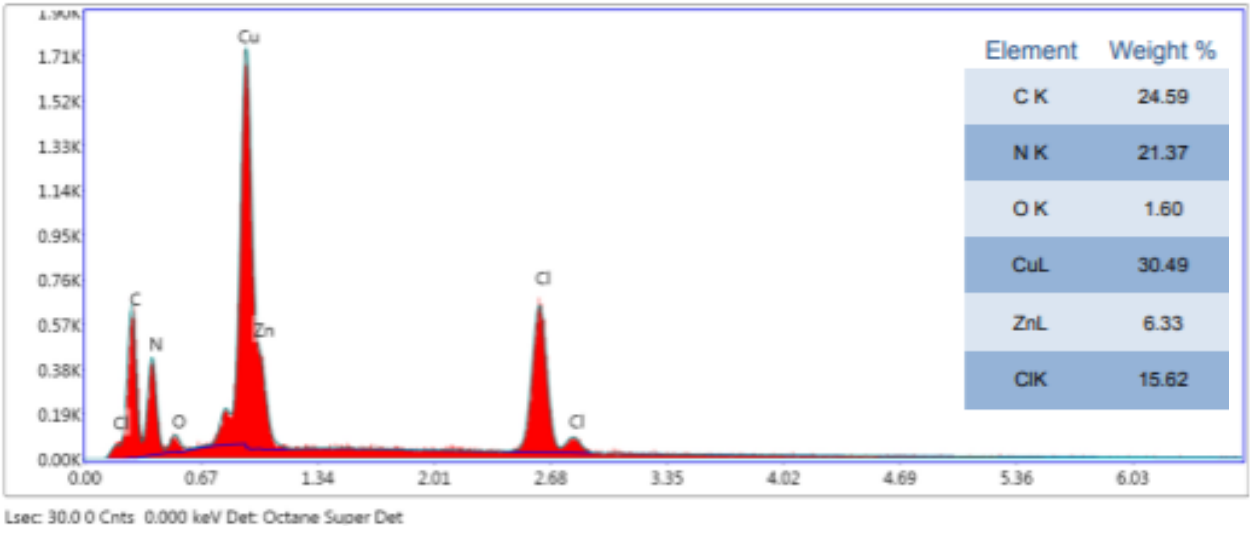

Figure 23: EDS Spectrum of "36 Hour" Sample

In the second sample, it was expected to see all the same elements as the "24 Hour" sample, however Copper was expected due to the sample being in the midst of the metal ion displacement.

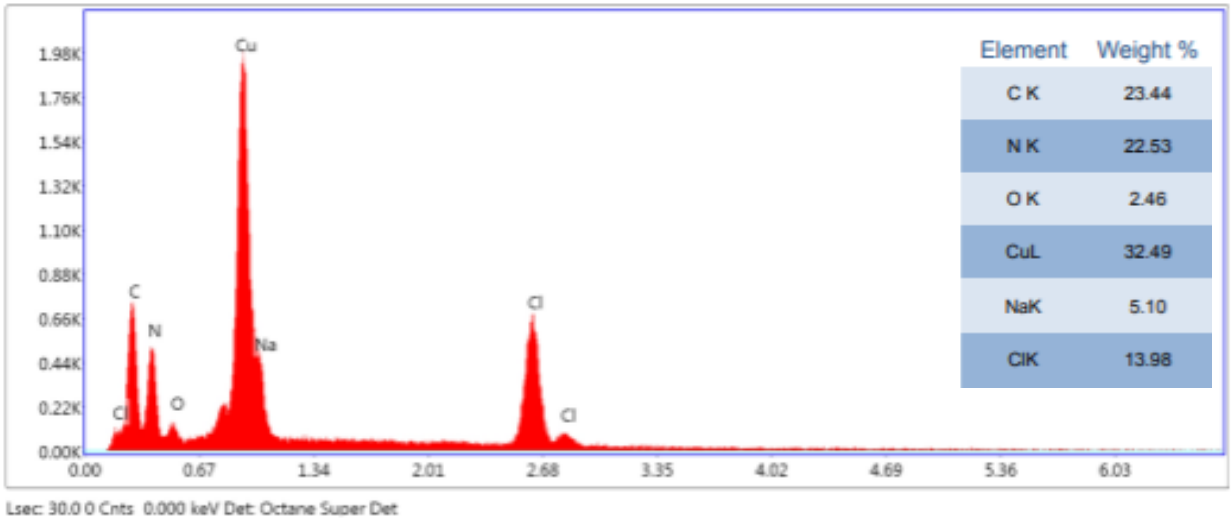

Figure 24: EDS Spectrum of "48 Hour" Sample

In the third sample, it was expected to see each element represented so far except Zinc. The "48 Hour" sample seen in Figure 24 is at the end of the metal ion displacement, where Copper has fully replaced Zinc in the MOF framework, completing the transition from Zn-MFU-4l to NU-2100

6. Conclusion

According to the SEM imaging and EDS spectrum, not only is each sample made of the expected chemicals, but each sample showcases the expected physical representation of it's process to full metal ion displacement. The "24 Hour" sample showing the beginnings of Zn-MFU-4l, the "36 Hour" showing the intermediary stage, with both Zn-MFU-4l and NU-2100 present, and the "48 Hour" sample showcasing NU-2100 in its entirety. After performing the BET analysis, while the adsorption measurements show a very small surface area and shallow pores, the adsorption calculations show a very large surface area of 800 m^2/g and a lucrative porosity, with pores 33.5 Å wide. It is believed that with more sample and more accurate parameters for the analysis, the measured results would match the calculated results.

7. Future Work

Due to insufficient resources, the measured adsorption/surface area of the samples was faulty. This can be ameliorated by resynthesizing the samples and setting at least 200 mg for the test of adsorption. Comparing it to the calculated adsorption/surface area of NU-2100 would be ideal to compare the theoretical with the experimental.

Due to facility and human errors, we were unable to perform a TGA analysis, which could be used to confirm the MOF is NU-2100 by comparing it to results in the reference paper.

Irradiation of the MOF could be used to determine what effect a fast neutron flux environment has on the surface area/porosity of the framework.

A. References

1. The Procedure and Reference data came from:
   Debabrata Sengupta, Patrick Melix, Saptasree Bose, Joshua Duncan, Xingjie Wang, Mohammad Rasel Mian, Kent O. Kirlikovali, Faramarz Joodaki, Timur Islamoglu, Taner Yildirim, Randall Q. Snurr, and Omar K. Farha, "Air-Stable Cu(I) Metal–Organic Framework for Hydrogen Storage", Journal of the American Chemical Society 2023 145(37), 20492-20502 "Materials", "Kinetic experiments of NU-2100 formation", S7
2. *A brief introduction to sem (scanning electron microscopy)*. SciMed. (2022, October 13). https://www.scimed.co.uk/education/sem-scanning-electron-microscopy/
3. *Simultaneous thermogravimetric analysis: Thermal Analysis: Hitachi High-Tech*. Hitachi High Tech Analytical Science. (n.d.). https://hha.hitachi-hightech.com/en/blogs-events/blogs/2022/08/03/what-is-simultaneous-thermogravimetric-analysis-sta/

B. Experimental Notes

1. Pour 10 mL of DMF solution into a 100 mL rounded flask
    a. Use a Graduated Cylinder no smaller than 15 mL
2. Carefully setup the eggplant flask above a magnetic stirring plate using a chemical stand
    a. Add the magnetic stirrer to the flask
    b. Turn on the magnetic stirring plate, do not heat the sample (set speed to 2-4)

3. Using a Laboratory Balance Scale, add 252.798 mg of $ZnCl_2$, 166.26 mg of $CuCl_2$, and 99.015 mg of H_2BBTA to the eggplant flask
    a. Add each chemical to the flask separately, waiting 1-5 minutes between each one

4. Once the mixture is fully homogenous, turn off the magnetic stirring plate

5. Place the flask within the sonicator (with support from clamp and chemical stand) and mix it for 10 minutes
    a. There is no reducing of power, just a dial to set time for sonication

6. Pour the contents of the flask into each vial equally
    a. First, weigh each vial and record initial weights
        a. Label one vial as "24 Hour", one as "36 Hour", and one as "48 Hour"

6. Once all sample has been divided, place each within the vacuum oven
    a. Set the oven to 413 K, and keep each sample in overnight
    b. DO NOT leave the lid on the vial; it will melt

7. Remove "24 Hour" sample once 24 hours has passed
    a. Remove with tongs and allow vial to cool down
    b. Mix with 10-15 mL of DMF until a homogeneous solution
    c. Pour sample into 2 centrifuge-safe containers, matching sample amount in each

d. Place containers in a centrifuge, making sure the positions of the vials are opposite of each other
e. Run the centrifuge at 3000 rpm for 10 minutes
    i. While running, clean 3-dram vial with 70% isopropyl alcohol or ethanol
f. After samples are done, pour out separated fluid into an appropriate waste container
    i. Scoop leftover precipitant back into 3-dram vial
g. After air drying for at most 24 hours, mix material into a powder and screw lid back onto the vial

8. Remove "36 Hour" sample once 36 hours has passed
    a. Repeat steps 6a-6g for the second sample
9. Remove "48 Hour" sample once 48 hours has passed
    a. Turn off oven
    b. Repeat steps 6a-6e for the third sample

10. For TGA analysis of each sample:
    a. Prepare 10 mg of sample using Laboratory Balance Scale
    b. Carefully add sample to an aluminum crucible (can withstand 600°C, does not waste materials meant for higher temperatures)
    c. Add empty aluminum powder bed to platinum (Pt) wire to calibrate TGA machine
        i. This is to zero the scale on the TGA machine before adding our sample
        ii. After calibration is finished:
        iii. Add sample to the aluminum powder bed
        iv. Hook powder bed on Pt wire
        v. Raise furnace to fully encapsulate the sample
    d. Set machine to only flow Nitrogen gas in and out of furnace
    e. Set furnace to run from room temperature (or 10°C) to 600°C at 10°C/min
        i. Full process should take approximately 1 hour
    f. After confirming settings with an associate at the laboratory, run the TGA analysis
    g. This is a destructive analysis; you will not be able to salvage the sample

11. For SEM and EDS analysis:
    a. Prepare three 0.5 cm long strips of carbon tape on a provided stainless-steel plate
    b. Label each strip with their corresponding oven time (24, 36, 48)
    c. Place a small spoonful of MOF on each corresponding strip
        i. Make sure to blow off any excess MOF not sticking to the carbon tape using a balloon-type blower
    d. Using the AMCC's proper procedure and machinery, coat the MOF in a gold-based coating
        i. Since the MOF is not inherently conductive, this is a necessary step
        ii. Seek the assistance of lab personnel
    e. After the coating is finished and approval has been given by personnel, turn on SEM machine
        i. Power on computer
        ii. Open program for SEM machine
        iii. Fill SEM chamber with gas

iv. Once finished, place sample plate within chamber
v. Close chamber, then purge gas from chamber
vi. Follow proper protocol listed at the SEM machine for preparing sample for analysis
vii. Take images at the appropriate locations and magnifications
    1. Two locations should be picked showing interesting MOF topography, crystal growth, or ideal crystals
    2. At each location, take 3 pictures: one at 2000x magnification, one at 5000x, and one at 10000x. If other magnifications are more ideal, then alter magnifications as necessary
viii. Once finished, if time permits, perform EDS as well
    1. Do not perform yourself: ask personnel
ix. Once finished, save sample pictures and data to OneDrive while filling chamber with air
x. Once chamber is full, remove sample and purge chamber of air
xi. Turn off computer

f. This is a destructive analysis; you will not be able to salvage the sample

12. For BET analysis:
    a. Prepare a bulb-shaped sample tube for the procedure
        i. Clean with methanol or use specified cleaning procedure in laboratory
    b. Prepare 10-20 mg of sample using a laboratory scale and square weighing paper
    c. Degas empty sample tube using BET machine (reach maximum temperature of 150°C
        i. After removing the sample tube from the BET machine, allow the tube to cool down to room temperature before moving on
        ii. DO NOT OPEN THE TUBE
    d. Next, weigh the sample tube on a laboratory scale
        i. The initial weight of the tube before adding the sample is required for the BET machine to properly analyze the sample
    e. After weighing the sample tube, open it up and pour the measured sample in the tube
    f. Repeat steps c and d
    g. Afterwards, inform personnel at the laboratory you are ready to run the analysis
    h. This is NOT a destructive analysis; you may salvage the sample if necessary.
    i. After the personnel perform the analysis, if necessary, remove the sample tube from the machine and pour the sample into a clean 1-dram vial
        i. Be sure to label the vial with the type of sample used and that it has been used for BET analysis

Day 1

	Empirical Formula	Weight (mg)	Theoretical Measurements (mg)	Actual Measurements (g)
Zinc Chloride	$ZnCl_2$	84.266	252.798	0.2523

Copper Chloride	$CuCl_2$	55.420	166.26	0.1668
H_2BBTA	$C_6H_4N_{64}H_4$	33.005	99.015	0.100

1. Scale is permanently set to grams, so have to round out some values for mg
2. Waited a while between adding Zn and Cu
3. 10 mL DMF, 0.2523 g ZNCl2, ~100 mg H2BBTA
    a. Poured bottle of H2BBTA directly into flask
4. See current setup for sonicator:



5. 10min sonication started at 2:59 pm 4/1/24
    a. Finished at 3:09 pm 4/1/24

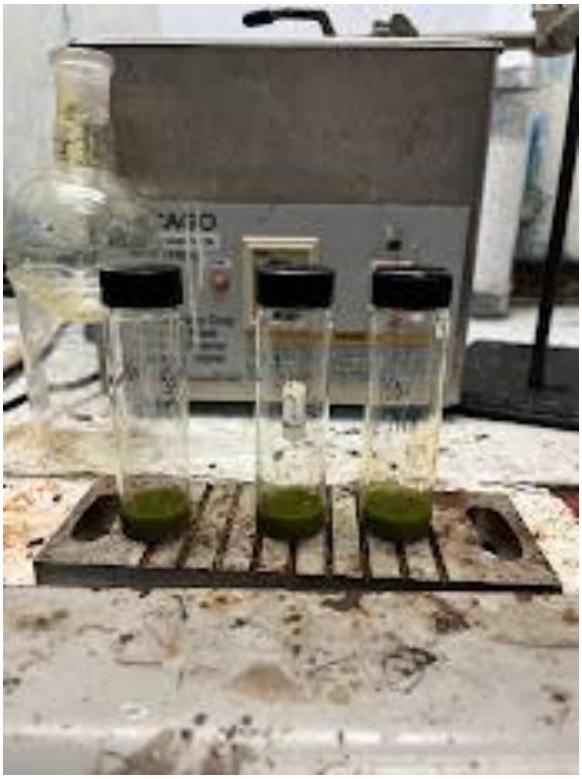

	Initial Weight (g) (without lid)	**Lid Weight (g)**	**Pre-Oven Weight (g) (with lid)**	**Final Weight (g) (without lid)**	**Yield (g)**
24 Hour	22.5323	2.1855	28.2807	22.7975	0.26652 (unlikely)
36 Hour	22.3557	3.4488	29.1554	22.3692	0.0135 (unlikely)
48 Hour	22.8103	1.5764	27.6016	22.7468	-0.0635 (impossible)

7. Samples went in non-vacuum oven at 3:56 pm 4/1/2024

Day 2

1. "24 hour" sample removed at 4:10 pm 4/2/2024
    a. Washed with 10 mL DMF
    b. Attempted to use Dr. Sun's centrifuge rather than Dr. Shanov's due to insufficient resources
    c. Yield will be minimal due to insufficient power
    d. Left out to air-dry

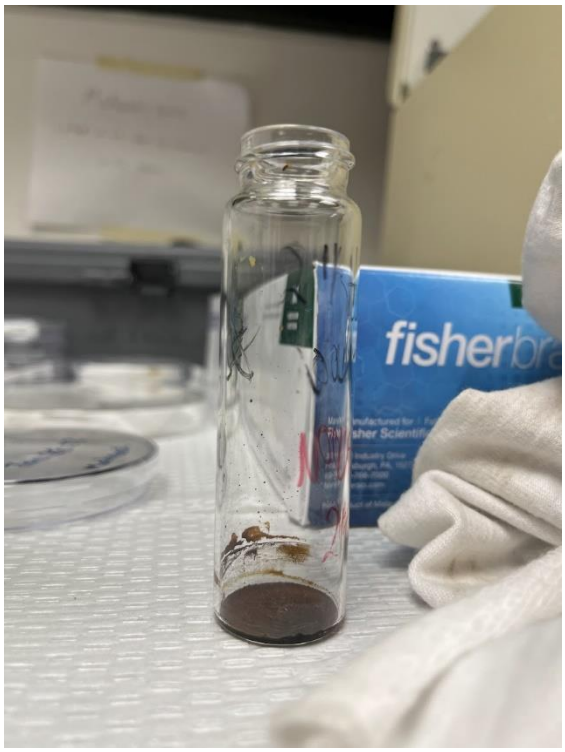

2. "48" hour" sample removed at 4:02 AM 4/3/2024
    a. New cleaning strategy:
        i. Pour 10mL DMF into a graduated cylinder
        ii. Pour 5mL DMF into the sample vial
        iii. Shake for 1 min, attempting to pick up Zinc particles not stuck to the surface
        iv. Carefully pour out into chemical waste container
        v. Pour final 5mL into sample vial
        vi. Shake until all particles have been picked up
        vii. Leave out to dry
    b. After following the new procedure, this is the result:

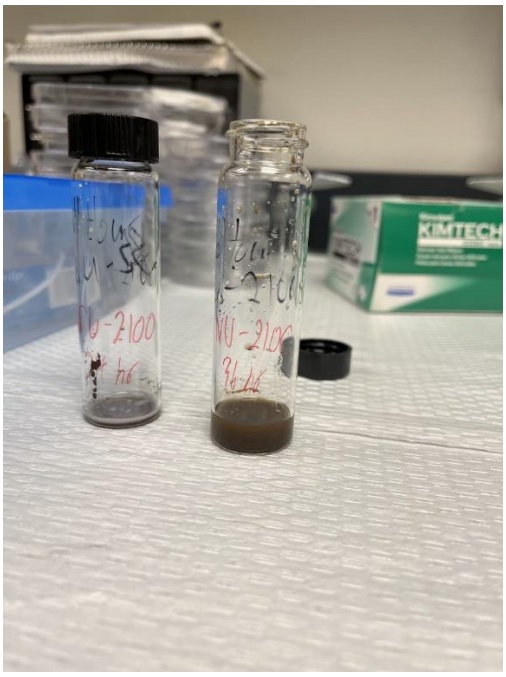

d. Has now been left out to air-dry
e. "24 Hour" sample weighed, seems to have a cloudy substance stuck to the bottom edges which could affect final weight
    i. Will compare to "36 Hour" sample once done air-drying

Day 3

1. "24 Hour" sample is only dry one, cloudy substance is possibly components of DMF
    a. The other 2 samples had contents settle to bottom, so attempted to remove DMF.
        i. Successfully removed most of DMF from "36 Hour" sample, but not "48 Hour" sample
    b. Attempting to use 50C method for half an hour to test the method, if not dry then will use vacuum oven in Dr. Iroh's laboratory
2. TGA start at 10 am, will do contents of "24 Hour" method
    a. The post-doc broke the wire hook required for TGA analysis, the TGA machine is down
3. New Plan evaporation plan:
    a. Use a pipette to remove as much DMF as possible
    b. Heat hot plate to 100C
    c. Place samples on hot plate for 6 hours
    d. Once DMF has dried, remove samples from hot plate and allow to sit and air-dry

Day 4

1. After sitting on the hot plate for 6 hours and air-drying for ~2 days, this is the result:

a. After successfully drying the samples, I took them to MD Pishnamazi to perform the BET analysis

2. New Analysis plan:
    a. Still do BET
    b. No TGA
    c. Use AMCC SEM and EDS
        i. Since ZnCl2 was borrowed, have extra money to spend for analysis

3. I removed a spoonful of MOF from each sample to perform SEM on Tuesday since the BET analysis will be until Thursday. During the BET analysis MD Pishnamazi will also be getting exact sample amounts, so a final yield will be determined. I will also weigh the yield I have since the previous method was faulty due to incorrect vial measurements

	SEM Sample Weight (mg)	**BET Sample Weight (mg)**	**Total Yield (mg)**
24 Hour	1.6	NCY	NCY
36 Hour	1.8	73.8	75.6
48 Hour	1.2	55.2	56.4

*NCY = Not collected yet

A. Master Document

THE MASTER DOC

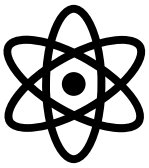

Conceptual Design of Molten Salt Test Loop for Fusion Reactor

UC-MSTL

UNIVERSITY OF CINCINNATI

1. PEOPLE

Team Members and Roles:

Jackson Stanley (stanljn@mail.uc.edu): Neutronics and Molten Salt Lead

Austin Michael (michaeau@mail.uc.edu): Heat Transfer and Fluid Flow Lead

Benjamin Kraus (krausbl@mail.uc.edu): Impurity Removal and Material Lead

Logan Powers (powerslg@mail.uc.edu): Impurity Removal and Material Engineer

Sam Haga (hagass@mail.uc.edu): Drafter and Design Engineer

CFS Contacts (supporting, not affiliated):

Ryanne Kennedy (rkennedy@cfs.energy) - Nuclear Engineering Lead

Megan Wart (mwart@cfs.energy) – Technical Lead for Neutronics

Austin Carter (acarter@cfs.energy) – Nuclear Engineer, data scientist

Amanda Johnson (ajohnson@cfs.energy) – Nuclear Engineer, project manager

2. DELIVERABLES

- Literature review
- Functional Requirements Document (FRD)
- Project Plan
- Rough design (SolidWorks) of test loop (down to equipment but not bolts, etc)
- Laboratory processes for gaseous byproduct removal and FLiBe chemical composition
- Shielding calculations and OpenMC models using unstructured mesh for irradiation of FLiBe.
- Complete conceptual Design Report of MSTL (report, standards and codes applicable for loop, calculations for thermofluidic heat transfer, sub-system design, and System Design Description)
- Filtering system experimental plan and results

3. MEETING NOTES

Monday, October 16, 2023 3:30 PM

Project Management

- Sam will take lead.
- We can use Ben's collection of Gantt Charts.
- Sam can use Microsoft Project on his computer.
- Sam will get Gantt Chart Started

First Deliverable

- Project Overview Report
    - Jackson taking lead on POR this week
    - Breakdown of subsystems and work for each subsystem
    - Actionable items
    - Start getting sets of equations

Research Results

- Ben
    - MOFs, tritium gas absorption, active copper sites, mostly theoretical
    - MOFs require a "shaving" of outer end to clear sites for gas absorption
        - Cleaning process of high/low temperatures, flash freezing, chemical washing
        - Ben knows process using Methanol to clean filter, available materials
    - Research on MOF separating gas from water vapor
    - Article on possible tritium absorption from MOF
    - Future discussion – what will MOF timeline look like?
        - Continuous or one time use
        - Document tradeoff between the two
    - Effects of purity of gaseous products on effectiveness of MOF
    - Tradeoff of purchasing new MOF instead of cleaning it
- Logan
    - Will look into filter materials that can withstand high temps/low temps/radiation environments.
    - Will look into filter materials.
- Sam
    - Researched corrosion
    - Corrosion from FLiBe
    - Corrosion from Radiation

    - Pipe Material of FLiBe
        - Replace with similar commercial alloys?
    - Gaseous Products – Beryllium Additives in Molten FLiBe reduces off-gassing of Fluoride
        - Beryllium is cheese, and a matter gun
    - Graph relating displacement per atom versus relative corrosion susceptibility
    - Need material that can withstand high neutron field
- Austin
    - Safety requirements of FLiBe salt in Fusion Reactor
- Jackson
    - Loops
    - Charles Forsberg papers
        - Initial thoughts on what loop will look like
        - Wall Structure
        - FLiBe can not be directly not to plasma
        - Mass Flow Rates
        - Removal of Tritium from Salt
            - Left at unknown – they do not know
        - Corrosion
        - Talks about challenges and things yet to be solved
    - Everyone should read above paper in Previous Examples of Loops Folder
    - "Fusion~1.pdf" – Previous Examples of Loops Folder
        - ANL Hard Data for FLiBe.
- Literature Review
    - Jackson's Approach is One table for each document.
    - Structure in whatever way is easy for you to follow.
    - Find holes in documents and what still needs researched.
    - After Literature Review is complete, format all the same and send over to CFS
    - Upload all tables into folder on OneDrive
        - Title document with title of the article

- Function Requirements Document Template
    - Sam has a little experience from project management standpoint
    - Jackson meeting with Amanda Johnson this week
    - We start flushing things out next week

Monday, October 23rd, 2023 3:30 PM

Round table:

Ben-

Completed several literature reviews:

- Several MOFs for the applicability of project- many are CU,ZN based (cheap)
- Researching videos and physical models to aid in education around MOF technology

Logan

- Several articles on honeycomb and membrane filters
- Narrowed down materials to porous ceramics/thermoplastics
- Researched pressure drop of several ranges of the filters, mat'l processes and novel hot gas filters.

Sam

- Completed literature reviews.
- Discovered beryllium as a tritium reducing agent- to be documented in project plan.

Austin

- Looking into sensors for radiation heat transfer.
- Multi-sensor radiation detection.
- Boron coated silicon sensors.
- Scintillators.

Jackson

- Researched previous loop ideas- SS, Argon, etc to be used?
- Operational systems for loops
- Types of systems for material timeline- decided no longer than 3 years of operation.

Going forward:

Meeting with Amanda at 3:00 PM on Friday- will send link.

See assigned work for direction. Plan to have all components done 10/30/23

Monday, October 30th, 2023 3:30 PM

Round table:

Ben- Will complete literature reviews today 10/30/2023. Ben will focus on the filtering system high level functional requirements for 11/6/2023.

Tech Talk: Equations for modeling MOF's – research and holes in literature.

- Issue around deformation of MOFs due to gasses filling up pores- a form of plenum gas conflict.
- Assumption has traditionally been that an MOF is linearly elastic- one DOF.

Logan- Completed literature review documents. Will help in creation of functional requirements for filtration and controls.

Sam- Out of meeting/sick. Nee to confirm:

1. Completion of literature review for documents.
2. Creation of simple diagrams.
3. Creation of simple equation sheet.

If completed, assigned to: develop functional requirements for controls and sampling. Also development of system/process flow diagram.

Austin- Created equations for the project plan. Completed literature reviews. Will combine literature reviews into one document. Will format functional requirements document. Will be out Monday the 6th of November.

Jackson- Finished literature review. Will finish and continue to work on FLiBe and Loop Requirements. Will look at completed literature review doc for formatting and executive summary. Will work with Will Hawkins on the development of the OpenMC code and XS file.

Going forward:

See assigned work for direction. Plan to have all components done **11/6/23.**

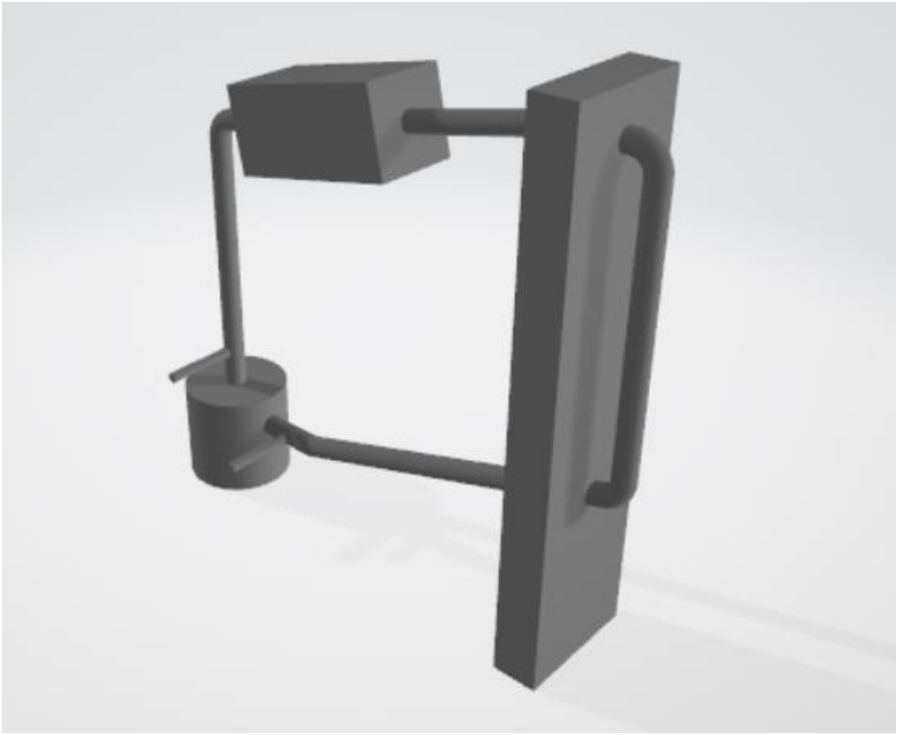

Monday, November 6th, 2023 3:30 PM

Ben- Finished literature review. Completed functional requirements. Would like to get into contact with people at CFS for data pertaining to FLiBe – to – tritium production. Would like to talk to Dr. Farnsworth- Jackson will facilitate.

Sam- Completed models and functional requirements. Will document assumptions into an assumptions log. Will document models in project plan.

Logan- out today. Will check master doc.

Austin- out today. Will check master doc.

Jackson- Completed functional requirements. Working with UC professor to get OpenMC working- hopefully by next week! Will get ahold of Ethan Peterson once unstructured mesh is generated. Will get concept model from Sam. Will help facilitate closing out of two documents- lit review and FRD.

Monday, November 13th, 2023 3:30 PM

- Caught up Austin and Logan on previous meeting.
- Met Dr. Jude Iroh and had a brief introduction.

Sam – Started details of loop layout considerations and pump characteristics. Working on completing characterization and formulating numerical assumptions.

Logan – Tritium storage in titanium, palladium, depleted uranium, erbium. Potential for metallic filter without need for MOF. Continuing research. Determining temperature range for filters. (~600-900C). Potential to research materials if want to use a membrane. Will do material traceability for different types of filtering techniques (membrane vs mesh filter).

Ben – Creating NX model of MOF filtering system. Potential for future research on degradation of Tritium inside of MOF.

Monday, November 20th, 2023 3:30 PM

Overview:

Updated the gant chart to represent functional requirements doc and lit review to be completed.

Everyone to look at lit review and function Req docs.

Scheduled meeting for all of us to go over nuclear aspects of loop.

Austin- Read through Func Req Docs. Quick call over concrete composition stuff. Look overflow sensors for flow sensing. Project plan population. Talk to Dr. Spitz.

Ben- Do research on degradation of tritum into helium inside MOFs. Dong project management tab in project plan. Creating 3D model of filter subsystem.

Sam- Deliverables and implementation plan for sections. Update concept model for shielding thickness.

Logan- Working on review of funct req doc and lit review. Fill out high level timeline on project plan. Continue working on computational model on airflow calcs to determine location of filter.

Jackson- Working on review of funct req doc and lit review. Play around with OpenMC to get cad file to load into system. Complete high level requirements in Project plan.

Monday, November 27, 2023

Overview: Continuation of previous goals:

Monday, December 4th, 2023

Overview: Continuation of previous goals:

Sam: Flight cancelled and moved, meeting on Saturday moved to Saturday at 1:00 or later would be beneficial

Monday, January 8th, 2024

Overview:

Review of CFS email and deliverables

Discussion surrounding funding for MOF selection and post processing.

The creation of the MOF type will not vary significantly in cost

A decision matrix will be utilized to select the best MOF for testing – due to funding constraints, we will only utilize one MOF.

Which MOF should we go with?						
		27	28	60	0	0
Options		Cu	UIO	VSB	option 4	option 5
Decision making factors	Weighting	Your Score	Your Score	Your Score	Your Score	Your Score
Material cost	3	3	3	5		
synthesis time	4	2	1	5		
Research pote	5	2	3	5		
factor 4						
factor 5						

Cu decided

3 samples

SEM Machine

ASAP Machine

TGA Machine – tentative -

Monday, January 15th, 2024

Overview: Met with Dr. Spitz and went over shielding calculation and NAA. He will go over shielding calc and provide comments- 0.13 result is in ballpark of correct, but he will check math. He also provided NAA calculation result discussion- utilize volume of material, microscopic cross section, and neutron flux (1E15 n/cm^2/s).

Ben will need to procure materials for testing asap. We will need to discuss with Huston ASAP to discuss funding.

Sam will need to provide volumes and materials for calculations.

Monday, January 22nd, 2024

Ben- Ben procuring chemicals. Applied for capstone funding ($400) for materials. Waiting for funding to order materials. Will work on SDD sections for filtering- very busy week.

Dr. Iroh was invited to the meeting but did not attend.

Monday, January 29th 2024

All- Working on producing PowerPoint and report for design review – work on SDD sections.

Austin – Waiting from Sam for NAA volume to finish up calc. Will work on documenting NAA and shielding calcs in OpenMC. Will also do research into neutron spectrum values for fusion reactor in 14MeV energy range and above.

Jackson - Finishing up OpenMC model such that we can produce results. Will meet with MIT this week. Working on FLiBe and sampling SDD sections. Working to document installation of OpenMC and deliverables.

Sam- Working on transferring models from NX to SolidWorks. Will provide Austin with the NAA volumes for calculations. Getting ready for new models with more complex loop designs.

Logan- Very busy this week. Will help out with SDD sections with Ben.

Going forward:

See assigned work for direction. Plan to have all SDD components done 2/12/2024.

Monday, January 29th, 2024

Austin- to work on example calcs for the shielding calc and NAA calc. Pumping SDD section.

Jackson- Finishing up OpenMC model such that we can produce results. Will meet with MIT this week. Working on FLiBe and sampling SDD sections. Working to document installation of OpenMC and deliverables.

Sam – Repair all surfaces for Jackson's CUBIT import functions.

Ben- work on getting chemicals procured. See table for SDD work.

Logan – Document filter SDD sections. Created video animations of filter mechanisms, and cad models.

Monday, February 5th, 2024

Austin- Working on OpenMC calc document and Pumping SDD section. Will meet with Jackson to check calculation for shielding and NAA.

Jackson- Working on preparing for status meeting following week. Brainstormed SDD sections, and more details for model. Working on SDD sections for flibe and sampling.

Sam – Worked on models and SDD sections. Will produce model images for SDD document.

Ben- Work on getting chemicals procured. See table for SDD work. Will work on 3D MOF model.

Logan – Document filter SDD sections. Created video animations of filter mechanisms, and cad models.

Monday, February 5th 2024

All- Working on producing PowerPoint and report for design review – work on SDD sections.

Monday, February 12th 2024

All- Working on producing PowerPoint and report for design review – work on SDD sections.

Monday, February 19th 2024

Ben – Working on getting the chemicals from sigma Aldrich – Dr. Spitz says he can provide help with producing chemicals and providing equipment. Looking at getting all chemicals in by March 4th. He will put in some work on progress report for MOF design updates.

Logan - Working on filter design and SDD controls section – could get SDD sections done by Friday. Idea to have model printed.

Austin – Work with Jackson on shielding Calc and SDD. Working on progress report.

Sam – Working on BOP SDD section. Integrating changes to model as they come in. Update Ghant Charts. On standby for filter assembly to integrate into final design.

Jackson – Shielding Calc, follow up with CFS. Completed FLiBe SDD section. Follow up on PowerPoint with regulations

Shielding Calc

SDD sections

OpenMC

Monday, February 26th 2024

- Sam is uploading new CAD files to shared drive
    - New CAD folder in Reference Section -> Concept Models and Assumptions
- Pipe Diameter is arbitrary but standard pipe size, 2” Schedule 40

Sam

- Design uploaded to drive
- Adding Jackson’s updates
- Request for Pictures in SDD
- Collecting images for Progress Report

Ben

- ZnCl2 still in transit
    - Arrives in 1-2 weeks
- Other chemicals in Dr. Iroh’s Lab and Ben’s office
- Start experiments on 3/4/2024
- Updating procedure for NU-2100

    - Will send over to Austin to add on Progress Report
- Jackson and Dr. Spitz in talking about radiating NU-2100 MOF
    - OSU reactor or Dr. Spitz Lab?
- Fellowship application approval decision coming in next few weeks
    - Dr. Lamkin runs the whole process
        - Application process takes about a month, could go through some red tape
    - Used for Lab tests and equipment usage
- BET is free from Dr. Shanov's Lab
- SEM and TGA
    - TGA 3 hours total, one hour per sample, $30/hour
    - SEM 1 hour total, $50/hour
- Extend time for heating NU-2100 samples
    - Becomes NU-2100 after 24 hours of heating, once all Zinc ions are replaced with Copper ions
        - 24, 36, 48 hours of heating
            - 1 sample for each

Logan

- Model of filter system moved to Wednesday.
- After model complete, throw into CFD software.

Austin

- Progress report completion
- Pump SDD work in progress
- NAA Calculation in contact with CFS for neutron flux values

** Ben will send out experimental schedule. Let Ben know if you want to attend.

- Best time to attend is very beginning with sonicator, or SEM analysis

Monday, March 4th 2024

All- Working on SDD sections. Jackson Working on OpenMC calcs – document finished and ready to be sent to Spitz for check.

Monday, March 11th 2024

WEEK OF 3/11: BREAK FOR SPRING BREAK. NO MEETING SHEDULED

Group

Took time to investigate best method for poster design, and toured lab spaces to get general ideas of poster. Created whiteboard drawings and diagrams to determine poster layout. Fellowship did not come in yet – assuming fellowship is not to be awarded.

Sam

- Design uploaded to drive
- Add Jackson's updates and Logans Filtering system into model
- Request for Pictures in SDD
- Collecting images for Progress Report

Austin

- Work on poster and video presentation – completed NAA work.

Ben

- Formulating protocol and writing procedures. Talk to Jackson about best way to prpoceed

Logan

- Working on poster and video presentation.

Jackson

- Working on poster and video presentation.

WEEK OF 3/11: BREAK FOR SPRING BREAK. NO MEETING SHEDULED

Monday, March 18th 2024

All- Teams meeting, many still traveling. Working individually with Jackson to get deliverables completed pre-video and poster. Sam not attending.

Monday, March 25th 2024

Group

Took time to investigate best method for poster design, and toured lab spaces to get general ideas of poster. Created whiteboard drawings and diagrams to determine poster layout. Fellowship did not come in yet – assuming fellowship is not to be awarded.

Sam

- Design uploaded to drive
- Add Jackson's updates and Logans Filtering system into model
- Request for Pictures in SDD

- Collecting images for Progress Report

Austin

- Work on poster and video presentation – completed NAA work.

Ben

- Formulating protocol and writing procedures.

Logan

- Working on poster and video presentation.

Jackson

- Working on poster and video presentation.

Monday April 1st , 2024

Group – Working on formatting presentation per requirements. Video scheduled for Tuesday at 3:00 PM.

Sam

Worked with Jackson and finished concept models. Models look great! Placed model in concept model images. Worked in importing them into poster. Finishing SDD section.

Austin

Worked on poster formatting and finished sections of project video.

Ben

Performing experiments for the MOF – will perform analysis on Wednesday, and post process by Friday. Working to document results and add to SDD.

Logan

Worked on poster formatting and finished sections of project video.

Jackson

Worked on poster formatting and finished sections of project video.

Monday April 8th , 2024

Group – virtual meeting due to eclipse! Planning to present with model of MSTL at expo.

Sam

Finished SDD sections and is ready to have them incorporated into final document.

Austin

Working on formatting final document for submission.

Ben

Performing experiments for the MOF – analysis pushed back due to constraints. Will be performing SEM on Tuesday afternoon and BET on Thursday.

Logan

Nothing to add- ready for expo! Will work on final presentation for Friday.

Jackson

Working on fixing some typos in the nuke calcs doc. Working on final presentation formatting for Friday.

4. ASSIGNED PROJECT-BASED WORK

10/2/2023

Person	Action Items	Date Due
Jackson	Research and produce 5 sources of information.	10/16/2023
Austin	…	…
Ben	…	…
Logan	…	…
Sam	…	…

10/16/2023

Person	Action Items	Date Due
Jackson	Create and populate project plan and Functional Requirements Document, and populate literature reviews	Literature Reviews, FRD, Project Plan- 10/23/2023 To do: Send Sam dates from handwritten notes Thoughts: SDD after FOR,
Austin	Literature Review Pumps and Sensors	Literature Reviews- 10/23/2023 10/23/2023
Ben	Research MOFs capable of Helium/Tritium Adsorption and literature reviews	Literature Reviews- 10/23/2023 10/23/2023
Logan	Research filter types and applications	Literature Reviews- 10/23/2023
Sam	Gantt Chart (General – WBS/Work Package Level) and Populate Literature Reviews Sketch Basic Spline Formation for FliBe Loop	Literature Reviews- 10/23/2023

10/23/2023

Person	Action Items	Date Due
Jackson	1. Create list of equations for radiation transport, documentation, etc.	10/30/23 Thoughts: SDD after FRD?
Austin	1. Finish literature reviews	10/30/2023 10/30/2023

	2. Create list of heat transfer equations	
Ben	1. Create list of equations for trit/byproduct removal	10/30/2023
Logan	1. Create list of equations for trit/byproduct removal	10/30/2023
Sam	1. Create list of fluid flow equations for molten salt/liquid metal flow	10/30/2023

10/30/2023

Person	Action Items	Date Due
Jackson	1. Finish Loop and FLiBe requirements. Start sampling requirements and support equip requirements. – leaving for team discussion. 2. Look over and format literature review. 3. Get OpenMC working!	11/6/2023
Austin	1. Format/compile literature reviews 2. FRD Pump Requirements 3. Fill in holes in Lit Review	11/06/2023
Ben	1. Finish literature reviews. 2. Complete functional requirement sections for high level byproduct removal. 3. Start development of experiment plan and procedure breakdown-	11/06/2023 11/20/2023

	list of experiments to do.	
Logan	1. Finish literature reviews. 2. Complete functional requirement sections for byproduct removal and partially complete controls section.	11/06/2023
Sam	1. Talk to Jackson. Available through zoom, teams, phone, etc!	11/06/2023

11/6/2023

Person	**Action Items**	**Date Due**
Jackson	1. Support conclusion of lit review. 2. Support Filtering system requirements. 3. Support BOP requirements. 4. Get OpenMC working! 5. Talk to Will about meetings and possible collaborations on future advising.	11/13/2023
Austin	1. Finish lit review- get in touch with Jackson to go over formatting. 2. Support on BOP requirements in FRD.	11/13/2023
Ben	1. Complete functional requirement	11/13/2023

	sections for filtering system. 2. Continue work on experiment plan and procedure breakdown- list of experiments to do. 3. Continue design work on filter. 4. Talk to Dr. Jude Iroh about meetings and possible collaborations on material decisions 5. Determine model for filter system	11/20/2023
Logan	1. Talk to Jackson- create a material traceability for filter type (membrane, honeycomb, etc.) 2. Talk to Ben- support functional requirements section for filtering system.	11/13/2023
Sam	1. Label and send image of system into project plan. 2. Document assumptions (materials, dimensions, etc.) 3. Convert gantt chart to excel and place in project management folder. 4. Calculate Mass Flow Rate for current concept	11/13/2023

	system -> Handoff to Ben	

11/13/2023

Person	Action Items	Date Due
Jackson		
Austin	Assist in location and type of sensors measuring flow. Shielding? Thickness?	11/20/2023
Ben	Research on inherent degradation of tritium while inside of a MOF	11/20/2023
Logan	Material Traceability for different types of filtering techniques (membrane vs mesh filter).	11/20/2023
Sam	Continuing work on loop and pump characteristics.	11/20/2023

11/20/2023

Person	Action Items	Date Due
Jackson	Working on Shielding Calcs- Will provide adjusted shielding thickness using custom concrete material. Work on populating project plan.	11/27/2023
Austin		11/27/2023
Ben	Create concept model for CFS on creating experiment for inner-MOF degradation. ~~Create experimental procedure.~~ Work on Project management section of Project Plan. ~~Review literature review.~~	11/27/2023
Logan		11/27/2023

Sam	Complete Deliverable and Work on Implementation Plan of Project Plan ~~Update Concept Model with New Thickness~~ ~~Include Dimensioned Diagram in Project Plan~~	11/27/2023

11/27/2023

Person	Action Items	Date Due
Jackson	Complete sections in project plan.	12/04/2023
Austin	Complete sections in project plan. Work on shielding calcs.	12/04/2023
Ben	Complete FRD review. ~~Complete project plan~~ deliverable and implementation sections.	12/01/2023 12/11/2023
Logan	Complete FRD review. Complete project plan deliverable and implementation sections.	12/01/2023 12/11/2023
Sam	Update Gantt Chart to Reflect Dates on Project Plan ~~Go Through Functional Requirements~~ ~~Complete Project Plan and Rough Design Sections of the Project Deliverable Breakdown~~ ~~Complete Project Plan and Rough Design Sections of the Implementation Plan~~	12/01/2023

12/04/2023

Person	Action Items	Date Due
Jackson	Complete sections in project plan.	12/11/2023
Austin	Complete sections in project plan. Work on shielding calcs.	12/11/2023

Ben	deliverable and implementation sections.	12/11/2023
Logan	Complete project plan deliverable and implementation sections.	12/11/2023
Sam	Update Gantt Chart to Reflect Dates on Project Plan	12/11/2023

12/11/2023

Person	**Action Items**	**Date Due**
Jackson	Review all docs- lit review, functional, and project plan. Work on shielding calcs.	12/15/2023
Austin	Review all docs- lit review, functional, and project plan. Work on shielding calcs.	12/15/2023
Ben	Review all docs- lit review, functional, and project plan. deliverable and implementation sections.	12/15/2023
Logan	Review all docs- lit review, functional, and project plan. Complete project plan deliverable and implementation sections.	12/15/2023
Sam	~~Update Gantt Chart to Reflect Dates on Project Plan~~ Determine High Level Material Composition (top 4 and/or 75% material composition) of Conceptual Loop Design. Update model of loop to represent changes made on 12/11/2023.	12/15/2023

1/8/2024

Person	Action Items	Date Due
Jackson	OpenMC IS WORKING: install dagmc and work with UC/CFS to get it ready to accept new model.	1/15/2024
Austin	Talk to Jackson about getting NAA study performed.	1/15/2024
Ben	Discuss plans for chemical analysis with department- reach out for funding and utility.	1/15/2024
Logan	Develop concept model for filtering mechanism.	1/15/2024
Sam	Update model per discussion with Jackson- update to include 3-in steel block, tungsten, and beryllium.	1/15/2024

1/15/2024

Person	Action Items	Date Due
Jackson	Complete NAA calculations and document in report format. Get OpenMC ready to accept model- install DAGMC and install Cubix.	1/19/2023
Austin	Complete NAA calculations and document in report format.	1/22/2023
Ben	Order chemicals and get ready to perform experiments. Talk to Dr. Huston to get everything ordered and paid for.	1/22/2023
Logan	Consider filtering mechanism concept. Sent total volume that MFC will occupy to Jackson and Auston. Perform CFD for airflow	1/22/2023

Sam	Send Jackson and Austin the total volumes of the steel piping, concrete, and FLiBe in cm^3. Work on the model to be ready for OpenMC implementation.	1/22/2023

1/22/2024

Would like to get SDD done 2/12

Person	**Action Items**	**Date Due**
Jackson	Get first results from OpenMC. Document results in neutronics doc FLiBe and Sample SDD sections.	1/26/2023
Austin	Document NAA and shielding calcs in the neutronics doc. Pump and help with FLiBe SDD.	1/29/2023
Ben	Filter of SDD – look at FRD doc for direction.	1/29/2023
Logan	Controls system and filter system sections of SDD.	1/29/2023
Sam	Update models from NX. Prepare for SDD images for sub-system designs. Balance of Plant SDD section.	1/29/2023

1/29/2024

Would like to get SDD done 2/12

Person	Action Items	Date Due
Jackson	Get first results from OpenMC. Document results in neutronics doc FLiBe and Sample SDD sections.	2/05/2023
Austin	Document NAA and shielding calcs in the neutronics doc. Pump and help with FLiBe SDD.	2/05/2023
Ben	Filter of SDD – look at FRD doc for direction.	2/05/2023
Logan	Controls system and filter system sections of SDD.	2/05/2023
Sam	Update models from NX. Prepare for SDD images for sub-system designs. Balance of Plant SDD section.	2/05/2023

2/5/2024

Would like to get SDD done 2/12

Person	Action Items	Date Due
Jackson	Get first results from OpenMC. Document results in neutronics doc FLiBe and Sample SDD sections. Write project status powerpoint. Correct shielding calculations and NAA calculations.	2/12/2023
Austin	Help document NAA and shielding calculations. Write project status update. Pump and help with FLiBe SDD.	2/12/2023
Ben	Filter of SDD – look at FRD doc for direction. Order chemicals. Work on MOF digital structure.	2/12/2023

Logan	Controls system and filter system sections of SDD.	2/12/2023
Sam	Update models from NX. Prepare for SDD images for sub-system designs. Balance of Plant SDD section.	2/12/2023

2/12/2024

Person	**Action Items**	**Date Due**
Jackson	Get first results from OpenMC. Document results in neutronics doc FLiBe and Sample SDD sections. Write project status powerpoint. Correct shielding calculations and NAA calculations.	2/19/2023
Austin	Help document NAA and shielding calculations. Write project status update. Pump and help with FLiBe SDD.	2/19/2023
Ben	Filter of SDD – look at FRD doc for direction. Order chemicals. Work on MOF digital structure. Write portion of presentation	2/19/2023 2/15/24
Logan	Controls system and filter system sections of SDD. Finish model of cyclone filter. Write portion of presentation.	2/19/2023 2/15/24
Sam	Update models from NX. Prepare for SDD images for sub-system designs. Balance of Plant SDD section.	2/19/2023

2/19/2024

Person	Action Items	Date Due
Jackson	~~**Progress report and PowerPoint must be done by Friday 2/23.**~~ ~~OpenMC Calcs – work to be done Wednesday with Austin C.~~ ~~SDD sampling section – finish sampling section.~~	2/23/2023 2/26/23
Austin	**Progress report and PowerPoint must be done by Friday 2/23.** Work with Jackson on NAA calc – which shielding/ neutron flux value to use? SDD pumping section – finish by 2/26.	2/23/2023 2/26/23
Ben	**Progress report and PowerPoint must be done by Friday 2/23.** Getting all chemicals in the first week of March. SDD filtering section – finish by 2/26.	2/23/2023 2/26/23
Logan	**Progress report and PowerPoint must be done by Friday 2/23.** SDD Controls/Filtering section: finish by 2/26.	2/23/2023 2/26/23
Sam	**Progress report and PowerPoint must be done by Friday 2/23.** Integrate all changes to model as requested.	2/23/2023 2/26/23

	-push all models to shared folder and update ghant chart-share ghant chart with Austin. BOP SDD section: Finish by 2/26.	

2/26/2024

Person	Action Items	Date Due
Jackson	Finish openmc calcs – post process data	3/1/2024
Austin	SDD Pump Rqmts – fix deterministic calcs	ASAP
Ben	Make changes to filtering system. Create document for filtering system analysis, experiments, and results	3/1/2024
Logan	Complete Filter Model Start CFD	Wednesday (2/28/2024)
Sam	Make changes to model – incorporate final changes from SDD into model. Work on support equipment section of SDD.	3/1/2024

3/04/2024

Person	Action Items	Date Due
Jackson	Finish openmc calcs – post process data	3/5/2024
Austin	Help Jackson with openmc calcs	3/5/2024
Ben	Make changes to filtering system. Create document for filtering system analysis, experiments, and results	3/5/2024
Logan	Complete Filter Model Start CFD	3/5/2024

Sam	Make changes to model – incorporate final changes from SDD into model. Work on support equipment section of SDD.	3/5/2024

3/18/2024

Person	**Action Items**	**Date Due**
Jackson	Openmc Calcs finished. Working on poster and video presentation.	3/25/2024
Austin	Help Jackson with poster and video presentation.	3/25/2024
Ben	Create document for filtering system analysis, experiments, and results – (2 weeks late). Order new chemicals – contact Dr. Spitz. Create experimental plans in document for filtering system.	3/25/2024
Logan	Add filtering system to poster – complete filter CFD.	3/25/2024
Sam	Make changes to model – incorporate final changes from SDD into model (Logan's filtering system and Jacksons model changes). Work on support equipment section of SDD. (3 weeks late).	3/25/2024

3/25/2024

Person	Action Items	Date Due
Jackson	Openmc Calcs finished. Working on poster and video presentation.	4/1/2024
Austin	Help Jackson with poster and video presentation.	4/1/2024
Ben	Create document for filtering system analysis, experiments, and results – (3 weeks late). Order new chemicals – contact Dr. Spitz. Create experimental plans in document for filtering system. Add filtering system to poster.	4/1/2024
Logan	Add cyclone filtering system to poster.	4/1/2024
Sam	Finish SDD section – add concept model to poster. Work on video.	4/1/2024

4/1/2024

Person	Action Items	Date Due
Jackson	Finalize poster and video presentation.	4/8/2024
Austin	Finalize poster and video presentation.	4/8/2024
Ben	Finalize poster and video presentation. Perform experiments and perform post process analysis for MOF filtration material.	4/8/2024
Logan	Finalize poster and video presentation.	4/8/2024
Sam	Finish SDD section. Finalize poster and video presentation.	4/8/2024

4/8/2024

Person	Action Items	Date Due
Jackson	Working on final presentation for Friday.	4/12/2024
Austin	Working on final presentation for Friday.	4/12/2024
Ben	Working on final presentation for Friday.	4/12/2024
Logan	Working on final presentation for Friday.	4/12/2024
Sam	Working on final presentation for Friday.	4/12/2024

5. PROJECT SCHEDULE

See the following page for the project Gantt Chart.

FliBe Test Loop Design

Project start: Mon, 10/9/2023

Display week: 1

TASK	ASSIGNED TO	PROGRESS	START	DURATION:	END
Literature Review					
Find Research Documents	ALL	100%	10/9/23	14	10/23/23
Complete Synopsis'	ALL	100%	10/16/23	14	10/30/23
Compile Synopsis'	AUSTIN	100%	10/30/23	7	11/6/23
Edit and Finalize Lit. Review	JACKSON	100%	11/6/23	7	11/13/23
Project Overview					
Create Schedule	SAM	100%	10/9/23	7	10/16/23
Create Project Plan	ALL	100%	10/16/23	28	12/11/23
Create Functional Requirements Document	ALL	100%	10/16/23	28	11/13/23
Find Applicable Equations For System Design	ALL	100%	10/23/23	7	12/11/23
FliBe Loop Design					
Determine Specific Sub-Systems and Processes	SAM	100%	10/30/23	3	11/2/23
Create Rough Model of FliBe Loop Layout	SAM	100%	11/3/23	10	11/13/23
Handoff System Parameters with Team (Flow/Pump/Heating Req)	SAM	100%	11/13/23	7	11/20/23
Detail Concept Model	SAM	100%	1/10/24	51	3/1/24
Compile Final System Parameterization	SAM	100%	3/1/24	31	4/1/24
Filtering Loop Design					
Design MOF Filtration System	BEN + LOGAN	100%	10/30/23	14	11/13/23
Determine Expirimentation Procedure	BEN	100%	11/13/23	21	12/4/23
Design Filtration/Loop System	LOGAN	100%	1/22/24	35	2/26/24
Perform Testing	BEN + LOGAN	100%	2/19/24	14	3/4/24
Handoff System Parameters with Team	BEN + LOGAN	100%	3/4/24	7	3/11/24
Detail Concept Models - post process analysis	BEN	50%	3/11/24	14	4/10/24
Expierimental Procedure					
Combine Materials	BEN + LOGAN	100%	3/26/24	13	4/8/24
Sonicating of Materials	BEN + LOGAN	100%	3/26/24	13	4/8/24
Trial 1 - 24 Hour Mixture	BEN + LOGAN	100%	3/26/24	13	4/8/24
Trial 2 - 36 Hour Mixture	BEN + LOGAN	100%	3/26/24	14	4/9/24
Trial 3 - 48 Hour Mixture	BEN + LOGAN	100%	3/26/24	14	4/9/24
SEM	BEN + LOGAN	100%	3/29/24	12	4/10/24
TGA	BEN + LOGAN	0%	3/29/24	5	4/3/24
BET	BEN + LOGAN	50%	4/1/24	3	4/4/24
Irradiation	BEN + LOGAN	0%	3/31/24	6	4/6/24
OpenMC Model/Simulation					
Learn About OpenMC / Get Working	JACKSON	100%	10/30/23	28	12/11/23
Import FliBe + Filter Loop	JACKSON + AUSTIN	100%	1/22/24	7	1/29/24
Perform Simulations	JACKSON	100%	1/29/24	32	3/1/24
1st Iteration Complete	JACKSON	100%	3/1/24	-21	2/9/24
2nd Iteration Complete	JACKSON	100%	3/4/24	8	3/12/24
3rd Iteration Complete	JACKSON	100%	3/12/24	8	3/20/24
Document Results	JACKSON + AUSTIN	100%	3/18/24	7	3/25/24
Investigate shielding requirements	JACKSON + AUSTIN	100%	11/6/23	14	11/20/23
Perform shielding calcs - get results checked by Dr. Spitz	JACKSON + AUSTIN	100%	11/27/23	7	12/4/23
Investigate NAA calcs - determine volumes of material, method, flux va	AUSTIN	100%	1/8/24	28	2/5/24
Perform NAA calcs - get results checked by Dr. Spitz	AUSTIN	100%	1/15/24	42	2/26/24
Closing					
Identify Standards and Codes	ALL	100%	3/25/24	7	4/1/24
Write Report	ALL	100%	4/1/24	14	4/1/24
Compile Deliverables Into Handoff Package	ALL	100%	4/1/24	14	4/15/24
Put Together Presentation	ALL	100%	4/1/24	7	4/8/24

Insert new rows ABOVE this one